

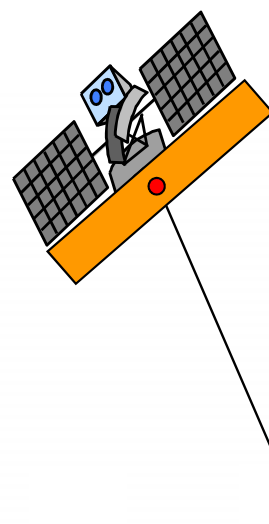
SAR Interferometry

A (very) short Introduction

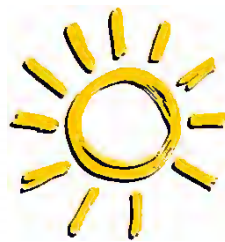
Konstantinos P. Papathanassiou

German Aerospace Center (DLR)
Microwaves and Radar Institute (DLR-HR)
Pol-InSAR Research Group

Oberpfaffenhofen, P.O. 1116, D-82234 Wessling
Tel./Fax.: ++49-(0)8153-28-2367/1149
Email: kostas.papathanassiou@dlr.de



SAR Image Phase Contribution

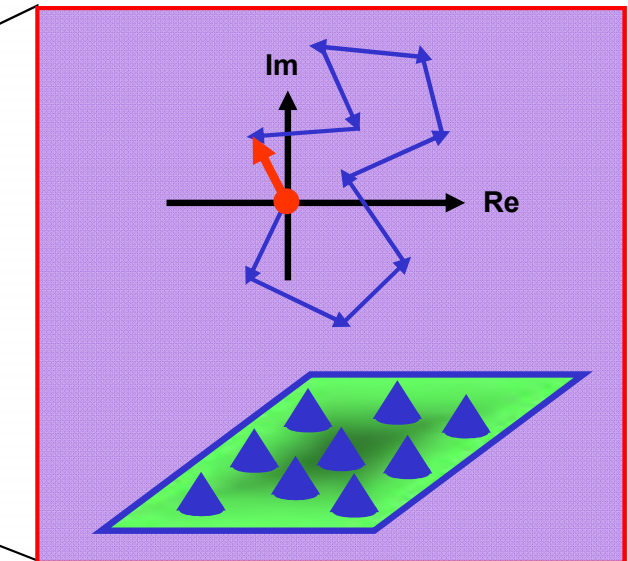
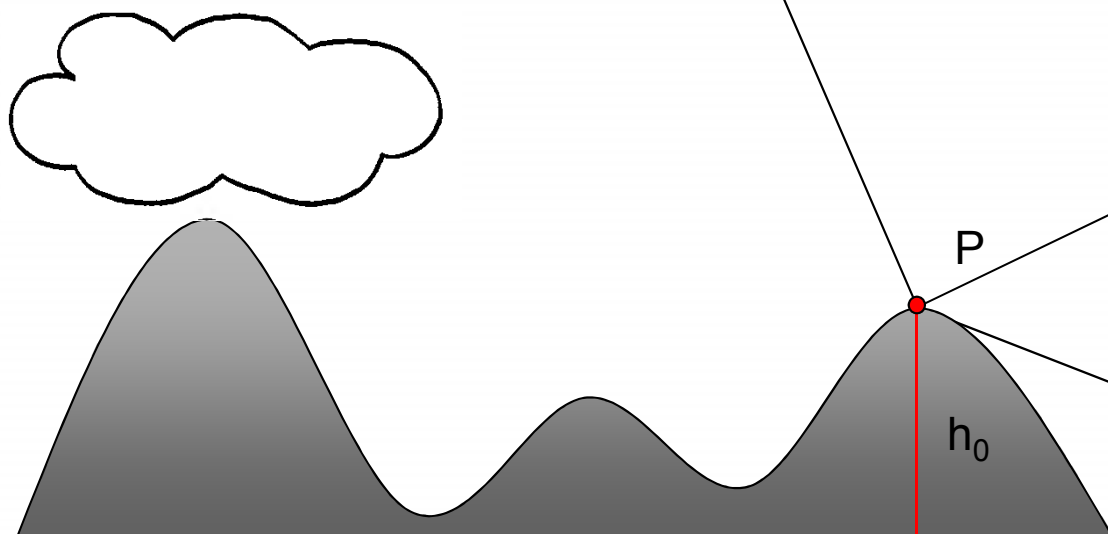


Signal from resolution cell P in Image 1: $i_1 = |i_1| \exp[-i(2\frac{2\pi}{\lambda}R_1) + \varphi_{S1}]$

Phase: $\varphi_1 = \arg(i_1) = (2\frac{2\pi}{\lambda}R_1) + \varphi_{S1}$

Term 1: Deterministic - proportional to the range distance R_1 of P

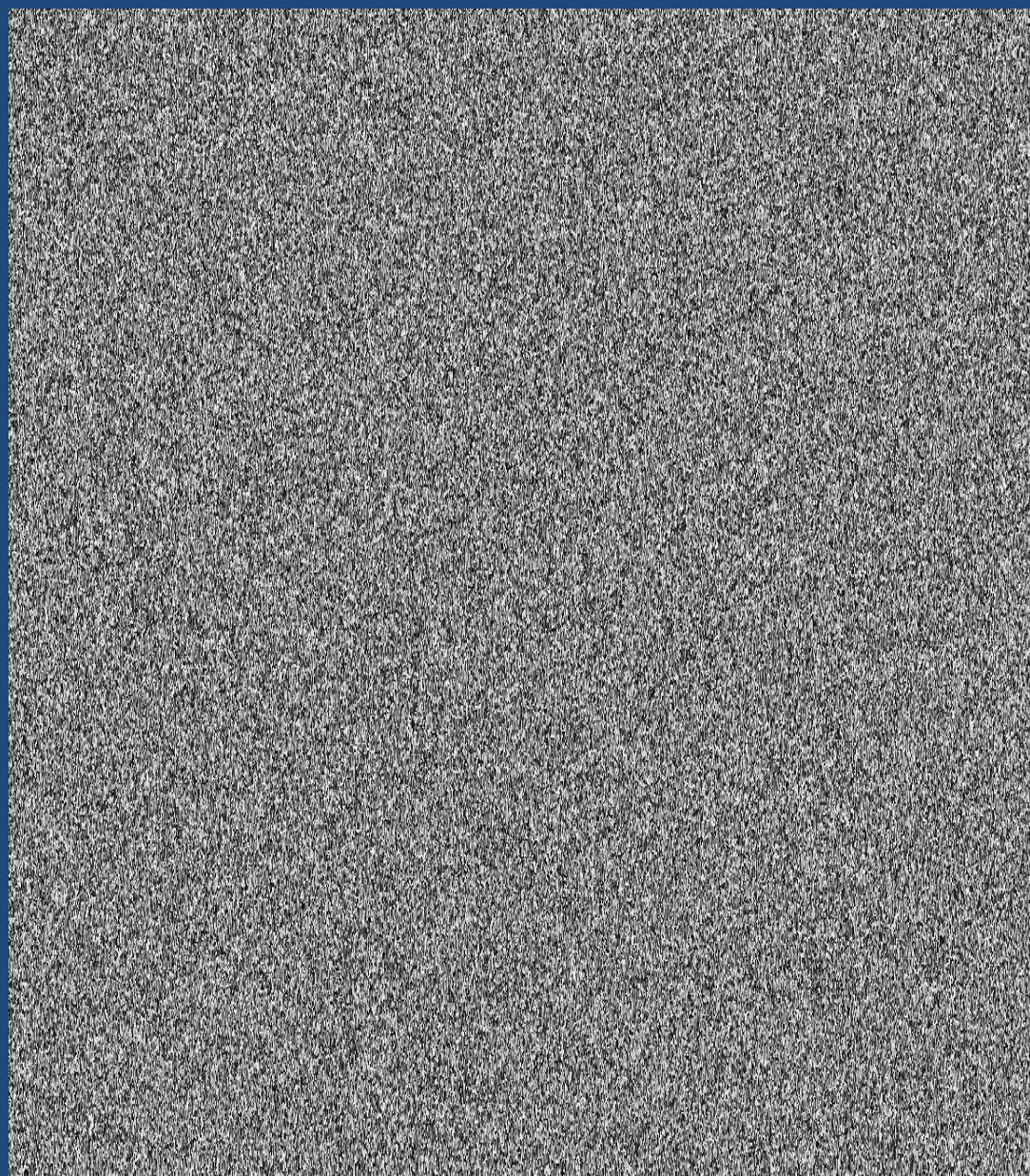
Term 2: Stochastic - induced by the scatterer (Speckle)



ERS – Bachu / China $\sim 100 \text{ km} \times 80 \text{ km}$



Amplitude Image 1

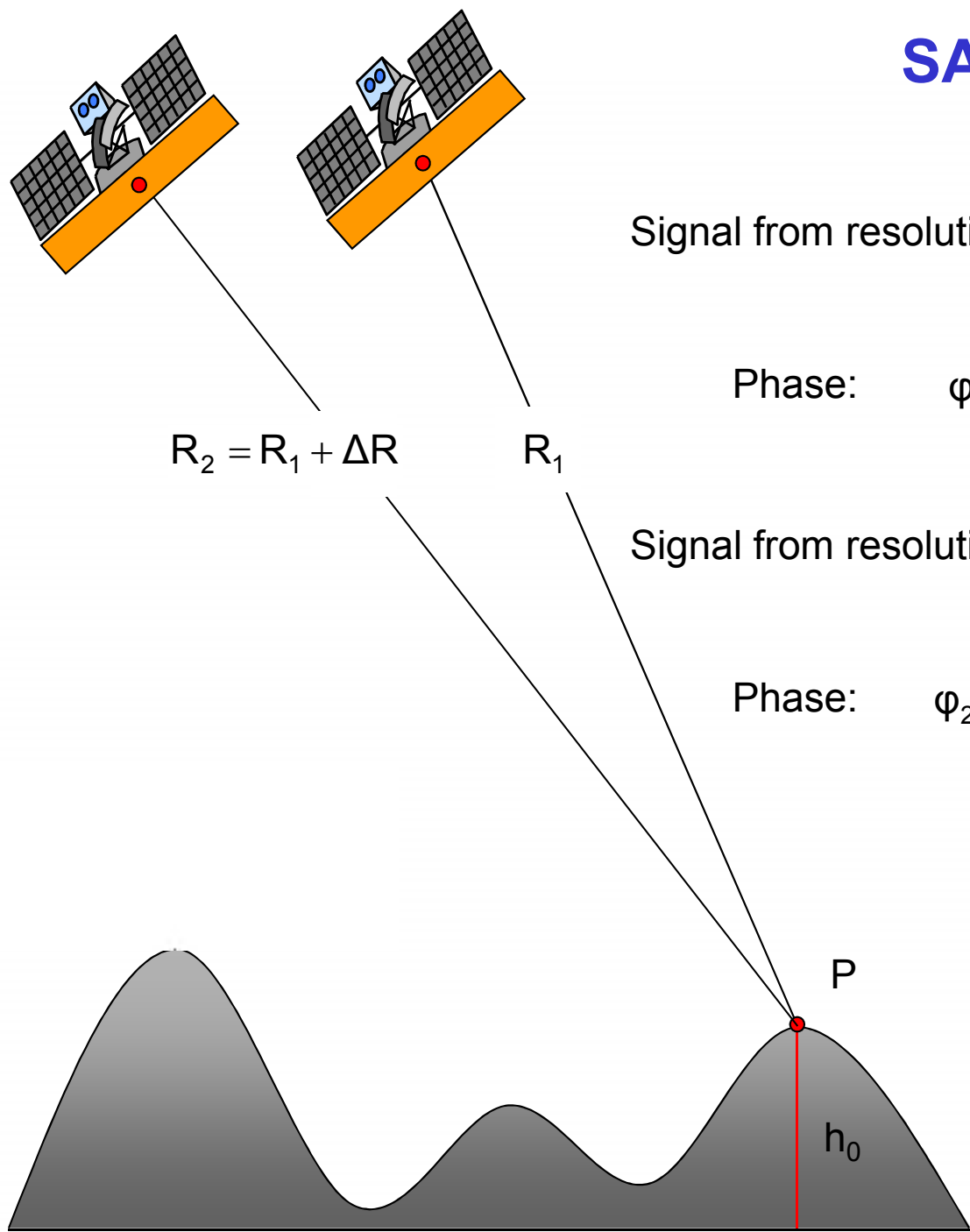


Phase Image 1





SAR Imaging



Signal from resolution cell P in Image 1: $i_1 = |i_1| \exp[-i(2\frac{2\pi}{\lambda}R_1) + \varphi_{s1}]$

Phase: $\varphi_1 = \arg(i_1) = (2\frac{2\pi}{\lambda}R_1) + \varphi_{s1}$

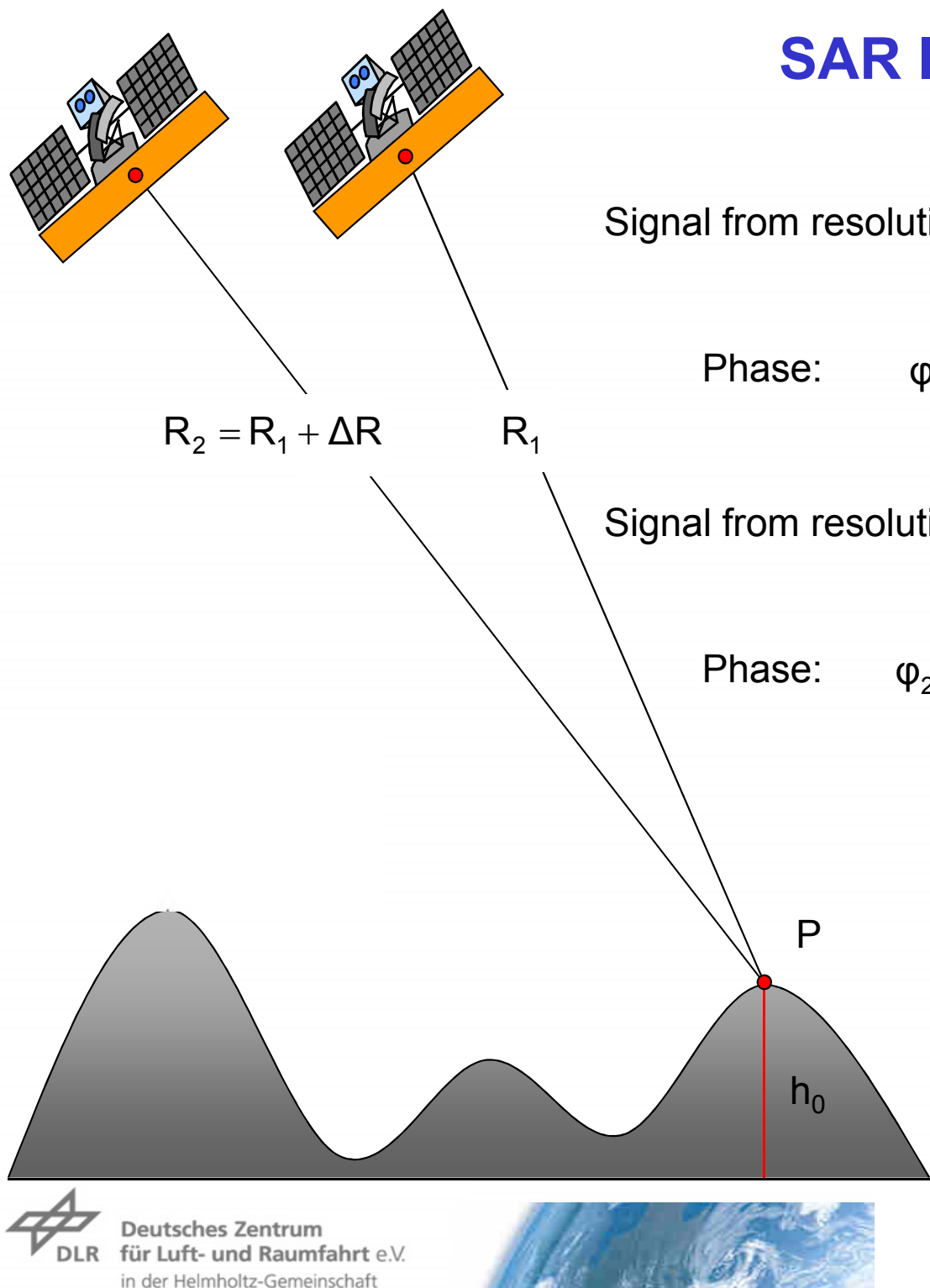
Signal from resolution cell P in Image 2: $i_2 = |i_2| \exp[-i(2\frac{2\pi}{\lambda}R_2) + \varphi_{s2}]$

Phase: $\varphi_2 = \arg(i_2) = (2\frac{2\pi}{\lambda}R_2) + \varphi_{s2}$





SAR Interferometry



Signal from resolution cell P in Image 1: $i_1 = |i_1| \exp[-i(2\frac{2\pi}{\lambda}R_1) + \varphi_{s1}]$

Phase: $\varphi_1 = \arg(i_1) = (2\frac{2\pi}{\lambda}R_1) + \boxed{\varphi_{s1}}$

Signal from resolution cell P in Image 2: $i_2 = |i_2| \exp[-i(2\frac{2\pi}{\lambda}R_2) + \varphi_{s2}]$

Phase: $\varphi_2 = \arg(i_2) = (2\frac{2\pi}{\lambda}R_2) + \boxed{\varphi_{s2}}$



Assuming $\varphi_{s1} = \varphi_{s2}$!!!

Interferogram: $i_1 i_2^* = |i_1 i_2^*| \exp[-i(2\frac{2\pi}{\lambda}\Delta R)]$

Phase: $\Phi_{int} = \frac{\text{Re}\{i_1 i_2^*\}}{\text{Im}\{i_1 i_2^*\}} = \boxed{2\frac{2\pi}{\lambda}\Delta R}$

Deterministic !!!

ERS – Bachu / China ~ 100 km × 80 km



Amplitude Image 1



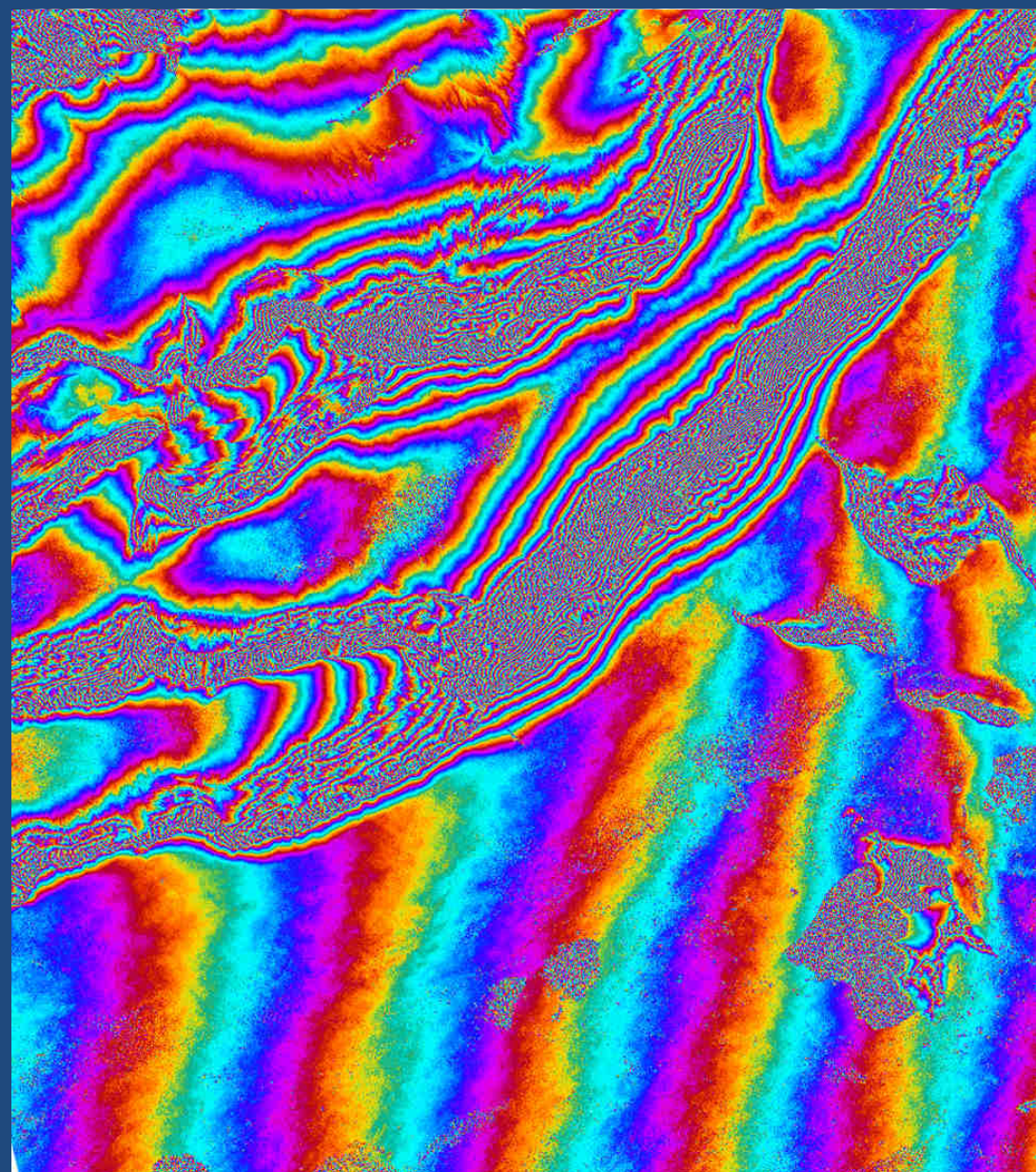
Amplitude Image 2



ERS – Bachu / China $\sim 100 \text{ km} \times 80 \text{ km}$

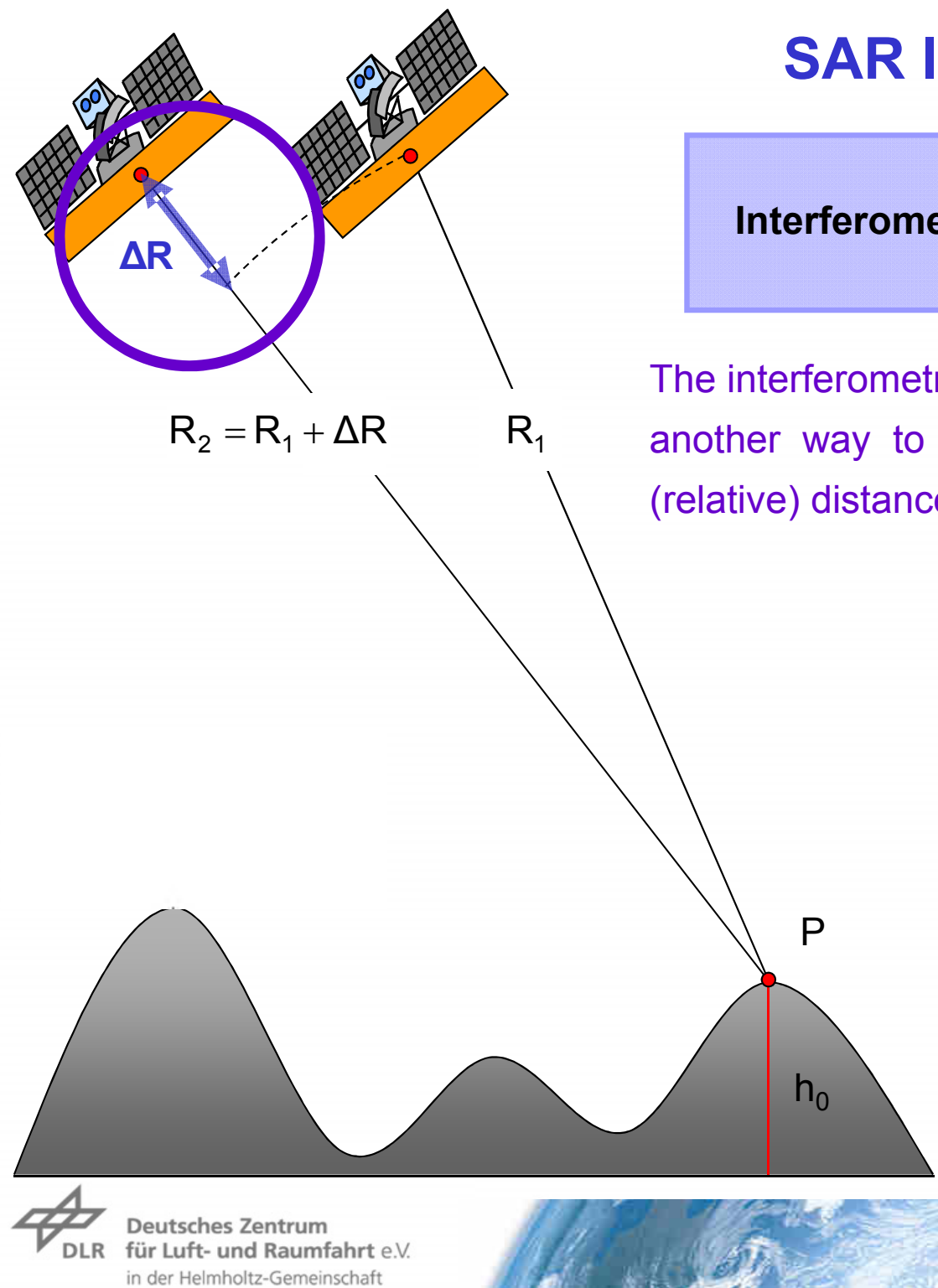


Amplitude Image 1



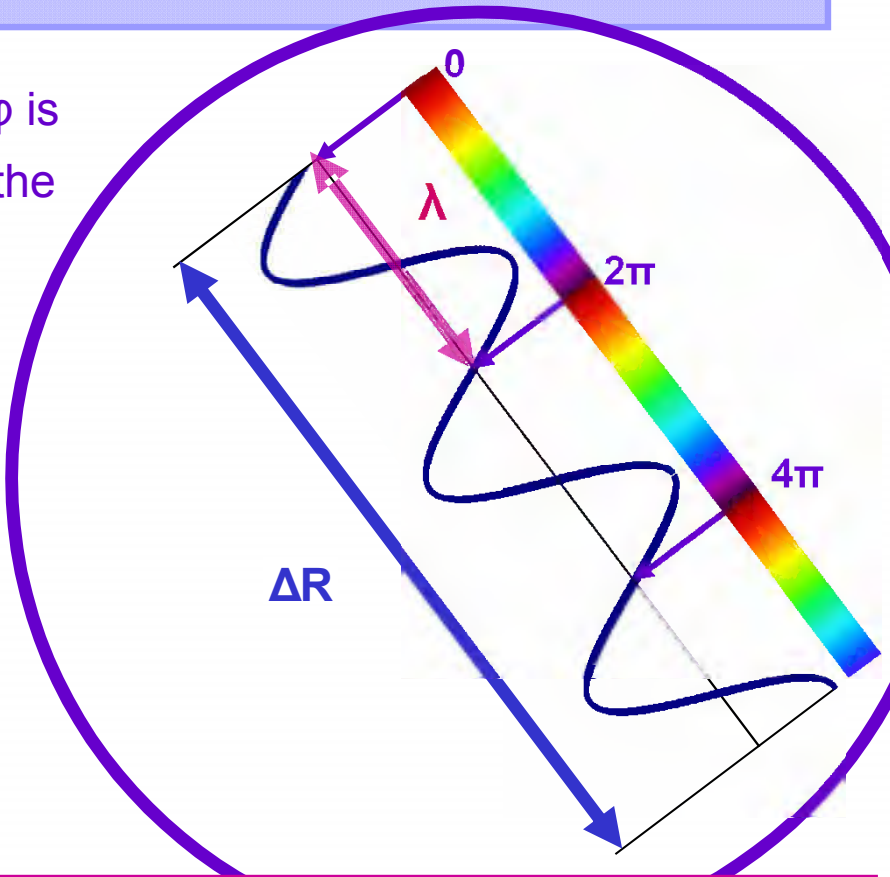
Interferometric Phase Image

SAR Interferometry



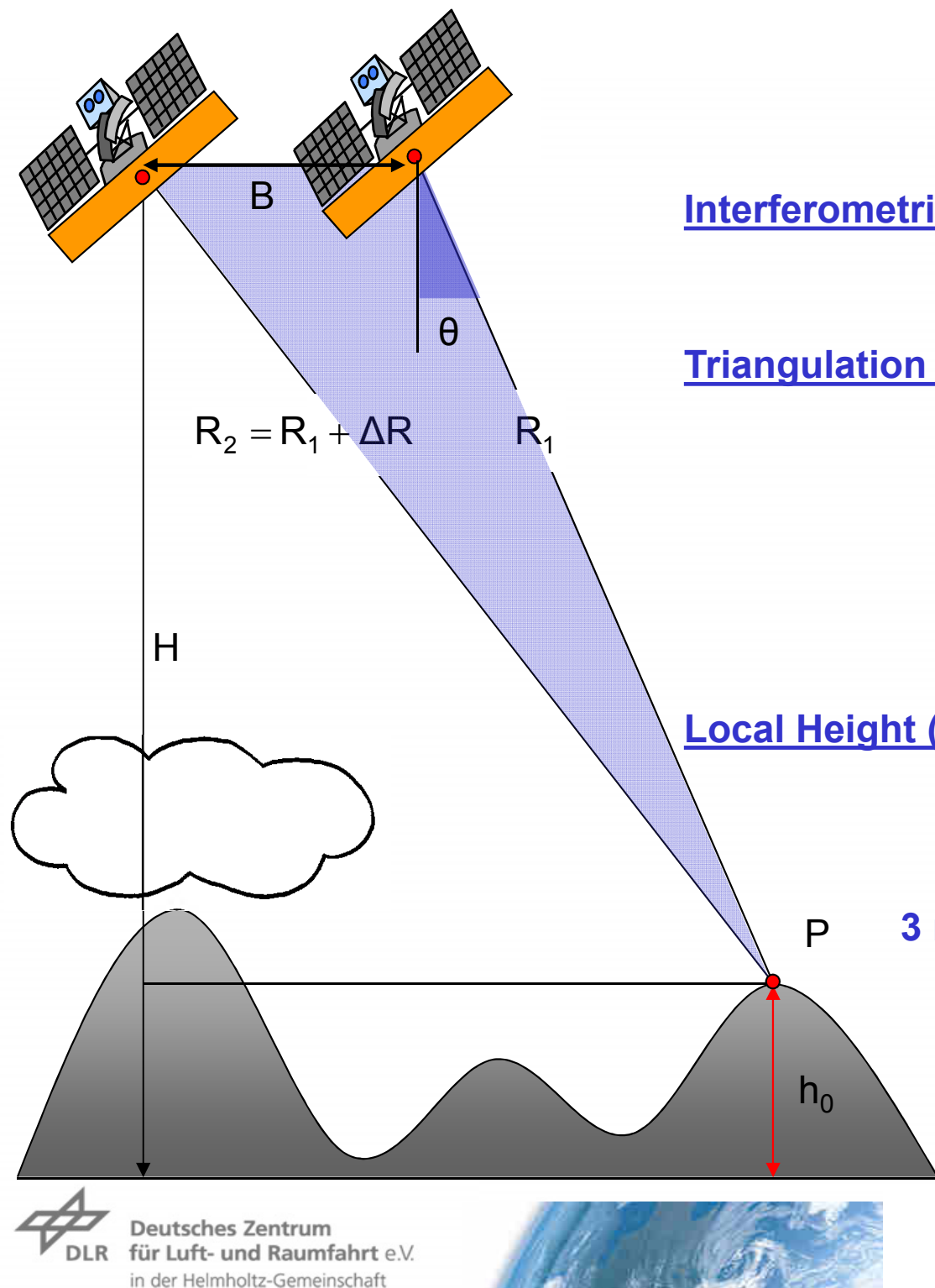
$$\text{Interferometric Phase: } \varphi = 2\frac{2\pi}{\lambda} \boxed{\Delta R}$$

The interferometric phase φ is another way to measure the (relative) distance Δr :



Phase measurements in interferometric systems can be made with a degree level accuracy. At radar wavelengths of 1-90cm (Ku to P-band) this corresponds to millimeter accuracy !!!

DEM Generation



Interferometric Phase (1): $\varphi = 2\frac{2\pi}{\lambda} \Delta R + 2\pi N \quad N = 0, \pm 1, \pm 2$

Triangulation (2): $(R_1 + \Delta R)^2 = R_1^2 + B^2 - 2R_1B \cos(\pi/2 + \theta) \rightarrow$

$$\rightarrow \sin(\theta) = \frac{(R_1 + \Delta R)^2 - R_1^2 - B^2}{2R_1B}$$

Local Height (3): $h_0 = H - (R_1 + \Delta R) \cos(\theta)$



3 non-linear Equations for 3 Unknowns ($h_0, \theta, \Delta R$)

B ... Spatial baseline and

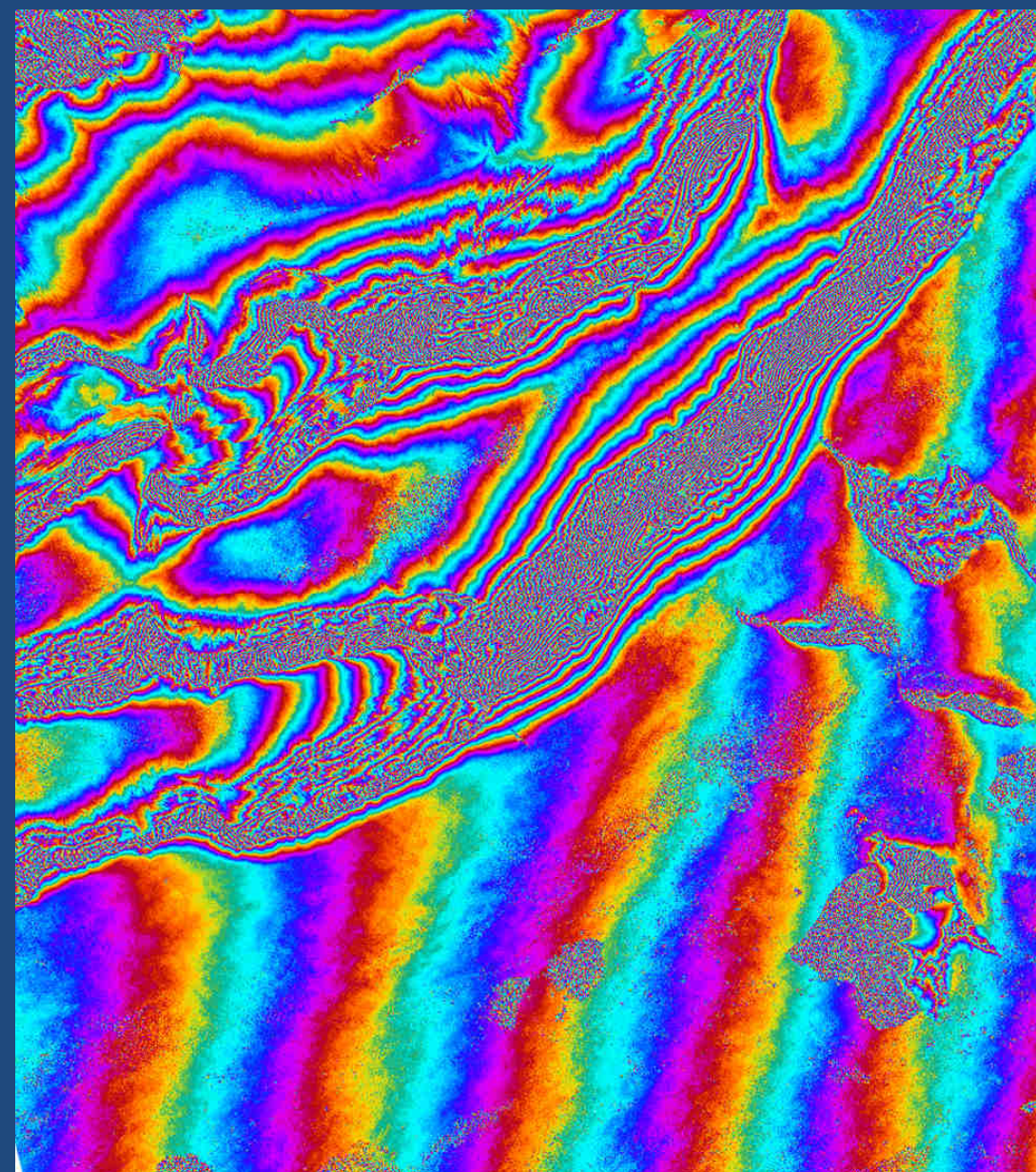
R_1 ... Range distance in Image 1 are known

Critical is the fact that the interferometric phase φ is initially measured modulo 2π ► **Phase Unwrapping**

ERS – Bachu / China $\sim 100 \text{ km} \times 80 \text{ km}$



Amplitude Image 1

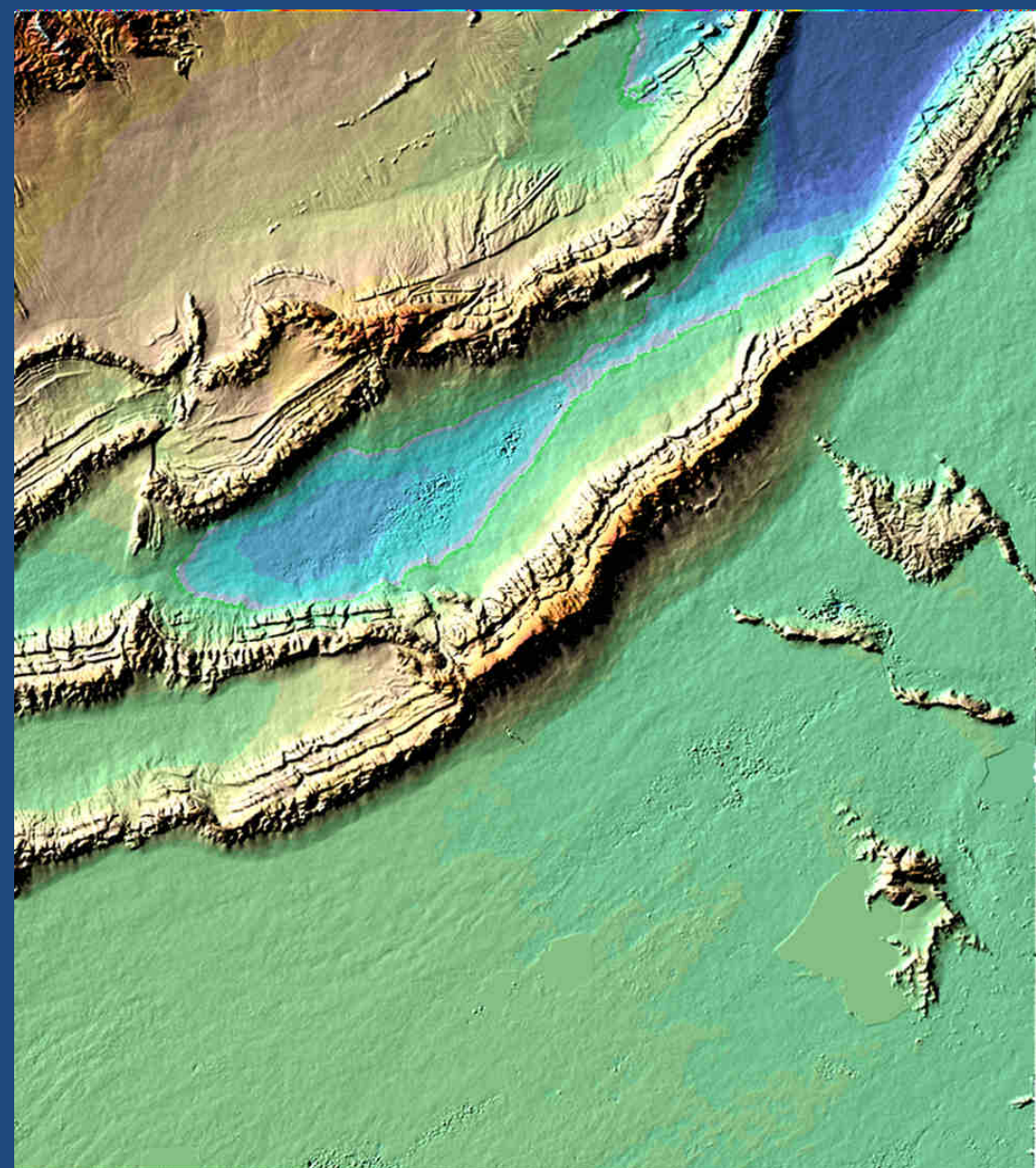


Interferometric Phase Image

ERS – Bachu / China ~ 100 km × 80 km



Amplitude Image



Digital Elevation Model with false colors

Interferometric SAR Implementations: Single vs. Repeat-Pass

Single-Pass or Simultaneous Interferometry

The two acquisitions are performed simultaneously
(Zero temporal baseline)



Single Platform
with two antennas

Two Platforms
flying in (close) formation

Repeat-Pass Interferometry

The two acquisitions are performed at different times
(Non-Zero temporal baseline)



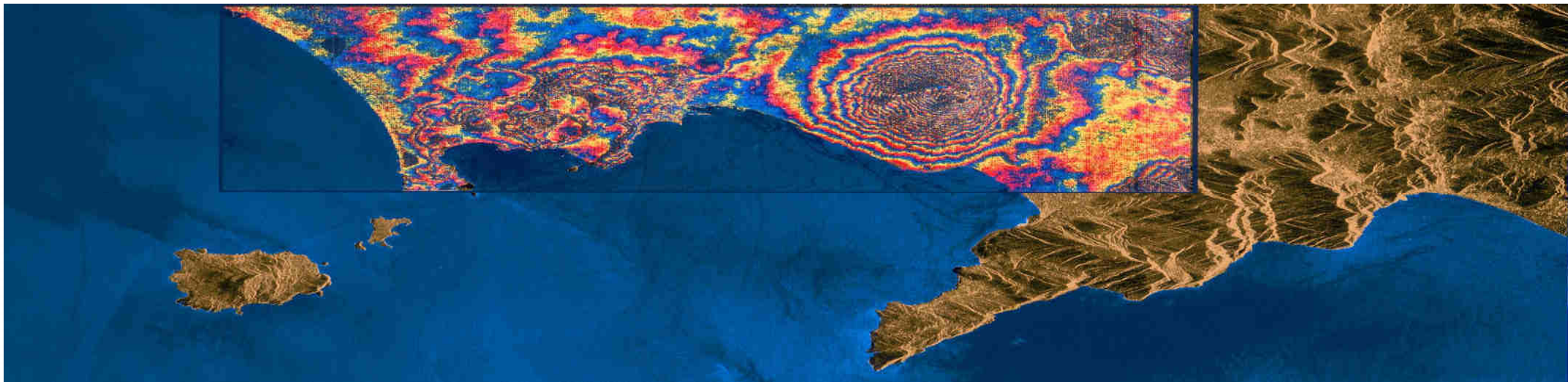
Single Platform
in repeated orbit(s)
or
Two Platforms
flying on the same orbit



European Remote Sensing Satellite (ERS-1)



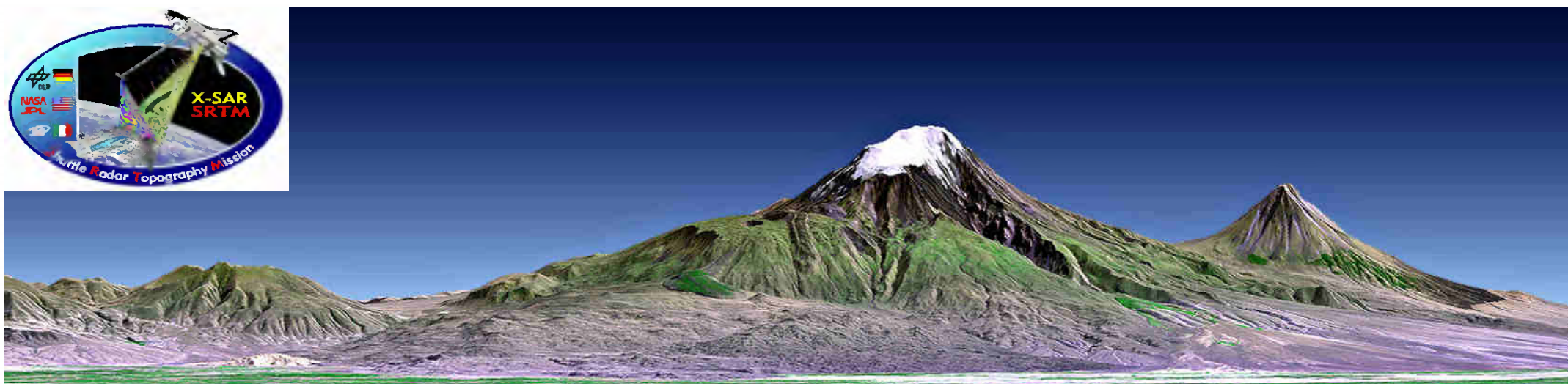
Launch	July 17, 1991
Duration	~9 years (+ March 10, 2000)
Orbit	~782 km / 35 Days
Height Accuracy	4-8 m (flat terrain)
	8-30 m (moderate relief)
Horizontal Resolution	25 m x 25 m
Coverage	Global
Wavelength	C-Band (5.6 cm)



Shuttle Radar Topography Mission (SRTM)



Launch	Feb 11, 2000
Duration	11 days
Altitude	~233 km
Height Accuracy	6 m (relative)
	16 m (absolute)
Horizontal Resolution	30 m x 30 m
Coverage	-56° to + 60° (80%)
Wavelength	5.6 cm + 3.1 cm



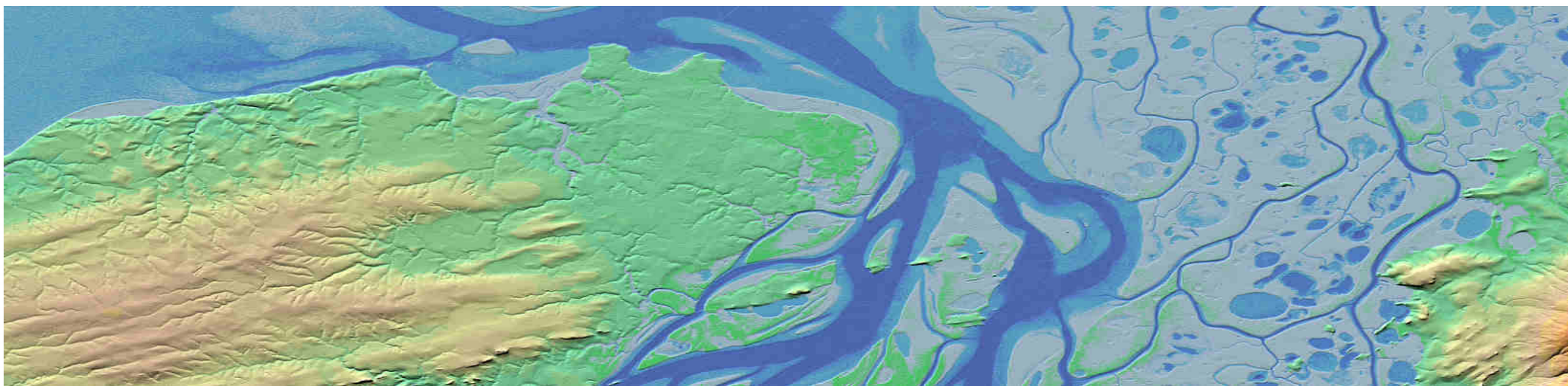
Deutsches Zentrum
für Luft- und Raumfahrt e.V.
in der Helmholtz-Gemeinschaft



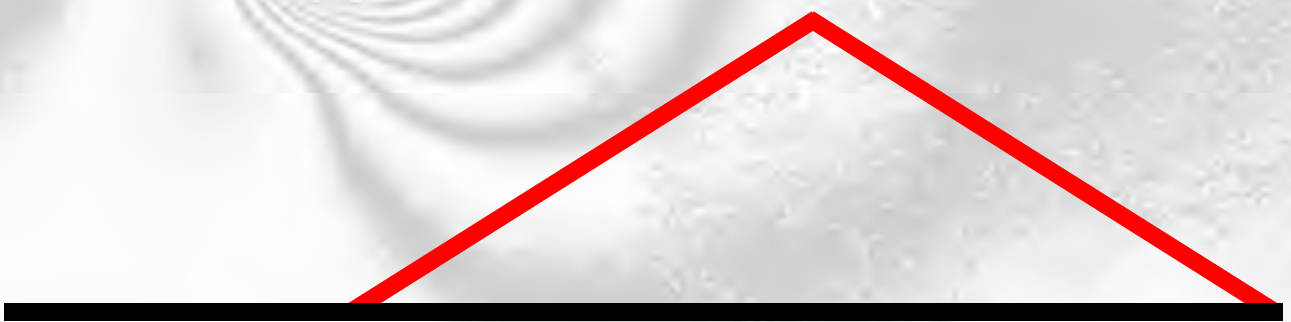
TanDEM-X: TerraSAR add-on for Digital Elevation Measurements

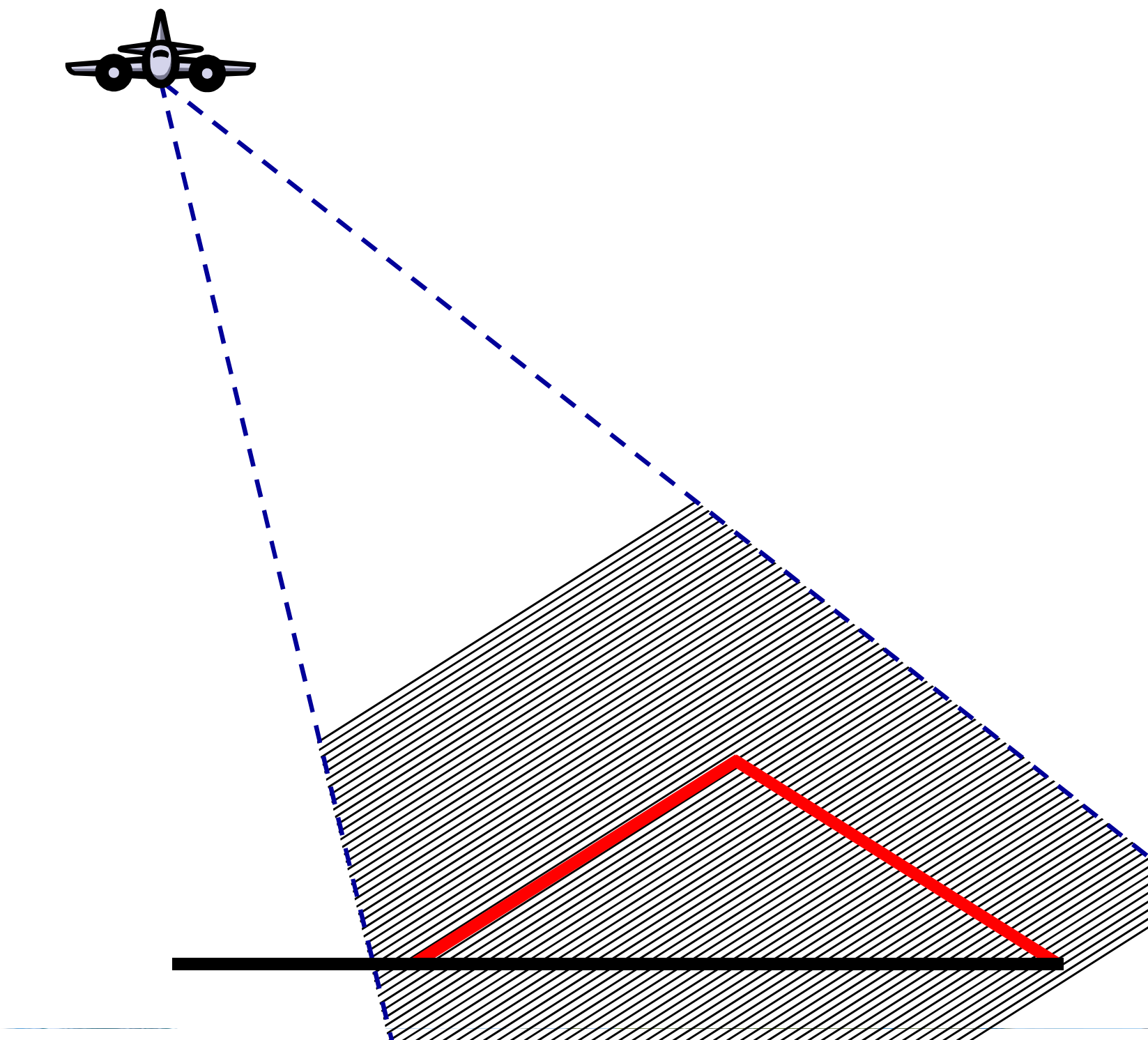


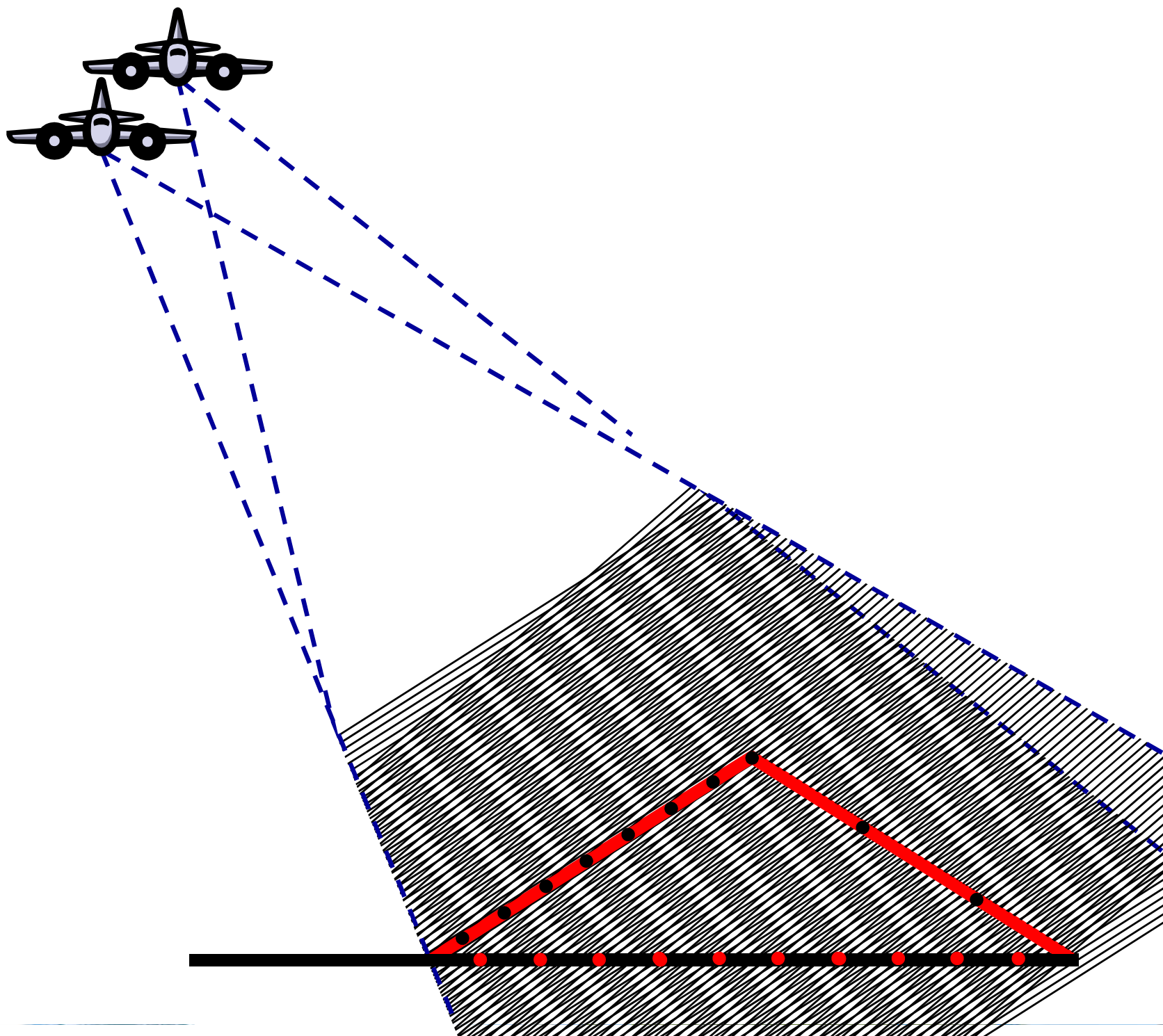
Launch	21 June 2010
Duration	3 Years
Orbit	514 km
Height Accuracy	2 m (relative)
	4 m (absolute)
Horizontal Resolution	12 m x 12 m
Coverage	Global (100%)
Wavelength	3.1 cm (X-band)

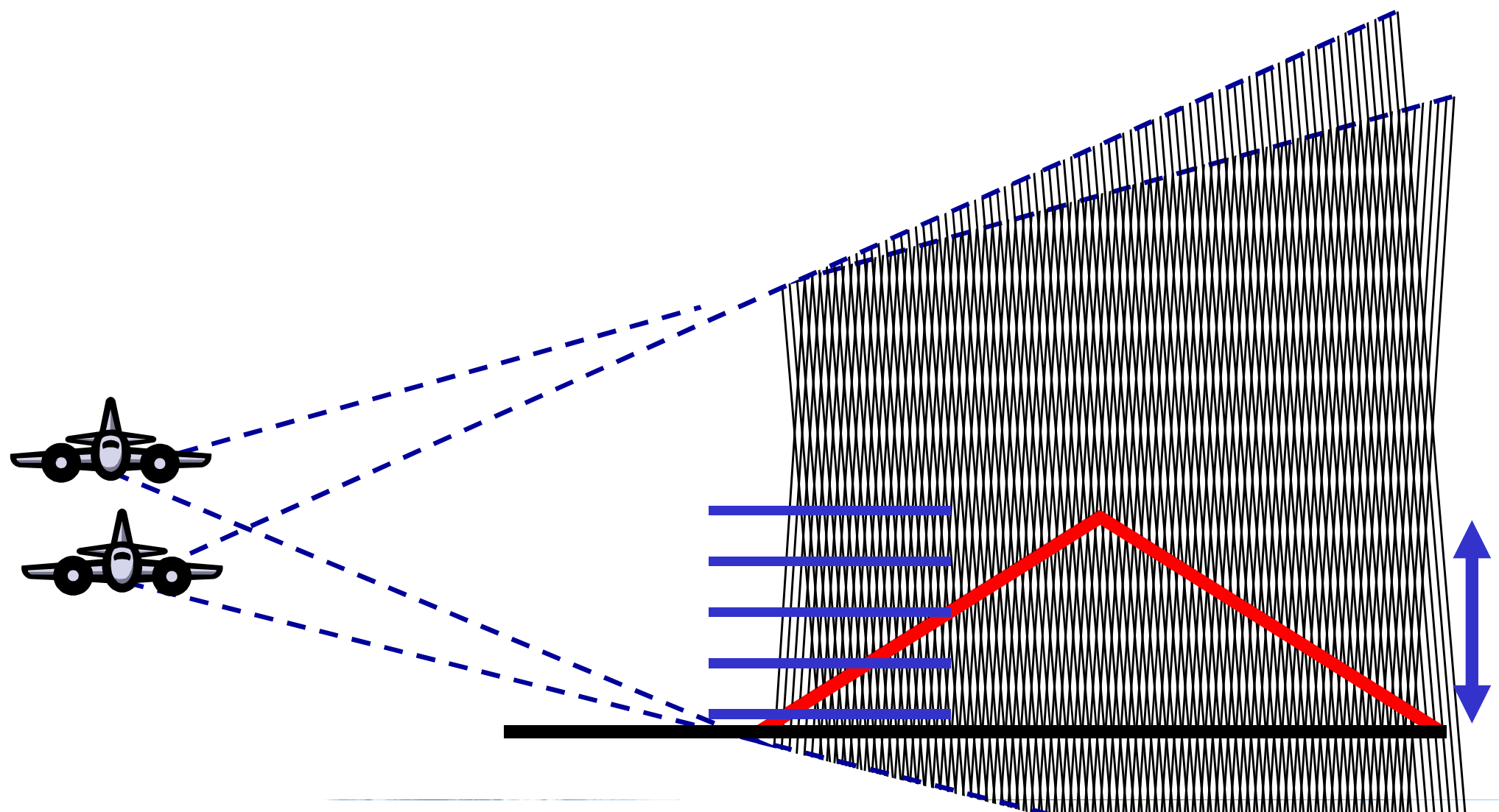


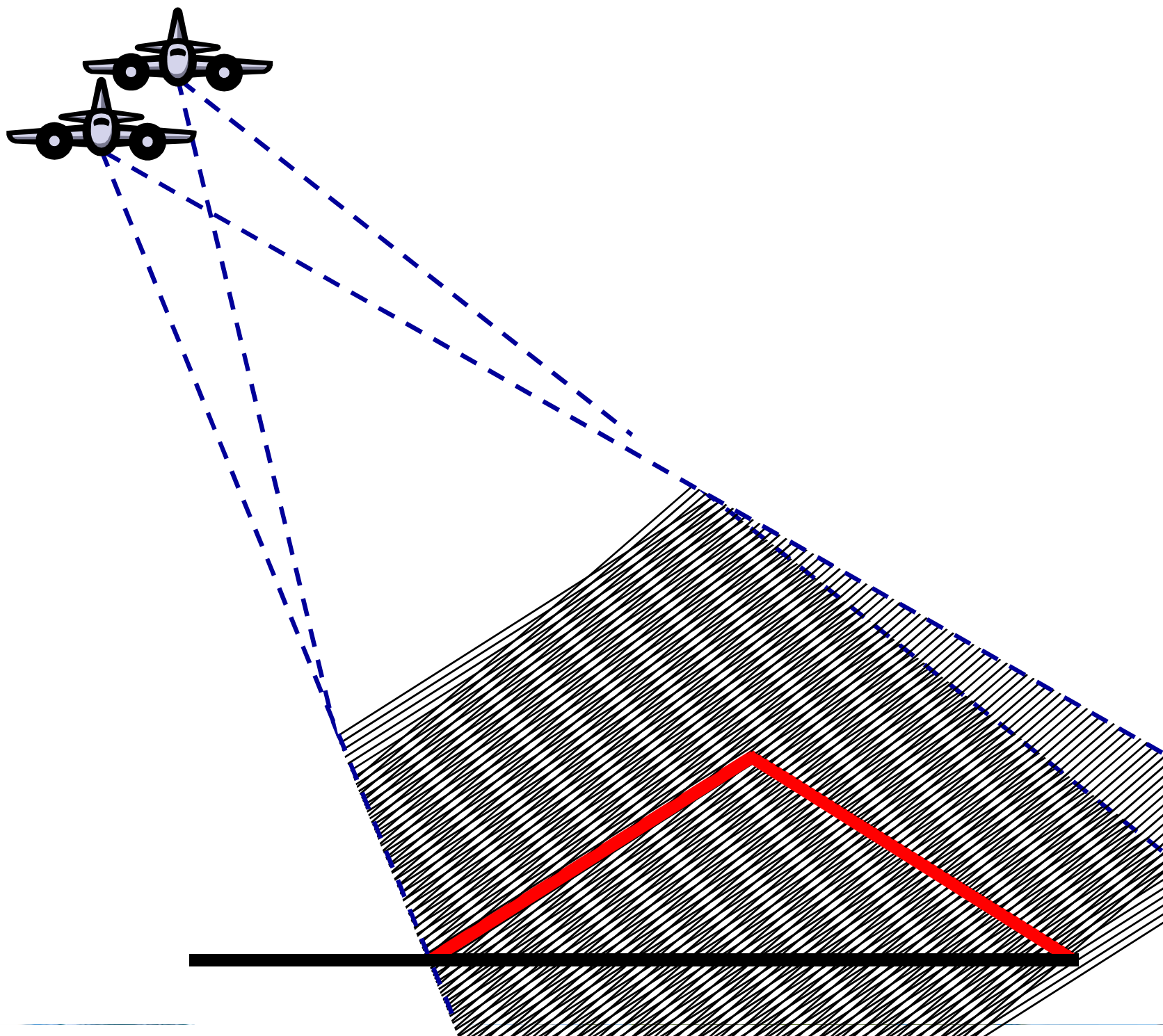
SAR Interferometry (InSAR)

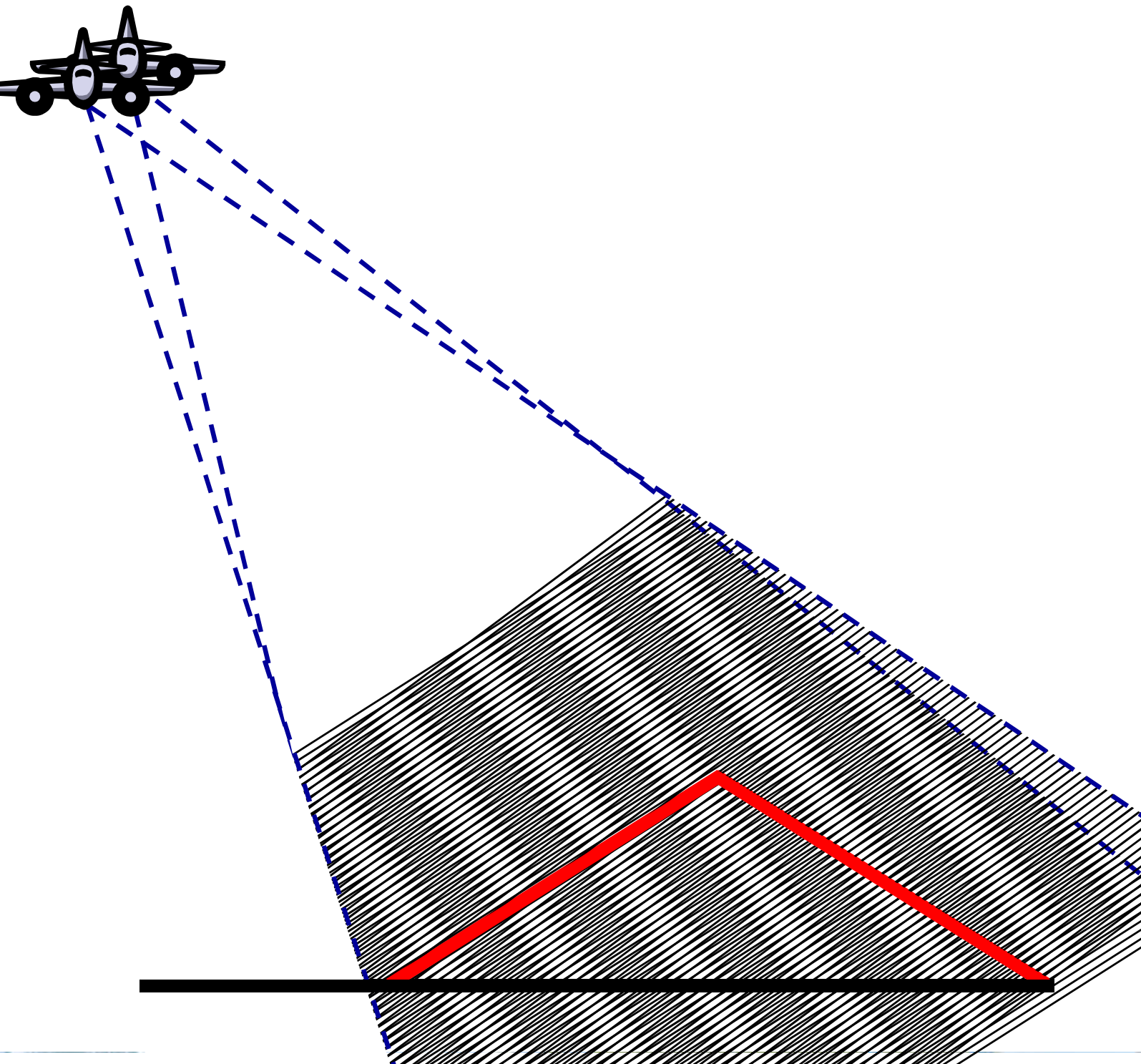


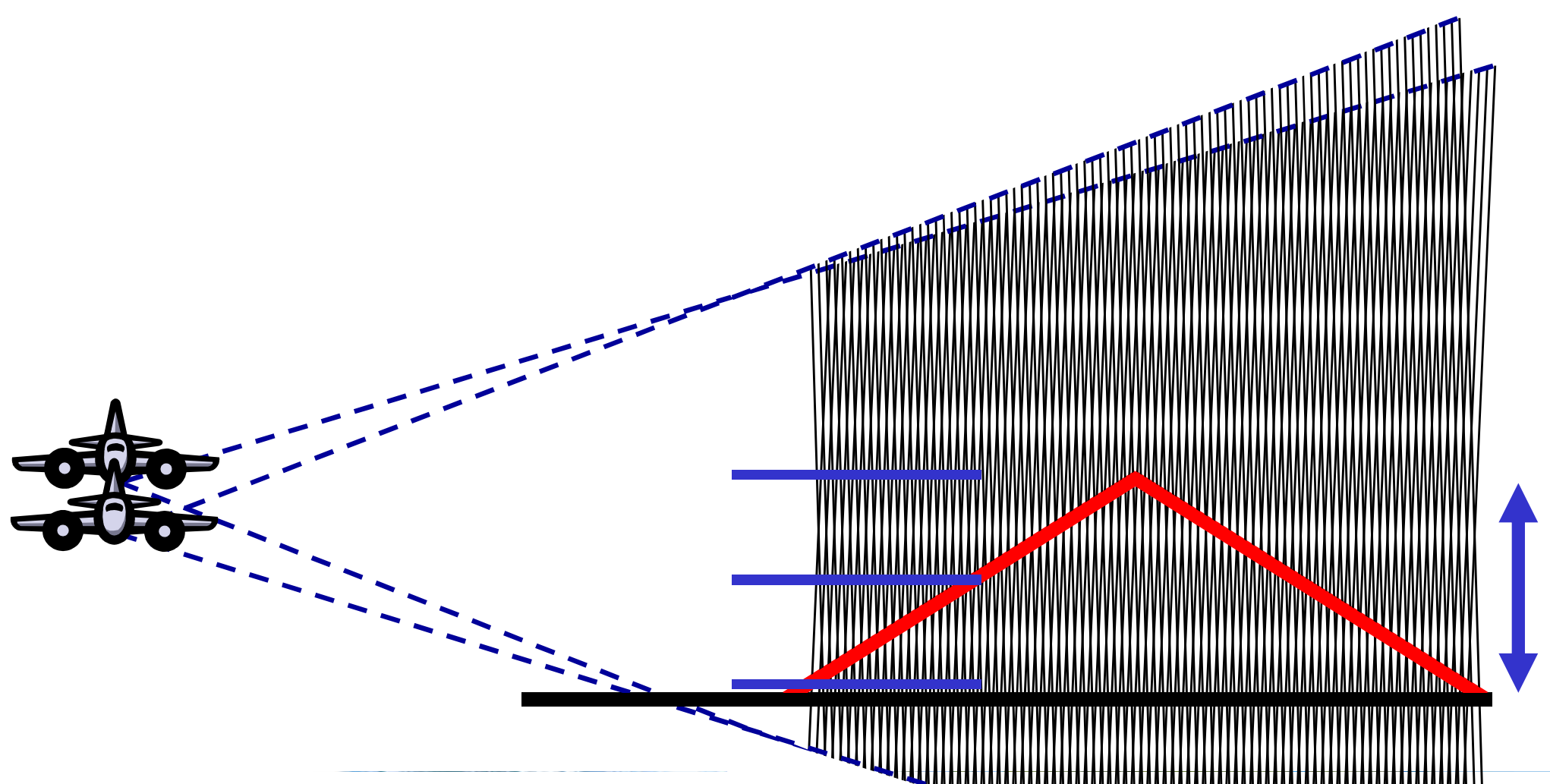




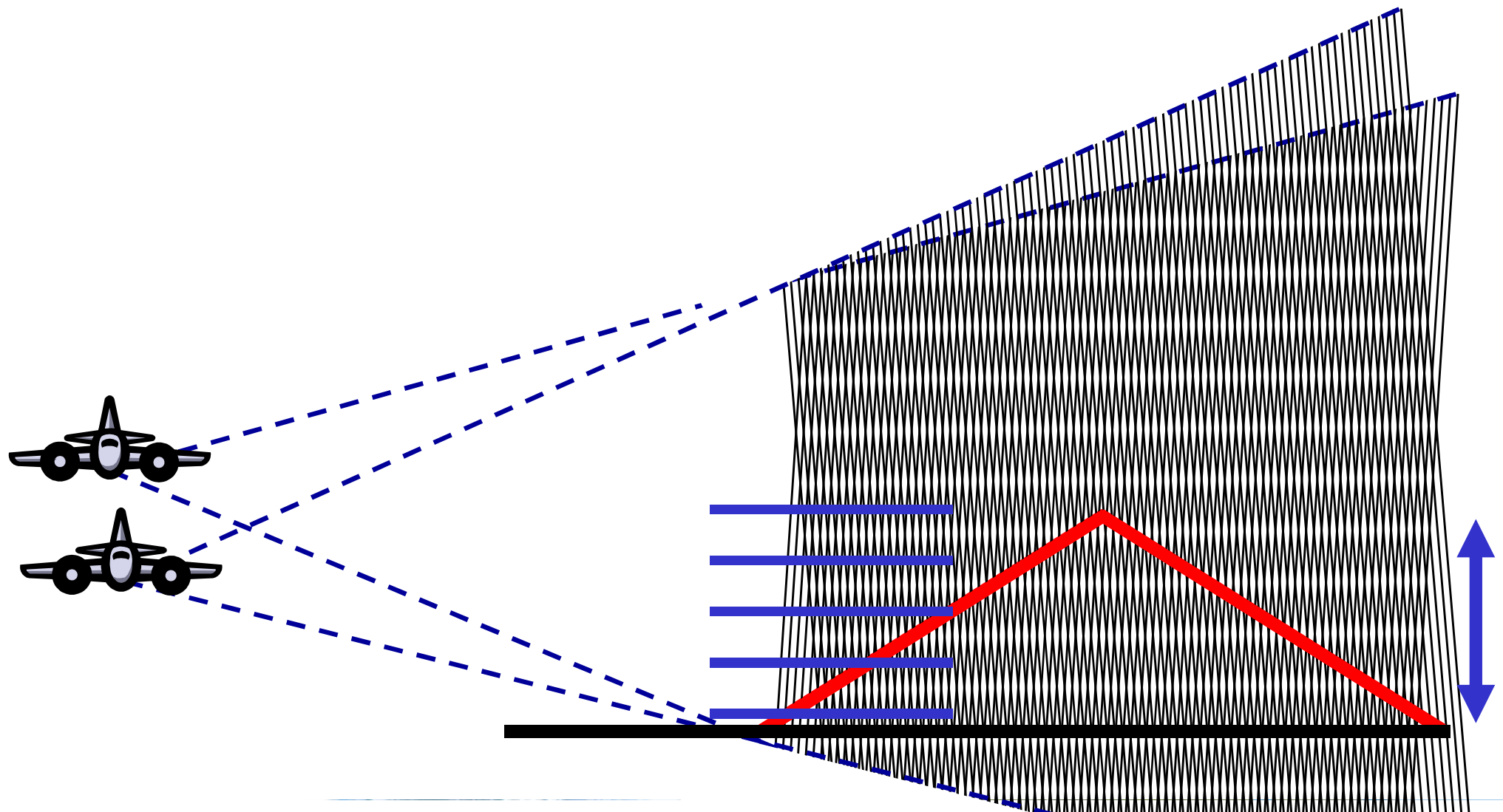








The Phase-to-Height Sensitivity increases with increasing the spatial baseline (i.e. $\Delta\theta$ or B_{\perp});





Interferometric Coherence

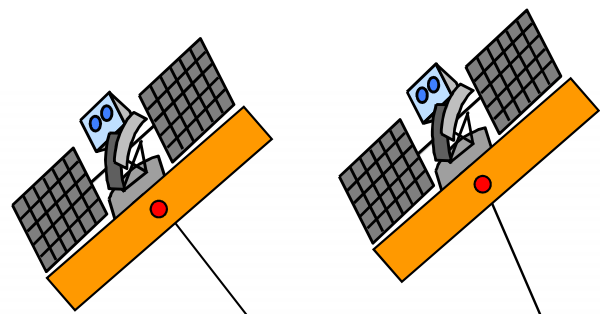


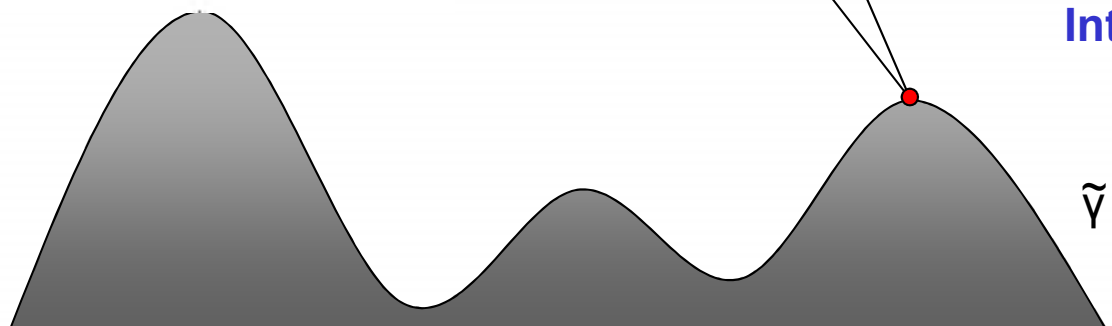
Image 1: $i_1 = |i_1| \exp[-i(2\frac{2\pi}{\lambda}R_1) + \phi_{S1}]$

Image 2: $i_2 = |i_2| \exp[-i(2\frac{2\pi}{\lambda}R_2) + \phi_{S2}]$

Interferometric Coherence: Normalised complex correlation coefficient

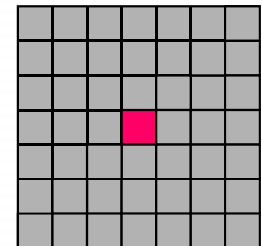
$$\tilde{\gamma} = \frac{E\{ i_1 i_2^* \}}{\sqrt{E\{ i_1 i_1^* \} E\{ i_2 i_2^* \}}} = \frac{|E\{ i_1 i_2^* \}| \exp(i\varphi)}{\sqrt{E\{ |i_1|^2 \} E\{ |i_2|^2 \}}}$$

$$0 \leq |\tilde{\gamma}| \leq 1$$



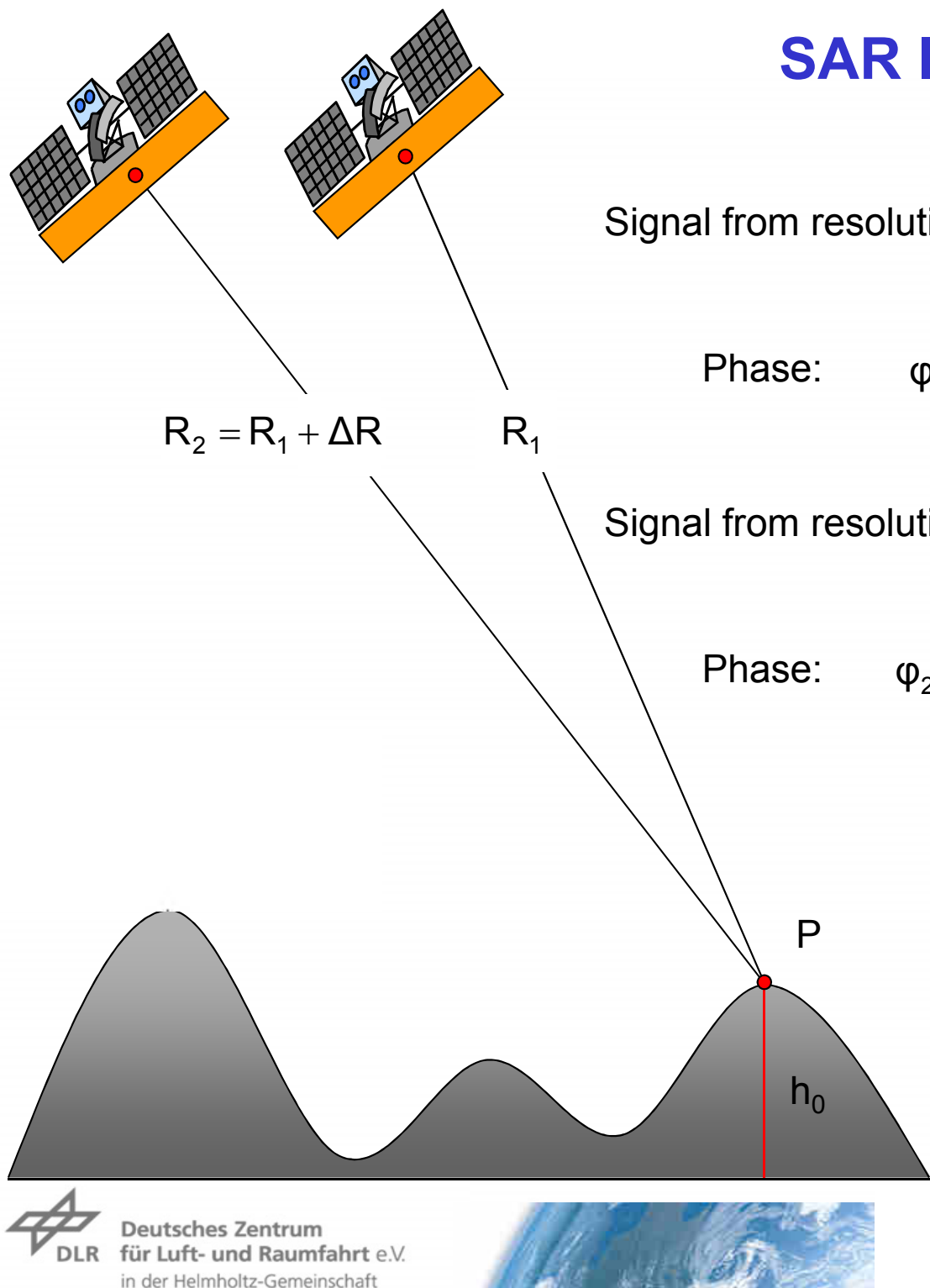
Interferometric Coherence Estimation:

$$\tilde{\gamma} = \frac{\sum_w i_1[i,j] i_2^*[i,j]}{\sqrt{\sum_w |i_1[i,j]|^2 \sum_w |i_2[i,j]|^2}} = \frac{\langle i_1 i_2^* \rangle}{\sqrt{\langle i_1 i_1^* \rangle \langle i_2 i_2^* \rangle}}$$





SAR Interferometry



Signal from resolution cell P in Image 1: $i_1 = |i_1| \exp[-i(2\frac{2\pi}{\lambda}R_1) + \varphi_{S1}]$

Phase: $\varphi_1 = \arg(i_1) = (2\frac{2\pi}{\lambda}R_1) + \boxed{\varphi_{S1}}$

Signal from resolution cell P in Image 2: $i_2 = |i_2| \exp[-i(2\frac{2\pi}{\lambda}R_2) + \varphi_{S2}]$

Phase: $\varphi_2 = \arg(i_2) = (2\frac{2\pi}{\lambda}R_2) + \boxed{\varphi_{S2}}$



Assuming $\varphi_{S1} = \varphi_{S2}$!!!

Interferogram: $i_1 i_2^* = |i_1 i_2^*| \exp[-i(2\frac{2\pi}{\lambda}\Delta R)]$

Phase: $\Phi_{Int} = \frac{\text{Re}\{i_1 i_2^*\}}{\text{Im}\{i_1 i_2^*\}} = \boxed{2\frac{2\pi}{\lambda}\Delta R}$

Deterministic !!!



Interferometric Coherence

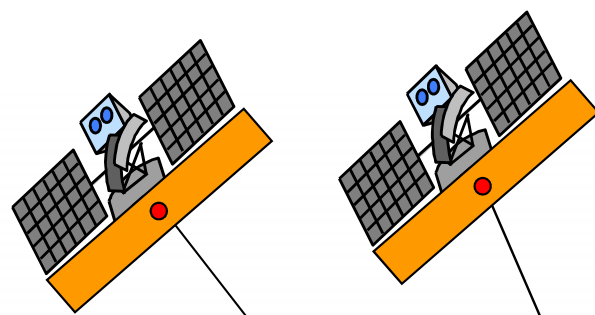


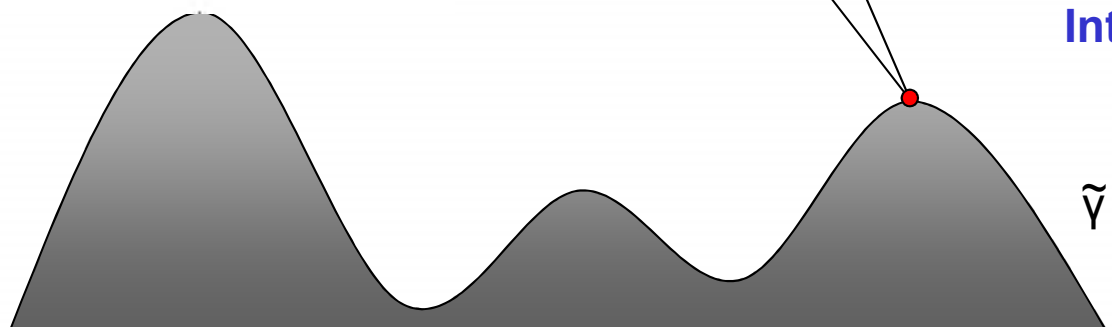
Image 1: $i_1 = |i_1| \exp[-i(2\frac{2\pi}{\lambda}R_1) + \phi_{s1}]$

Image 2: $i_2 = |i_2| \exp[-i(2\frac{2\pi}{\lambda}R_2) + \phi_{s2}]$

Interferometric Coherence: Normalised Complex Correlation Coefficient

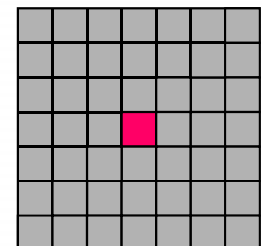
$$\tilde{\gamma} = \frac{E\{ i_1 i_2^* \}}{\sqrt{E\{ i_1 i_1^* \} E\{ i_2 i_2^* \}}} = \frac{|E\{ i_1 i_2^* \}| \exp(i\varphi)}{\sqrt{E\{ |i_1|^2 \} E\{ |i_2|^2 \}}}$$

$$0 \leq |\tilde{\gamma}| \leq 1$$



Interferometric Coherence Estimation:

$$\tilde{\gamma} = \frac{\sum_w i_1[i,j] i_2^*[i,j]}{\sqrt{\sum_w |i_1[i,j]|^2 \sum_w |i_2[i,j]|^2}} = \frac{\langle i_1 i_2^* \rangle}{\sqrt{\langle i_1 i_1^* \rangle \langle i_2 i_2^* \rangle}}$$



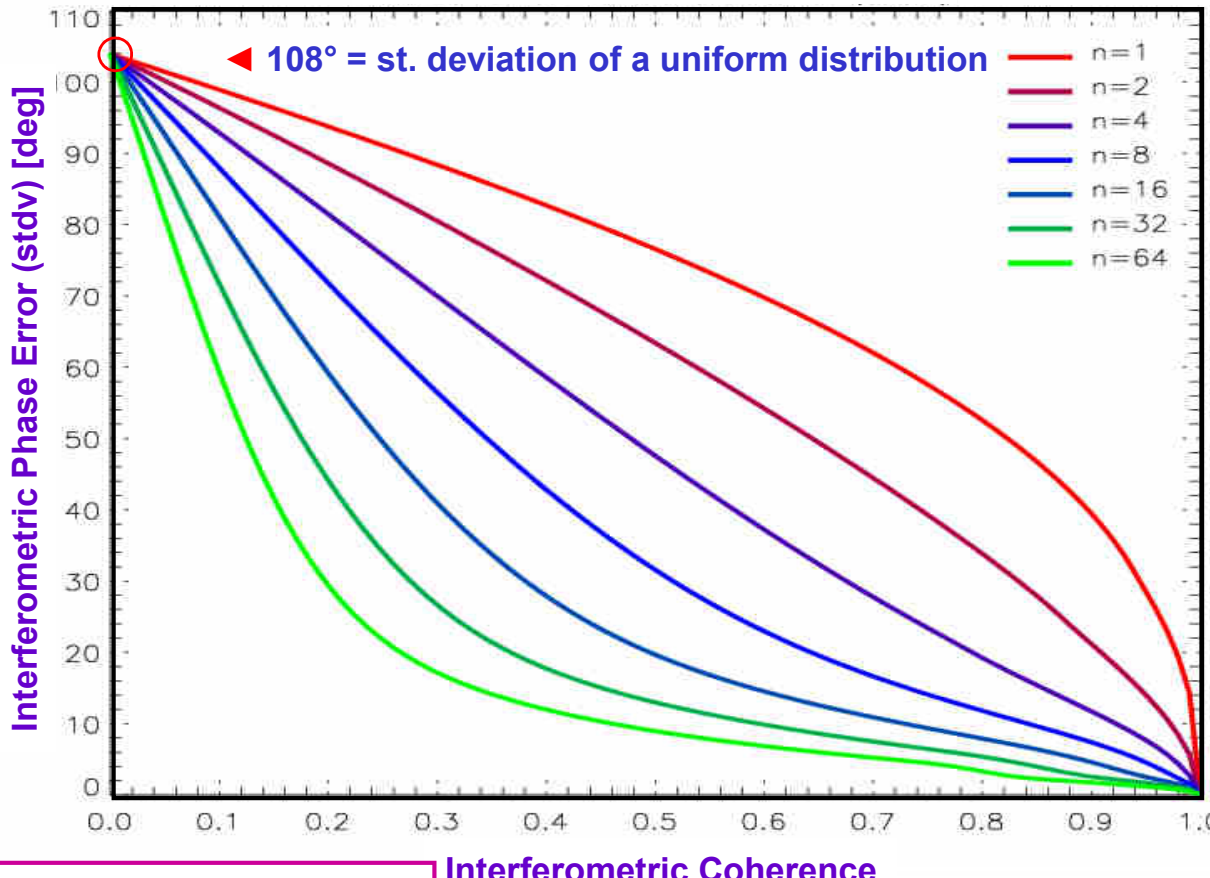
Interferometric coherence

... as a Measure of Interferogram Quality:

Standard Deviation of the InSAR Phase ϕ :

$$\sigma_\phi = \sqrt{\int_{-\pi}^{\pi} \phi^2 \text{pdf}(\phi) \cdot d\phi}$$

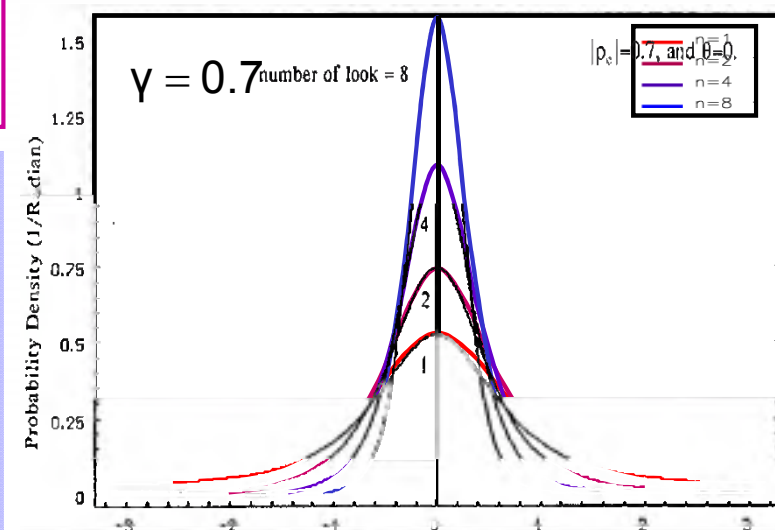
depends on ► the underlying coherence &
► the number of looks N.



A increase in decorrelation (= loss in coherence) is associated with an increase in the phase variance;
► Increased phase variance leads to increased height errors.

where: $\text{pdf}(\phi, \gamma, N) = \frac{\Gamma(N + 1/2)(1 - |\gamma|^2)^2 \beta}{2\sqrt{\pi}\Gamma(N)(1 - \beta^2)^{N+1/2}} + \frac{(1 - |\gamma|^2)^N}{2\pi} F(N, 1; 1/2; \beta^2)$

- F is a Gauss hypergeometric function and $\beta = |\gamma| \cos(\phi - \bar{\phi})$
- N is the number of Looks

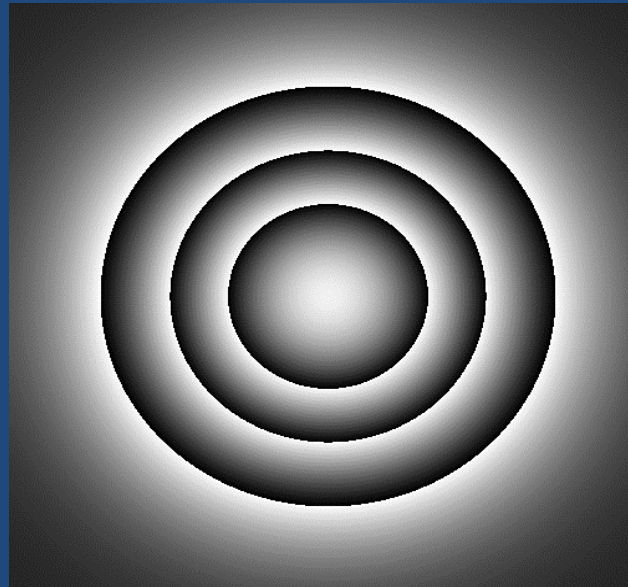


Interferometric Phase Images

Simulation

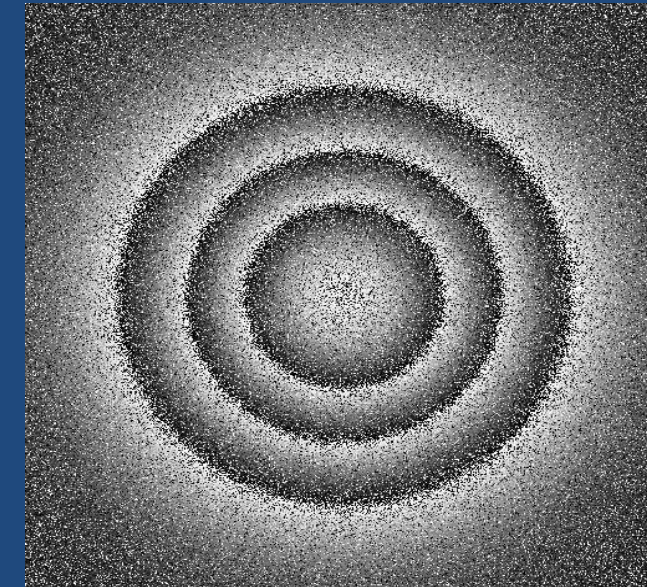


Absolute Phase



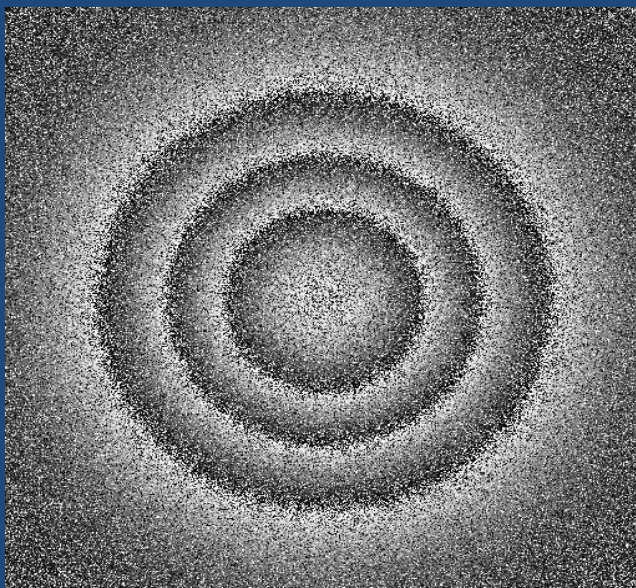
Coherence=1.0

Looks=1



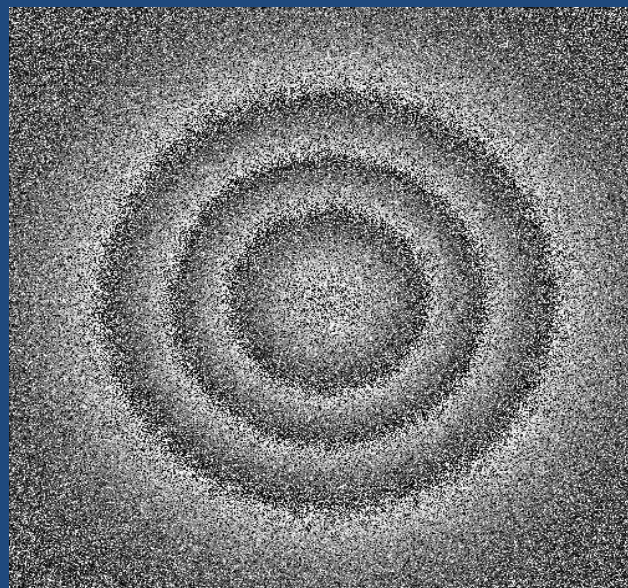
Coherence=0.8

Looks=1



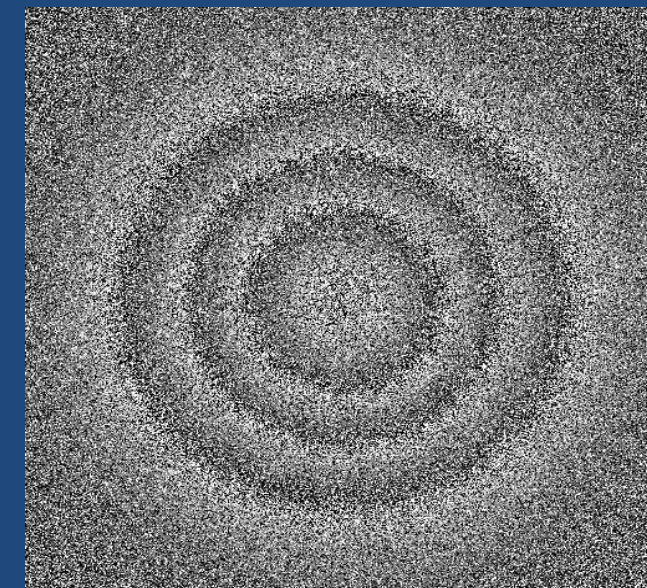
Coherence=0.6

Looks=1



Coherence=0.4

Looks=1



Coherence=0.2

Looks=1



SAR Interferometry

A (very) short Introduction

Konstantinos P. Papathanassiou

German Aerospace Center (DLR)
Microwaves and Radar Institute (DLR-HR)
Pol-InSAR Research Group

Oberpfaffenhofen, P.O. 1116, D-82234 Wessling
Tel./Fax.: ++49-(0)8153-28-2367/1149
Email: kostas.papathanassiou@dlr.de

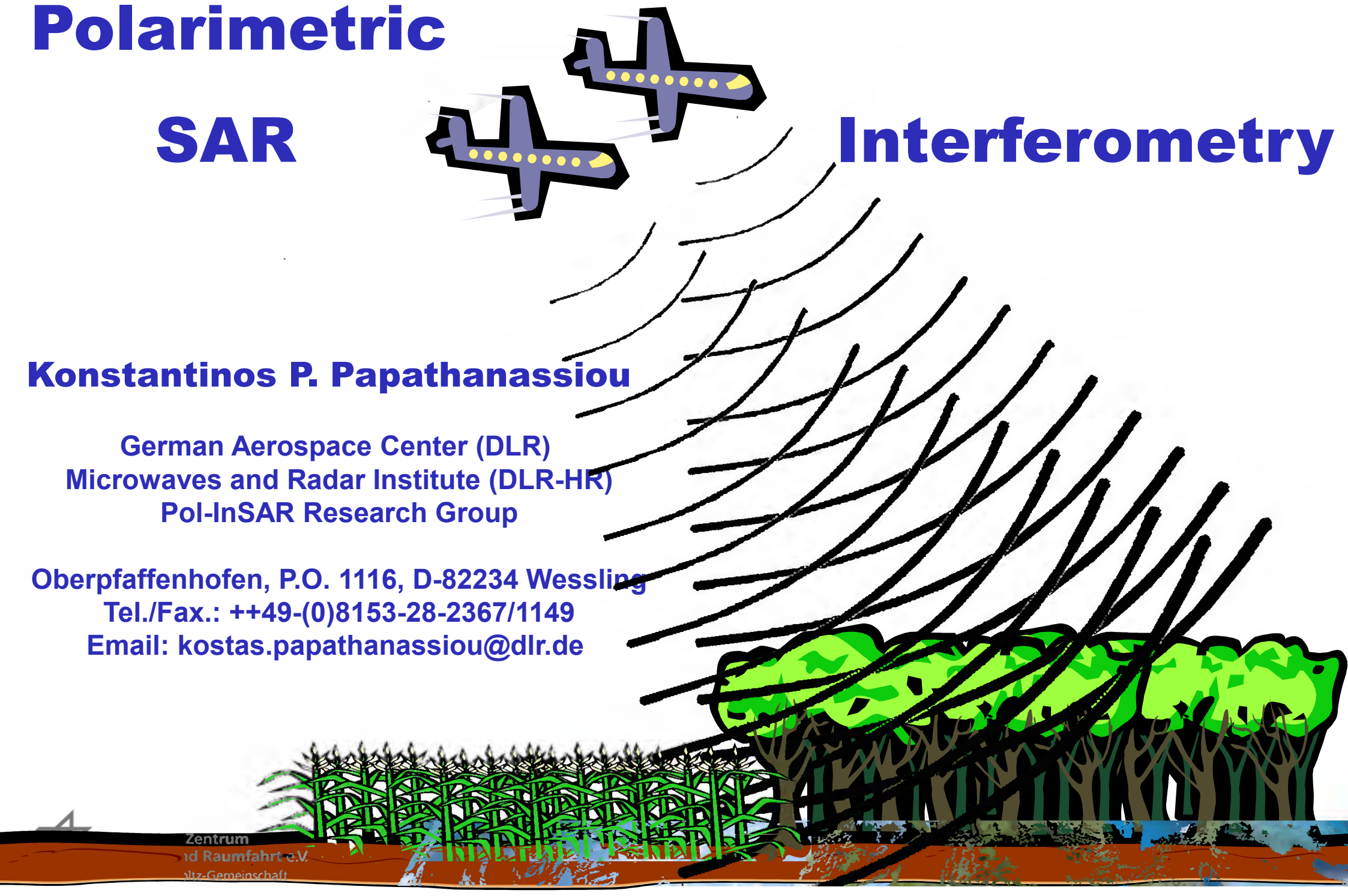
Polarimetric SAR

Interferometry

Konstantinos P. Papathanassiou

German Aerospace Center (DLR)
Microwaves and Radar Institute (DLR-HR)
Pol-InSAR Research Group

Oberpfaffenhofen, P.O. 1116, D-82234 Wessling
Tel./Fax.: ++49-(0)8153-28-2367/1149
Email: kostas.papathanassiou@dlr.de

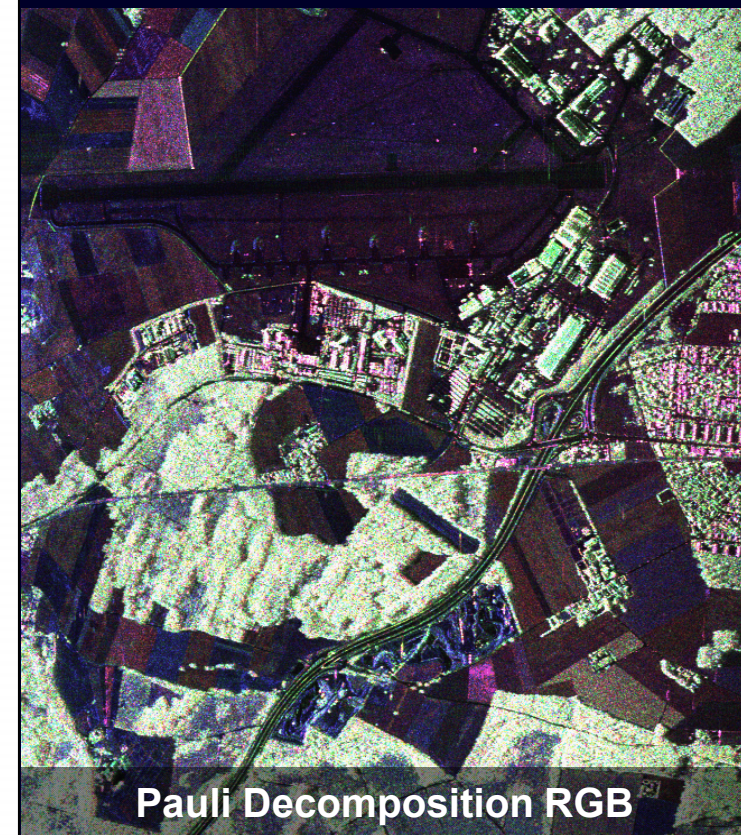


SAR Polarimetry (PolSAR)

Allows the identification / decomposition of different scattering processes occurring inside the resolution cell

SAR Interferometry (InSAR)

Allows the location of the effective scattering center inside the resolution cell



Pauli Decomposition RGB



VV Channel Image



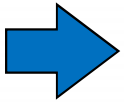
InSAR DEM

Polarimetric SAR Interferometry (Pol-InSAR)

Potential to separate in height different scattering processes occurring inside the resolution cell.

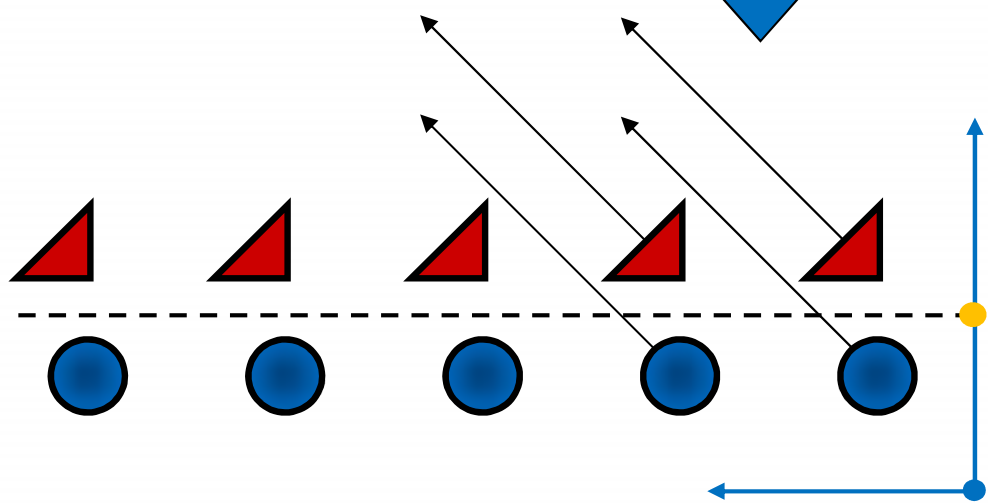
Interferometry vs. Polarimetry

$$S_{HH}^1 = A_D^1 + A_S^1$$



$$\varphi = \arg\{ S_{HH}^1 \quad S_{HH}^{2*} \}$$

$$S_{HH}^2 = A_D^2 + A_S^2$$

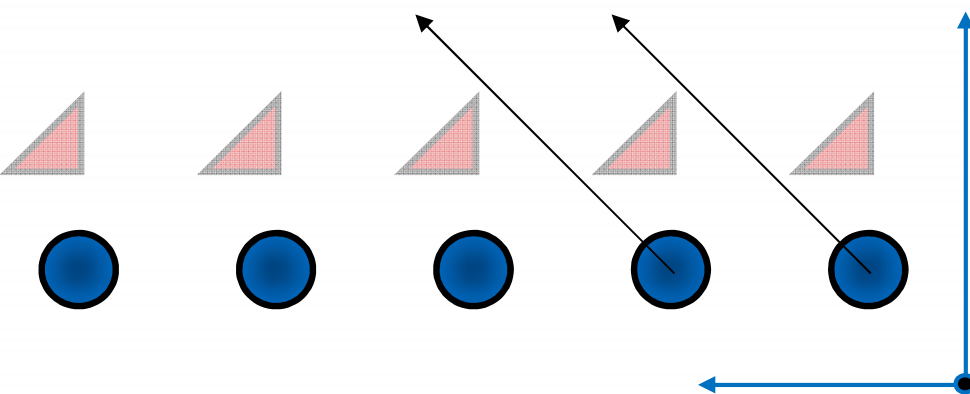


$$[S_D] = \begin{bmatrix} S_{HH} & S_{HV} \\ S_{VH} & S_{VV} \end{bmatrix} = A_D \begin{bmatrix} 1 & 0 \\ 0 & -1 \end{bmatrix}$$

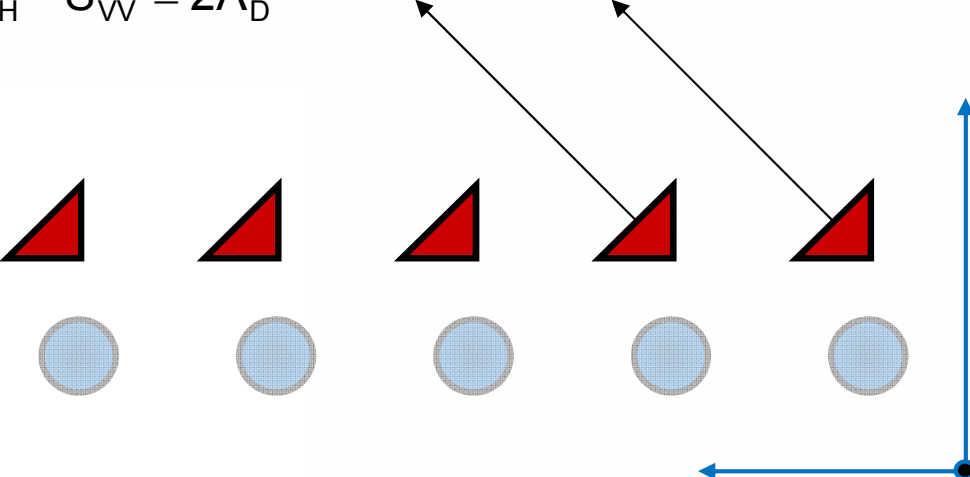


$$[S_S] = \begin{bmatrix} S_{HH} & S_{HV} \\ S_{VH} & S_{VV} \end{bmatrix} = A_S \begin{bmatrix} 1 & 0 \\ 0 & 1 \end{bmatrix}$$

$$S_{HH} + S_{VV} = 2A_S$$



$$S_{HH} - S_{VV} = 2A_D$$

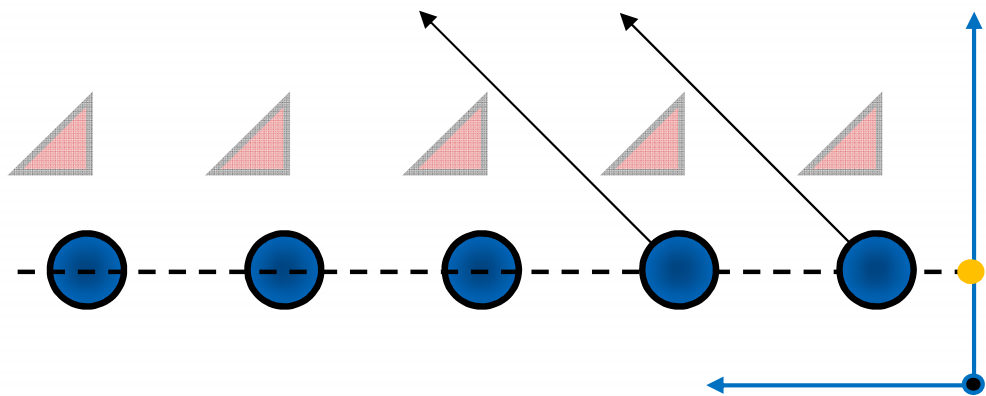


Polarimetric Interferometry

$$i_{1S} = S_{HH}^1 + S_{VV}^1 = 2A_S^1$$

$\rightarrow \varphi_S = \arg\{ i_{1S} \ i_{2S}^* \}$

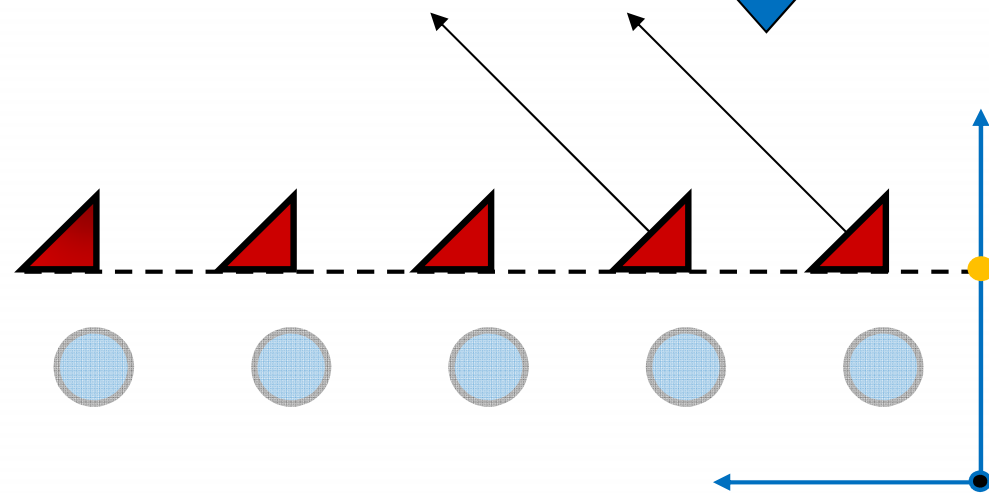
$$i_{2S} = S_{HH}^2 + S_{VV}^2 = 2A_S^2$$



$$i_{1D} = S_{HH}^1 - S_{VV}^1 = 2A_D^1$$

$\rightarrow \varphi_D = \arg\{ i_{1D} \ i_{2D}^* \}$

$$i_{2D} = S_{HH}^2 - S_{VV}^2 = 2A_D^2$$

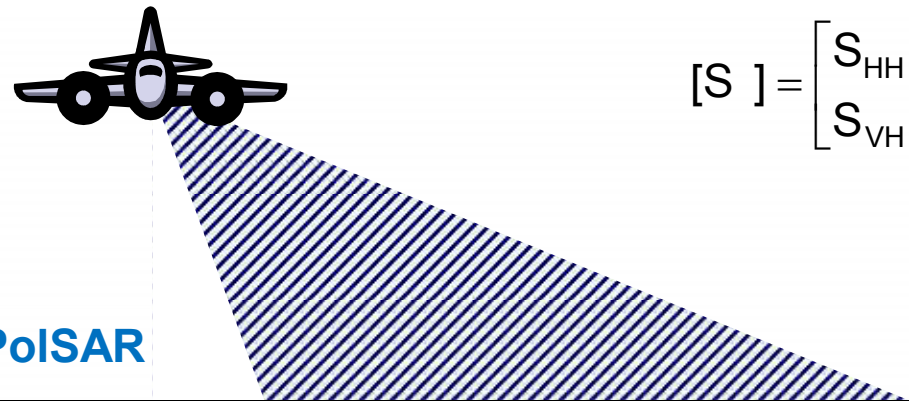


$$[S_D] = \begin{bmatrix} S_{HH} & S_{HV} \\ S_{VH} & S_{VV} \end{bmatrix} = A_D \begin{bmatrix} 1 & 0 \\ 0 & -1 \end{bmatrix}$$

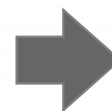


$$[S_S] = \begin{bmatrix} S_{HH} & S_{HV} \\ S_{VH} & S_{VV} \end{bmatrix} = A_S \begin{bmatrix} 1 & 0 \\ 0 & 1 \end{bmatrix}$$



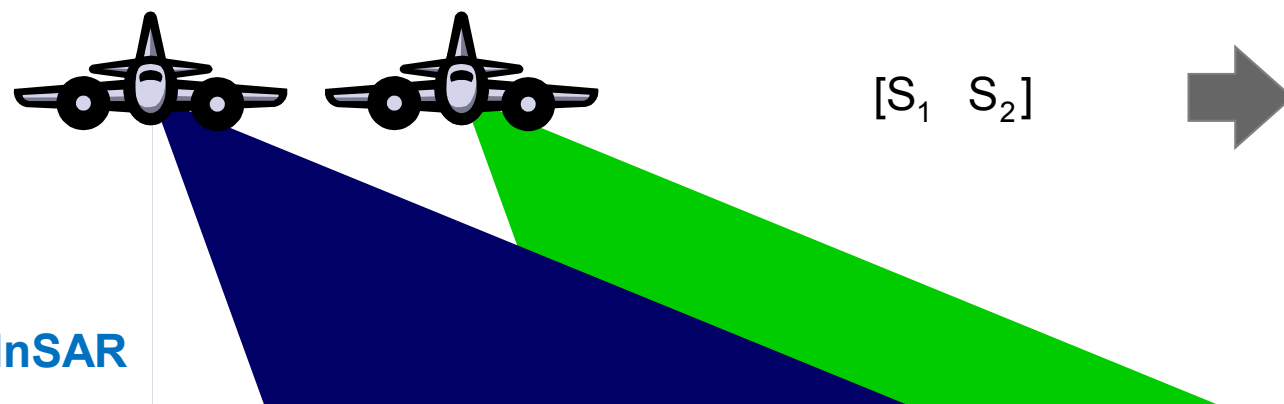


$$[S] = \begin{bmatrix} S_{HH} & S_{HV} \\ S_{VH} & S_{VV} \end{bmatrix}$$

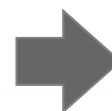


Polarimetric Coherences

$$\tilde{\gamma}(S_{ij} S_{mn}) = \frac{\langle S_{ij} S_{mn}^* \rangle}{\sqrt{\langle S_{ij} S_{ij}^* \rangle \langle S_{mn} S_{mn}^* \rangle}}$$

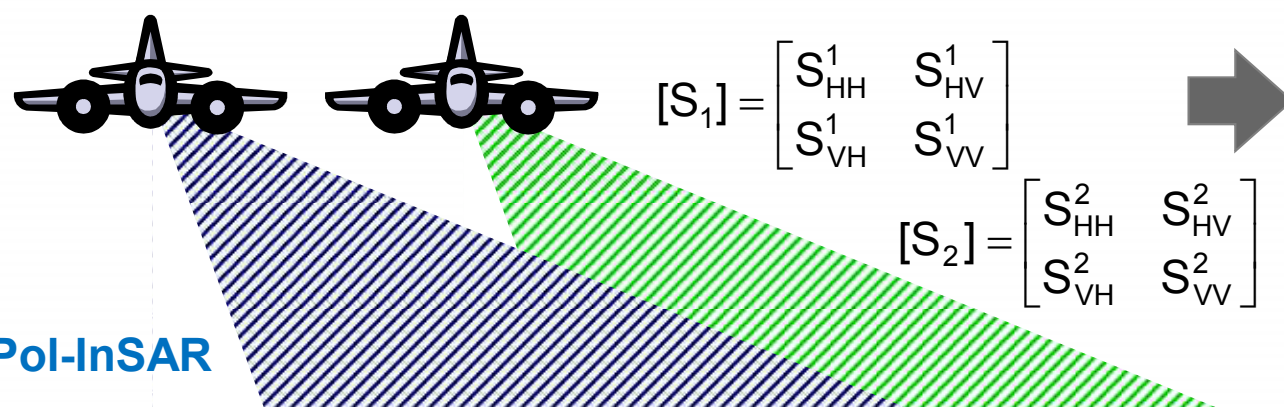


$$[S_1 \quad S_2]$$



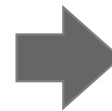
Interferometric Coherences

$$\tilde{\gamma}(S_1 S_2) = \frac{\langle S_1 S_2^* \rangle}{\sqrt{\langle S_1 S_1^* \rangle \langle S_2 S_2^* \rangle}}$$



$$[S_1] = \begin{bmatrix} S_{HH}^1 & S_{HV}^1 \\ S_{VH}^1 & S_{VV}^1 \end{bmatrix}$$

$$[S_2] = \begin{bmatrix} S_{HH}^2 & S_{HV}^2 \\ S_{VH}^2 & S_{VV}^2 \end{bmatrix}$$



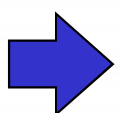
Polarimetric / Interferometric Coherences

$$\tilde{\gamma}(S_{ij}^1 S_{mn}^2) = \frac{\langle S_{ij}^1 S_{mn}^{2*} \rangle}{\sqrt{\langle S_{ij}^1 S_{ij}^{1*} \rangle \langle S_{mn}^2 S_{mn}^{2*} \rangle}}$$



The Complex Coherence

$$\tilde{\gamma} = \frac{< S_1 S_2^* >}{\sqrt{< S_1 S_1^* > < S_2 S_2^* >}}$$



$$\tilde{\gamma} = \frac{\sum_{k=1}^N S_1(k)S_2^*(k)}{\sqrt{\sum_{k=1}^N S_1(k)S_1^*(k) \sum_{k=1}^N S_2(k)S_2^*(k)}}$$

Multi-look phase difference

$$\varphi = \text{Arg} \left[\frac{1}{N} \sum_{k=1}^N S_1(k)S_2^*(k) \right]$$

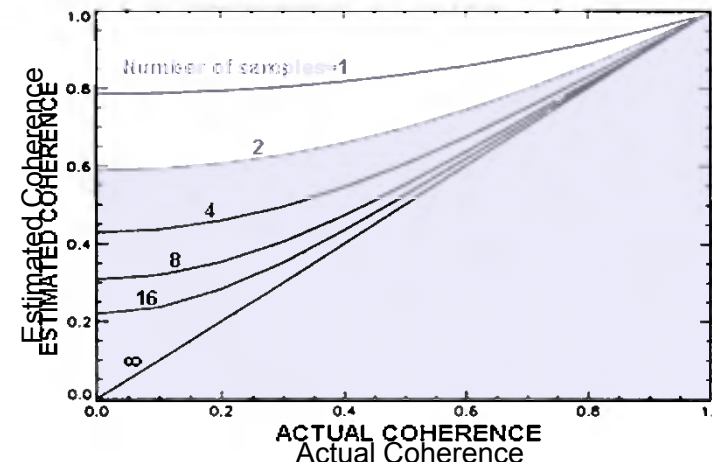
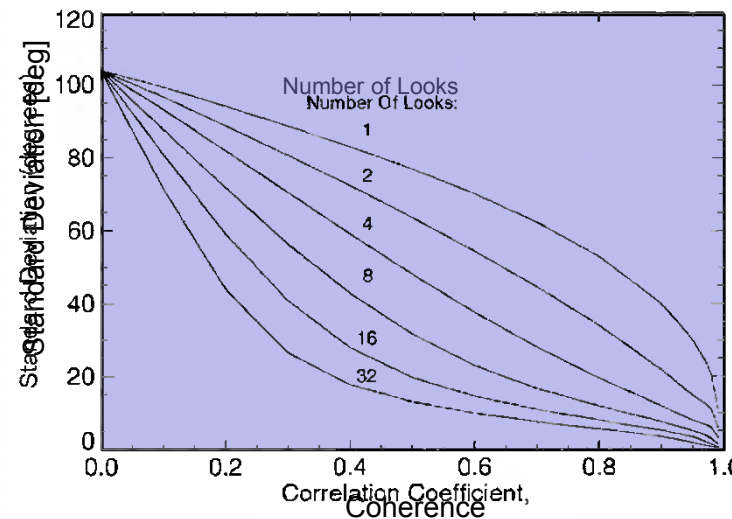
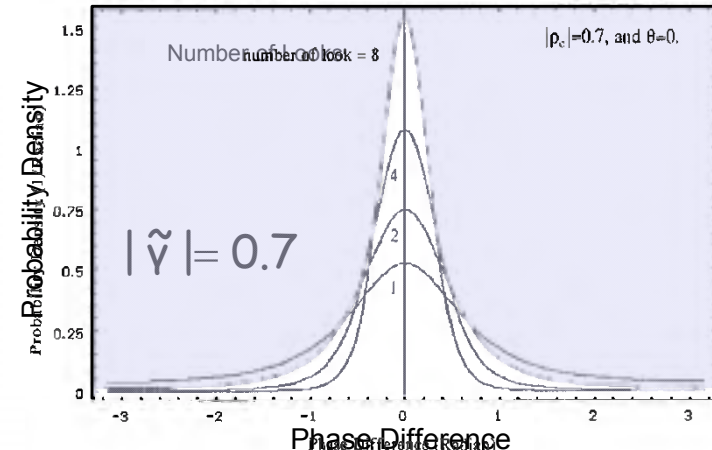
pdf: $p_\varphi(\varphi) = \frac{\Gamma(N+1/2)(1-|\gamma|^2)^2 \beta}{2\sqrt{\pi} \Gamma(N)(1-\beta^2)^{N+1/2}} + \frac{(1-|\gamma|^2)^N}{2\pi} F(N, 1; 1/2; \beta^2),$

where N is the number of Looks

and F is a Gauss hypergeometric function. $\beta = |\gamma| \cos(\varphi - \bar{\theta})$

Correlation Coefficient

$$|\tilde{\gamma}| = \frac{|\sum_{k=1}^N S_1(k)S_2^*(k)|}{\sqrt{\sum_{k=1}^N S_1(k)S_1^*(k) \sum_{k=1}^N S_2(k)S_2^*(k)}}$$



Complex Coherences on the Unit Circle (UC)

$$\tilde{\gamma} := \frac{\sum_{k=1}^N S_1(k)S_2^*(k)}{\sqrt{\sum_{k=1}^N S_1(k)S_1^*(k) \sum_{k=1}^N S_2(k)S_2^*(k)}} = \exp(i \operatorname{Arg}(\tilde{\gamma})) \cdot |\tilde{\gamma}|$$

Correlation Coefficient

$$0 \leq |\tilde{\gamma}| = \gamma \leq 1$$

Interferometric Phase

$$0 \leq \operatorname{Arg}(\tilde{\gamma}) = \varphi \leq 2\pi$$

Cramer Rao Bounds:

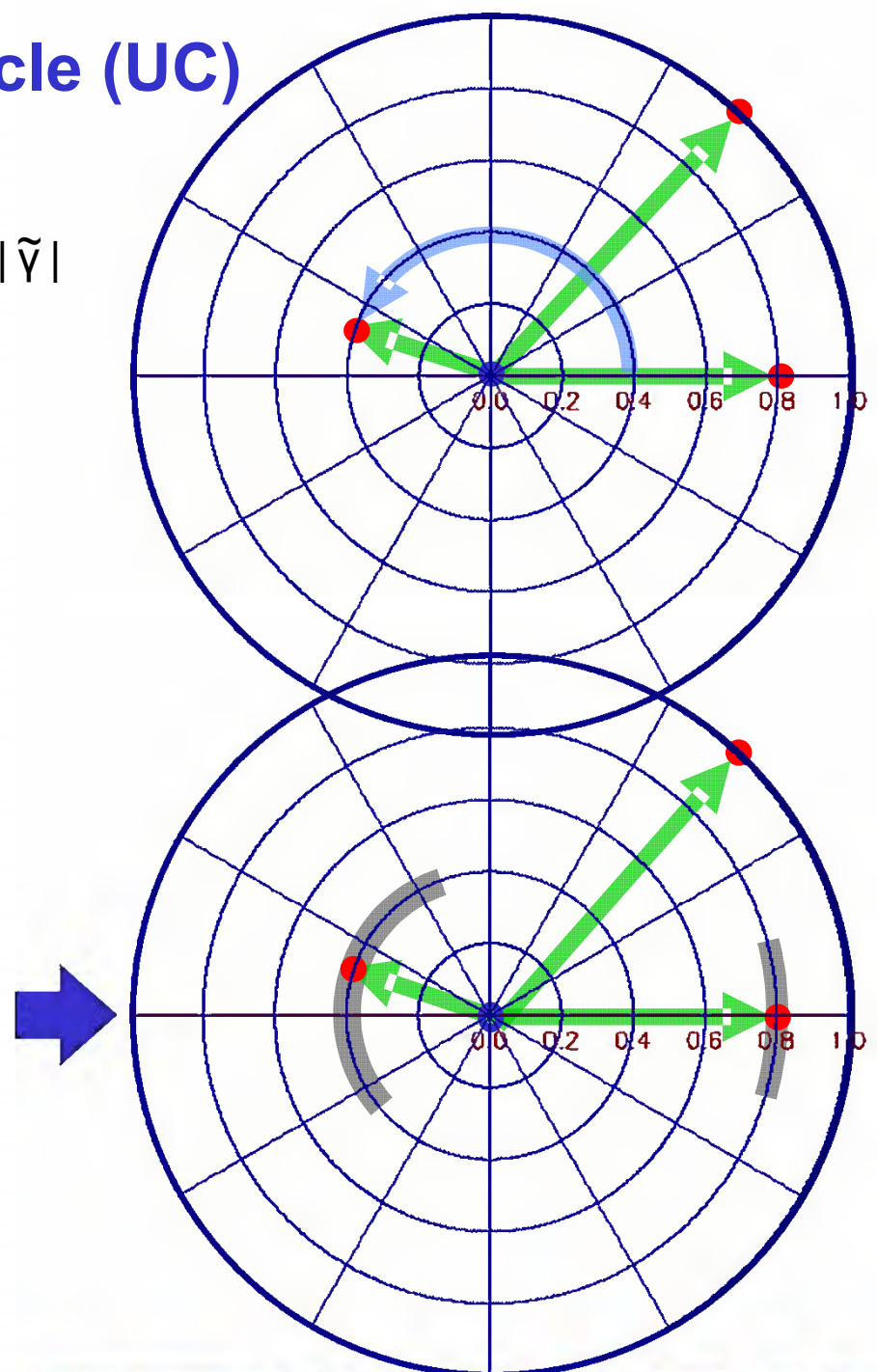
Correlation Coefficient

$$\operatorname{VAR}(|\tilde{\gamma}|)_{\text{CR}} = \frac{(1 - |\gamma|^2)^2}{2N}$$

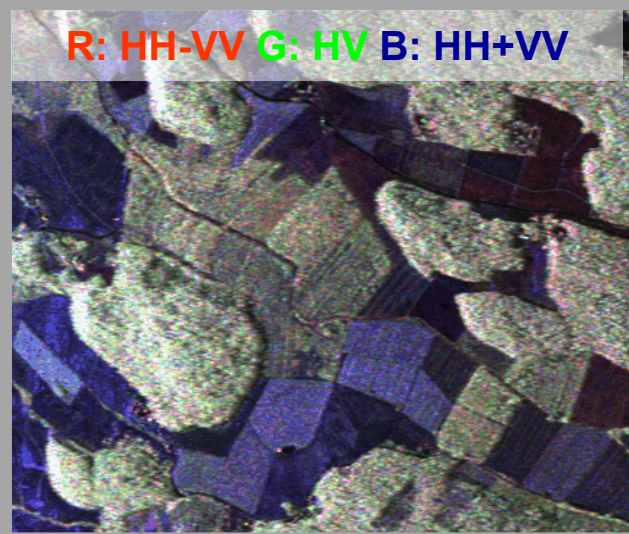
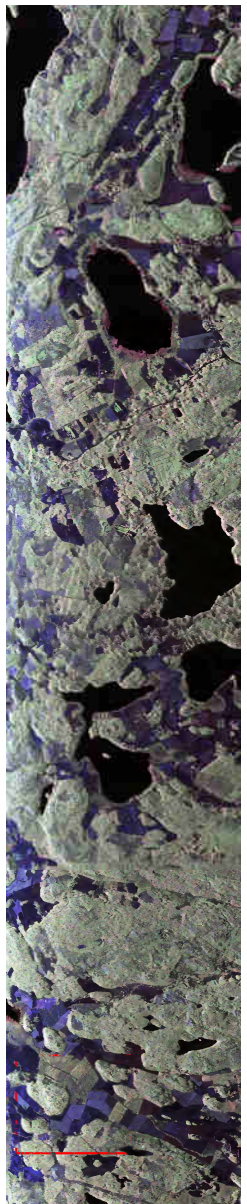
Interferometric Phase

$$\operatorname{VAR}(\varphi)_{\text{CR}} = \frac{1 - |\gamma|^2}{2N|\gamma|^2}$$

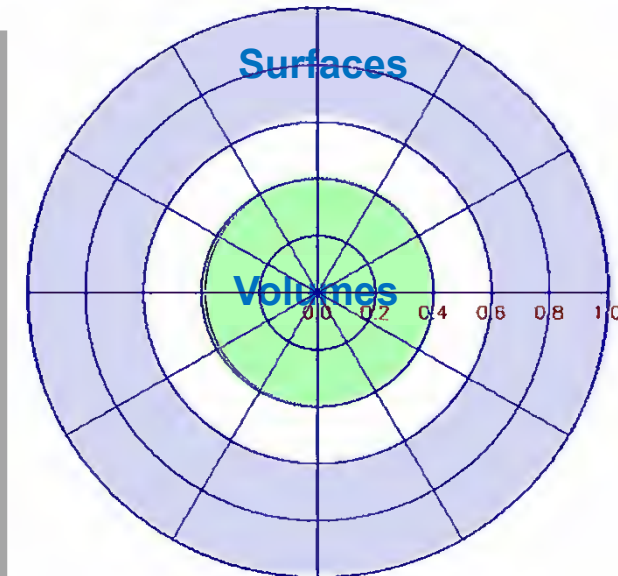
$\varphi = \arg(\tilde{\gamma})$ and N is the number of Looks



Why is Interferometry important for Volume Scatterers?



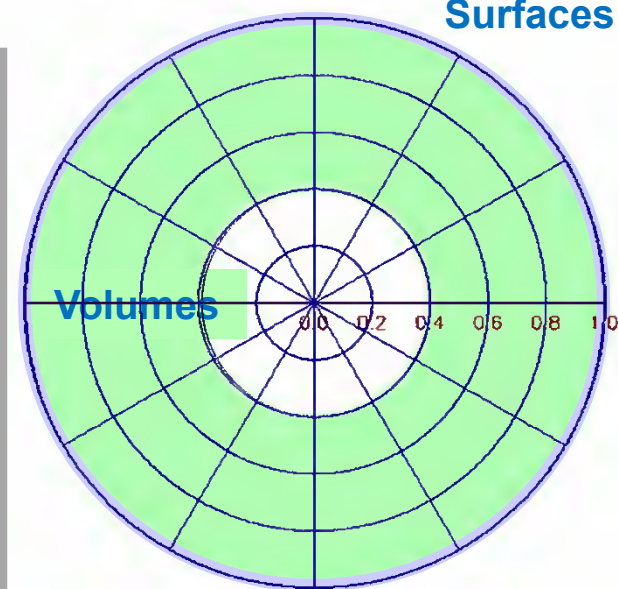
HH-VV Coherence

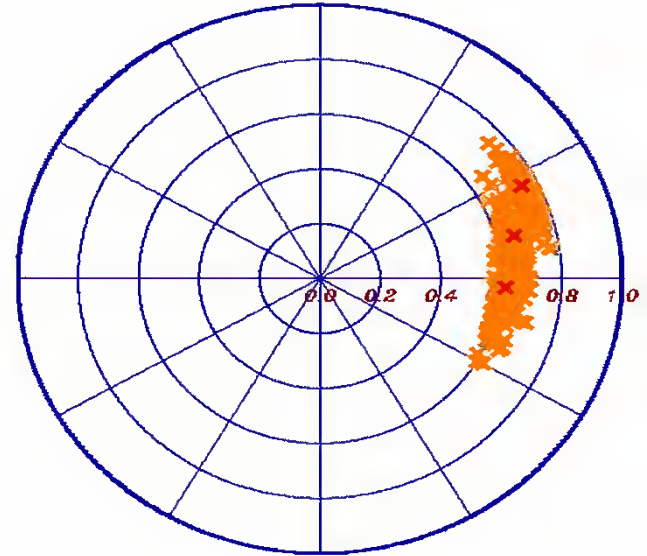
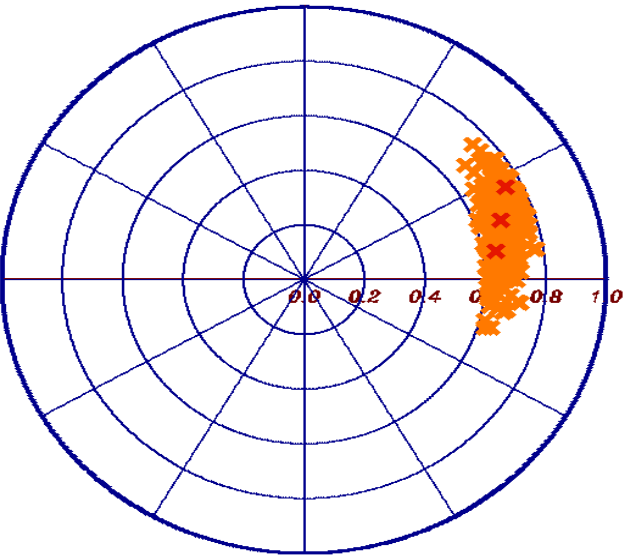
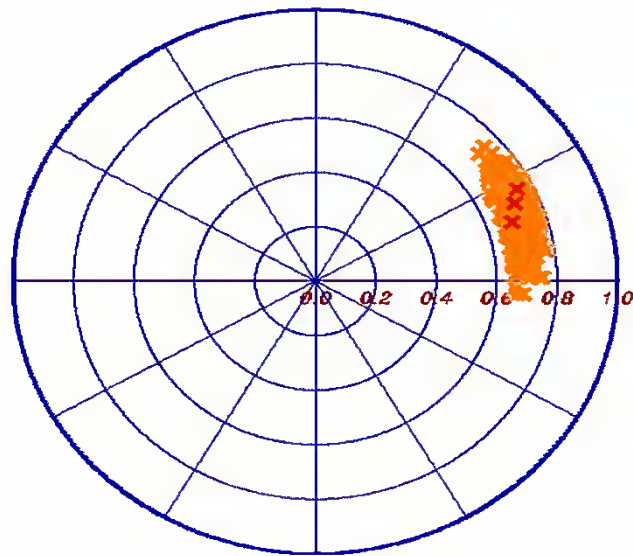


HH-HH Coherence

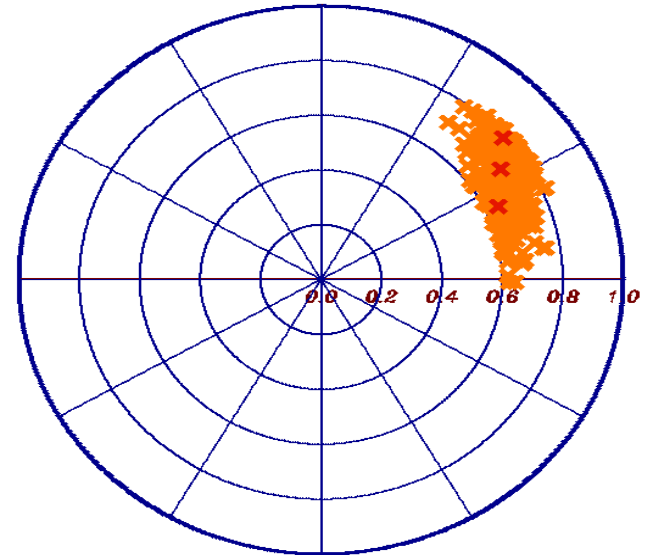
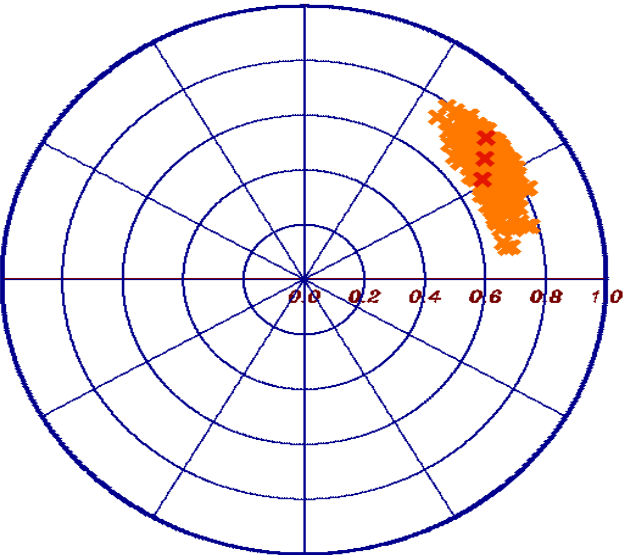
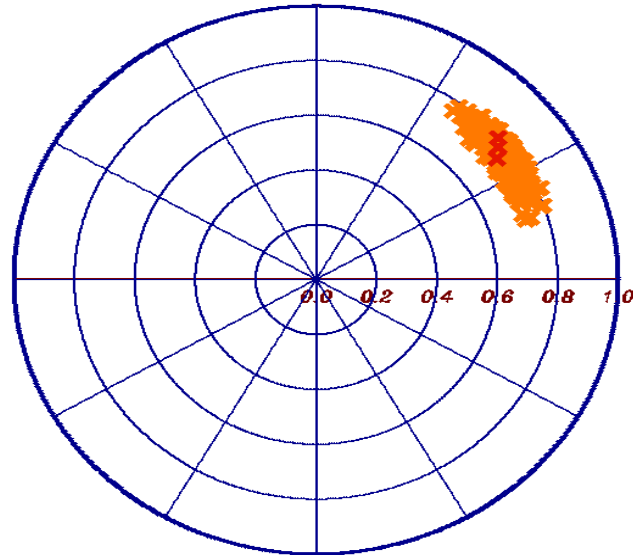


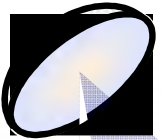
Surfaces





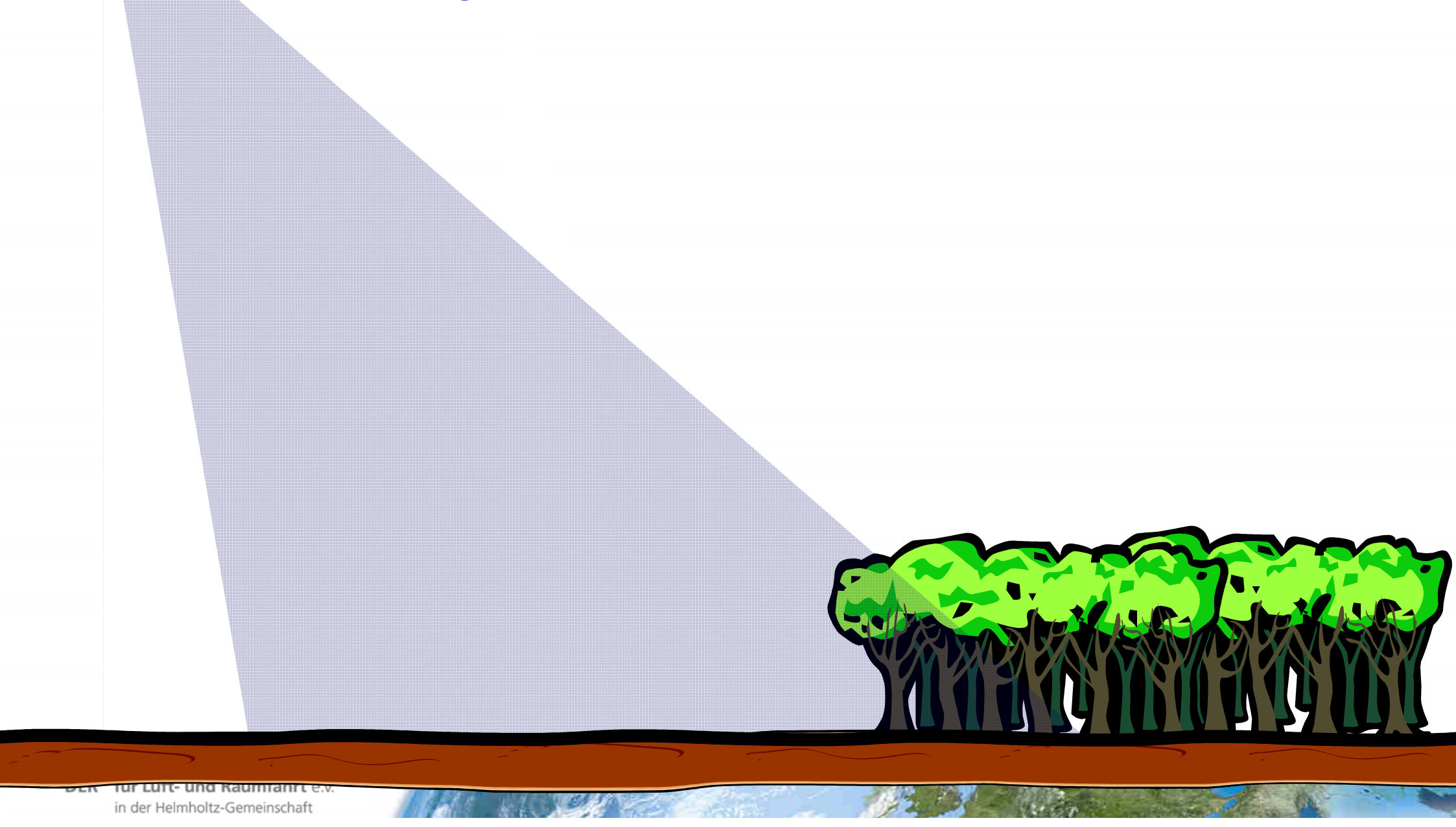
Pol-InSAR: Basic Principles & Ideas

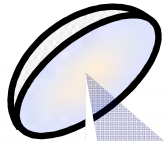
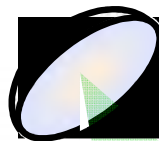




S_1

SAR Interferometry for Volume Structure



 S_1 S_2 

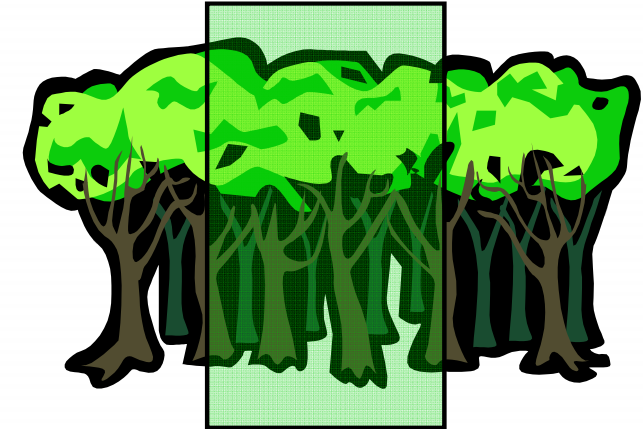
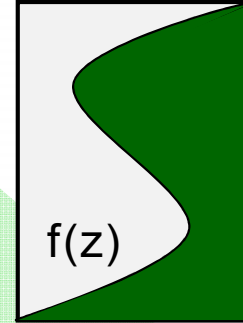
Interferometric Coherence

$$\tilde{\gamma}(S_1, S_2) = \frac{\langle S_1 S_2^* \rangle}{\sqrt{\langle S_1 S_1^* \rangle \langle S_2 S_2^* \rangle}}$$

SAR Interferometry for Volume Structure

Volume Coherence

$$\tilde{\gamma}_{\text{Vol}}(f(z), k_z) = e^{ik_z z_0} \frac{\int_0^{h_v} f(z) e^{ik_z z} dz}{\int_0^{h_v} f(z) dz}$$

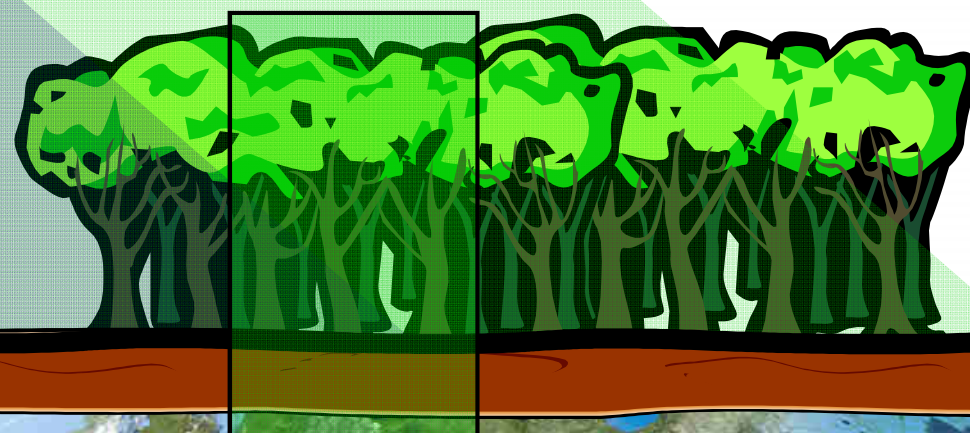


$f(z)$... vertical reflectivity function

$$\tilde{\gamma} = \tilde{\gamma}_{\text{Temporal}} \gamma_{\text{SNR}} \tilde{\gamma}_{\text{Vol}}$$

- $\tilde{\gamma}_{\text{Temporal}}$... temporal decorrelation
- γ_{SNR} ... additive noise decorrelation
- $\tilde{\gamma}_{\text{Volume}}$... geometric decorrelation

$$\text{Vertical Wavenumber: } k_z = \frac{\kappa \Delta \theta}{\sin(\theta_0)}$$



 S_1 S_2 

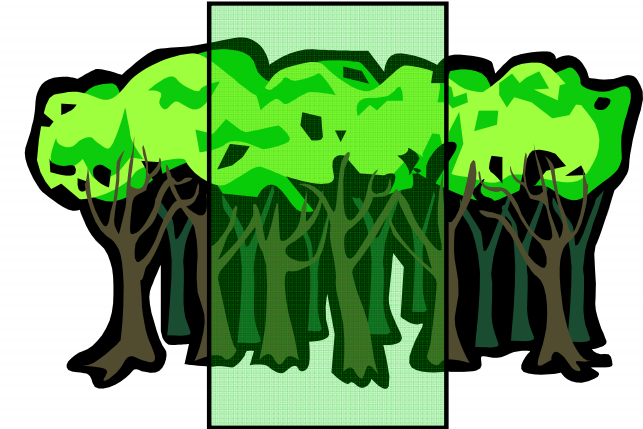
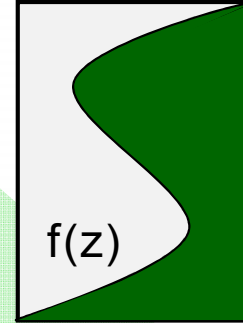
Interferometric Coherence

$$\tilde{\gamma}(S_1, S_2) = \frac{\langle S_1 S_2^* \rangle}{\sqrt{\langle S_1 S_1^* \rangle \langle S_2 S_2^* \rangle}}$$

SAR Interferometry for Volume Structure

Volume Coherence

$$\tilde{\gamma}_{\text{Vol}}(f(z), k_z) = e^{ik_z z_0} \frac{\int_0^{h_v} f(z) e^{ik_z z} dz}{\int_0^{h_v} f(z) dz}$$



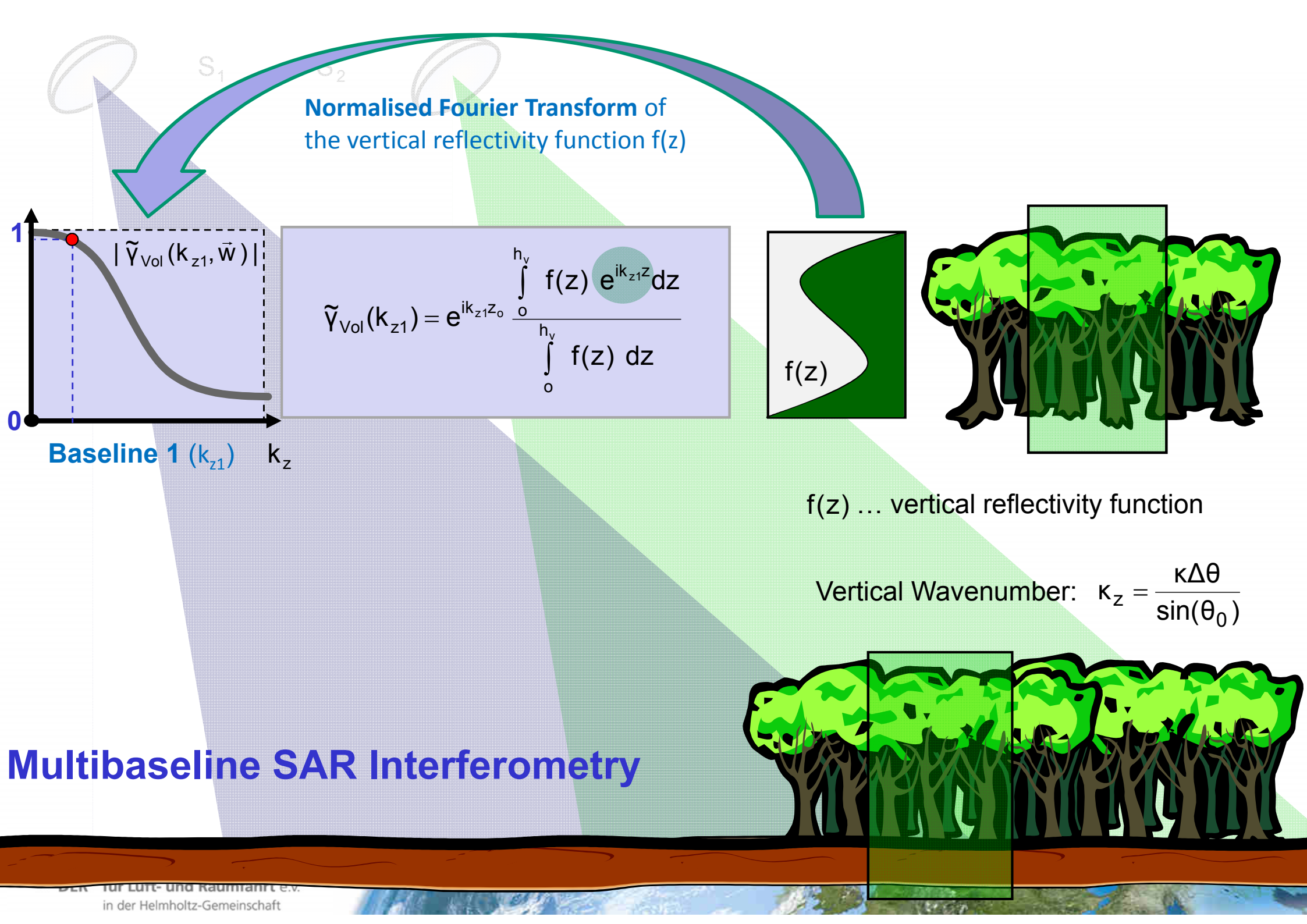
$f(z)$... vertical reflectivity function

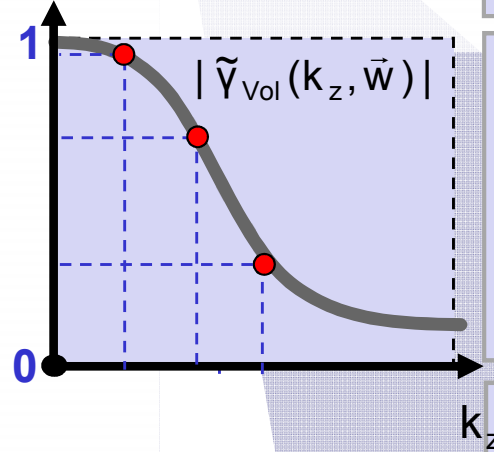
$$\tilde{\gamma} = \tilde{\gamma}_{\text{Temporal}} \gamma_{\text{SNR}} \tilde{\gamma}_{\text{Vol}}$$

- $\tilde{\gamma}_{\text{Temporal}}$... temporal decorrelation
- γ_{SNR} ... additive noise decorrelation
- $\tilde{\gamma}_{\text{Volume}}$... geometric decorrelation

$$\text{Vertical Wavenumber: } k_z = \frac{\kappa \Delta \theta}{\sin(\theta_0)}$$

SAR interferometry allows to reconstruct the vertical reflectivity function $f(z)$ of a volume scatterer by means of interferometric (volume) coherence measurements at different vertical wavenumbers k_z , i.e. at different spatial baselines.

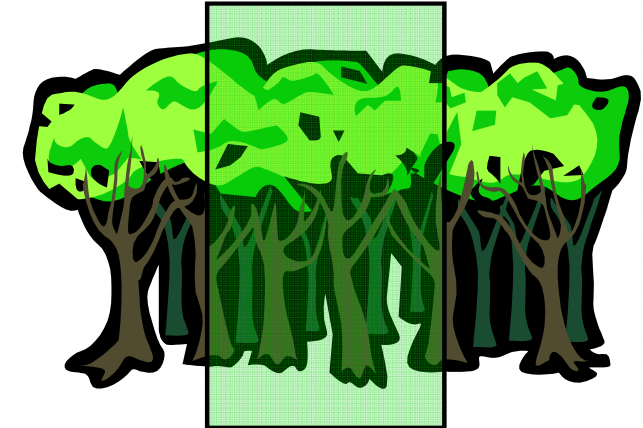
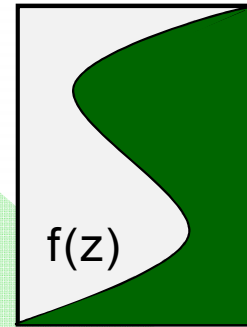


 S_1 Baseline 3 (k_{z3})Baseline 2 (k_{z2})

$$\tilde{Y}_{\text{Vol}}(k_{z2}) = e^{ik_z z_o} \frac{\int_0^{h_v} f(z) e^{ik_{z2} z} dz}{\int_0^{h_v} f(z) dz}$$

$$\tilde{Y}_{\text{Vol}}(k_{z1}) = e^{ik_z z_o} \frac{\int_0^{h_v} f(z) e^{ik_{z1} z} dz}{\int_0^{h_v} f(z) dz}$$

$$\tilde{Y}_{\text{Vol}}(k_{z3}) = e^{ik_z z_o} \frac{\int_0^{h_v} f(z) e^{ik_{z3} z} dz}{\int_0^{h_v} f(z) dz}$$



f(z) ... vertical reflectivity function

$$\text{Vertical Wavenumber: } \kappa_z = \frac{\kappa \Delta \theta}{\sin(\theta_0)}$$

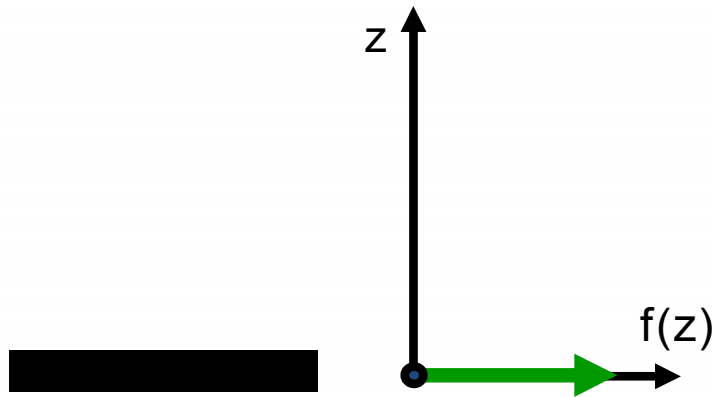


Multibaseline SAR Interferometry

Multi-baseline measurements allow to sample the spectrum of the vertical reflectivity $\text{FT}\{f(z)\}$ @ different (spatial) frequencies (k_z).

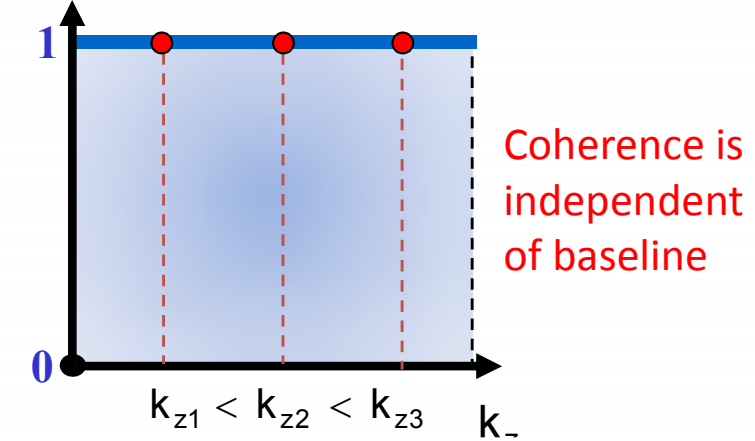
Vertical Reflectivity Function $f(z)$

Surface Scatterer

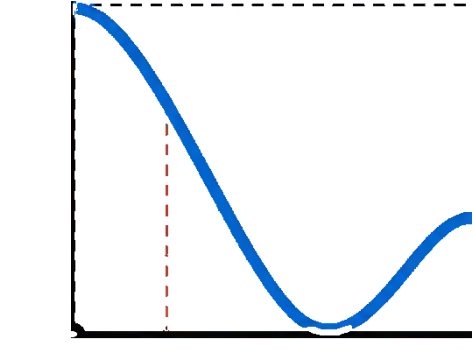
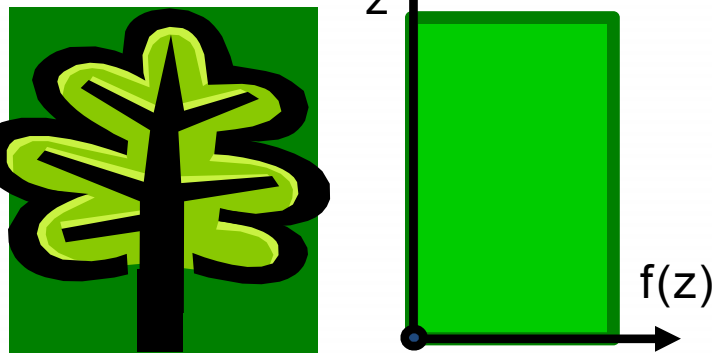


$$|\tilde{\gamma}_{\text{Vol}}(k_z)| = \frac{\left| \int_0^{h_v} f(z) e^{ik_z z} dz \right|}{\int_0^{h_v} f(z) dz}$$

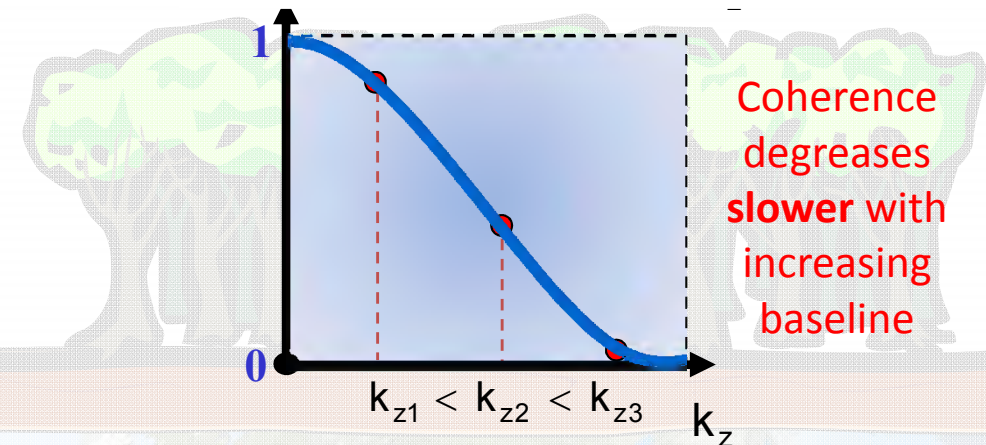
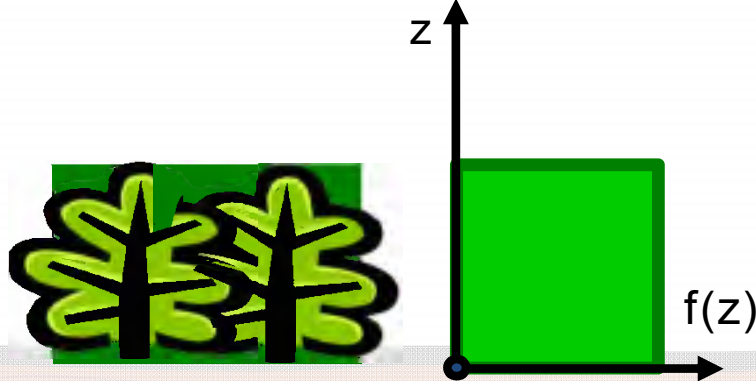
InSAR Volume Coherence $|\tilde{\gamma}_{\text{Vol}}(k_z)|$



Tall Vegetation



Short Vegetation



Amplitude Image



Amplitude Image HH

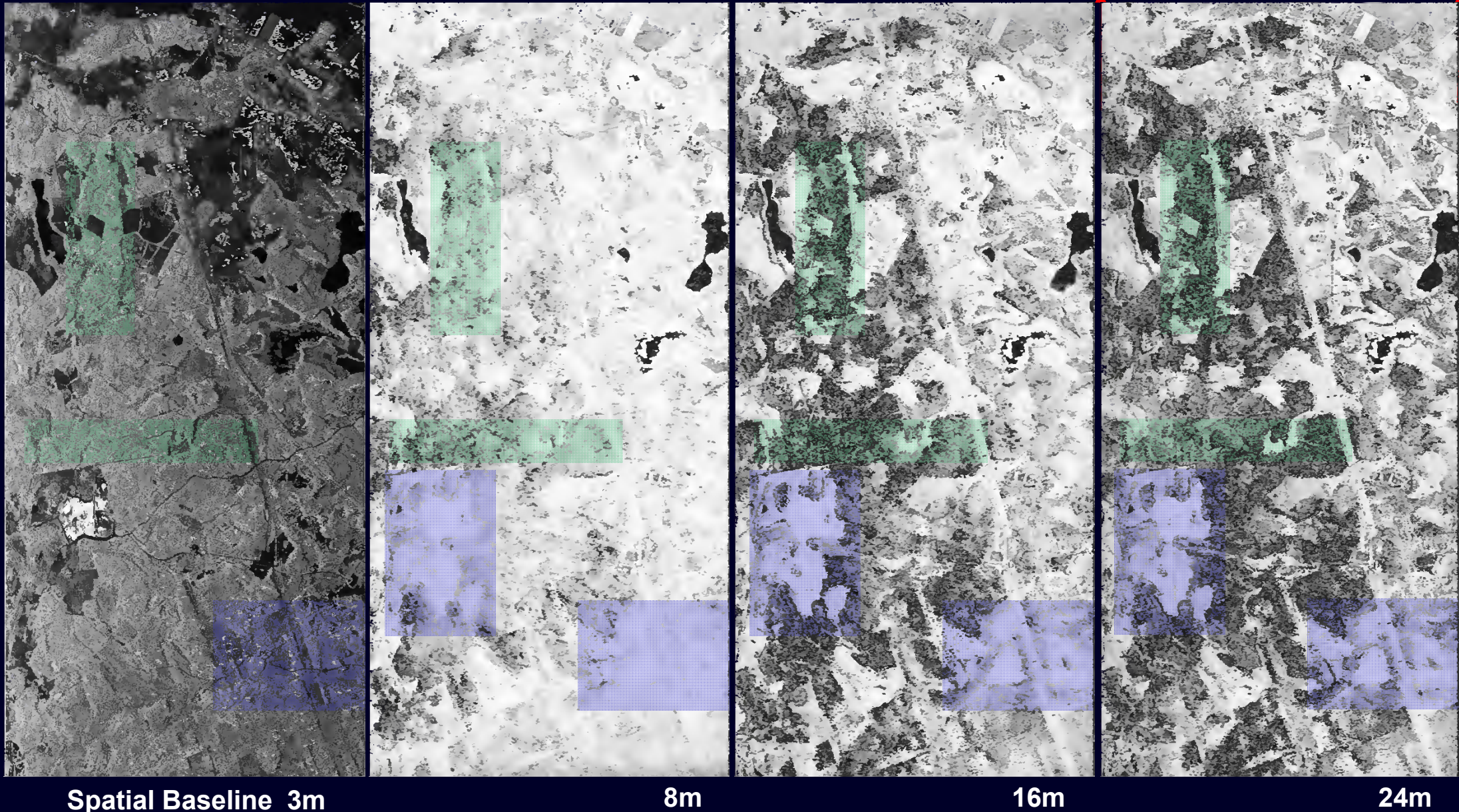


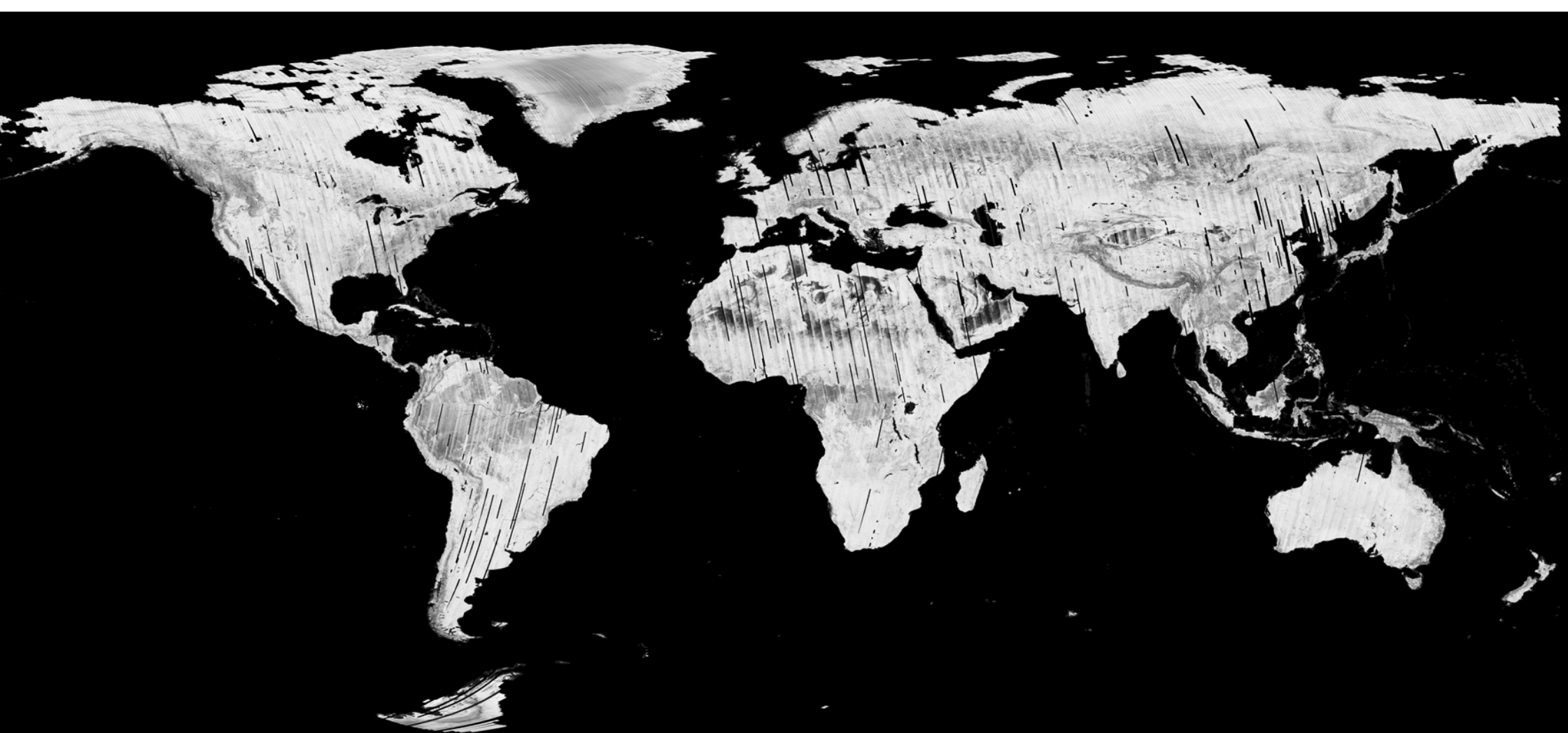
Interferometric Coherence: Volume Decorrelation

25°

Incidence Angle

55°





0

1



By DLR-HR-STL

500x500 m² resolution

Polarimetric SAR Interferometry

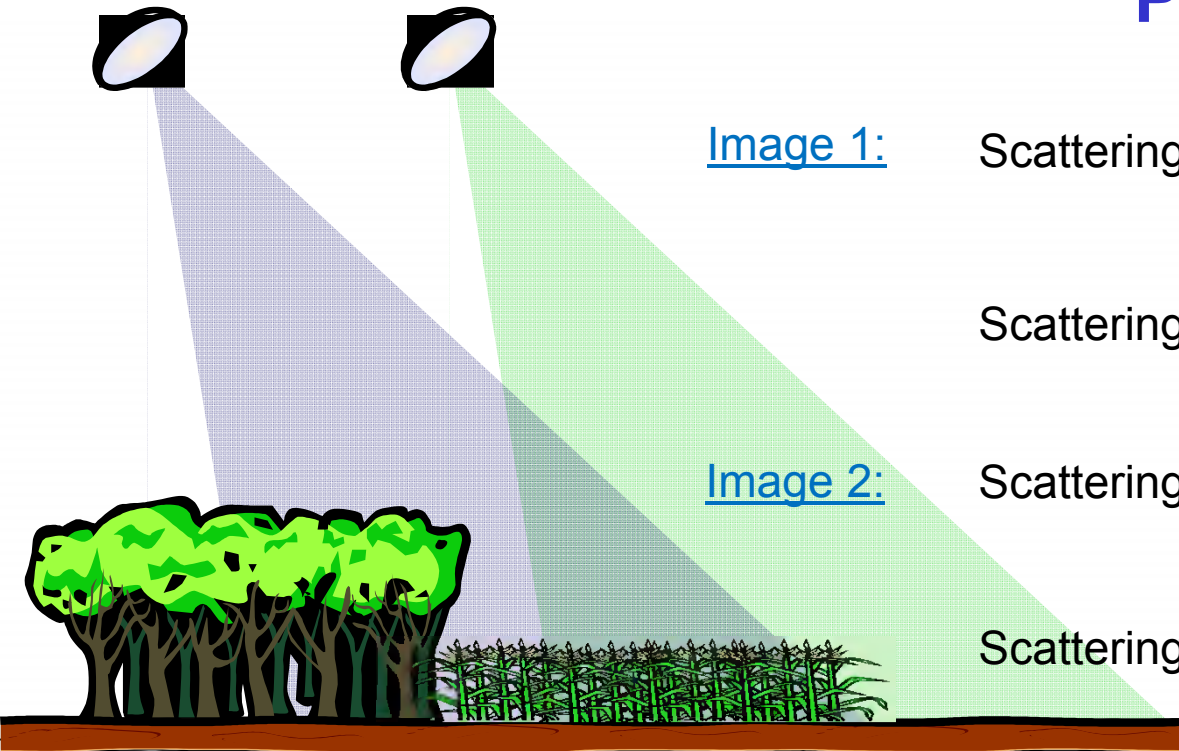


Image 1:

Scattering Matrix:

$$[S_1] = \begin{bmatrix} S_{HH}^1 & S_{HV}^1 \\ S_{VH}^1 & S_{VV}^1 \end{bmatrix}$$

Scattering Vector:

$$\vec{k}_1 = \frac{1}{\sqrt{2}} [S_{HH}^1 + S_{VV}^1, S_{HH}^1 - S_{VV}^1, 2S_{HV}^1]^T$$

Scattering Matrix:

$$[S_2] = \begin{bmatrix} S_{HH}^2 & S_{HV}^2 \\ S_{VH}^2 & S_{VV}^2 \end{bmatrix}$$

Scattering Vector:

$$\vec{k}_2 = \frac{1}{\sqrt{2}} [S_{HH}^2 + S_{VV}^2, S_{HH}^2 - S_{VV}^2, 2S_{HV}^2]^T$$

Image formation:

$i_1 = \vec{w}_1^+ \cdot \vec{k}_1$ and $i_2 = \vec{w}_2^+ \cdot \vec{k}_2$... projection of the scattering vector on a (complex) unitary vector \vec{w}_i

\vec{w}_i used to select a given polarisation out of all possible polarisations provided by $[S]$

Example: $S_{HH} + S_{VV}$ image: $\vec{w} = [1 \ 0 \ 0]^T \rightarrow i = \vec{w}^+ \cdot \vec{k}_j = \frac{1}{\sqrt{2}} (S_{HH}^j + S_{VV}^j)$

S_{HH} image: $\vec{w} = [1/\sqrt{2} \ 1/\sqrt{2} \ 0]^T \rightarrow i_j = \vec{w}^+ \cdot \vec{k}_j = S_{HH}^j$



Polarimetric SAR Interferometry

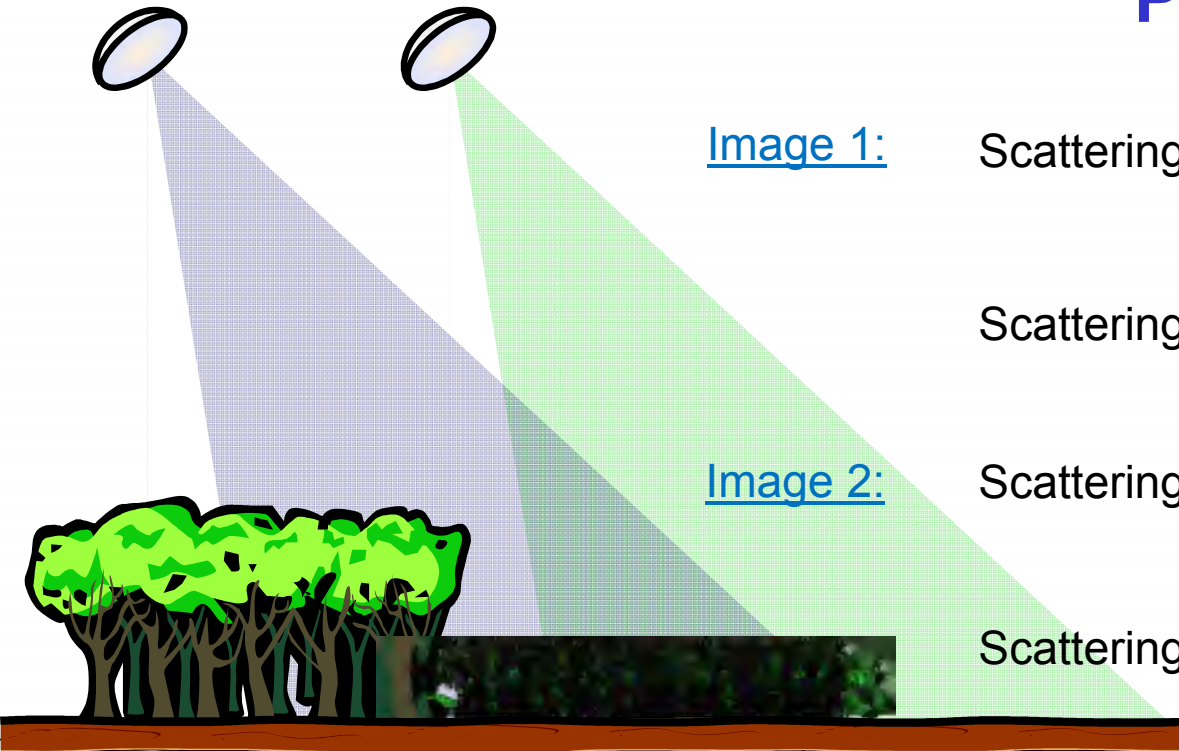


Image 1:

Scattering Matrix:

$$[S_1] = \begin{bmatrix} S_{HH}^1 & S_{HV}^1 \\ S_{VH}^1 & S_{VV}^1 \end{bmatrix}$$

Scattering Vector:

$$\vec{k}_1 = \frac{1}{\sqrt{2}} [S_{HH}^1 + S_{VV}^1 \quad S_{HH}^1 - S_{VV}^1 \quad 2S_{HV}^1]^T$$

Scattering Matrix:

$$[S_2] = \begin{bmatrix} S_{HH}^2 & S_{HV}^2 \\ S_{VH}^2 & S_{VV}^2 \end{bmatrix}$$

Scattering Vector:

$$\vec{k}_2 = \frac{1}{\sqrt{2}} [S_{HH}^2 + S_{VV}^2 \quad S_{HH}^2 - S_{VV}^2 \quad 2S_{HV}^2]^T$$

Image formation: $i_1 = \vec{w}_1^+ \cdot \vec{k}_1$ and $i_2 = \vec{w}_2^+ \cdot \vec{k}_2$ where \vec{w}_i are complex unitary vectors*

Interferogram formation:

$$i_1 i_2^* = (\vec{w}_1^+ \cdot \vec{k}_1)(\vec{w}_2^+ \cdot \vec{k}_2)^* = \vec{w}_1^+ (\vec{k}_1 \cdot \vec{k}_2^+) \vec{w}_2 = \vec{w}_1^+ [\Omega] \vec{w}_2$$

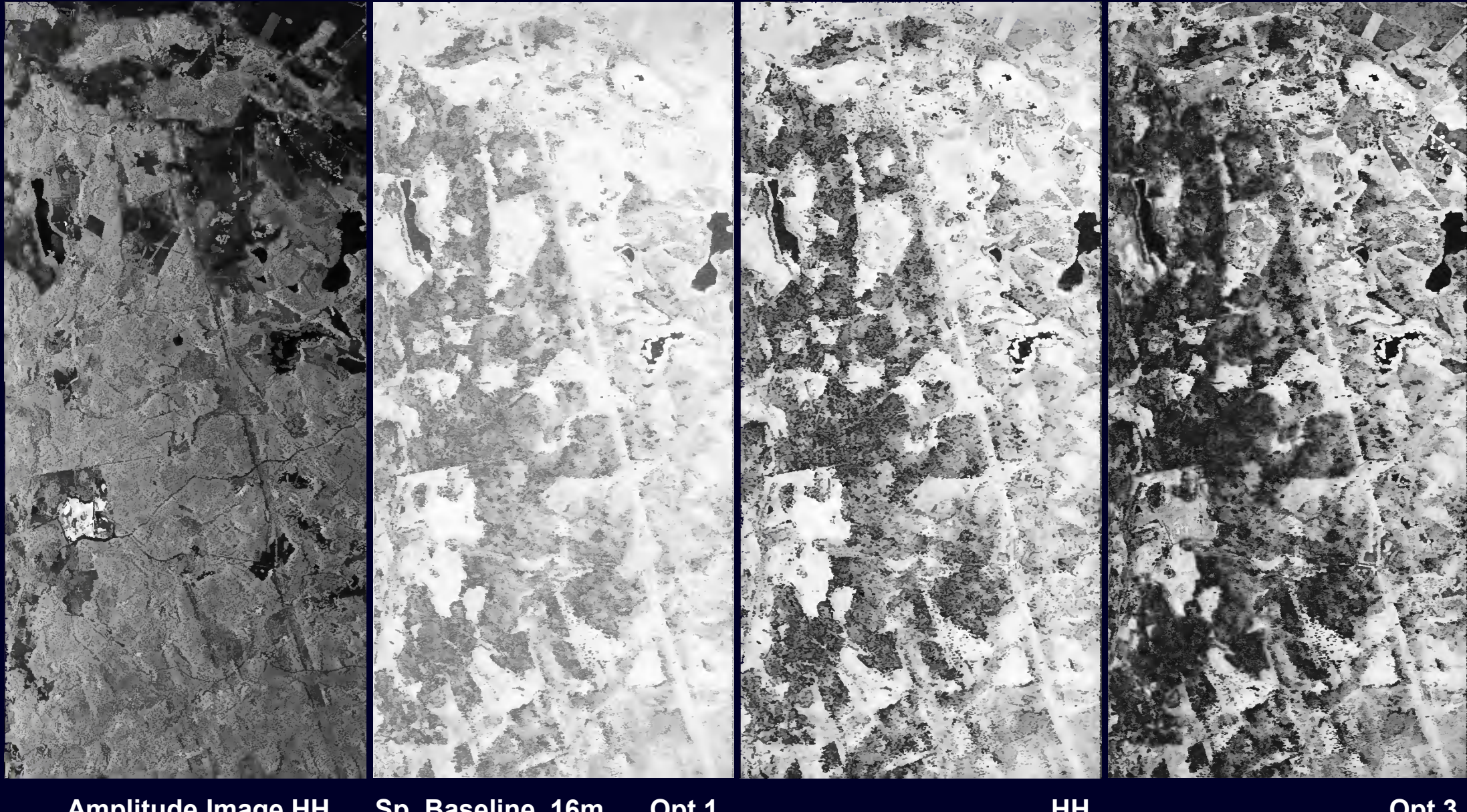
Interferometric Coherence:

$$\tilde{\gamma}(\vec{w}_1, \vec{w}_2) = \frac{\langle i_1 i_2^* \rangle}{\sqrt{\langle i_1 i_1^* \rangle \langle i_2 i_2^* \rangle}} = \frac{\langle \vec{w}_1^+ [\Omega] \vec{w}_2 \rangle}{\sqrt{\langle (\vec{w}_1^+ [\Omega] \vec{w}_1) \rangle \langle (\vec{w}_2^+ [\Omega] \vec{w}_2) \rangle}}$$

where $[T_{11}] = \langle \vec{k}_1 \cdot \vec{k}_1^+ \rangle$ $[T_{22}] = \langle \vec{k}_2 \cdot \vec{k}_2^+ \rangle$ and $[\Omega] = \langle \vec{k}_1 \cdot \vec{k}_2^+ \rangle$

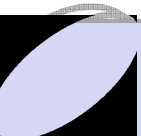
\vec{w}_i used to select a polarisation state out of all possible polarisations provided by the scattering matrix [S]

Interferometric Coherence: Volume Decorrelation

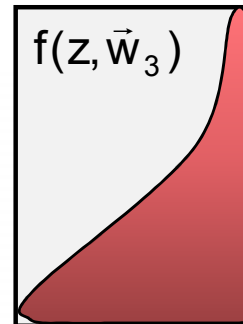




Polarisation 3 (w₃):



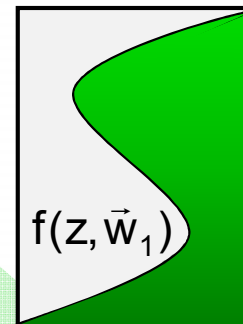
$$\tilde{\gamma}_{\text{Vol}}(f(z, \vec{w}_3)) = e^{ik_z z_0} \frac{\int_0^{h_v} f(z, \vec{w}_3) e^{ik_z z} dz}{\int_0^{h_v} f(z, \vec{w}_3) dz}$$



Polarisation 1 (w₁):



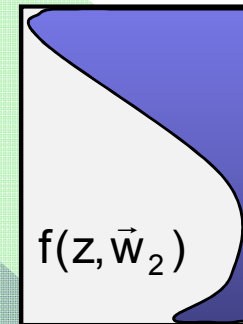
$$\tilde{\gamma}_{\text{Vol}}(f(z, \vec{w}_1)) = e^{ik_z z_0} \frac{\int_0^{h_v} f(z, \vec{w}_1) e^{ik_z z} dz}{\int_0^{h_v} f(z, \vec{w}_1) dz}$$



Polarisation 2 (w₂):

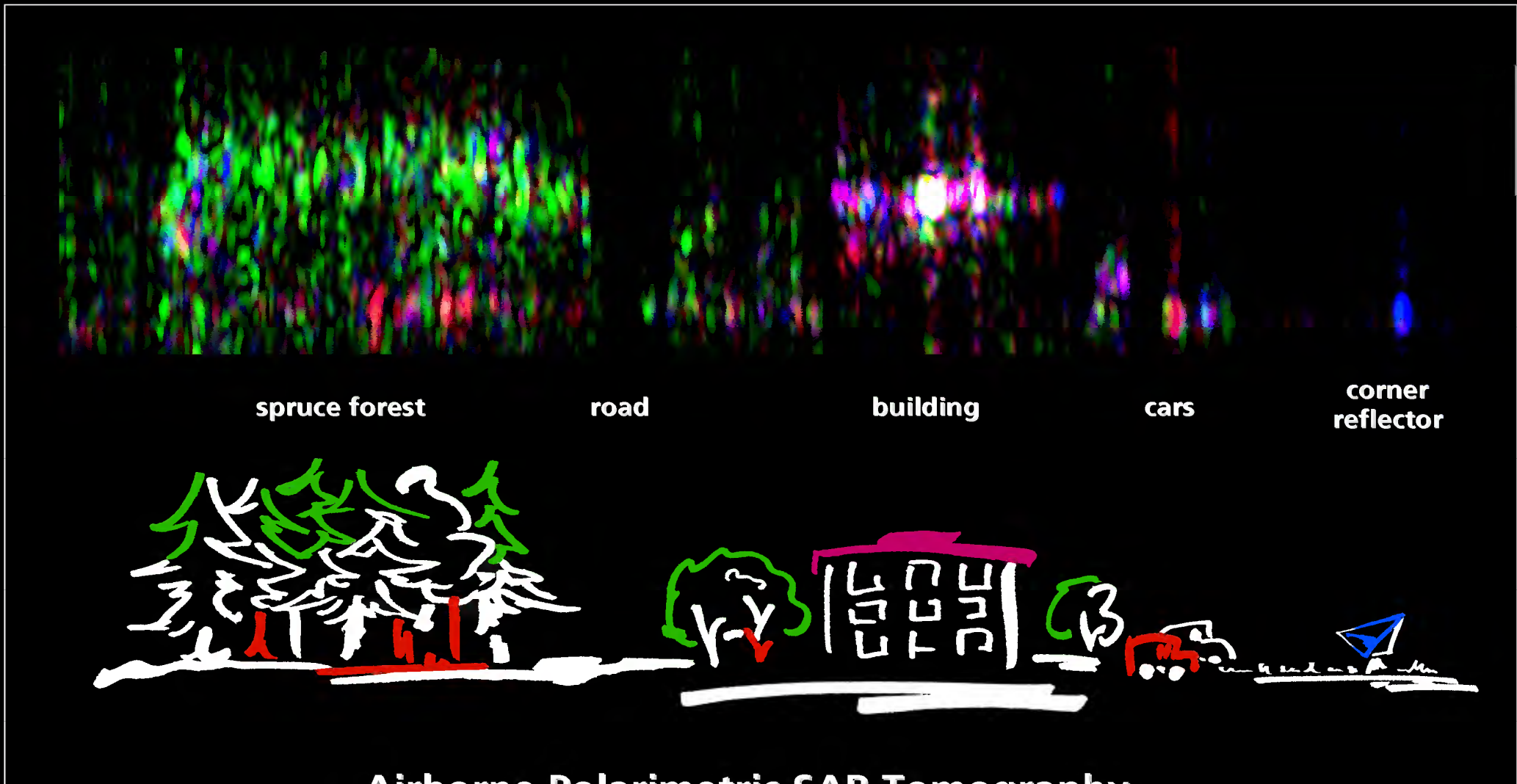


$$\tilde{\gamma}_{\text{Vol}}(f(z, \vec{w}_2)) = e^{ik_z z_0} \frac{\int_0^{h_v} f(z, \vec{w}_2) e^{ik_z z} dz}{\int_0^{h_v} f(z, \vec{w}_2) dz}$$



$f(z, \vec{w})$...vertical reflectivity function

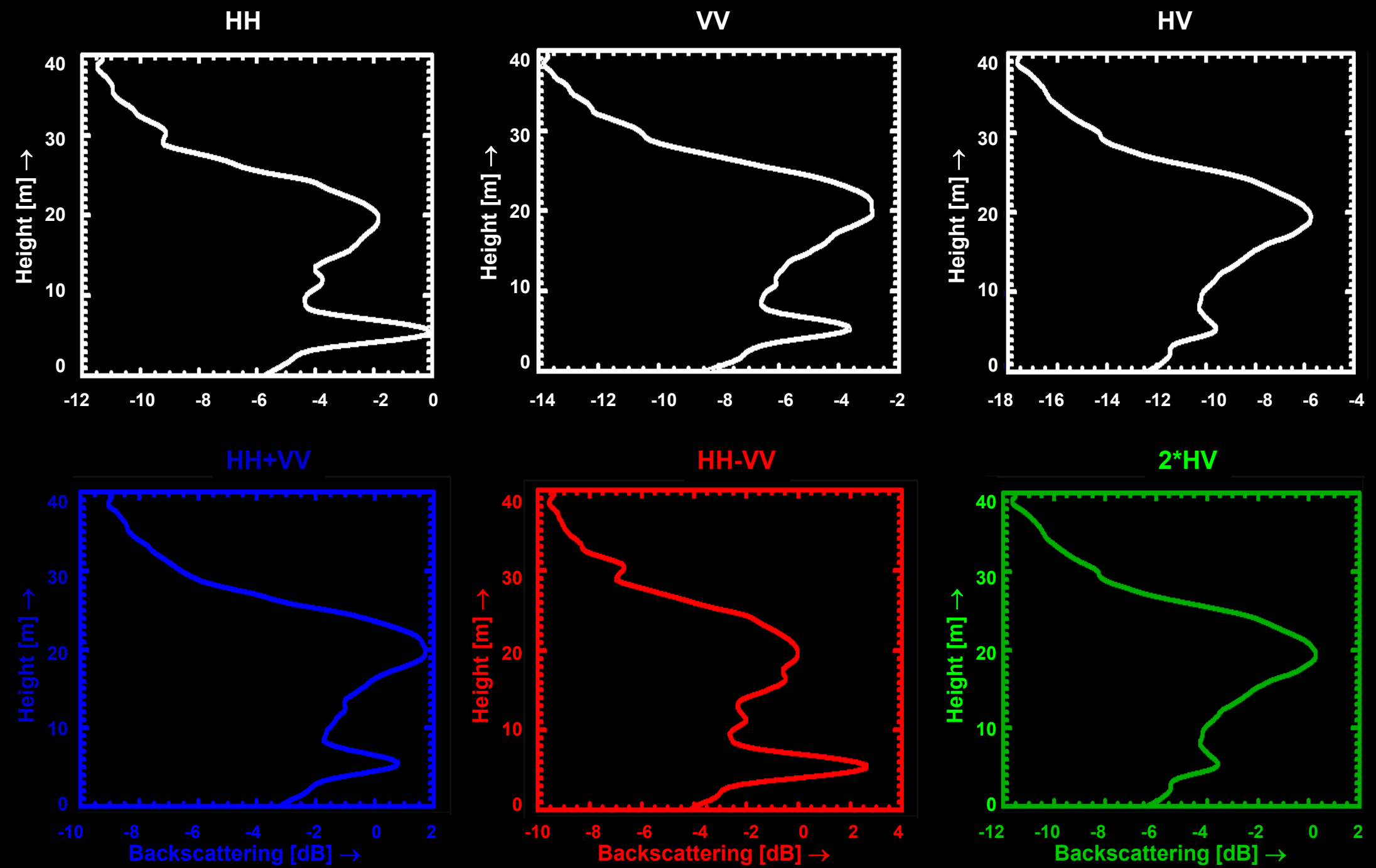
Polarimetric SAR Interferometry



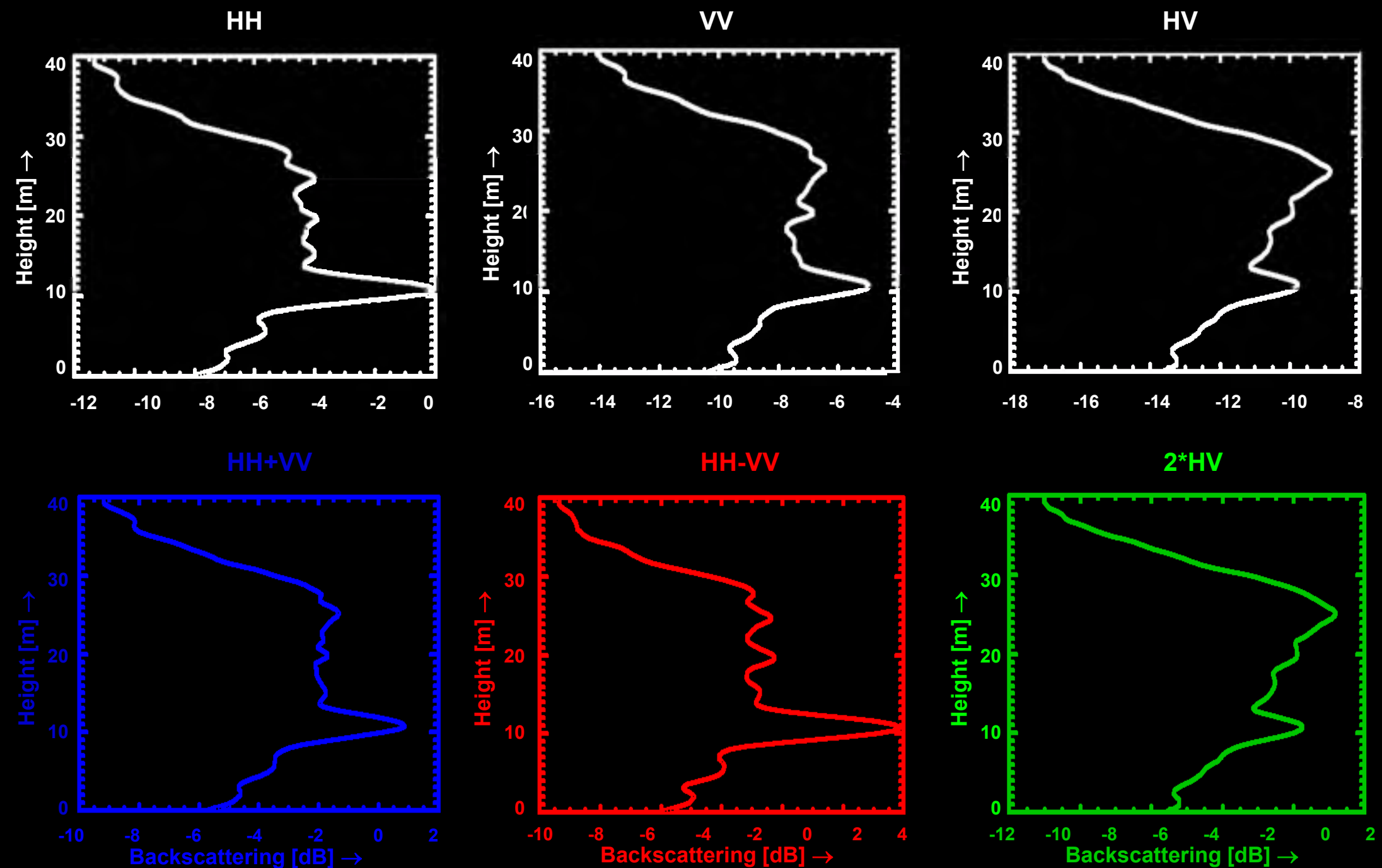
Airborne Polarimetric SAR Tomography

Upper image: Polarimetric color composite (L-band) of a tomographic slice in the height/azimuth-direction
■ HH+VV, ■ HH-VV, ■ 2*HV

Lower image: Schematic view of the imaged area



Spruce Forest Backscattering Profiles (15-20 m height)

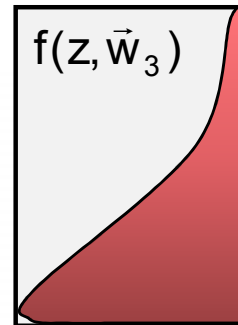


Mixed Forest Backscattering Profiles (12-20 m height)



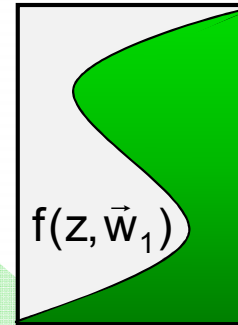
Polarisation 3 (w₃):

$$\tilde{\gamma}_{\text{Vol}}(f(z, \vec{w}_3)) = e^{ik_z z_0} \frac{\int_0^{h_v} f(z, \vec{w}_3) e^{ik_z z} dz}{\int_0^{h_v} f(z, \vec{w}_3) dz}$$



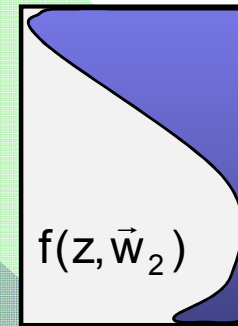
Polarisation 1 (w₁):

$$\tilde{\gamma}_{\text{Vol}}(f(z, \vec{w}_1)) = e^{ik_z z_0} \frac{\int_0^{h_v} f(z, \vec{w}_1) e^{ik_z z} dz}{\int_0^{h_v} f(z, \vec{w}_1) dz}$$

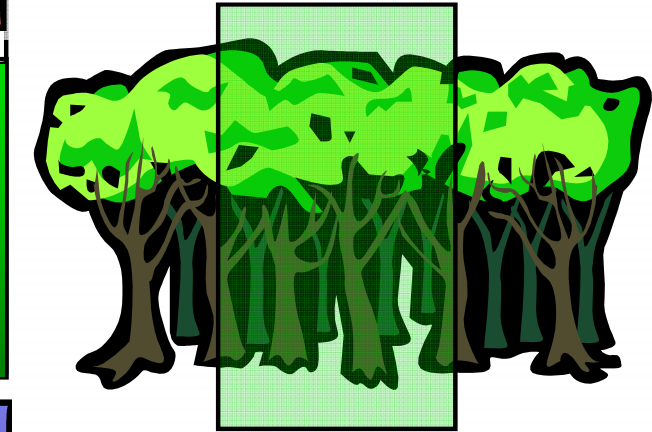


Polarisation 2 (w₂):

$$\tilde{\gamma}_{\text{Vol}}(f(z, \vec{w}_2)) = e^{ik_z z_0} \frac{\int_0^{h_v} f(z, \vec{w}_2) e^{ik_z z} dz}{\int_0^{h_v} f(z, \vec{w}_2) dz}$$

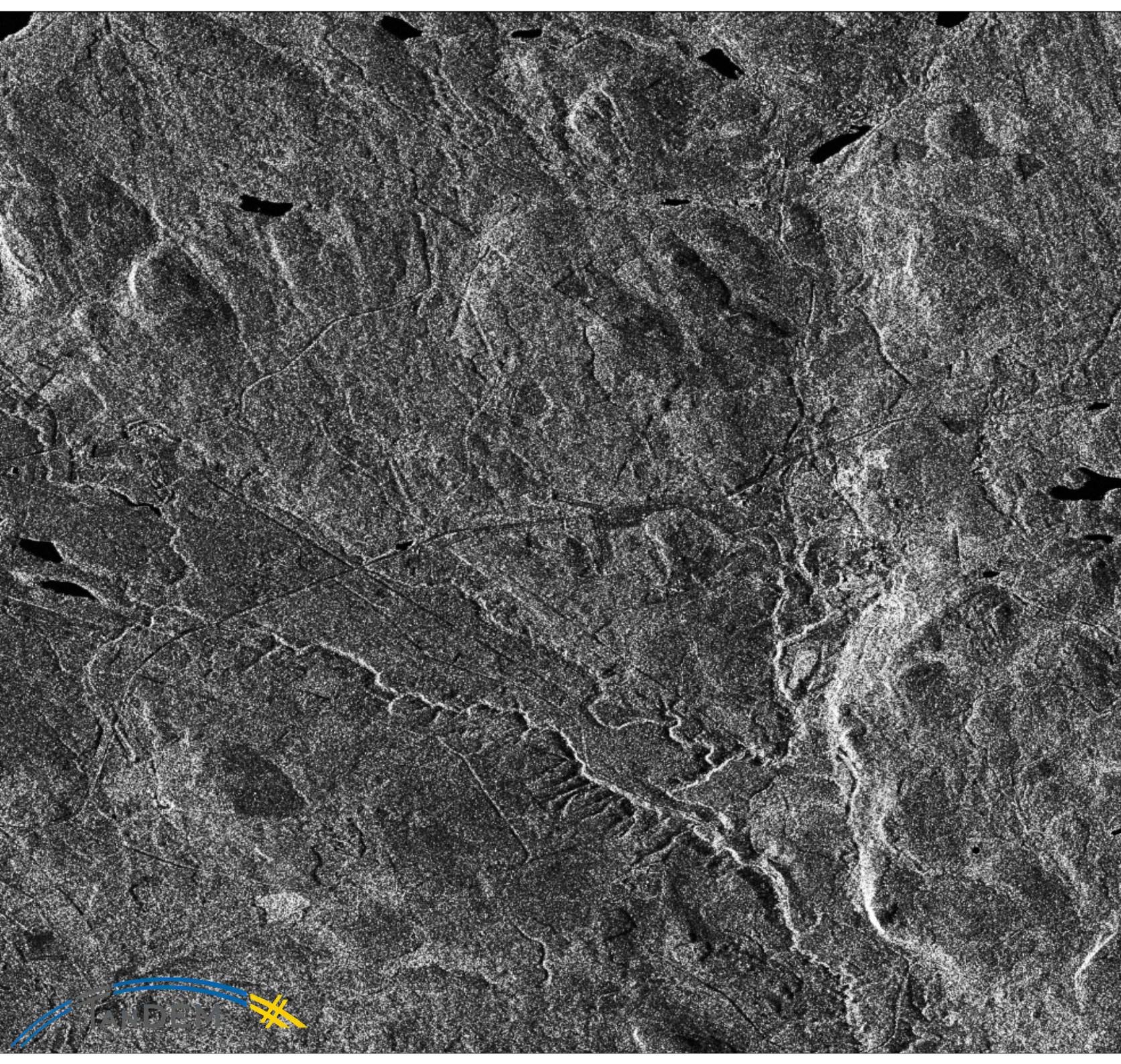


$f(z, \vec{w})$...vertical reflectivity function



Polarimetric SAR Interferometry

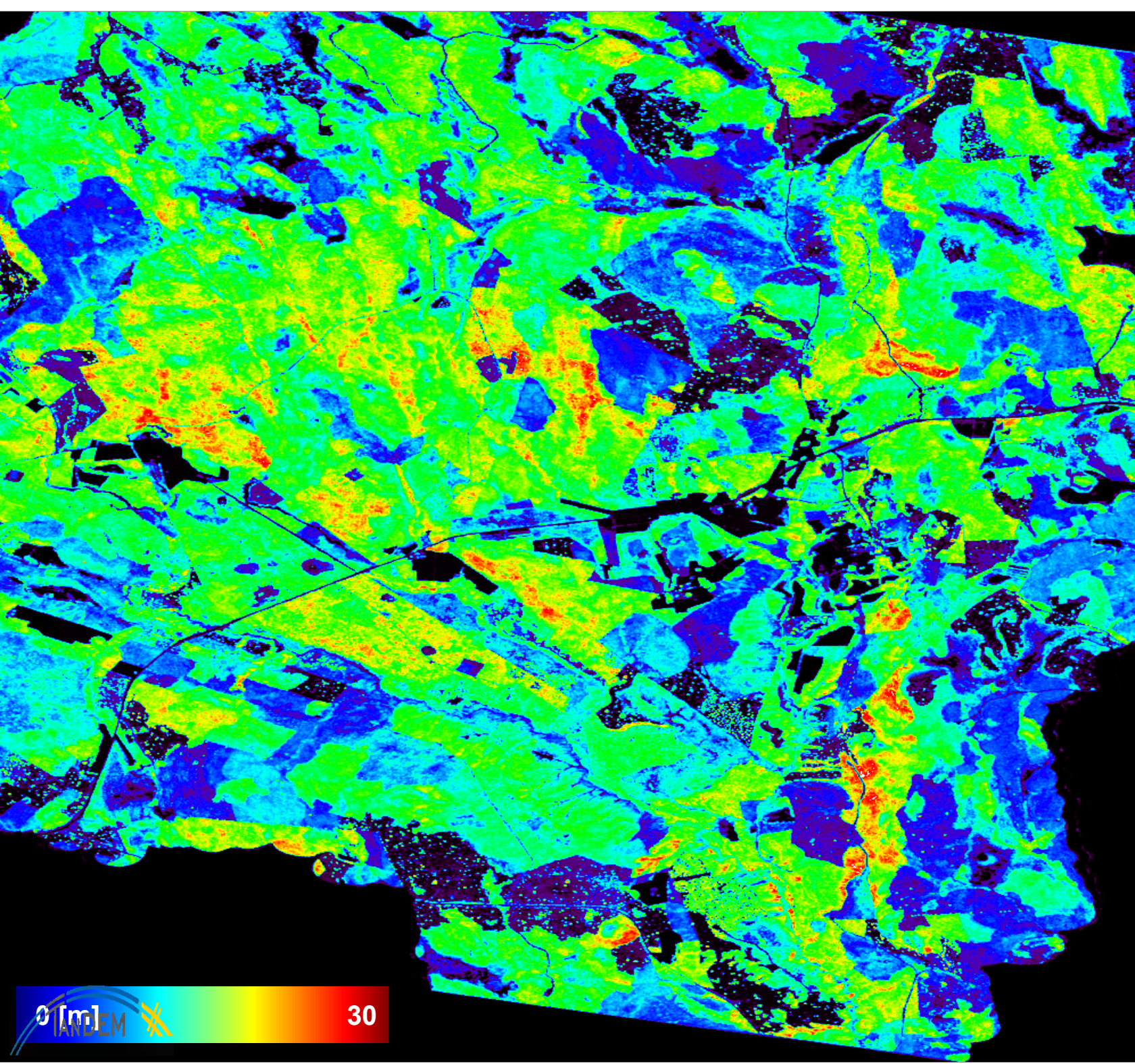
By changing the polarisation the contrast between the individual components consisting the vertical reflectivity $f(z)$ of a (volume) scatterer changes.



**Test Site: Krycklan,
Sweden**



Test Site: Krycklan,
Sweden





**Test Site: Krycklan,
Sweden**

Structure Parameters & Applications

Forest

- Forest Height
- Forest (Vertical) Structure
- Forest Biomass
- Underlying Topography



- Forest Ecology
- Forest Management
- Ecosystem Modeling
- Climate Change

Agriculture

- Underlying Soil Moisture
- Moisture of Vegetation Layer
- Height of Vegetation Layer
- Soil Roughness



- Farming Management
- Ecosystem Modeling
- Water Cycle / CC
- Desertification

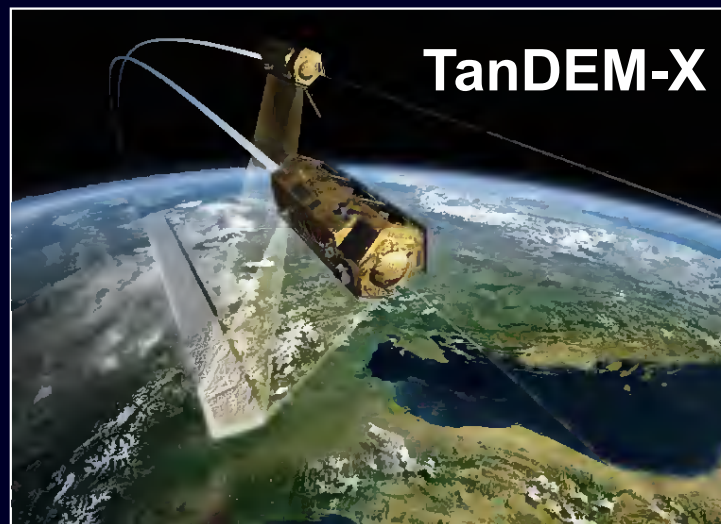
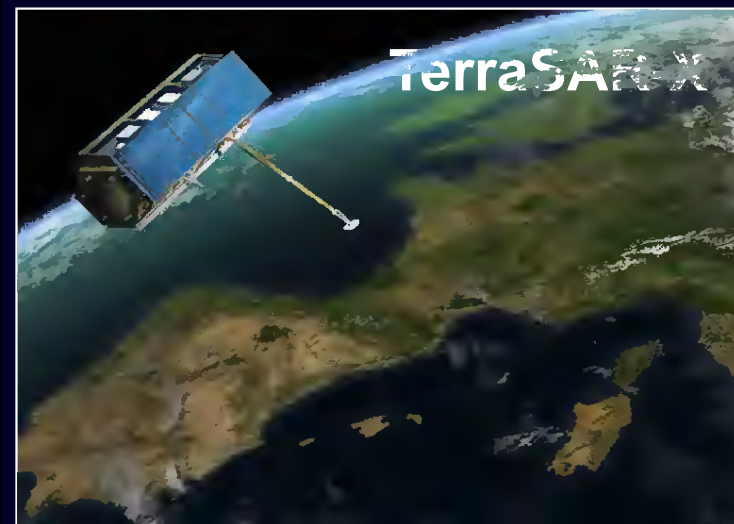
Snow & Ice

- Ice Layer Structure
- Penetration Depth (Ice)
- Snow Layer Thickness
- Snow Water Equivalent

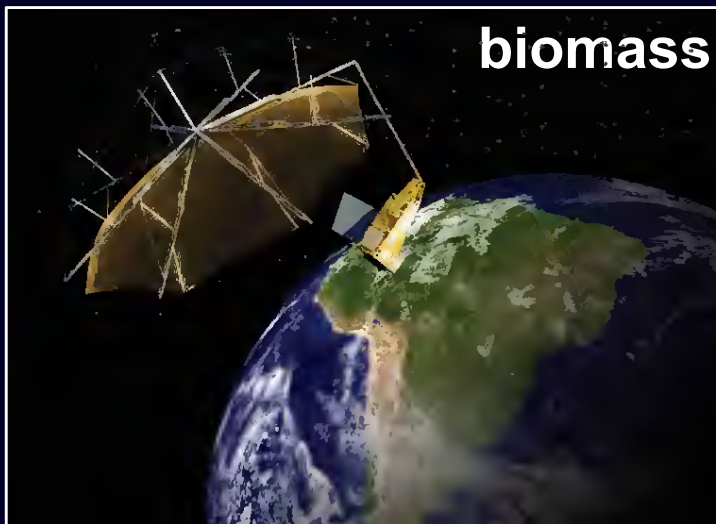
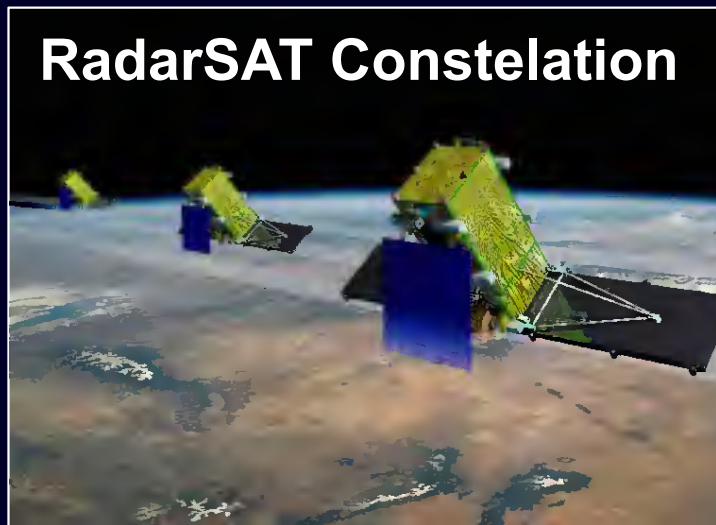
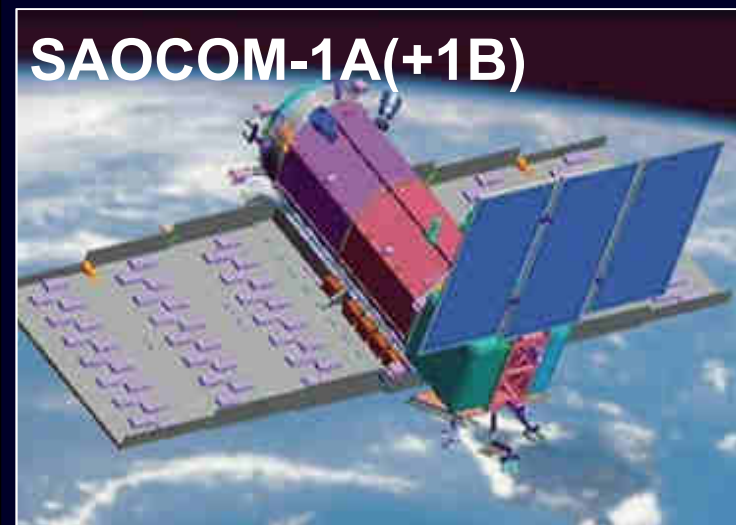


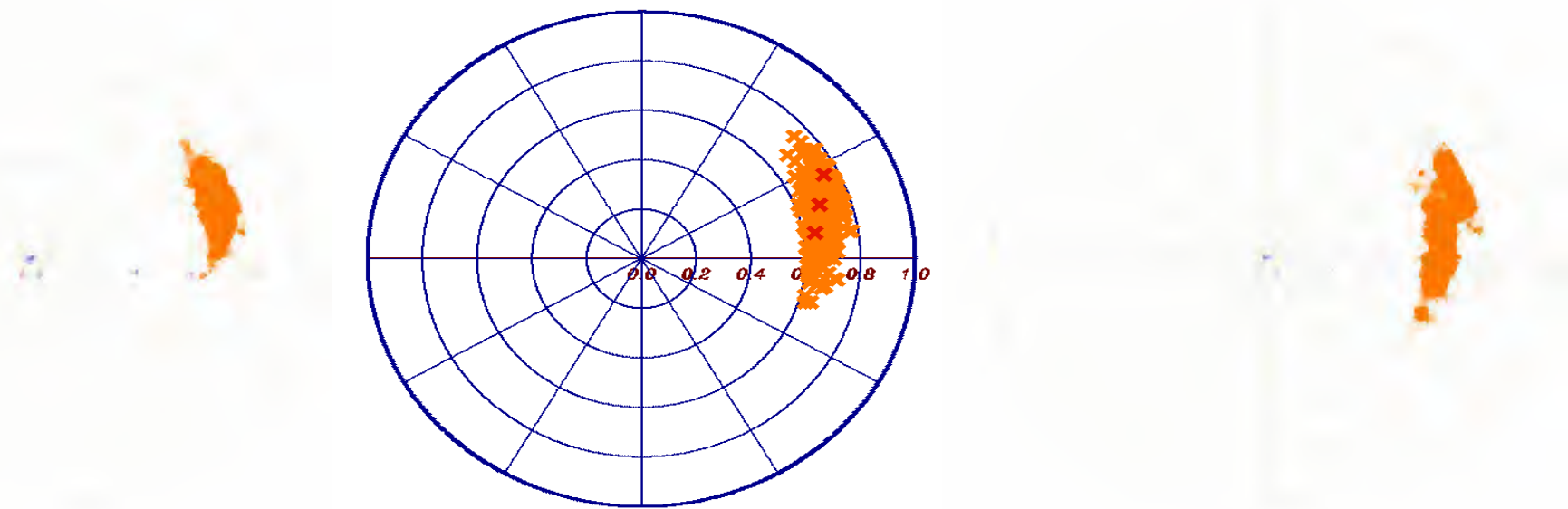
- Ecosystem Change
- Water Cycle
- Water Management

Pol-InSAR In Orbit

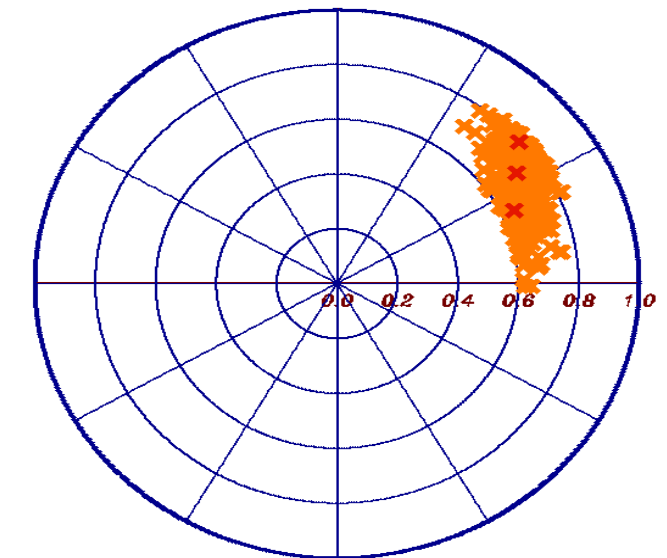
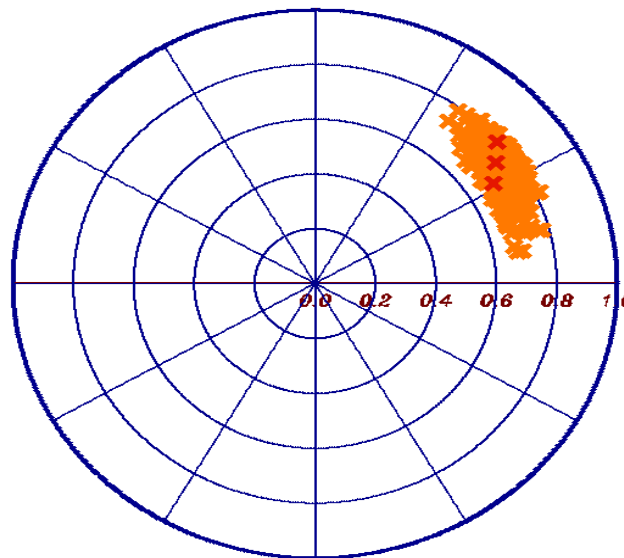
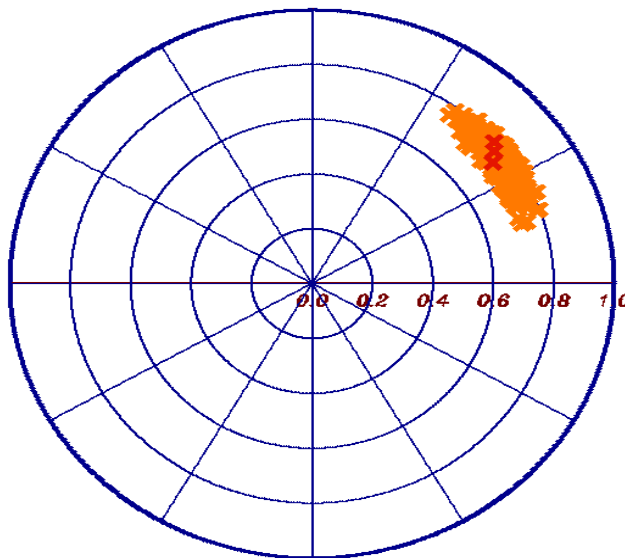


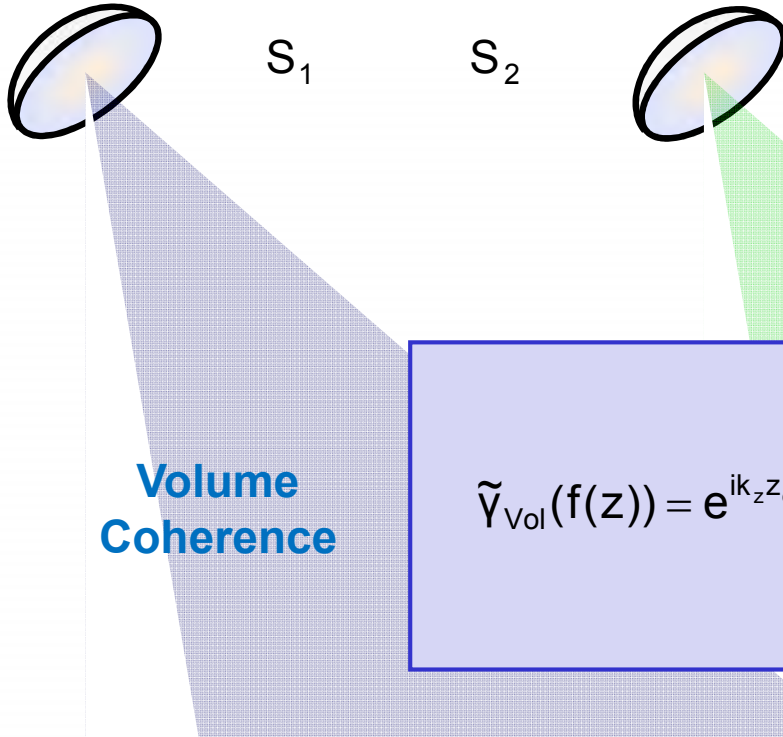
Pol-InSAR In Orbit





Pol-InSAR: Modelling and Inversion

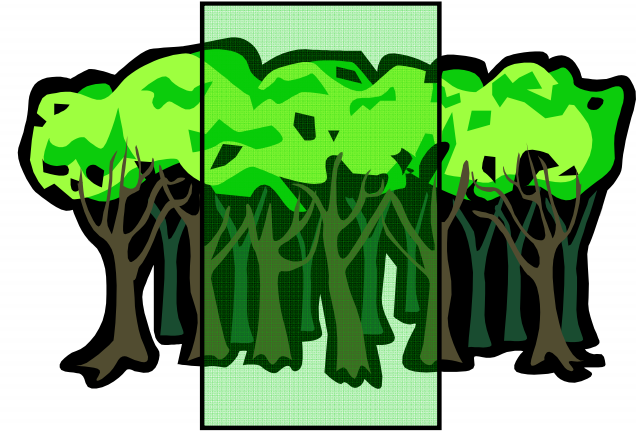
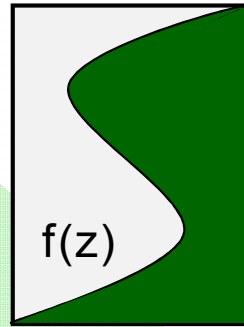




Interferometric Coherence

$$\tilde{\gamma}(S_1, S_2) = \frac{\langle S_1 S_2^* \rangle}{\sqrt{\langle S_1 S_1^* \rangle \langle S_2 S_2^* \rangle}}$$

$$\tilde{\gamma}_{Vol}(f(z)) = e^{ik_z z_0} \frac{\int_0^{h_v} f(z) e^{ik_z z} dz}{\int_0^{h_v} f(z) dz}$$



Volume Layer Ground Layer

$$f(z) = m_V f_V(z) + m_G \delta(z - z_0)$$

$f_V(z)$... volume reflectivity function

2 Layer Inversion Model

$$\tilde{\gamma}_{Vol} = \exp(i\phi_0) \frac{\tilde{\gamma}_V + m}{1+m}$$

Volume Coherence

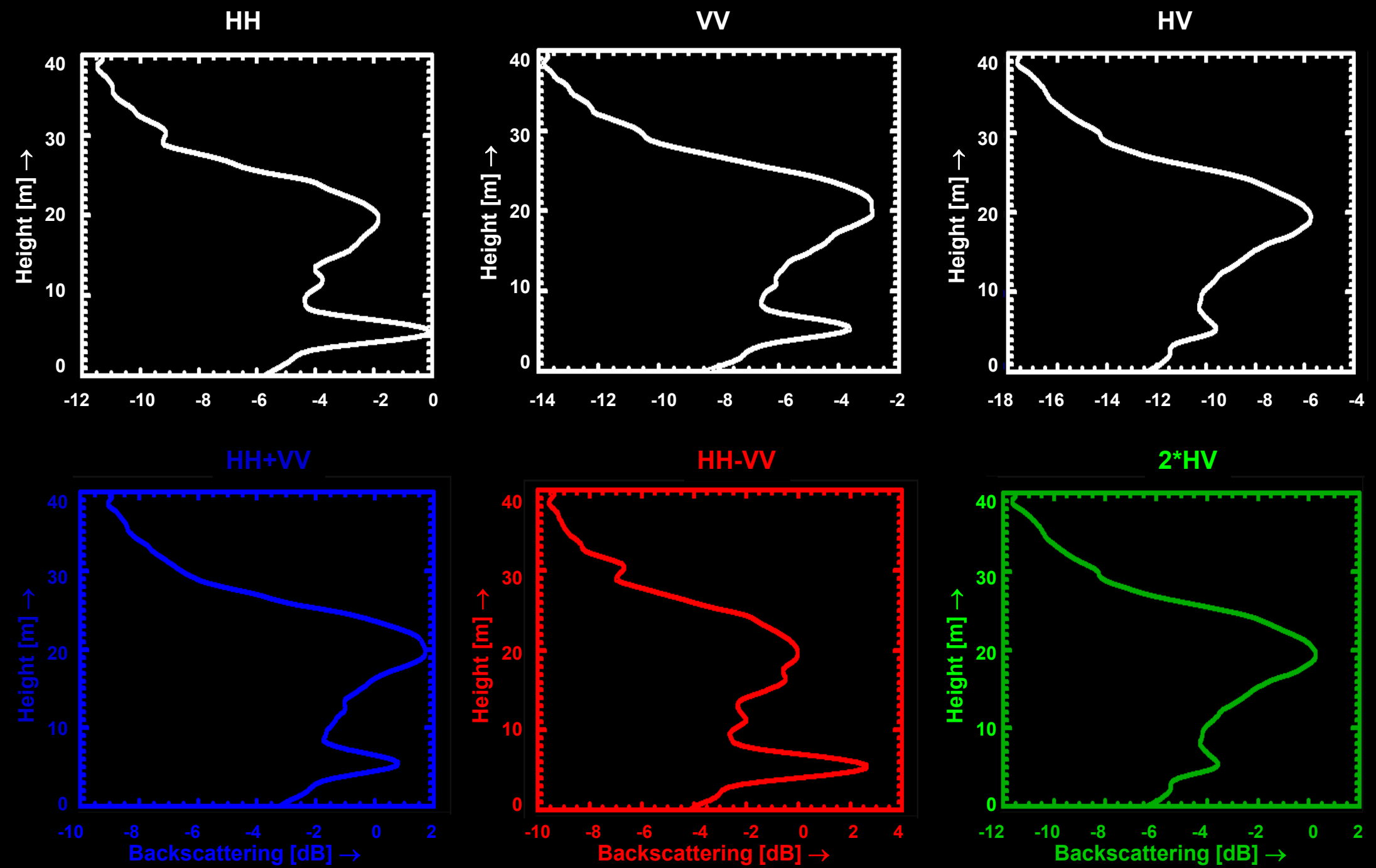
$$\tilde{\gamma}_V = \frac{I}{I_0} \quad \left\{ \begin{array}{l} I = \int_0^{h_v} \exp(i\kappa_z z') f_V(z') dz' \\ I_0 = \int_0^{h_v} f_V(z') dz' \end{array} \right.$$

with

$$m = \frac{m_G}{m_V I_0}$$

$$\kappa_z = \frac{\kappa \Delta \theta}{\sin(\theta_0)}$$

$f_V(z)$ parameterised by N parameters	
Vol. Height	h_v
Topography	ϕ_0
G / V Ratio	m

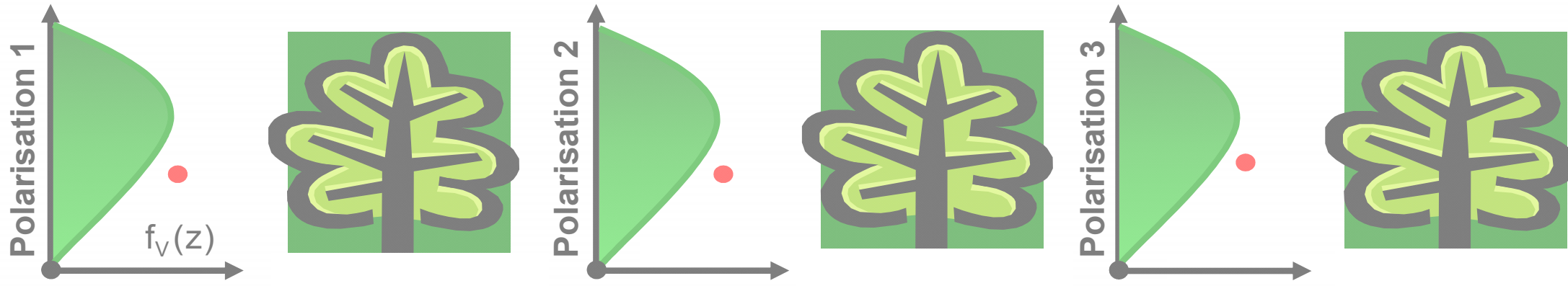


Spruce Forest Backscattering Profiles (15-20 m height)

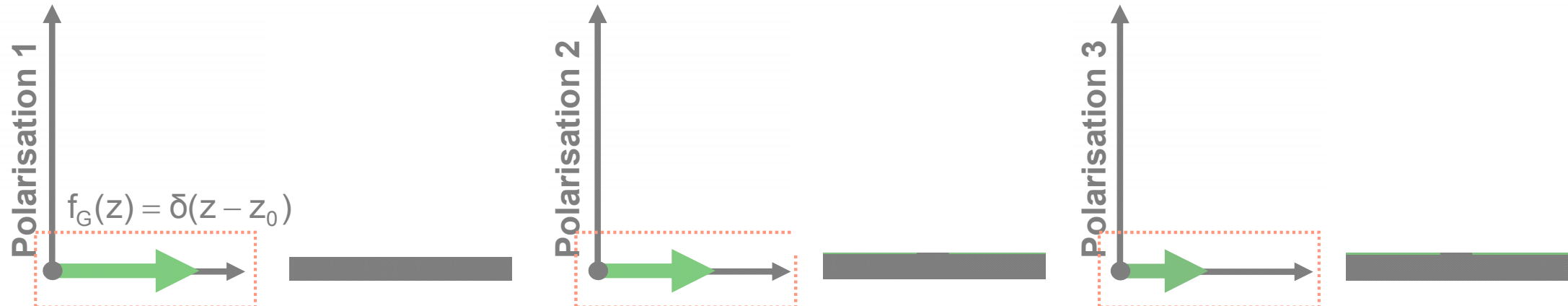
The Random Volume over Ground (RVoG) Model

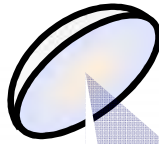
The RVoG model relies on two assumptions:

1. The vertical reflectivity function of the volume layer $f_v(z)$ is (up to a scaling factor $m_v(\vec{w})$) the same for all polarisations. All polarisations see the same (vertical) distribution of scatterers in the volume;



2. The Ground is impenetrable, i.e. the vertical reflectivity of the bare ground is given by a Dirac delta modulated by an (strongly) polarimetric dependent amplitude $m_G = m_G(\vec{w})$.



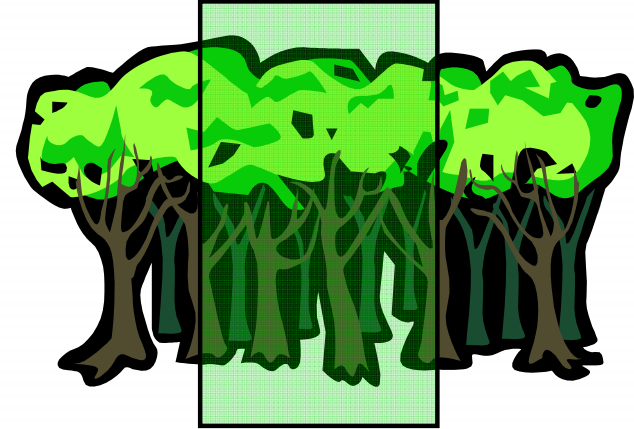
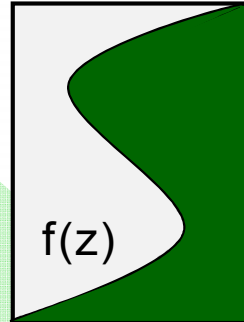
 S_1 S_2 

Interferometric Coherence

$$\tilde{\gamma}(S_1, S_2) = \frac{\langle S_1 S_2^* \rangle}{\sqrt{\langle S_1 S_1^* \rangle \langle S_2 S_2^* \rangle}}$$

Volume Coherence

$$\tilde{\gamma}_{Vol}(f(z)) = e^{ik_z z_0} \frac{\int_0^{h_v} f(z) e^{ik_z z} dz}{\int_0^{h_v} f(z) dz}$$



Volume Layer Ground Layer

$$f(z, \vec{w}) = m_V(\vec{w}) f_V(z) + m_G(\vec{w}) \delta(z - z_0)$$

2 Layer Inversion Model

$$\tilde{\gamma}_{Vol}(\vec{w}) = \exp(i\varphi_0) \frac{\tilde{\gamma}_V + m(\vec{w})}{1 + m(\vec{w})}$$

$f_V(z)$... volume reflectivity function

Volume Coherence

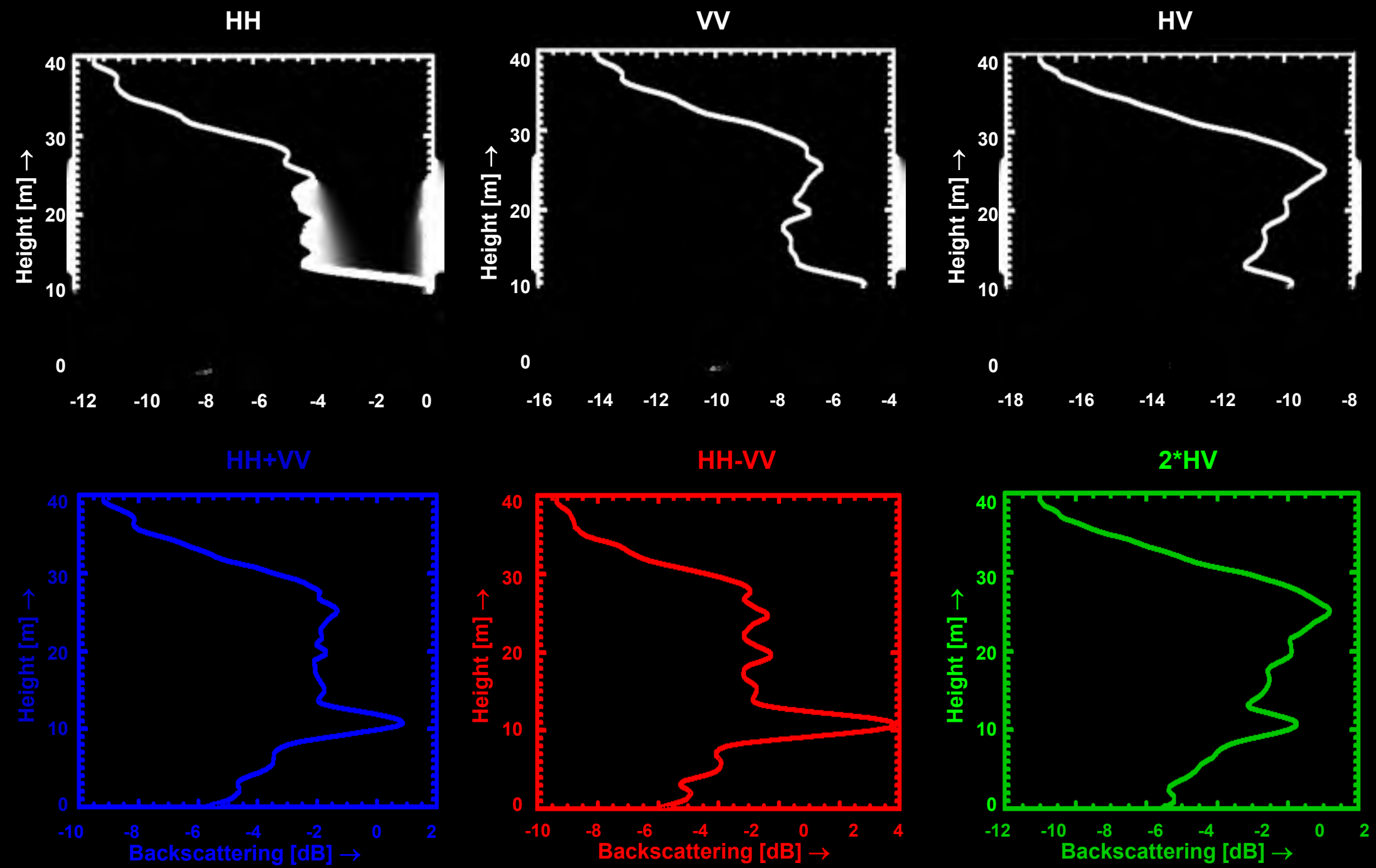
$$\tilde{\gamma}_V = \frac{I}{I_0} \quad \left\{ \begin{array}{l} I = \int_0^{h_v} \exp(i\kappa_z z') f_V(z') dz' \\ I_0 = \int_0^{h_v} f_V(z') dz' \end{array} \right.$$

with

$$m(\vec{w}) = \frac{m_G(\vec{w})}{m_V(\vec{w}) I_0}$$

$$\kappa_z = \frac{\kappa \Delta \theta}{\sin(\theta_0)}$$

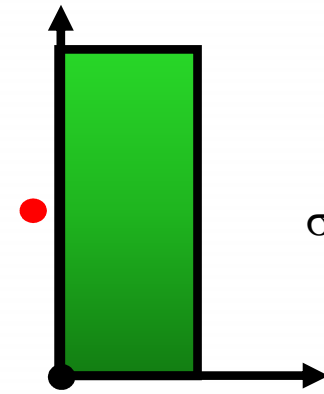
- $f_V(z)$ parameterised by N parameters
- Vol. Height h_v
- Topography φ_0
- G / V Ratio $m(\vec{w})$



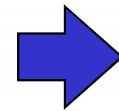
Mixed Forest Backscattering Profiles (12-20 m height)

Simple Models for $\sigma_v(z)$

Constant Profile

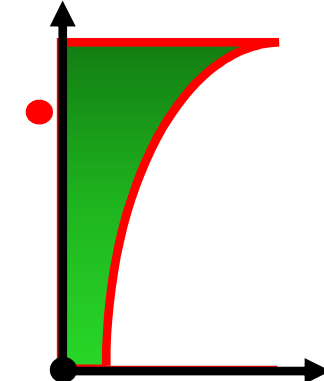


$$\sigma_v(z) = \text{ct.}$$



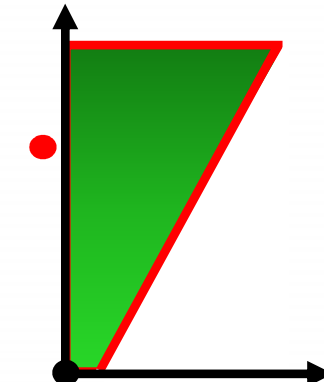
$$\tilde{\gamma}_{\text{vol}} = \exp[i(\frac{\kappa_z h_v}{2} + \phi_0)] \frac{\sin(\frac{\kappa_z h_v}{2})}{\frac{\kappa_z h_v}{2}}$$

Exponential Profile



$$\sigma_v(z) = \sigma_{v0} \exp\left(\pm \frac{2 \sigma z}{\cos \theta_0}\right)$$

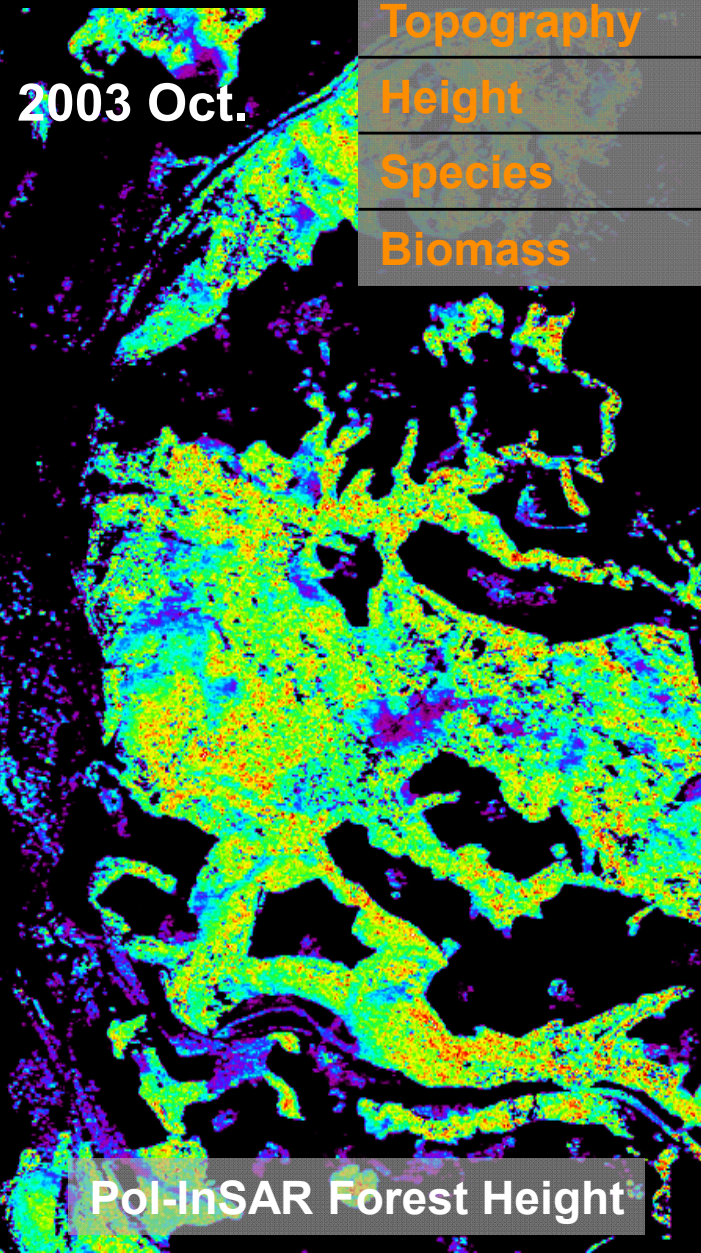
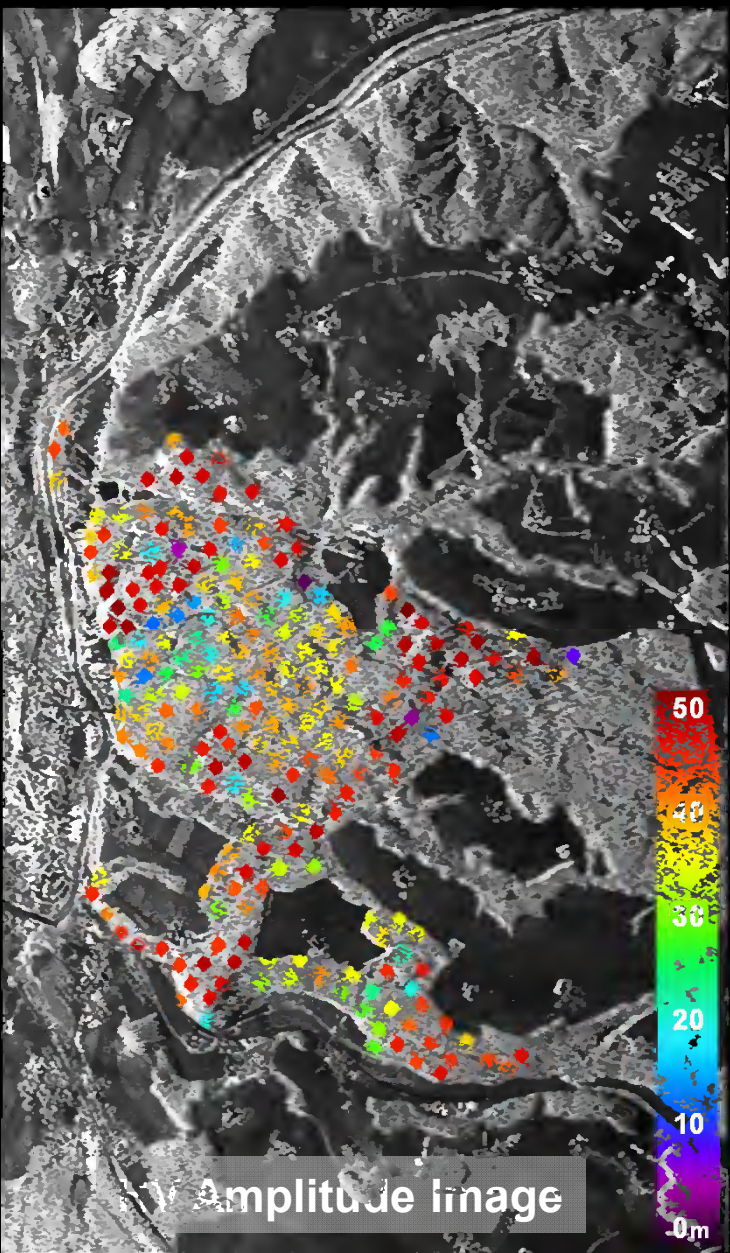
Linear Profile



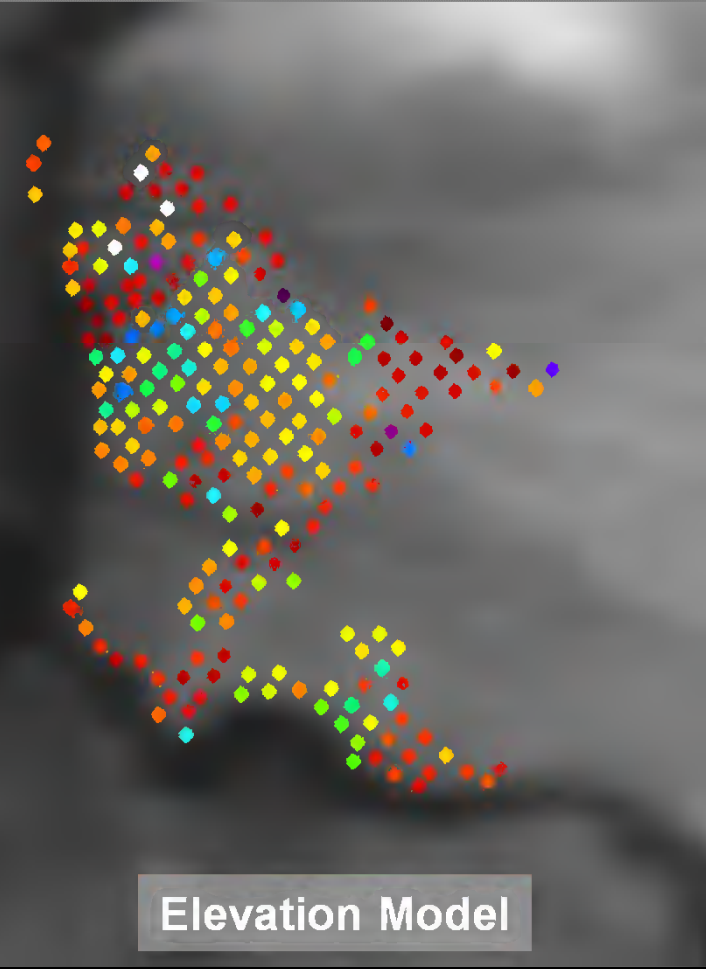
$$\sigma_v(z) = \sigma_{v0} \left(\pm \frac{2 \sigma z}{\cos \theta_0} + 1 \right)$$



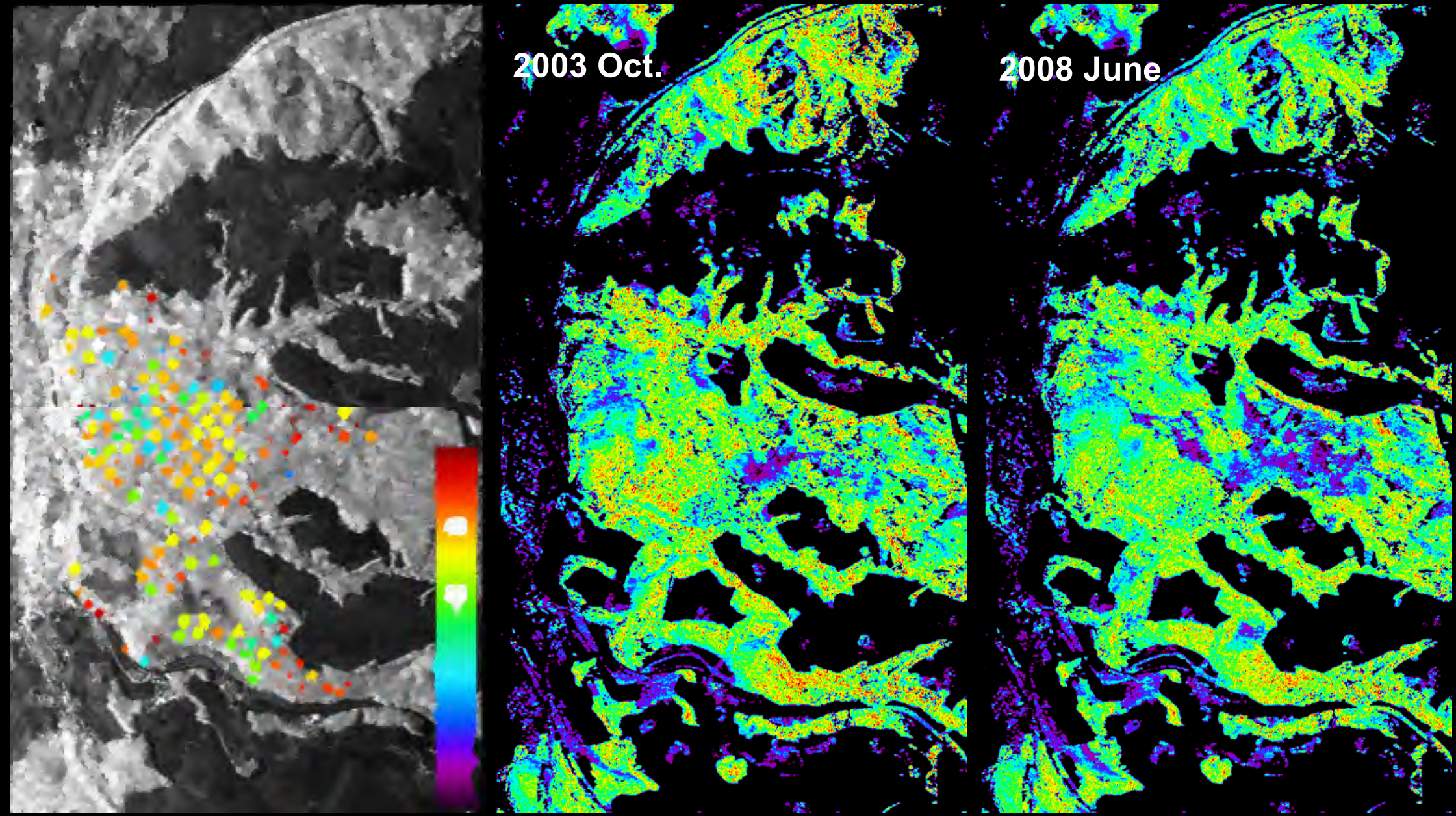
Traunstein Test Site



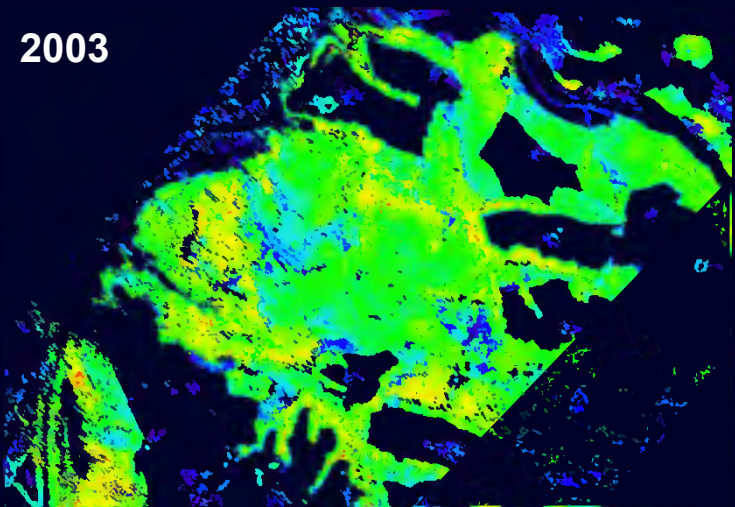
Forest type	Temperate
Topography	Moderate slopes
Height	25 ~ 35m
Species	N. Spruce, E. Beech, White Fir
Biomass	40 ~ 450 t/ha



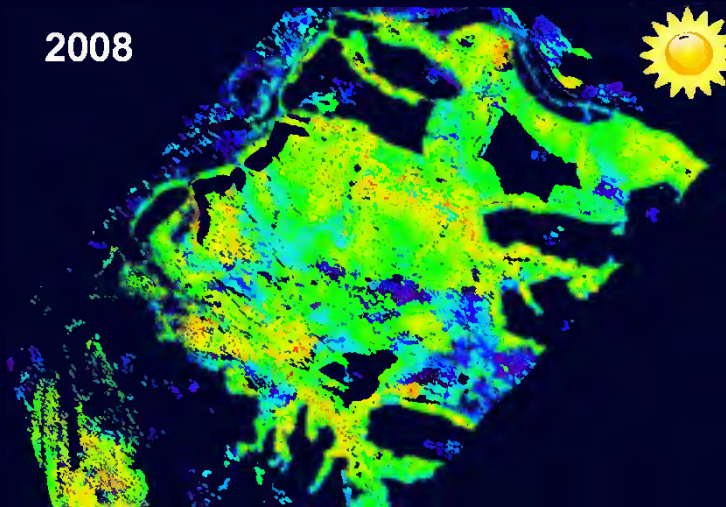
Traunstein Test Site



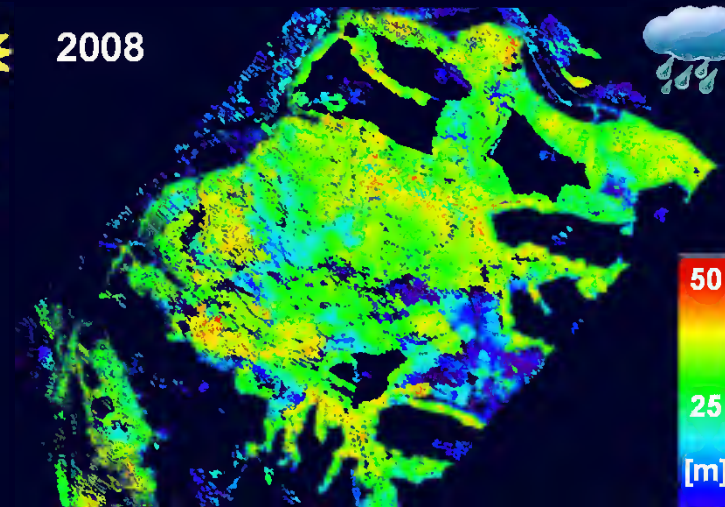
2003



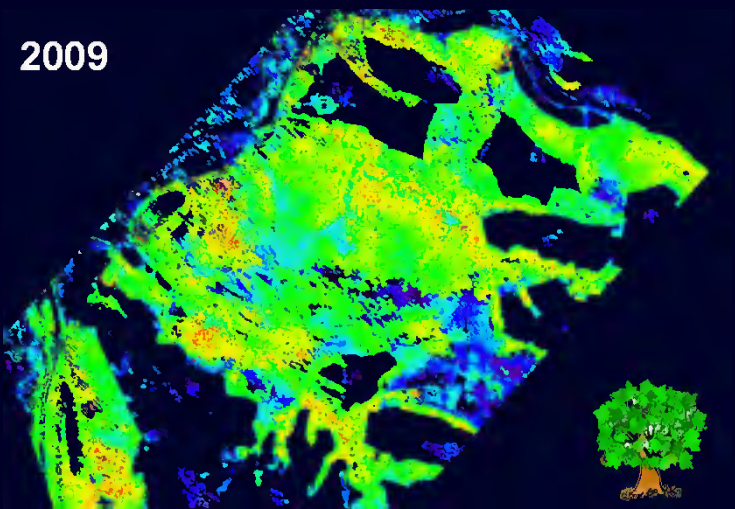
2008



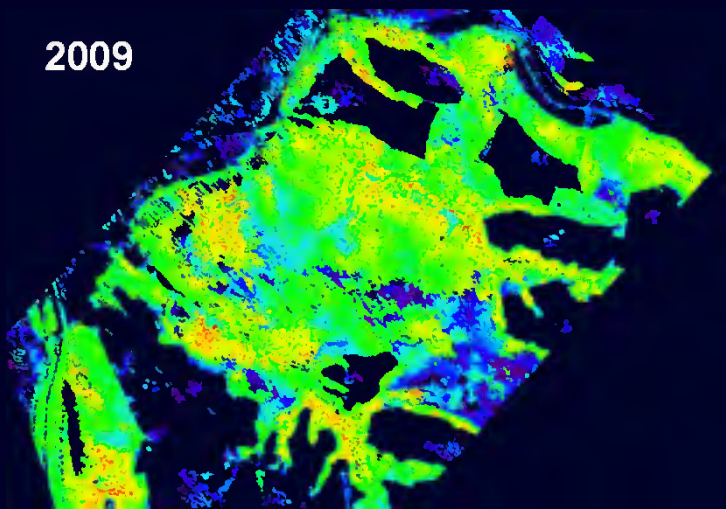
2008



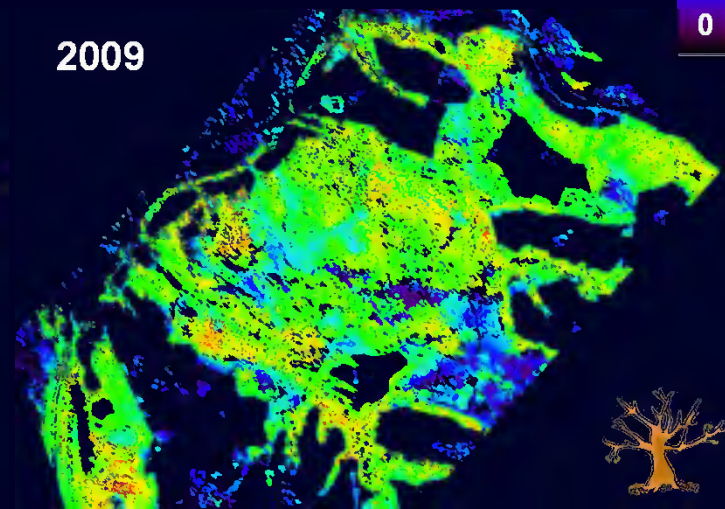
2009



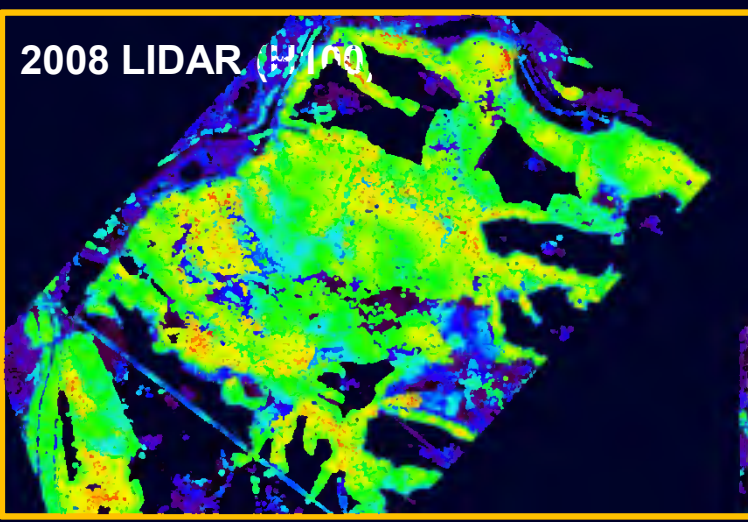
2009



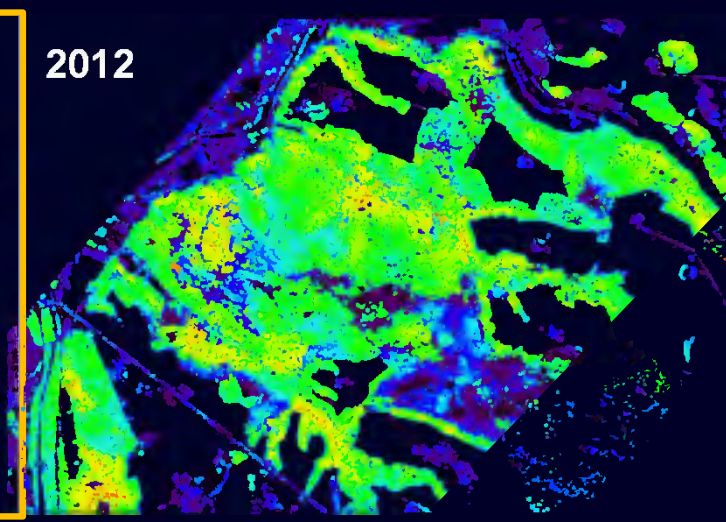
2009



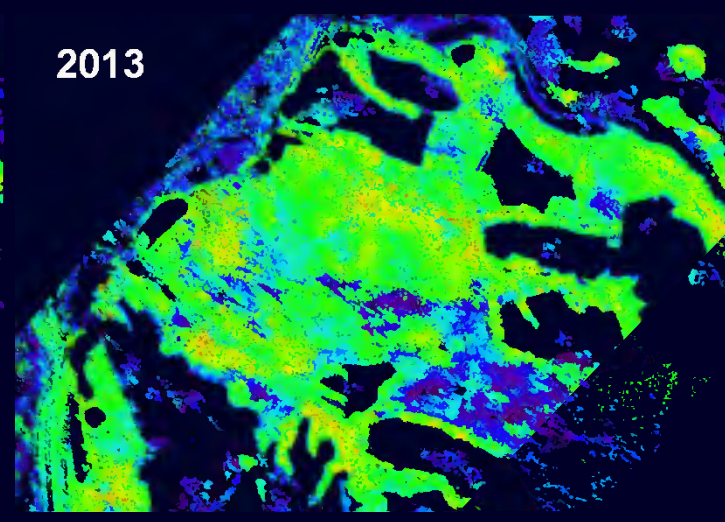
2008 LIDAR (WFO)



2012

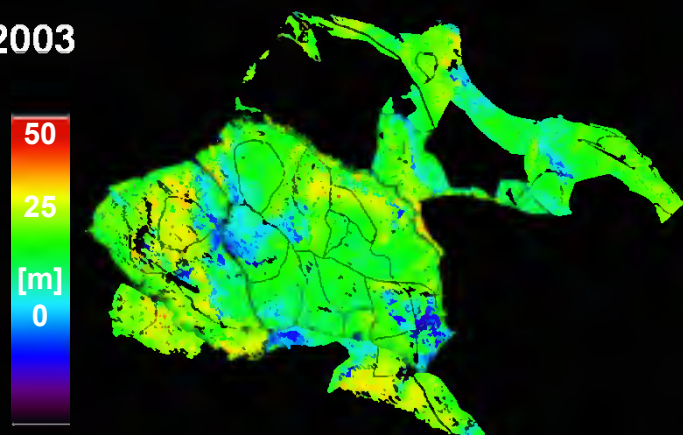


2013

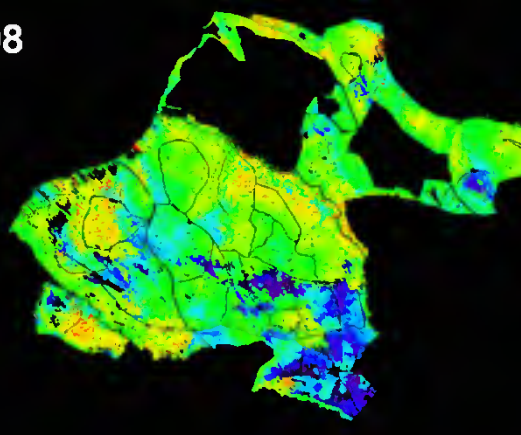


50
25
[m]
0

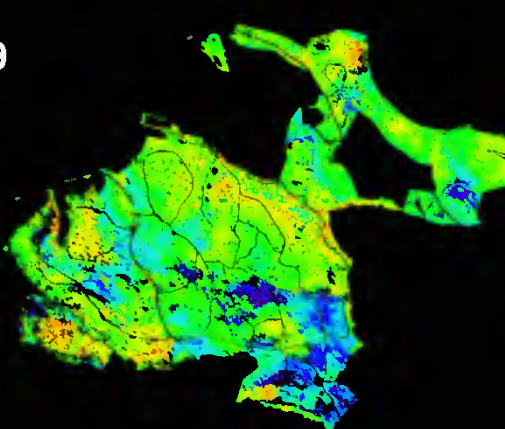
2003



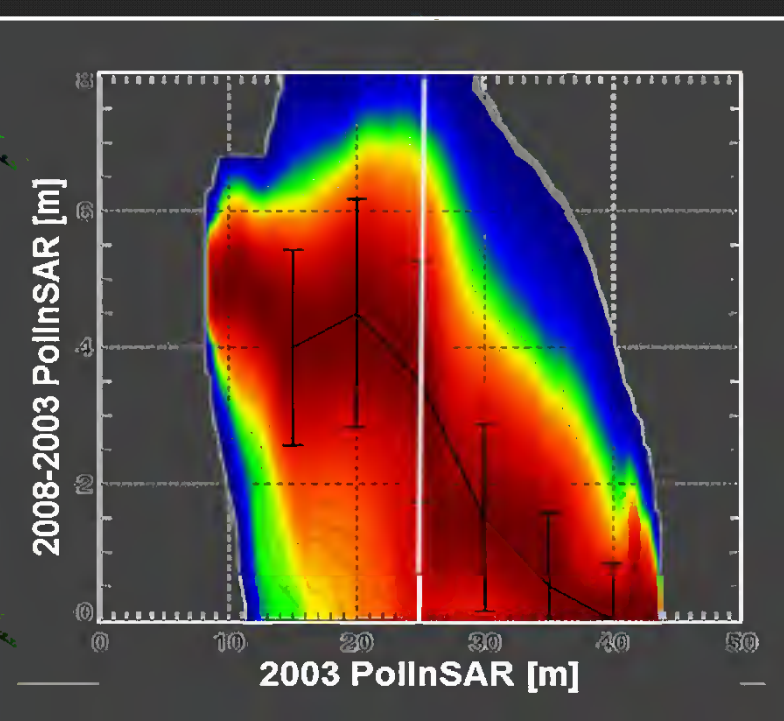
2008



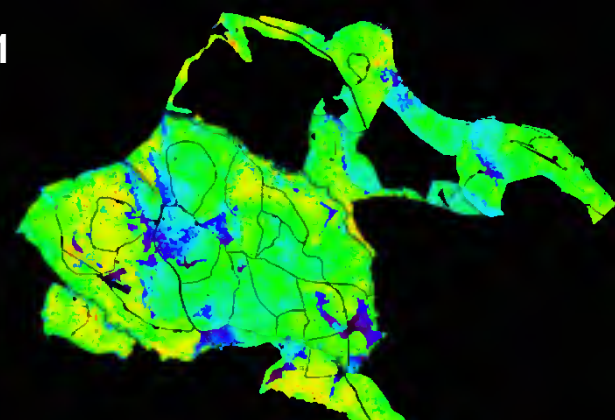
2009



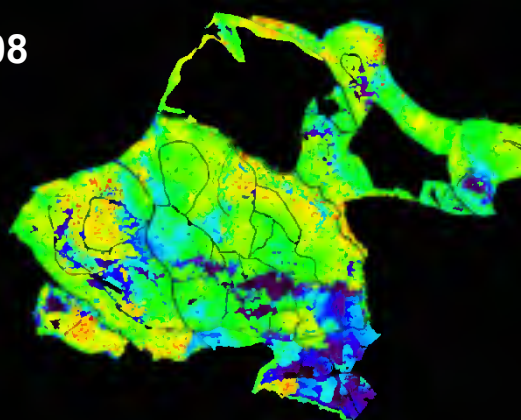
Pol-InSAR Height (H100) Estimates / L-band / Traunstein, Germany



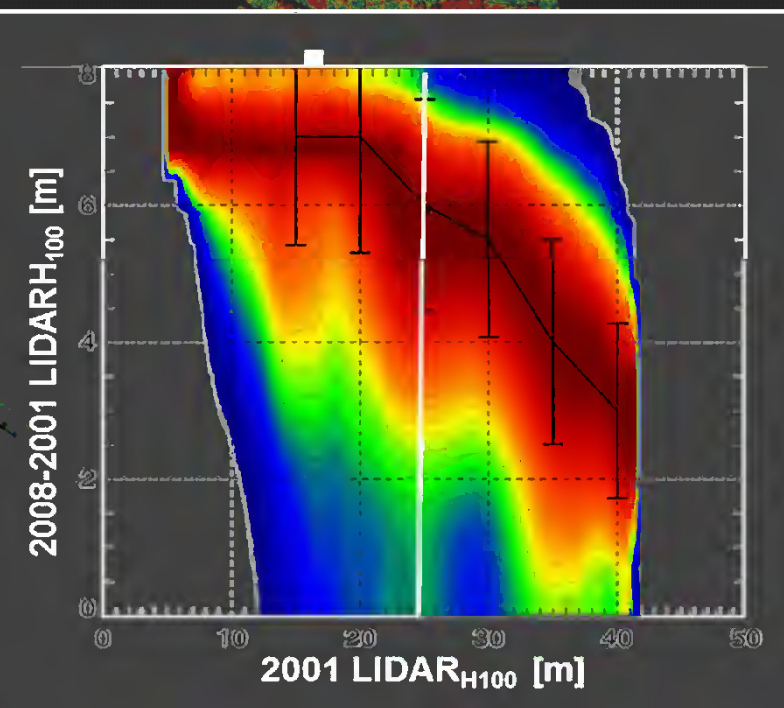
2001



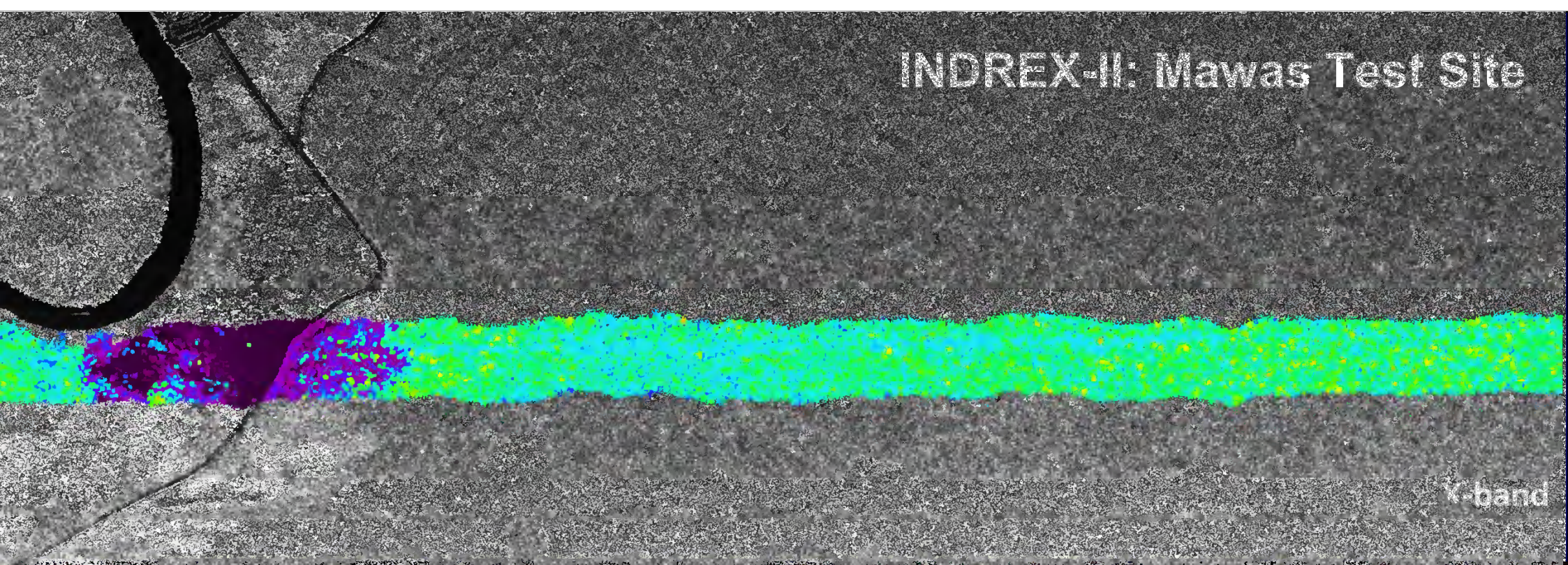
2008



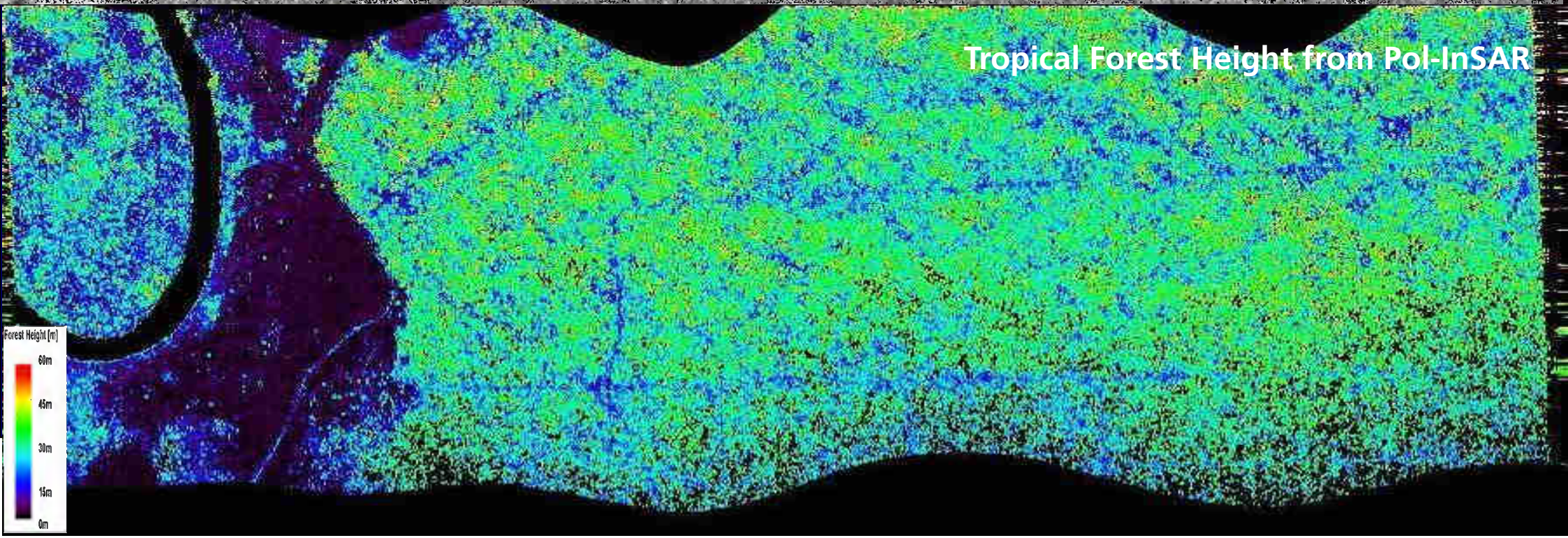
Airborne Lidar Height (H100) Estimates / L-band / Traunstein, Germany



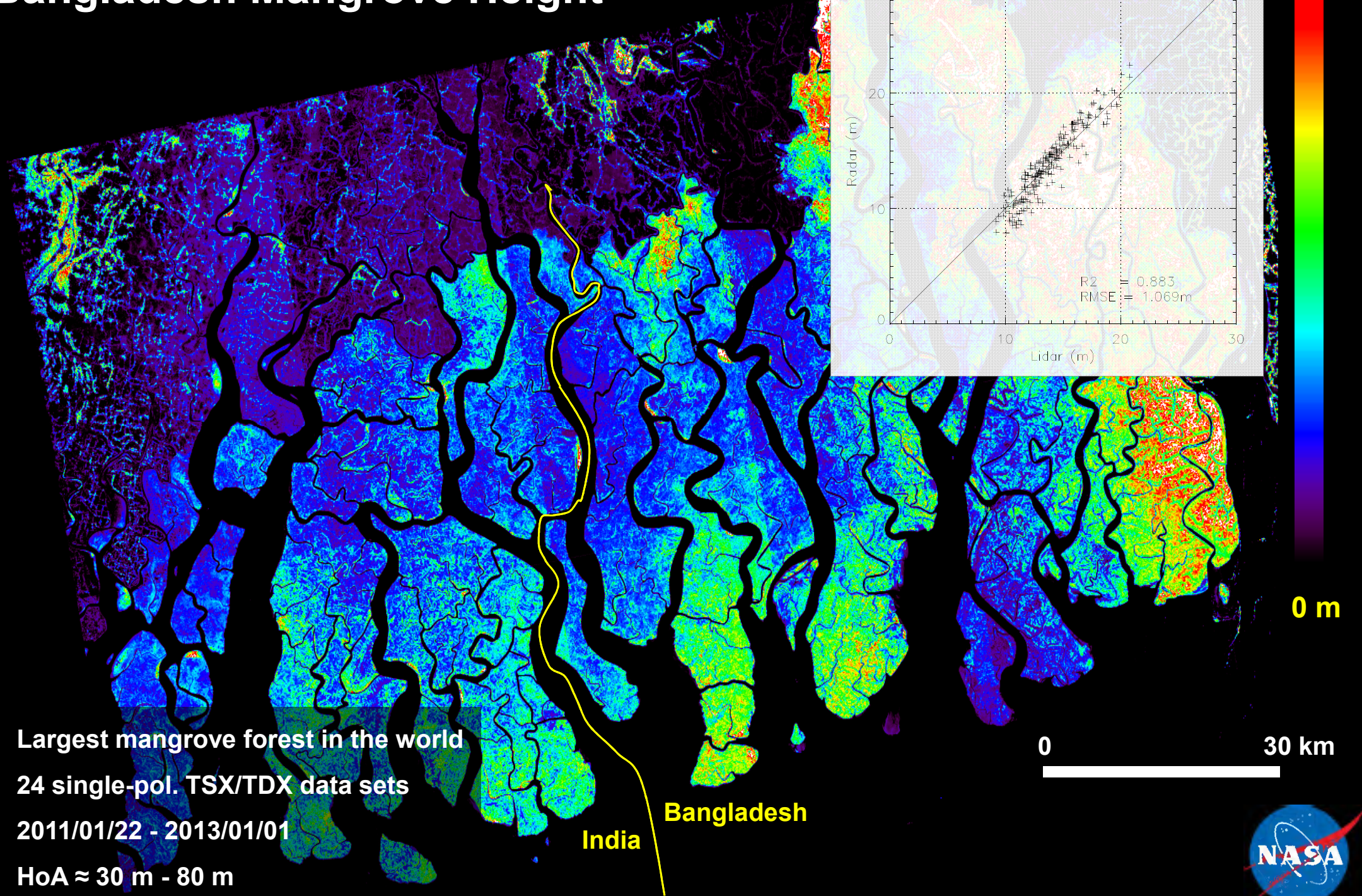
INDREX-II: Mawas Test Site

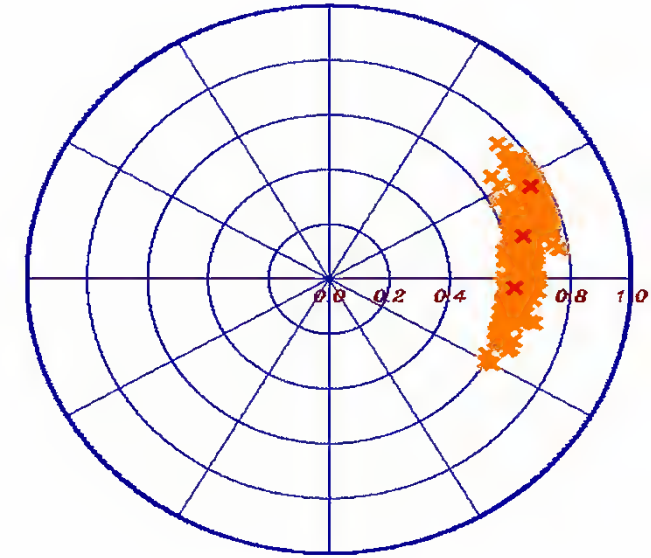
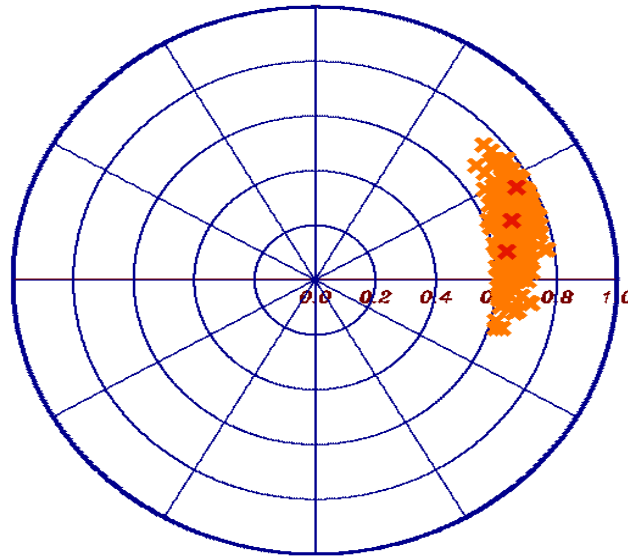
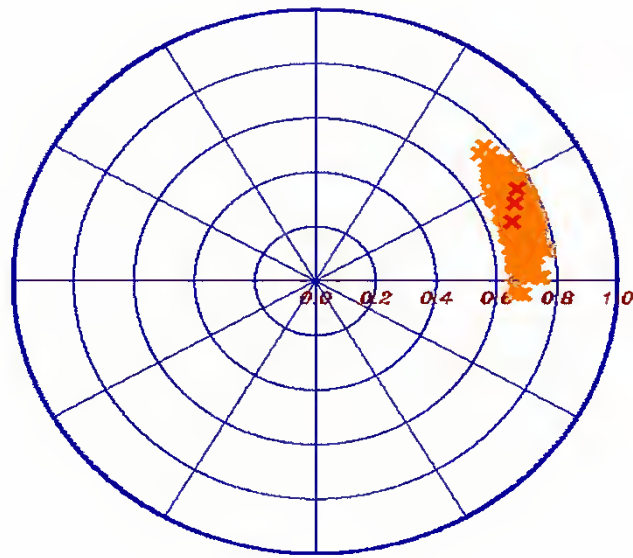


Tropical Forest Height from Pol-InSAR

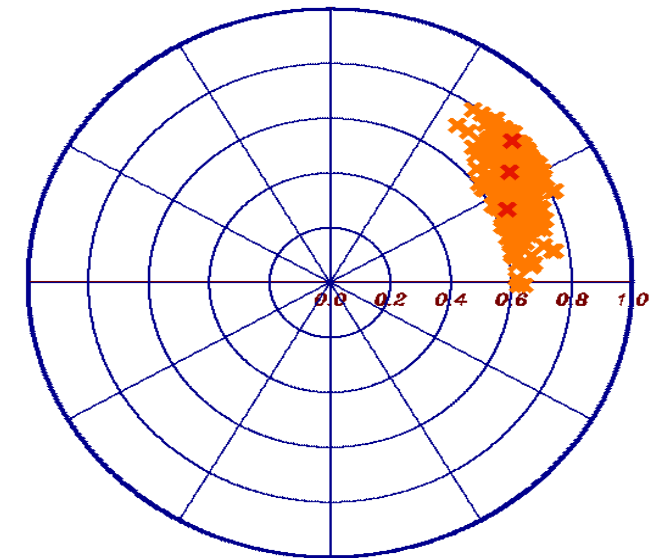
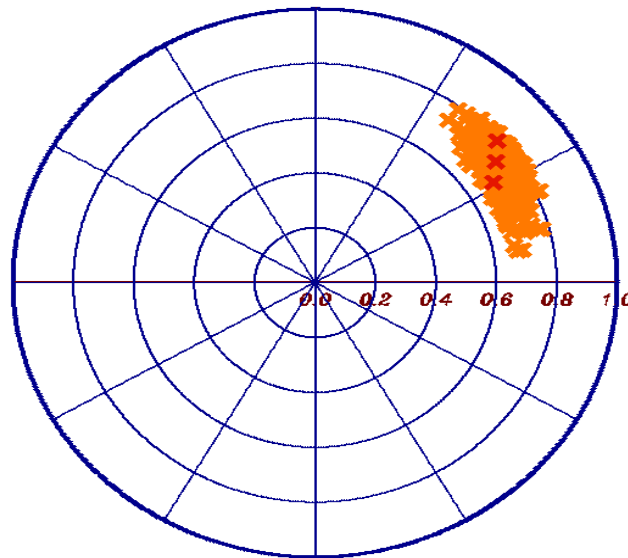
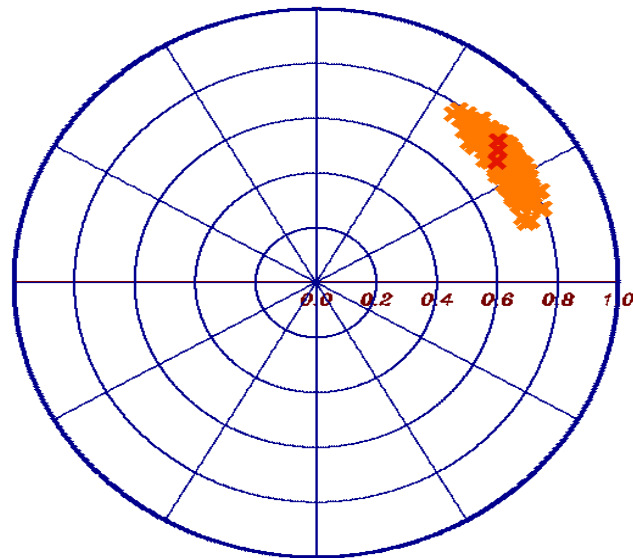


Bangladesh Mangrove Height





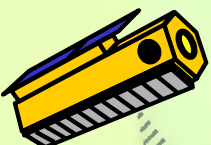
Agriculture Vegetation



Agriculture Pol-InSAR Applications

Pol-SAR

$$[\mathbf{S}] = \begin{bmatrix} S_{HH} & S_{HV} \\ S_{VH} & S_{VV} \end{bmatrix}$$



Pol-InSAR

$$[\mathbf{S}_1] = \begin{bmatrix} S_{HH}^1 & S_{HV}^1 \\ S_{VH}^1 & S_{VV}^1 \end{bmatrix}$$

$$[\mathbf{S}_2] = \begin{bmatrix} S_{HH}^2 & S_{HV}^2 \\ S_{VH}^2 & S_{VV}^2 \end{bmatrix}$$

Bare Surfaces: Isolated Scattering Center

- Low Entropy scatterers -> High polarimetric coherence

Vegetated Surfaces: Volume Scatterers

- High Entropy scatterers -> Low polarimetric coherence

Agricultural vs. Forest Vegetation

Orientation effects in the vegetation layer ➡

Thinner / shorter vegetation layer ➡

Short crop / plant phenological cycle ➡

Variety of crop / plant str.

Increased Importance
Large scattering volumes

Short crop / plant phenological cycle

Abstract

Volume Scattering

Scatterers



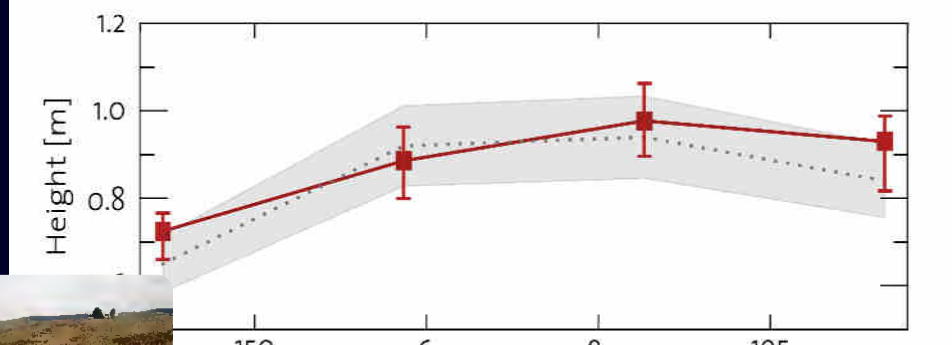
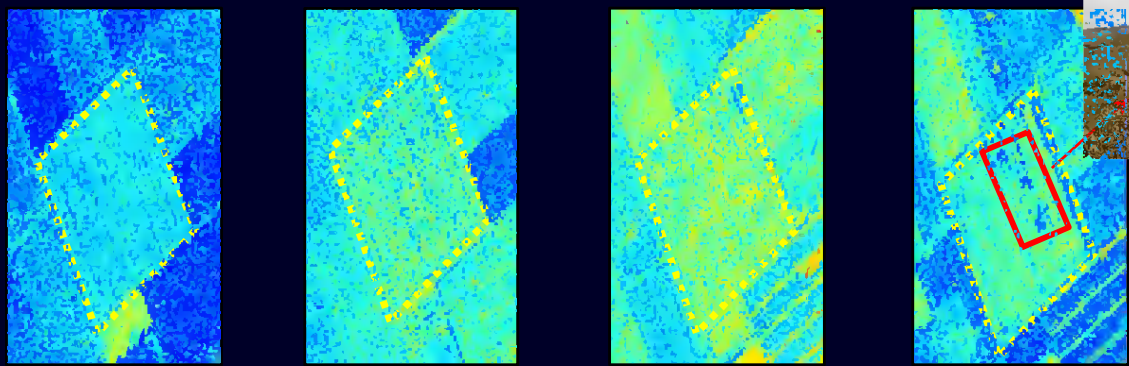
Wheat



May 22 Jun 12

Jul 03

Jul 24



■ Estimated height
··· In-situ height
□ 10% uncertainty

Sensor: DLR's F-SAR

Frequency: C-Band (≈ 5 GHz)

Number of spatial baselines: 2

Max. temporal baseline: 90 minutes

Equivalent Number of Looks: 100

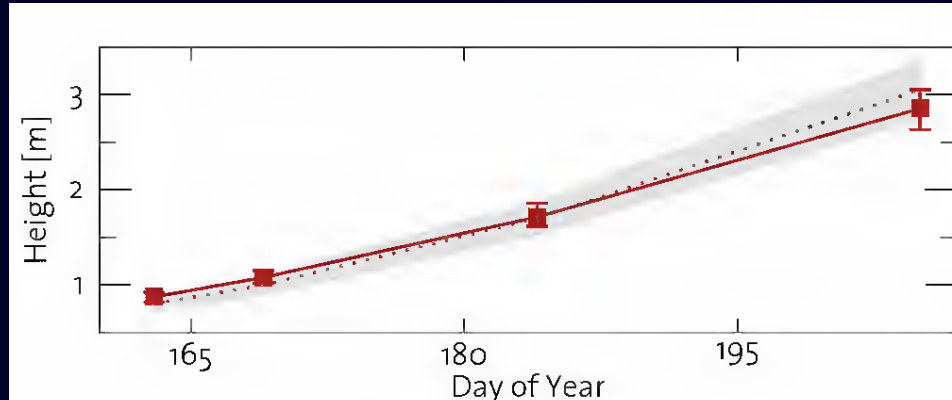
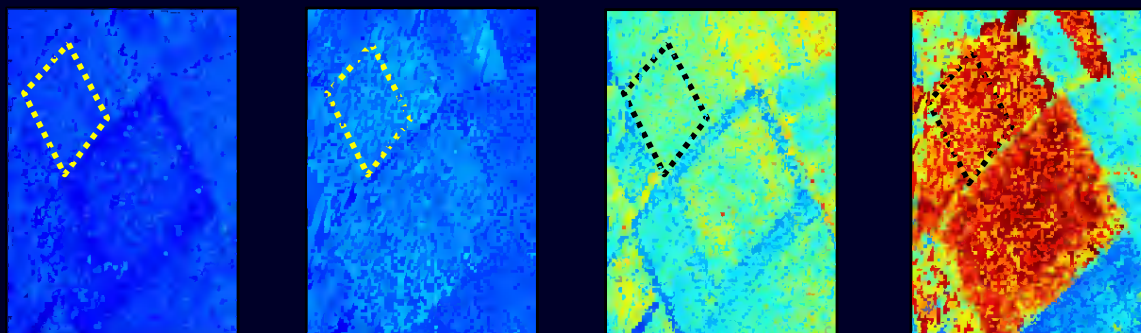
Corn (Maize)



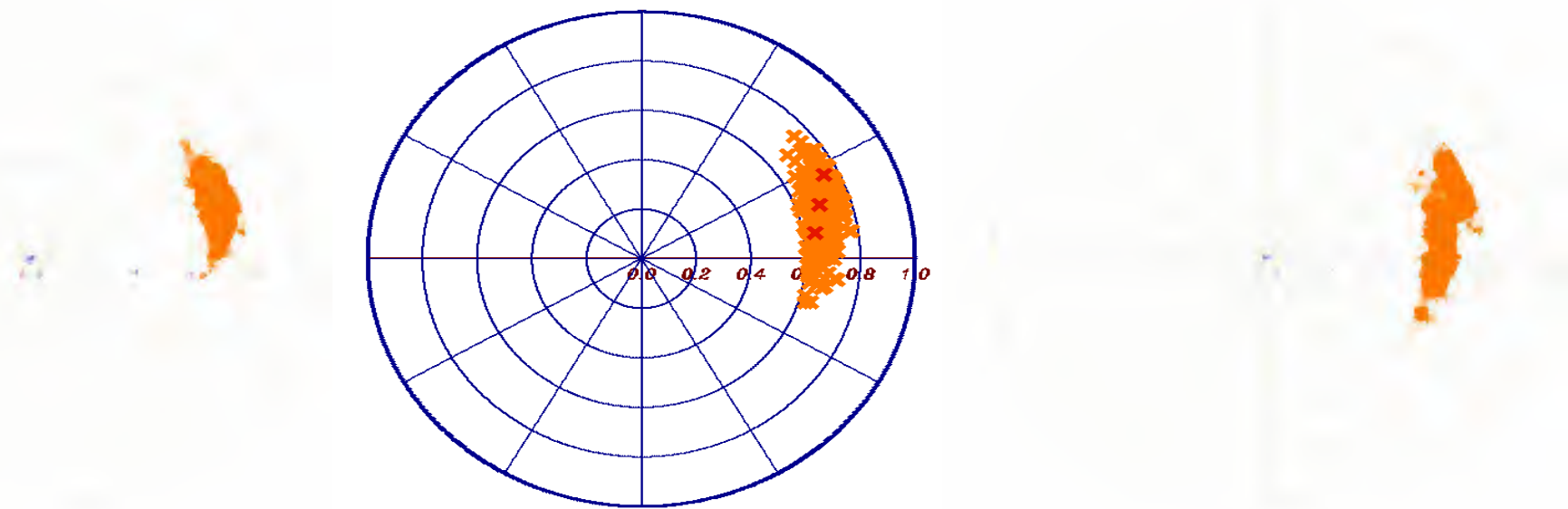
Jun 12 Jun 18

Jul 03

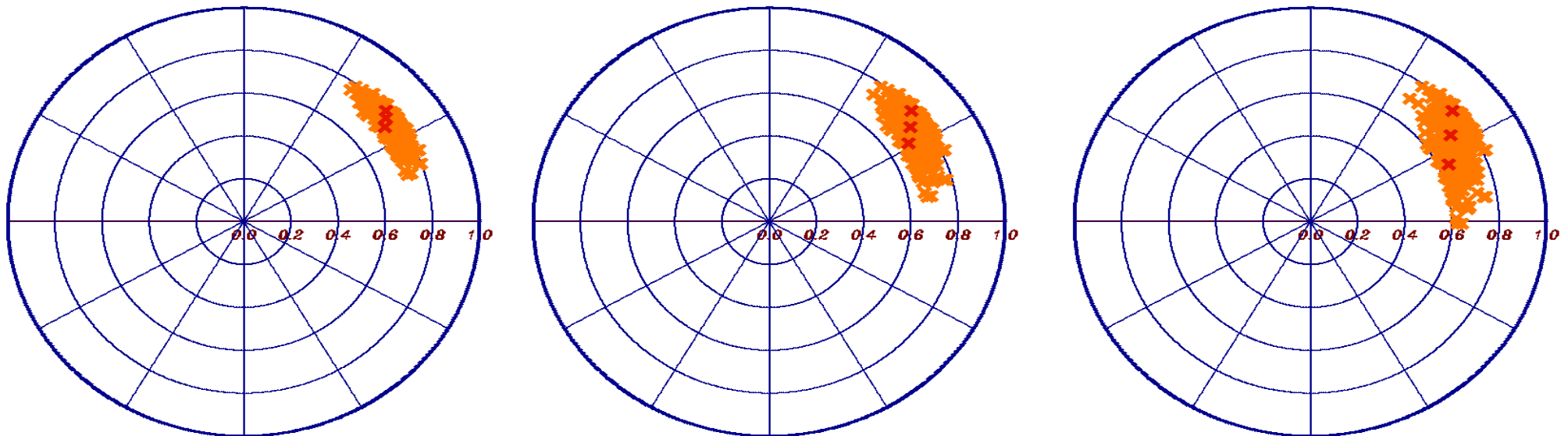
Jul 24



■ Estimated height
··· In-situ height
□ 10% uncertainty



Generalised Polarimetric Decomposition



Polarimetric Decompositions

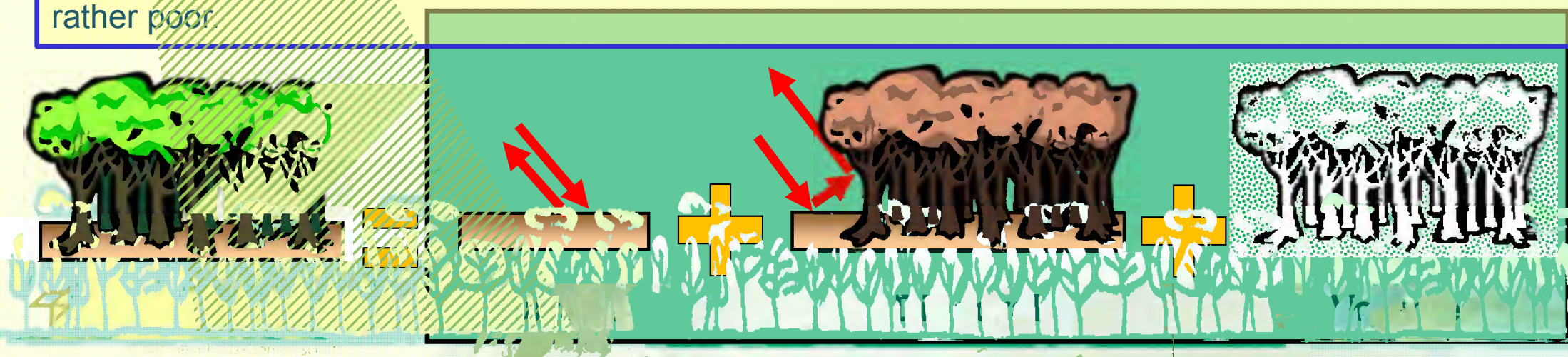


$$[S] = \begin{bmatrix} S_{HH} & S_{HV} \\ S_{VH} & S_{VV} \end{bmatrix} \rightarrow \vec{k} = \frac{1}{\sqrt{2}} [S_{HH} + S_{VV} \quad S_{HH} - S_{VV} \quad 2S_{HV}]^T \rightarrow [T_T] = \langle \vec{k} \cdot \vec{k}^+ \rangle$$

Covariance (Coherence) Matrix: $[T_T] = [T_G] + [T_V]$ Ground + Volume; $[T_G] = [T_S] + [T_D]$ Surface + Dihedral

- Unique solutions are obtained only for non-depolarising (rank 1) surface and/or dihedral contributions.
- Only 5 independent parameters available (reflexion symmetry) in the covariance matrix limit the complexity of the polarimetric models used to model the covariance matrix of the individual contributions.

In conclusion: The performance of polarimetric decomposition approaches is constrained by the (rather low) dimension of the observation space. Qualitative conclusions are possible, quantitative estimates rather poor.

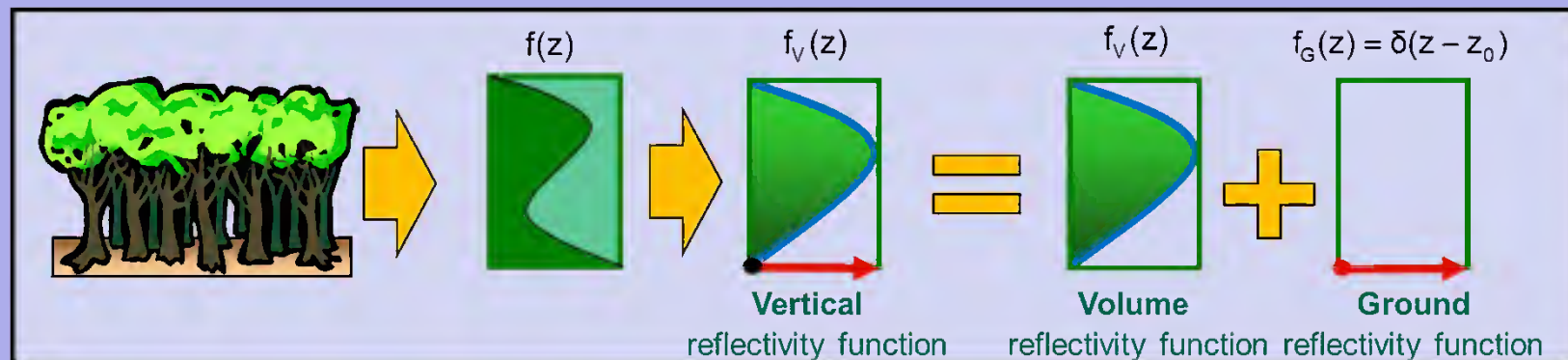


Volume	Ground
$f(z, \vec{w}) = m_v f_v(z) + m_g(\vec{w}) \delta(z - z_0)$	

$$\tilde{\gamma}_{vol}(\vec{w}, \kappa_z) = e^{ik_z z_0} \frac{\int_0^{h_v} f(z, \vec{w}) e^{ik_z z} dz}{\int_0^{h_v} f(z, \vec{w}) dz} \rightarrow \tilde{\gamma}_{vol}(\vec{w}, \kappa_z) = e^{ik_z z_0} \frac{\tilde{\gamma}_v(\kappa_z) + m(\vec{w})}{1 + m(\vec{w})}$$

Volume Only Coherence: $\tilde{\gamma}_v = \frac{1}{I_0}$ $I = \int_0^{h_v} \exp(ik_z z') f_v(z') dz'$ $I_0 = \int_0^{h_v} f_v(z') dz'$ $m(\vec{w}) = \frac{m_g(\vec{w})}{m_v(\vec{w}) I_0}$ $\kappa_z = \frac{\kappa \Delta \theta}{\sin(\theta_0)}$

Ground Only Coherence: $\tilde{\gamma}_g = e^{ik_z z_0}$

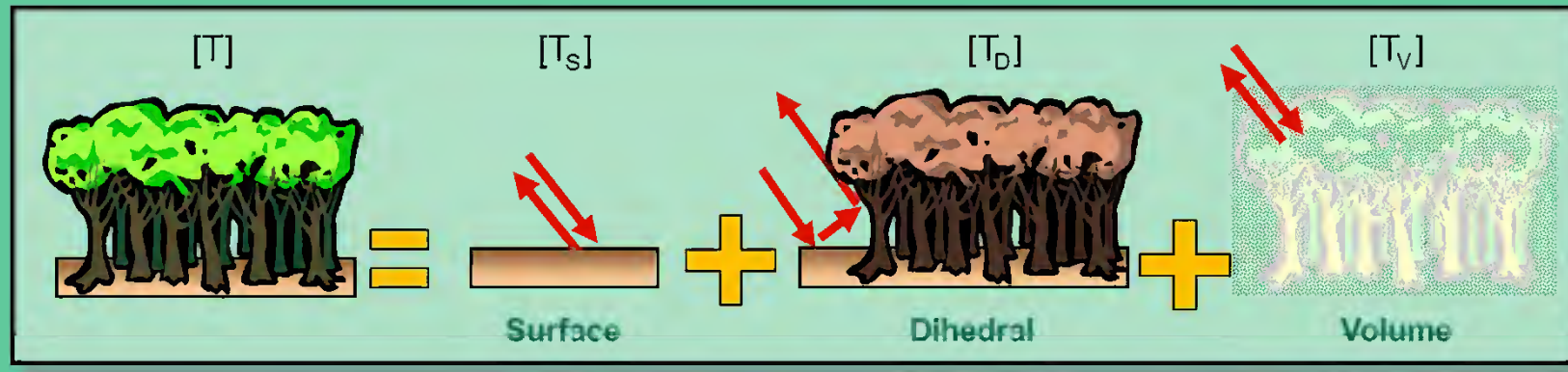


InSAR Decomposition:

PolSAR Decomposition:

$$[T] = P_s[T_s] + P_d[T_d] + P_v[T_v] = P_g[T_g] + P_v[T_v]$$

Surface + Dihedral + Volume;



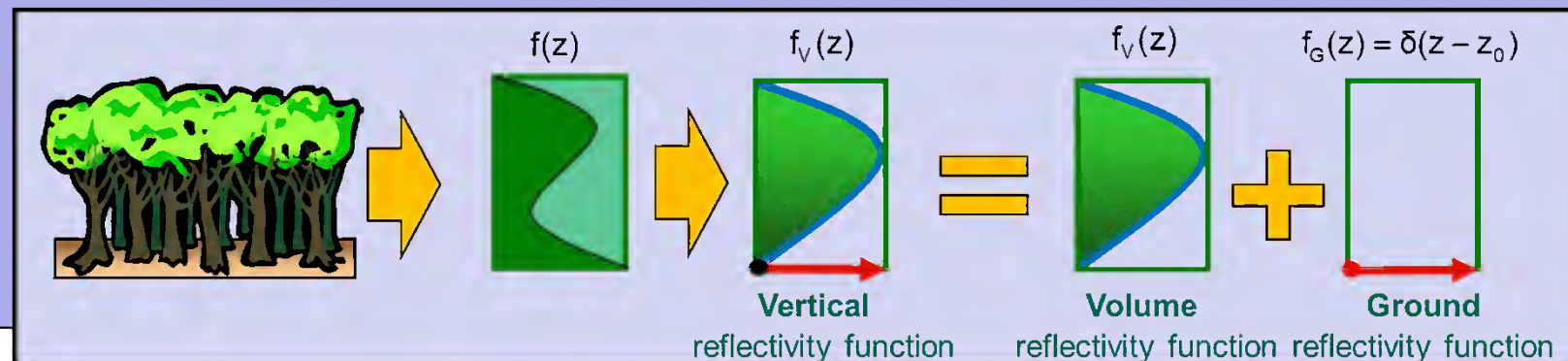
Volume **Ground**

$$f(z, \vec{w}) = m_v f_v(z) + m_g(\vec{w}) \delta(z - z_0)$$

$$\tilde{\gamma}_{vol}(\vec{w}, \kappa_z) = e^{ik_z z_0} \frac{\int_0^{h_v} f(z, \vec{w}) e^{ik_z z} dz}{\int_0^{h_v} f(z, \vec{w}) dz} \rightarrow \tilde{\gamma}_{vol}(\vec{w}, \kappa_z) = e^{ik_z z_0} \frac{\tilde{\gamma}_v(\kappa_z) + m(\vec{w})}{1 + m(\vec{w})}$$

Volume Only Coherence: $\tilde{\gamma}_v = \frac{1}{I_0}$ $I = \int_0^{h_v} \exp(ik_z z') f_v(z') dz'$ $I_0 = \int_0^{h_v} f_v(z') dz'$ $m(\vec{w}) = \frac{m_g(\vec{w})}{m_v(\vec{w}) I_0}$ $\kappa_z = \frac{\kappa \Delta \theta}{\sin(\theta_0)}$

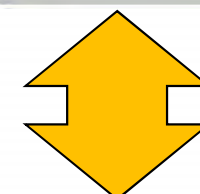
Ground Only Coherence: $\tilde{\gamma}_g = e^{ik_z z_0}$



InSAR Decomposition:

$$P_G[T_G] = f(\tilde{\gamma}_v(\kappa_z), e^{ik_z z_0})$$

$$P_V[T_V] = f(\tilde{\gamma}_v(\kappa_z), e^{ik_z z_0})$$

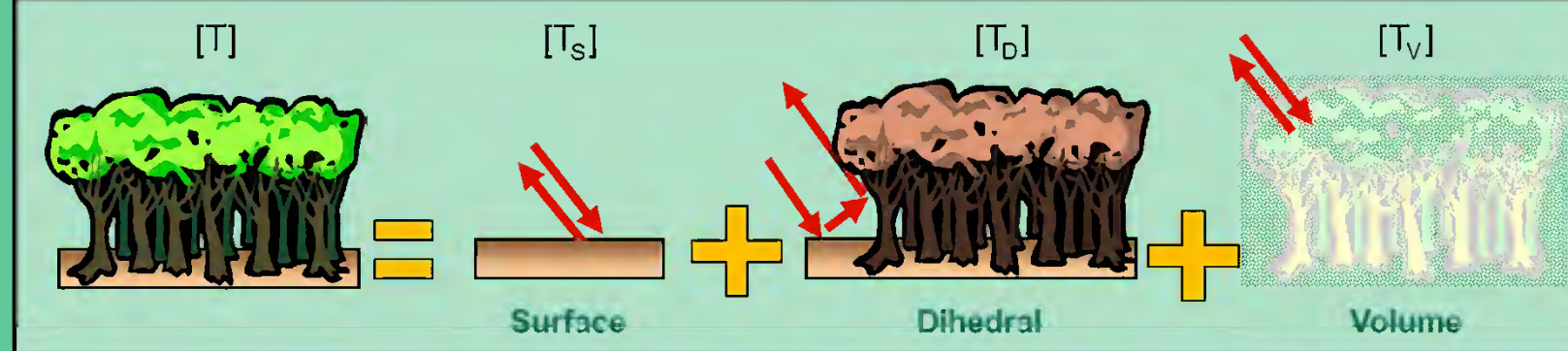


The two formulations are linked by the Ground-to-Volume ratio:

$$m(\vec{w}) = \frac{P_G}{P_V} \frac{\vec{w}^+ [T_G] \vec{w}}{\vec{w}^+ [T_V] \vec{w}}$$

PolSAR Decomposition:

$$[T] = P_G[T_G] + P_V[T_V]$$



[S₁] [S₂]

Pol-InSAR 2 layer Model Ground & Volume estimation

The ground & volume (polarimetric) coherency matrices T_{gw} and T_{vw} are estimated from the (interferometric) ground & volume coherence estimates γ_{ij}^g and γ_{ij}^v in the context of the Random Volume over Ground Model.



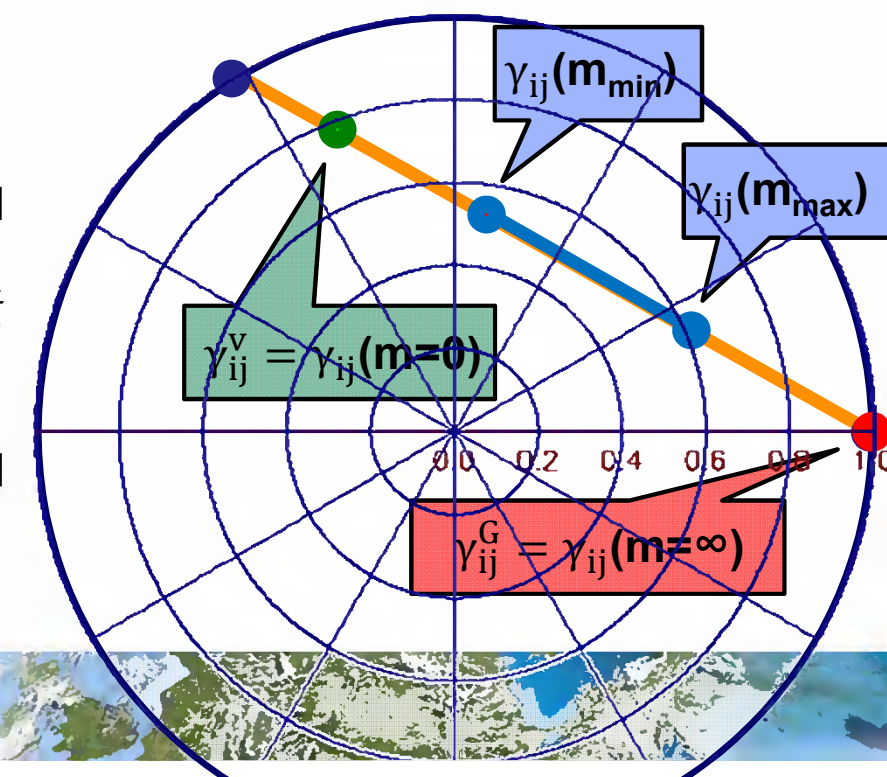
$$k_1 = [s_{HH}^1, \sqrt{2} s_{HV}^1, s_{VV}^1] \quad k_2 = [s_{HH}^2, \sqrt{2} s_{HV}^2, s_{VV}^2] \quad \left\{ \begin{array}{l} T_{ii} = \langle k_i k_i^H \rangle \\ \Omega_{ij} = \langle k_i k_j^H \rangle \end{array} \right.$$

After de-whitening ground and volume components are obtained

$$T_{gw} = \frac{\Pi_{ij} - \gamma_{ij}^v I}{\gamma_{ij}^g - \gamma_{ij}^v}$$

$$T_{vw} = \frac{\Pi_{ij} - \gamma_{ij}^g I}{\gamma_{ij}^v - \gamma_{ij}^g}$$

$$\Pi_{ij} = T_{ii}^{-\frac{1}{2}} \Omega_{ij} T_{jj}^{-\frac{1}{2}}$$



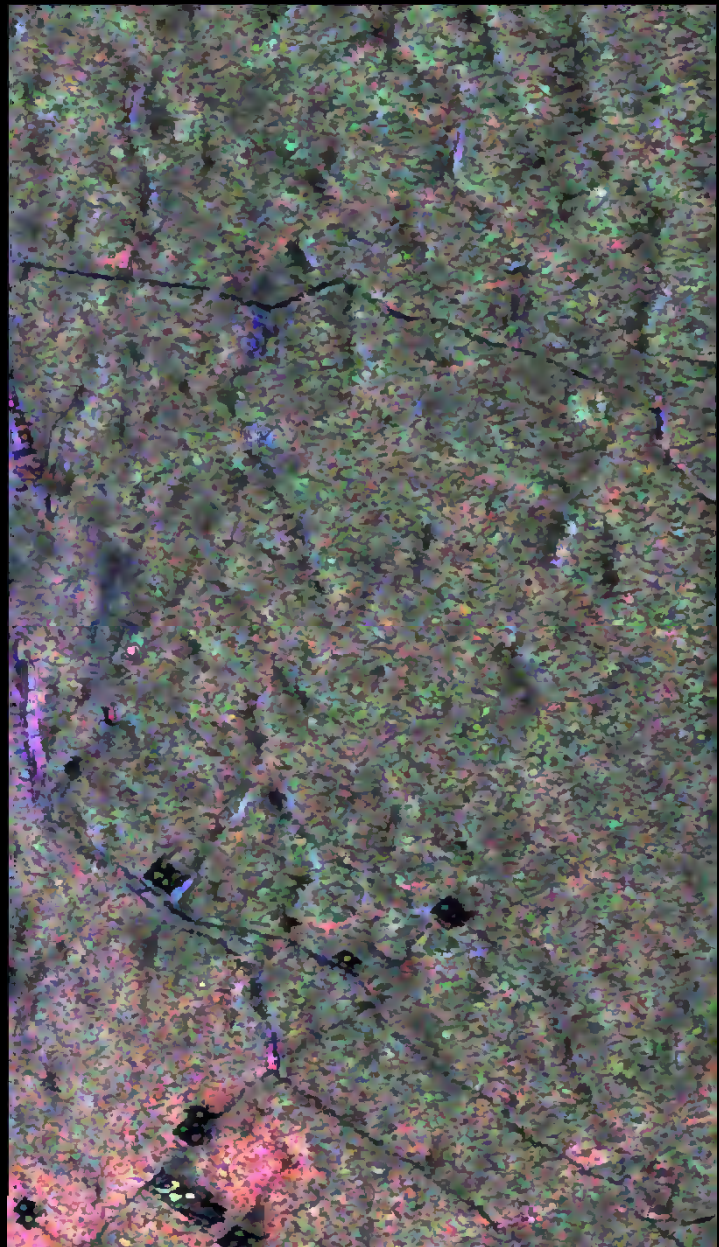
After de-whitening ground and volume components are obtained

$$T_{gii} = T_{ii}^{\frac{1}{2}} T_{gw} T_{ii}^{\frac{1}{2}}$$

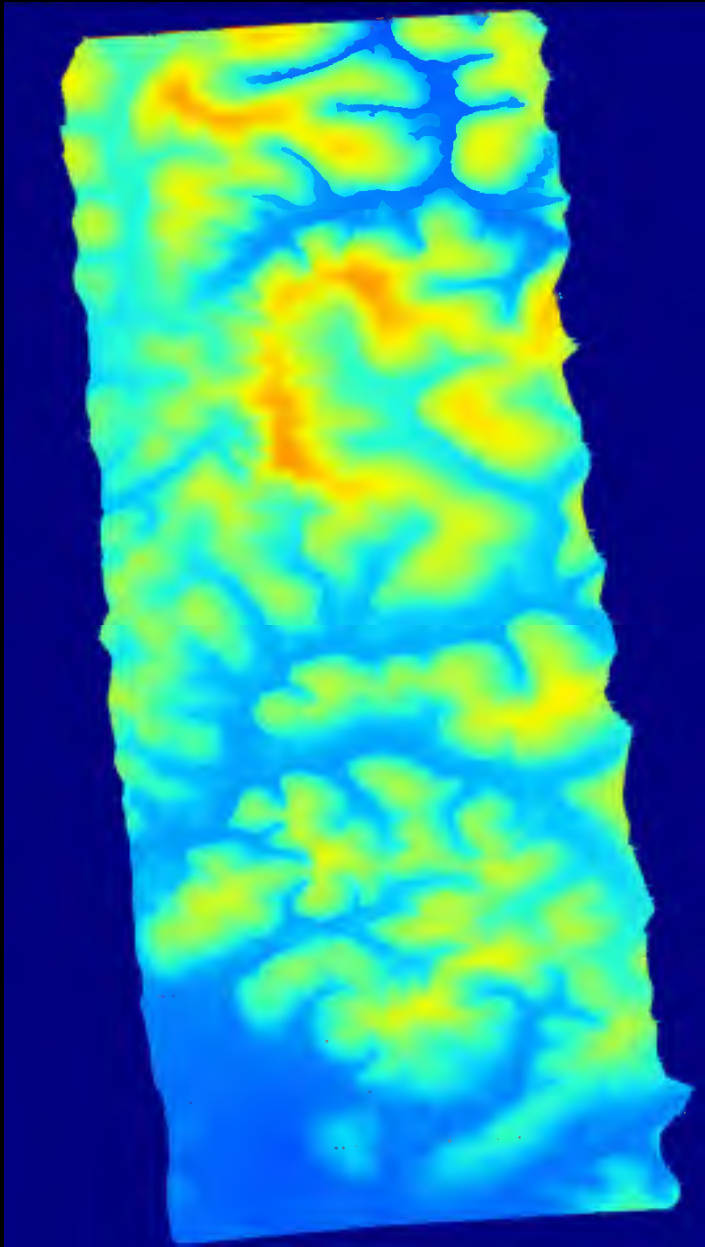
$$T_{vii} = T_{ii}^{\frac{1}{2}} T_{vw} T_{ii}^{\frac{1}{2}}$$

$$T_{ii} = T_{gii} + T_{vii}$$

AfriSAR Rabi Testsite: F-SAR P-band

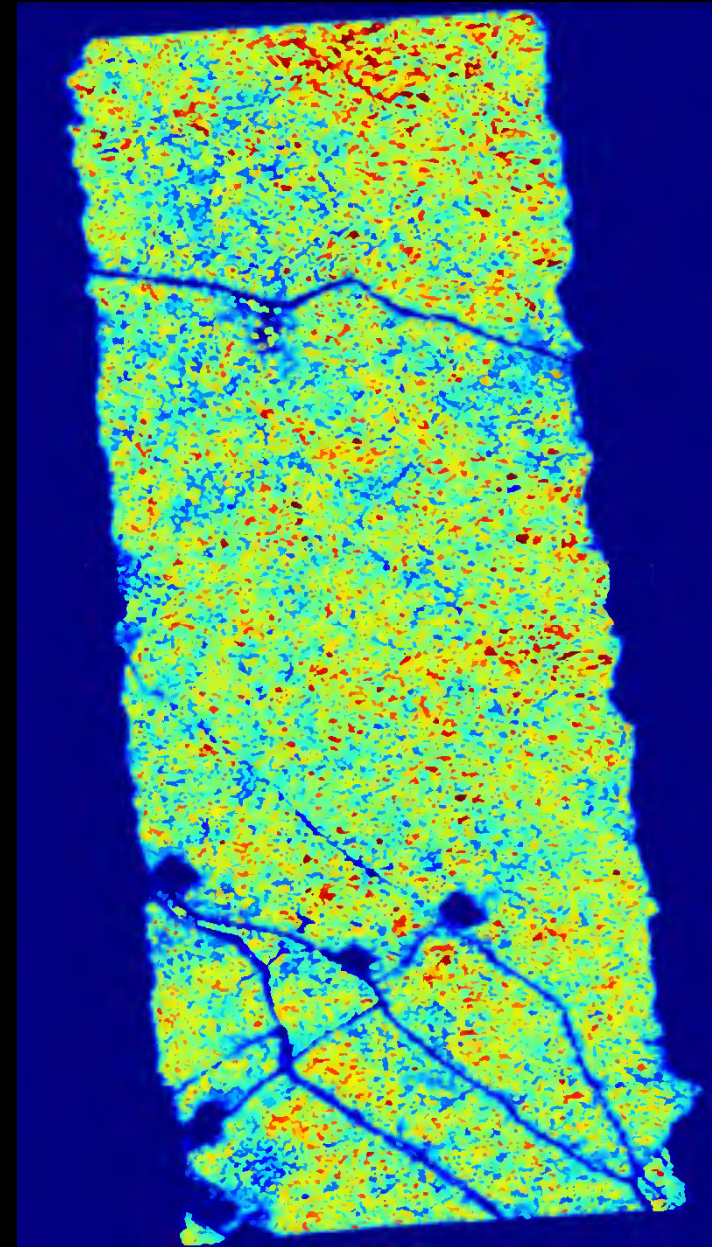


Pauli RGB



0m 100m

Lidar DTM

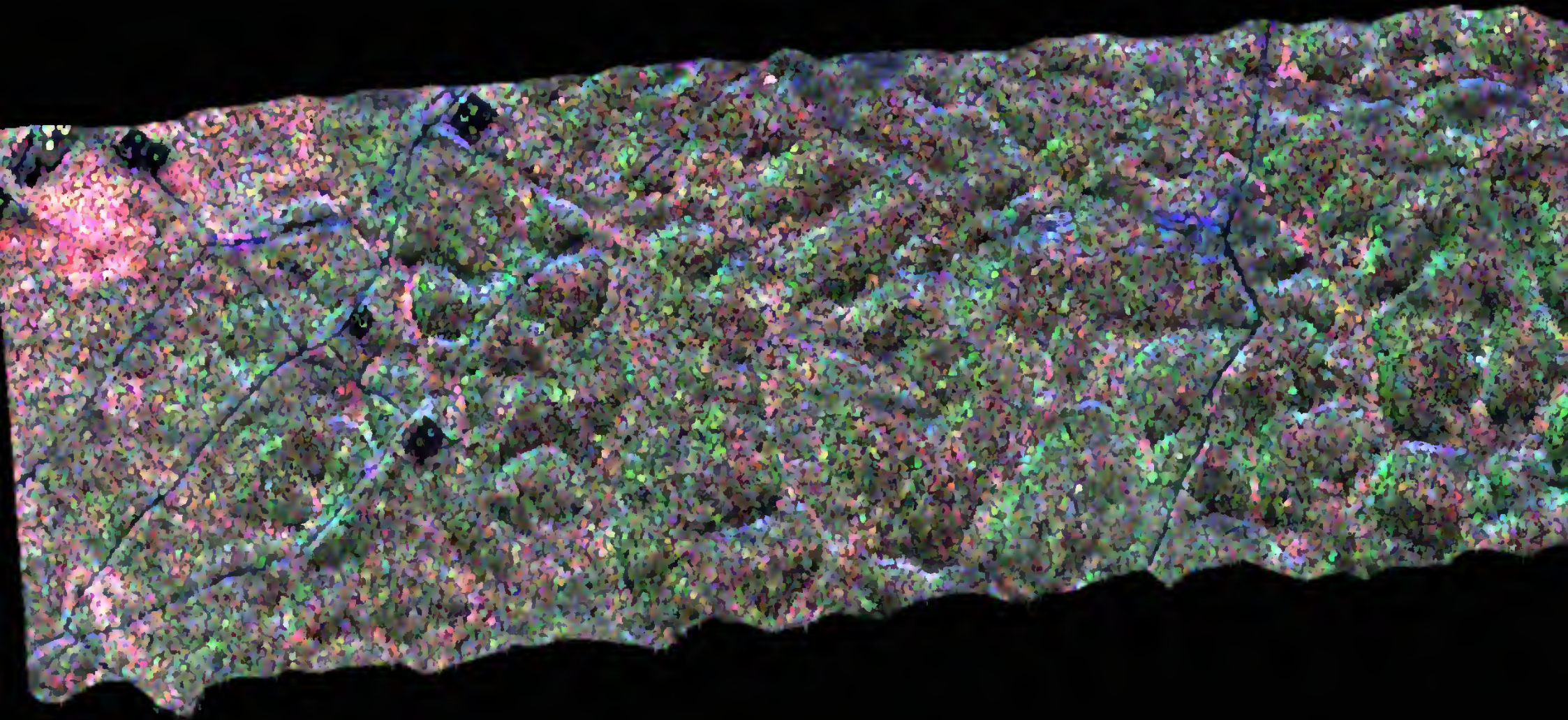


0m 50m

Lidar DSM

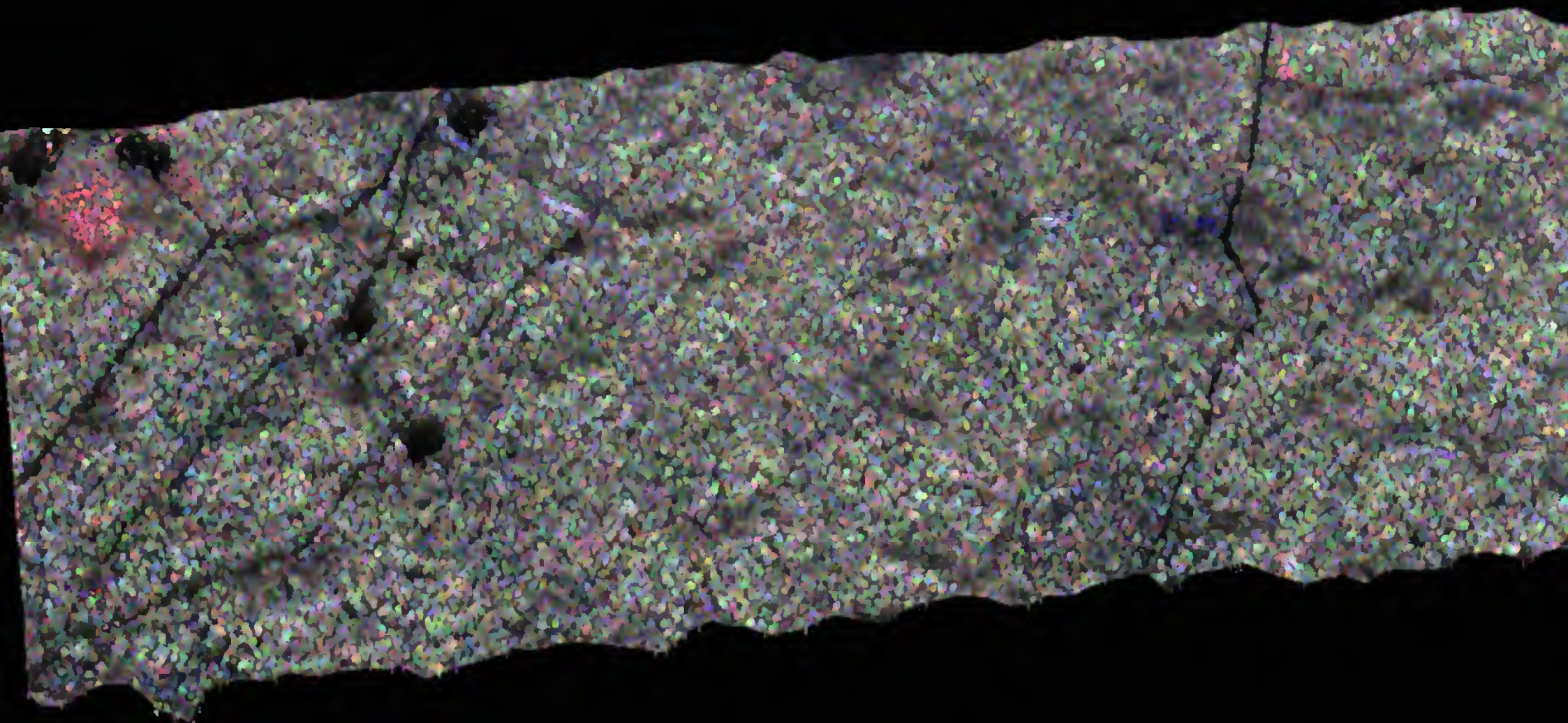
PollInSAR Ground-Volume Separation

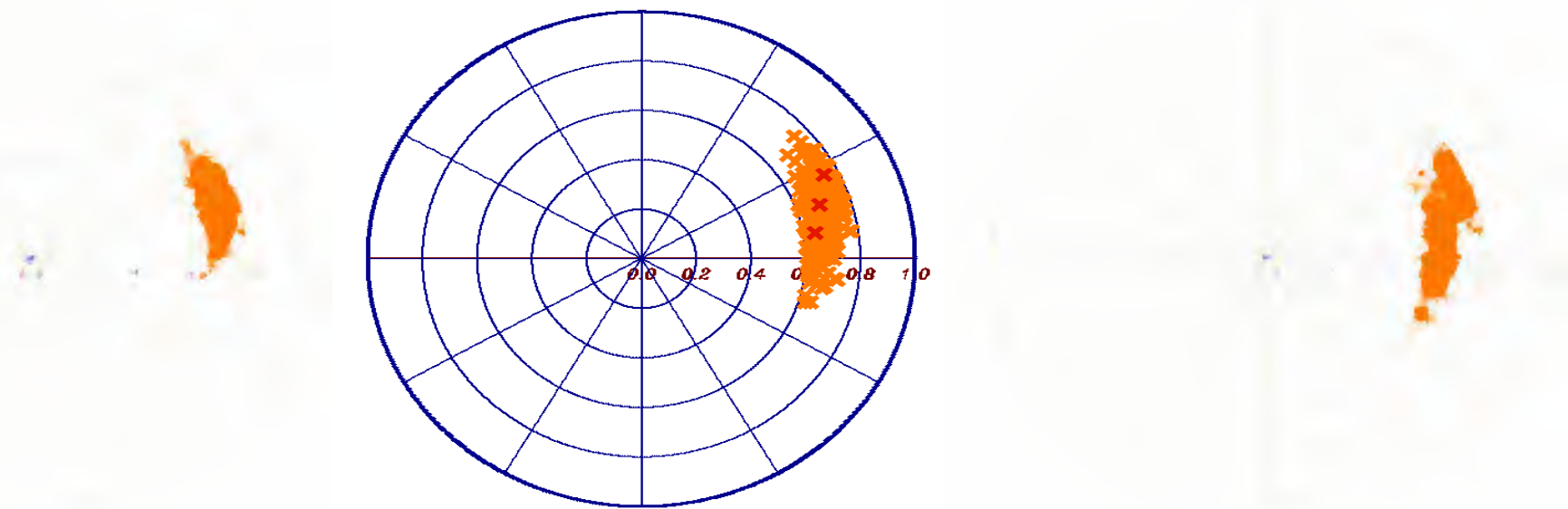
Ground component - Pauli RGB |HH+VV||HH-VV||HV+VH|



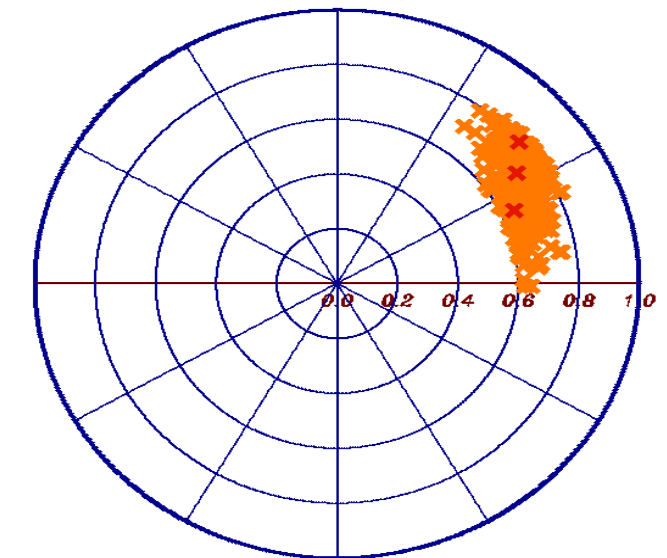
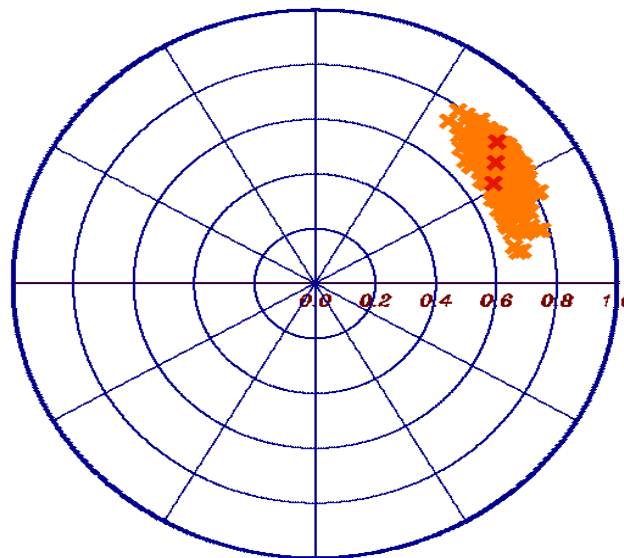
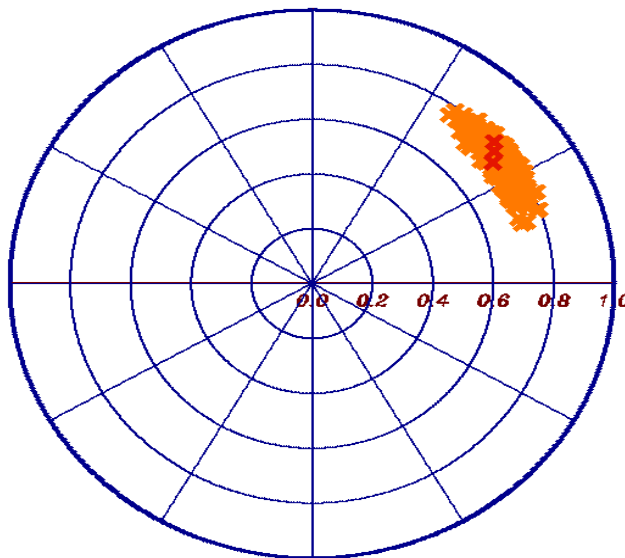
PollInSAR Ground-Volume Separation

Volume component - Pauli RGB |HH+VV||HH-VV||HV+VH|

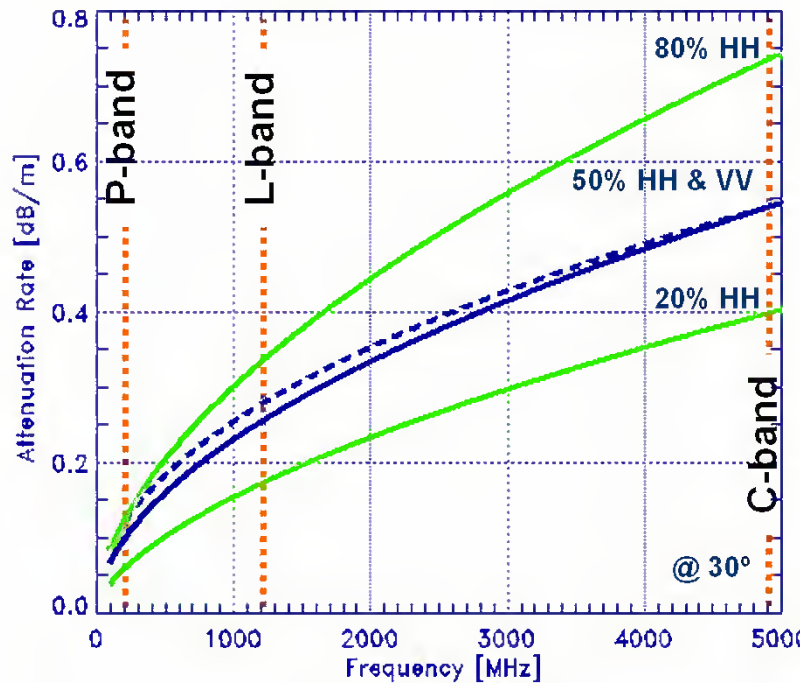




Pol-InSAR: Frequency Effects

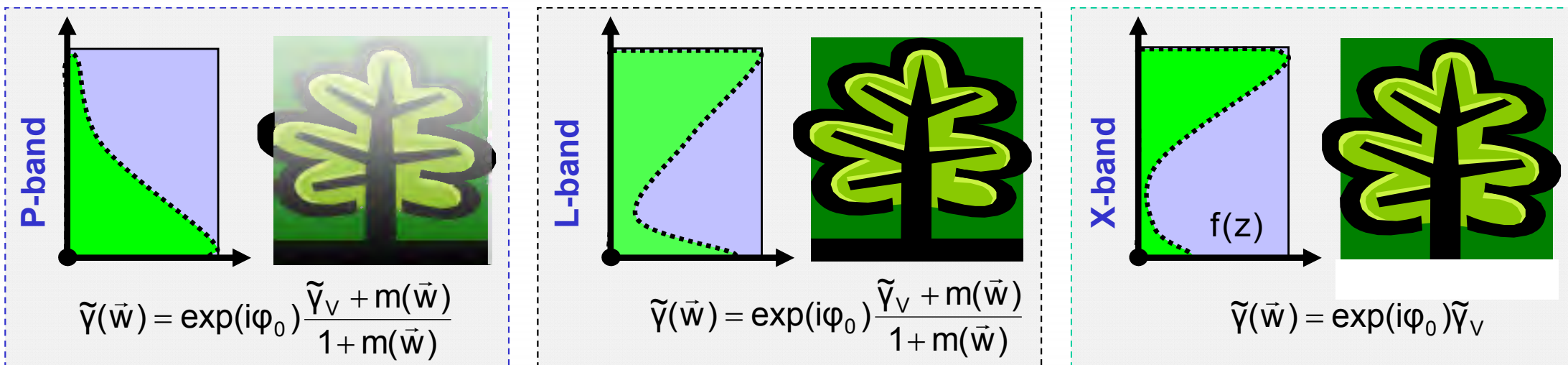


Frequency Dependency

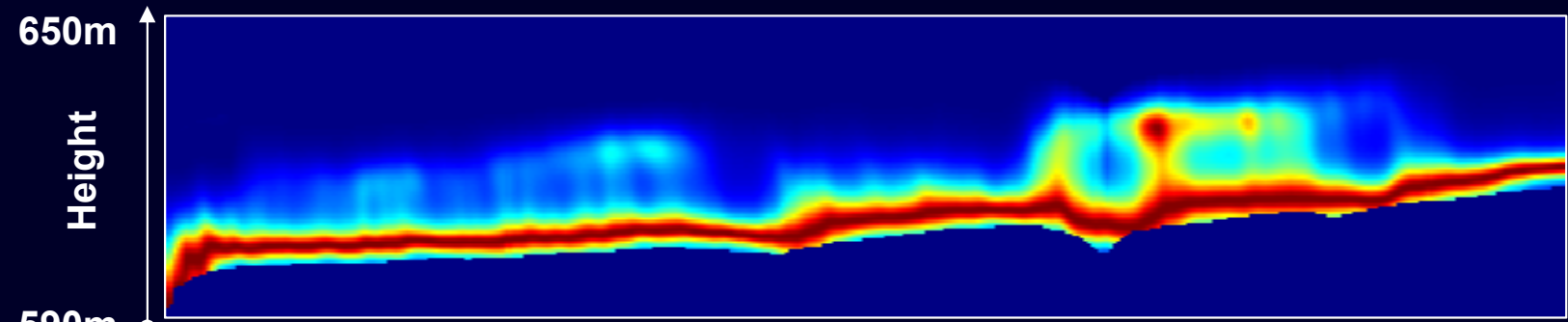
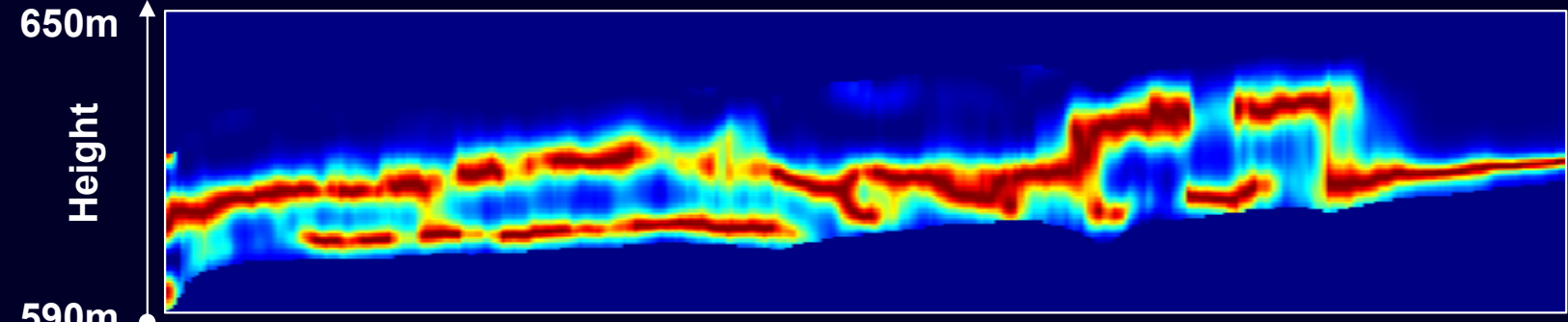
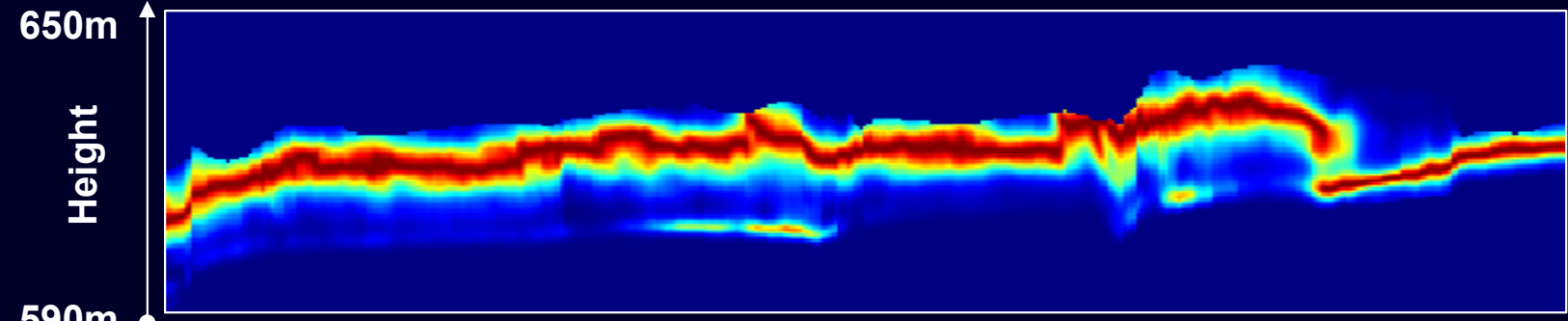
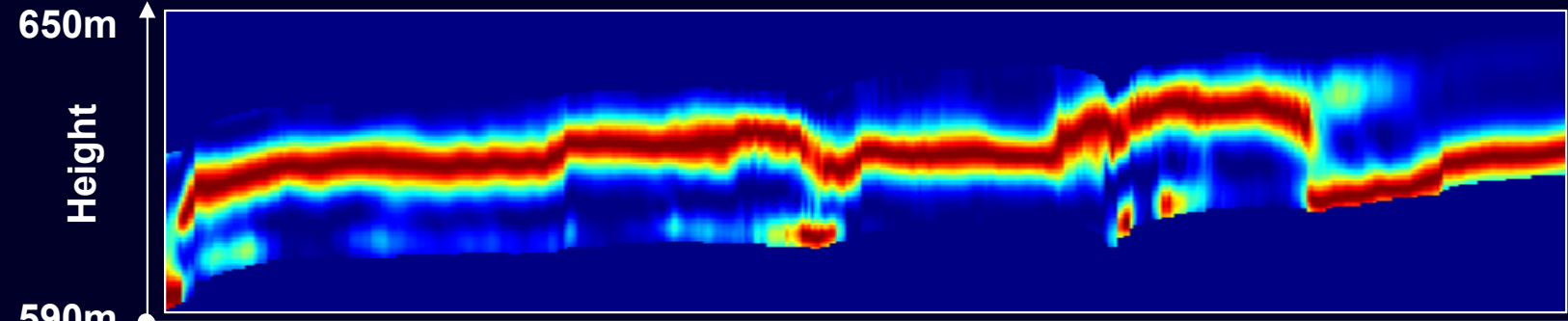


With decreasing frequency:

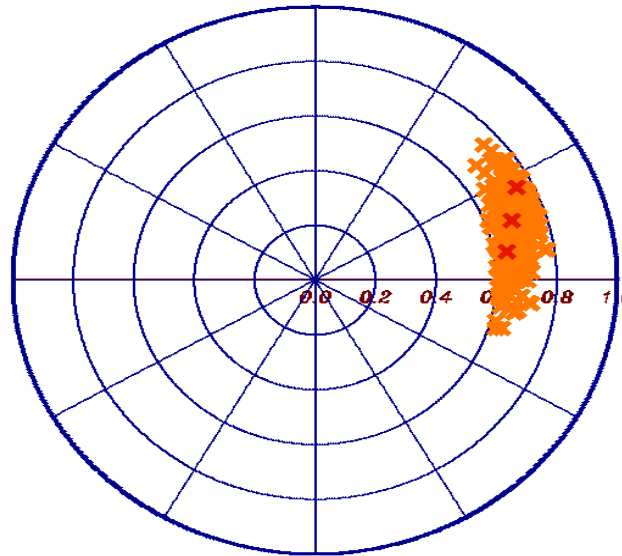
- The attenuation through the vegetation decreases;
- The relative importance of the volume decreases;
- The relative importance of the ground increases;
- The effective scatterers and their distribution changes.



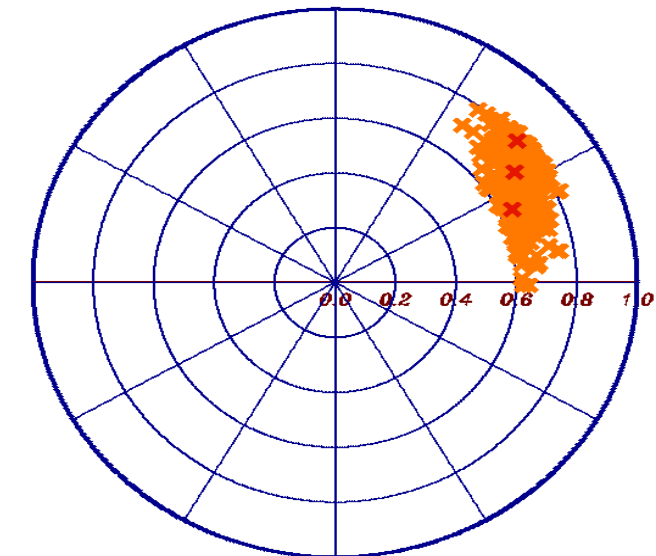
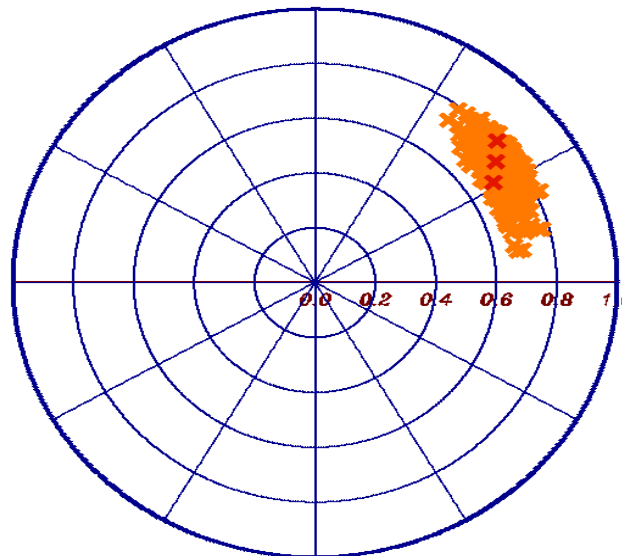
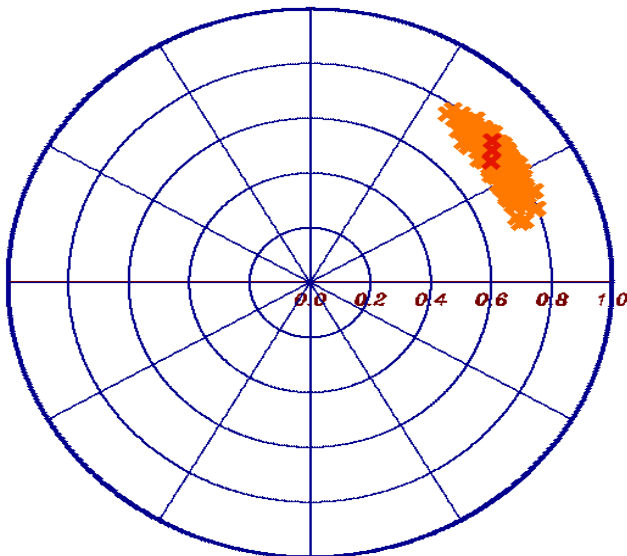
L.Bessette, S.Ayasli "Ultra Wide Band P-3 and Carabas II Foliage Attenuation and Backscatter Analysis", Proceedings of IEEE Radar Conference, 2001.

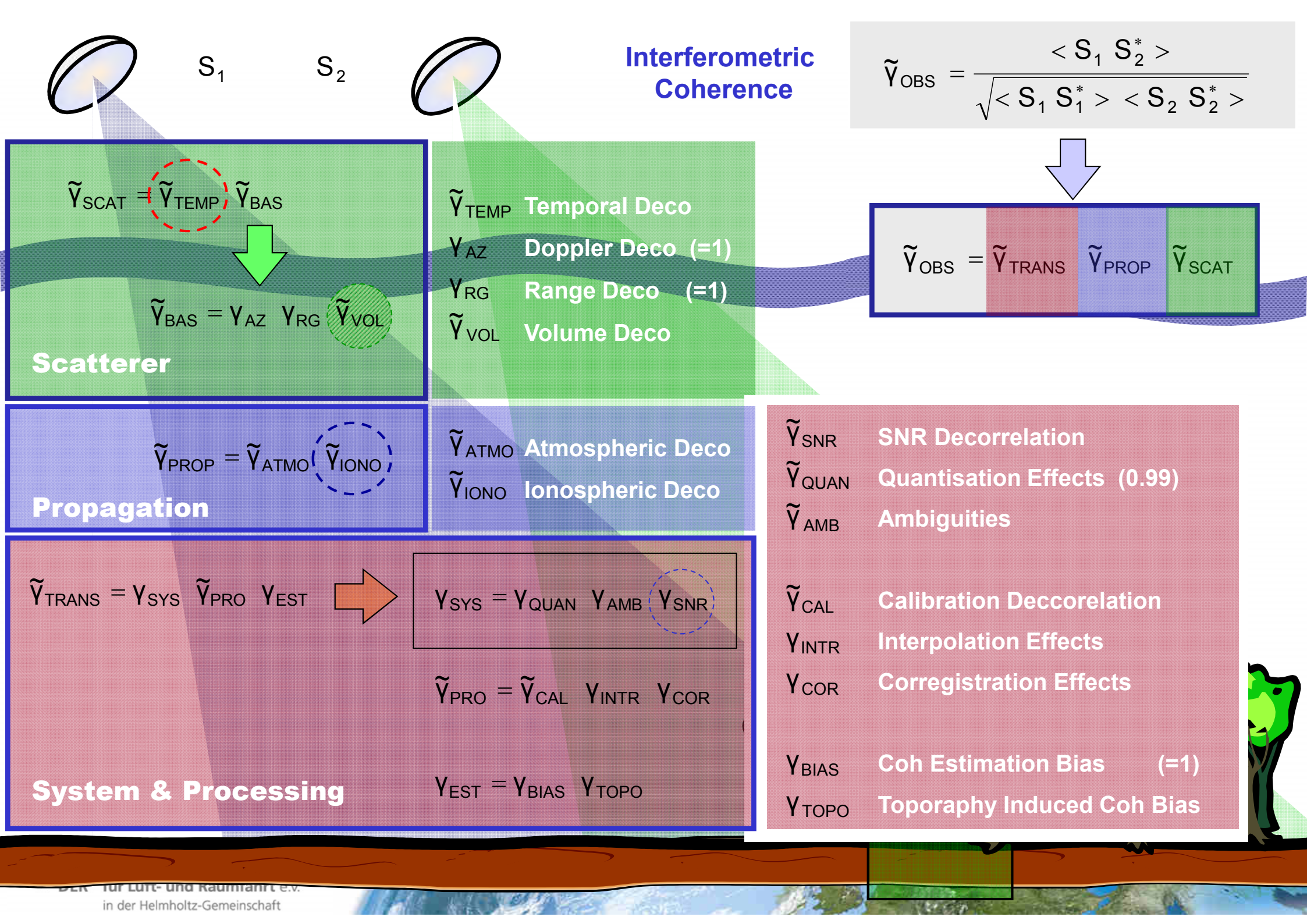
P-band**L-band****S-band****X-band**

Slant range (0.6Km)



Non-Volumetric Decorrelation Effects





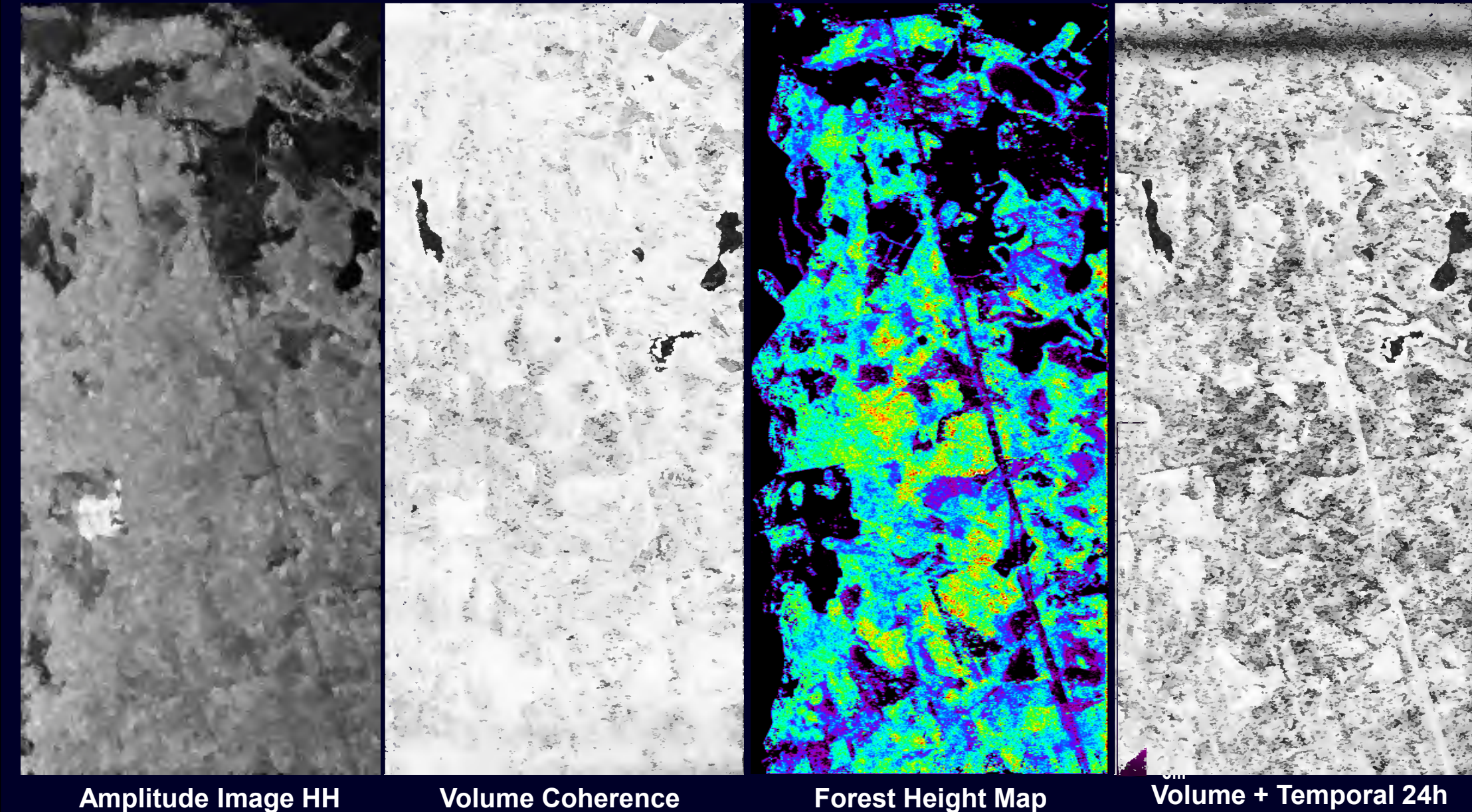
Amplitude Image



Amplitude Image HH



Interferometric Coherence: Volume vs Temporal Decorrelation



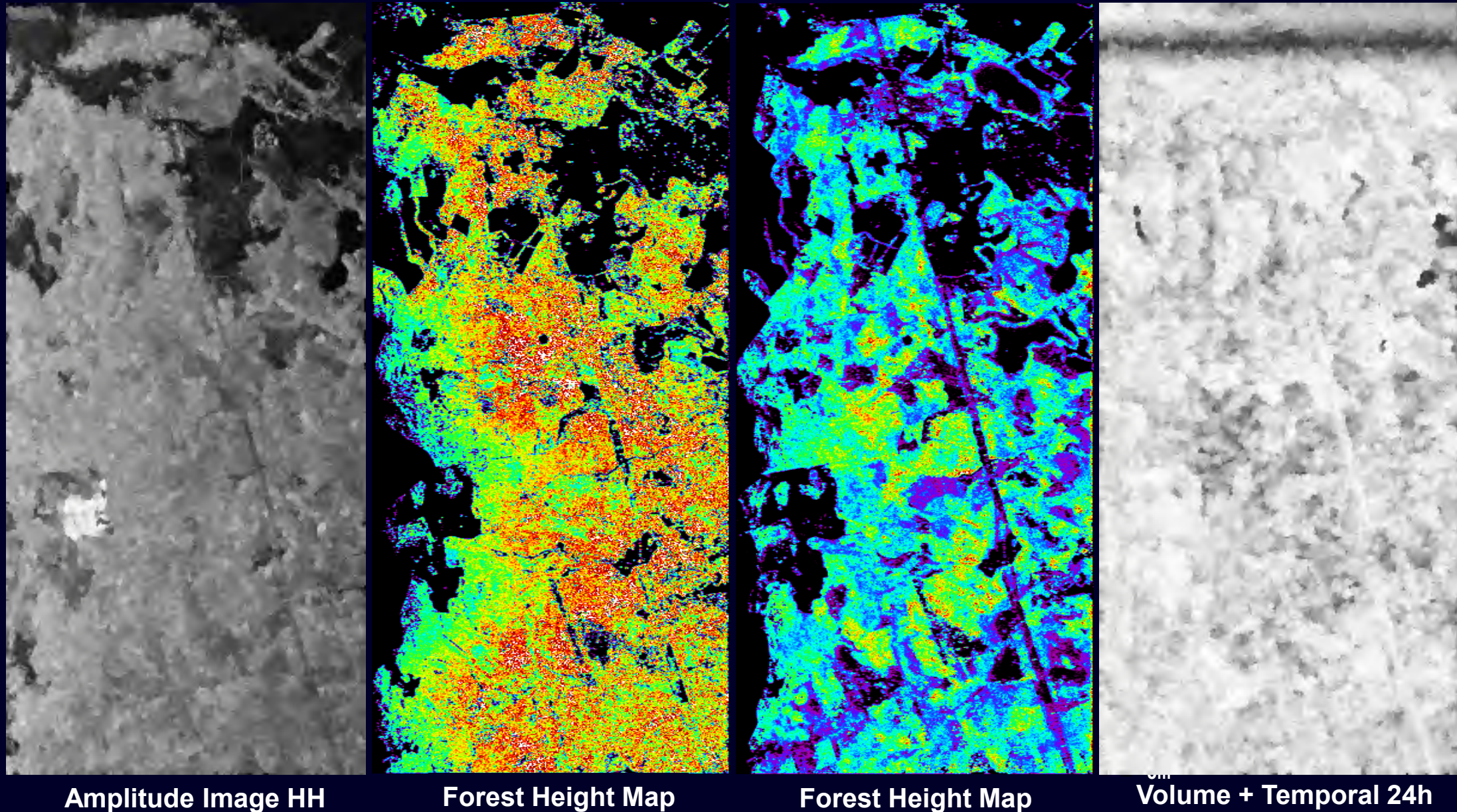
Amplitude Image HH

Volume Coherence

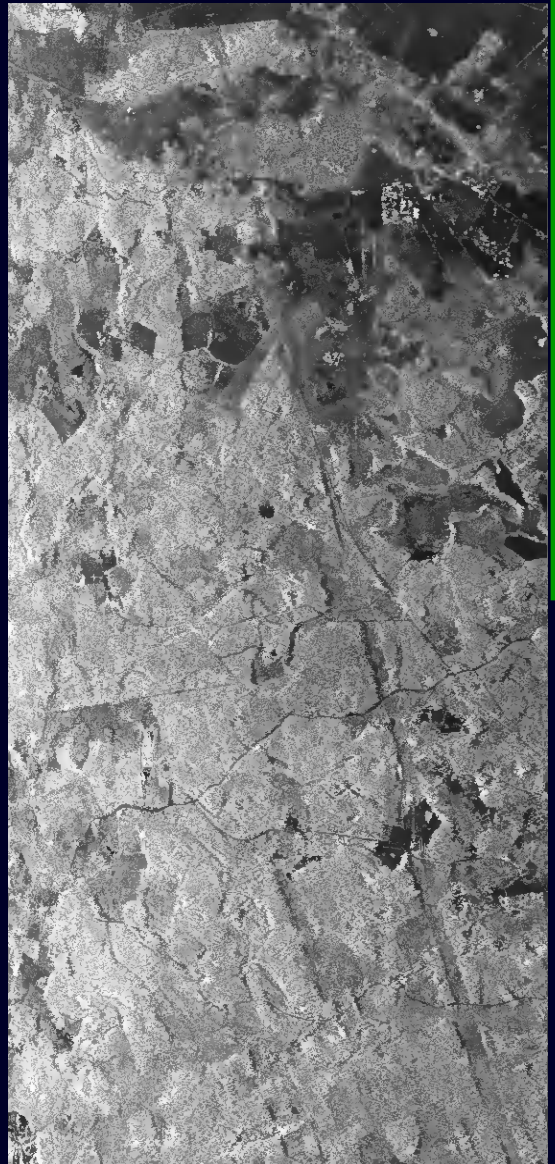
Forest Height Map

Volume + Temporal 24h

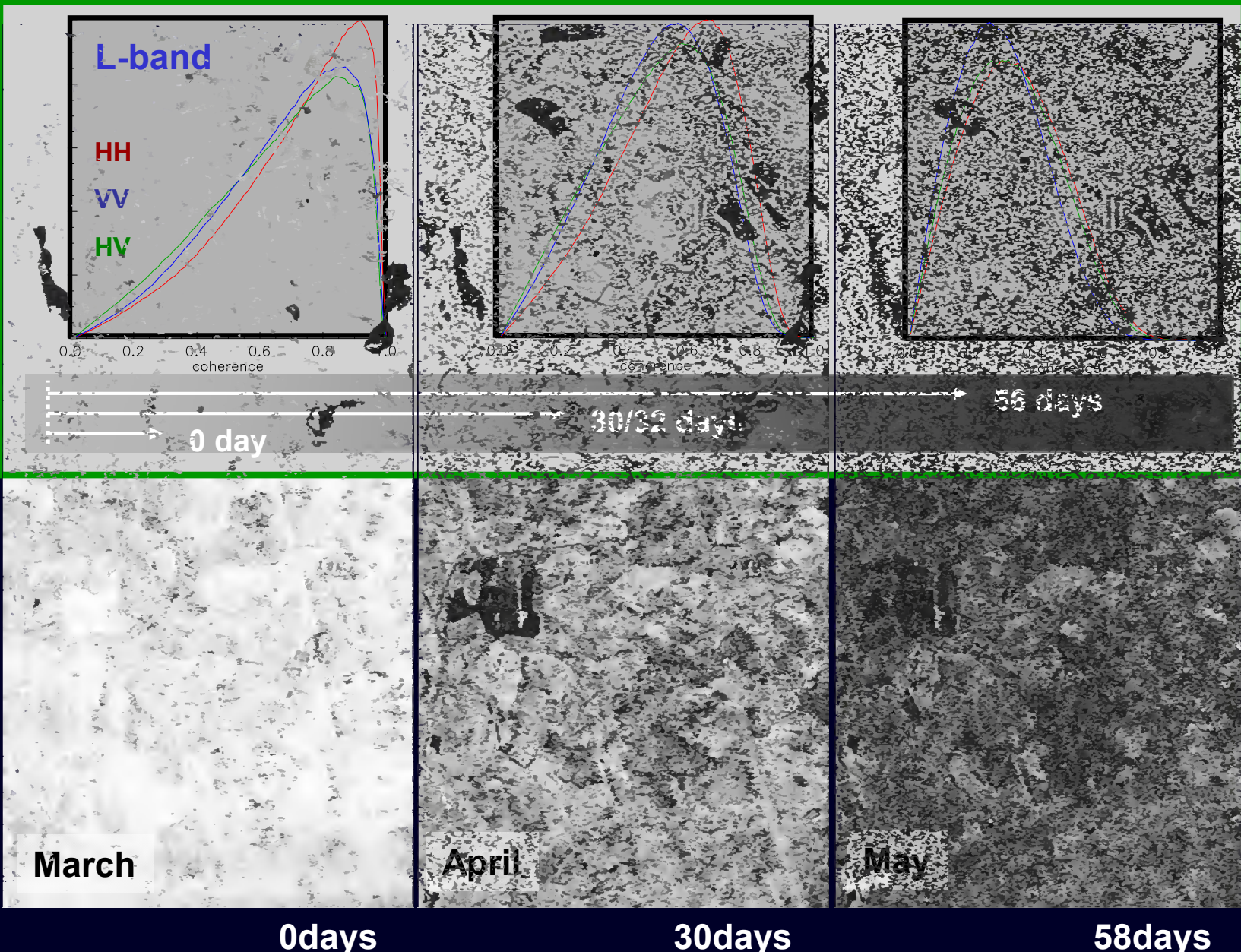
Interferometric Coherence: Volume vs Temporal Decorrelation



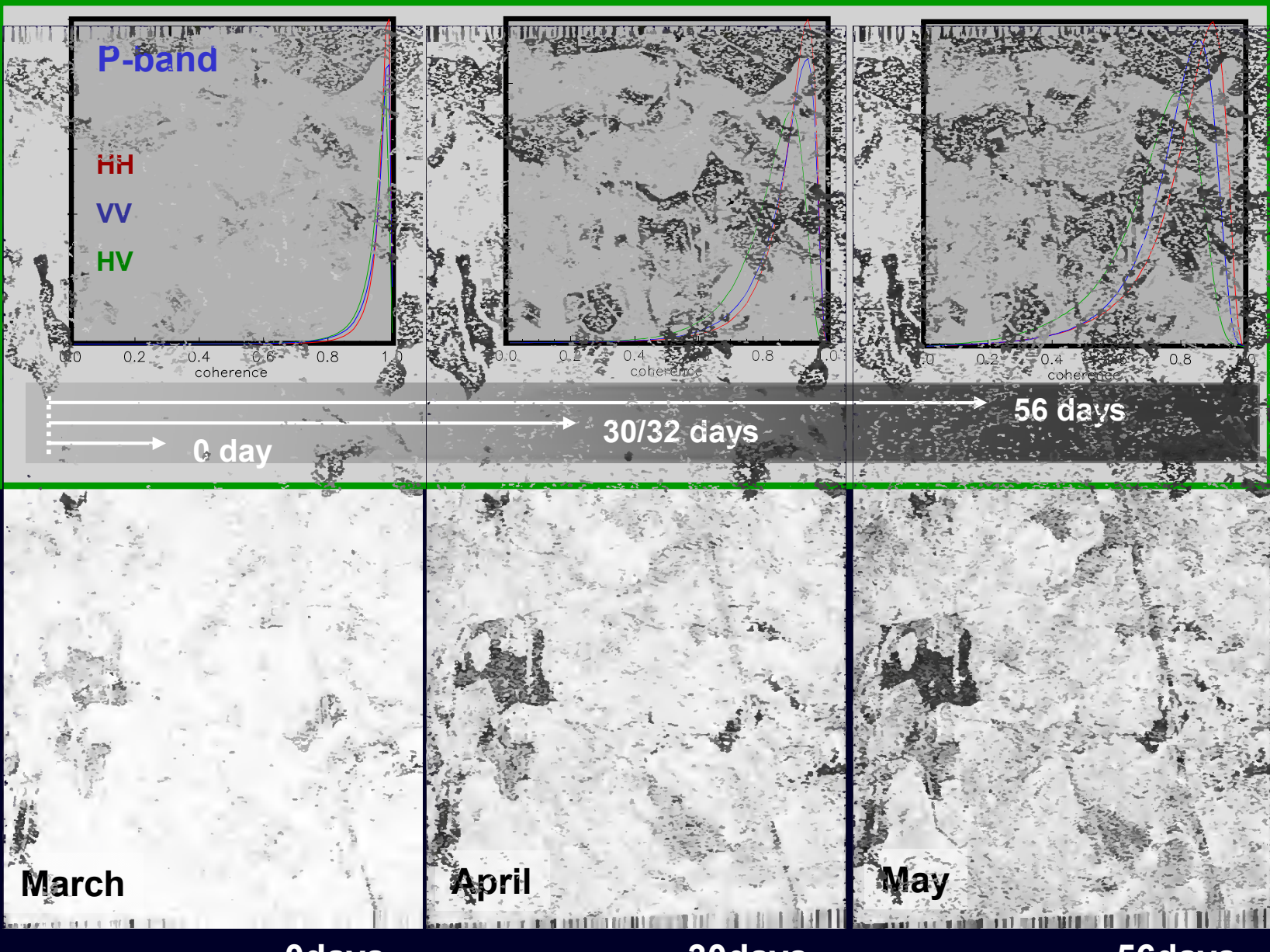
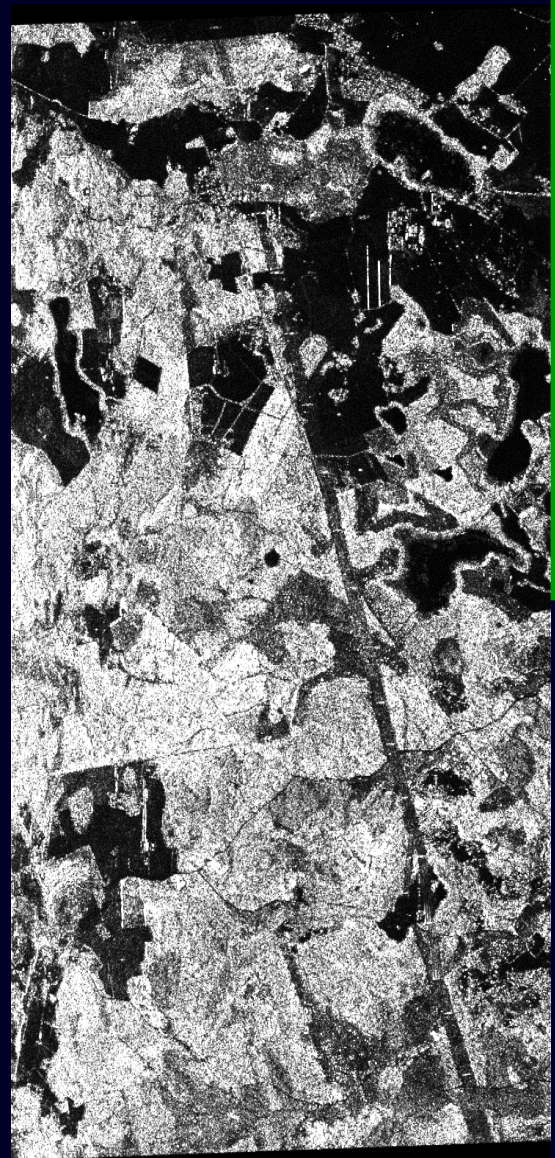
Remnningstorp Test Site: Temporal Decorrelation: L-band



HV Amplitude Image



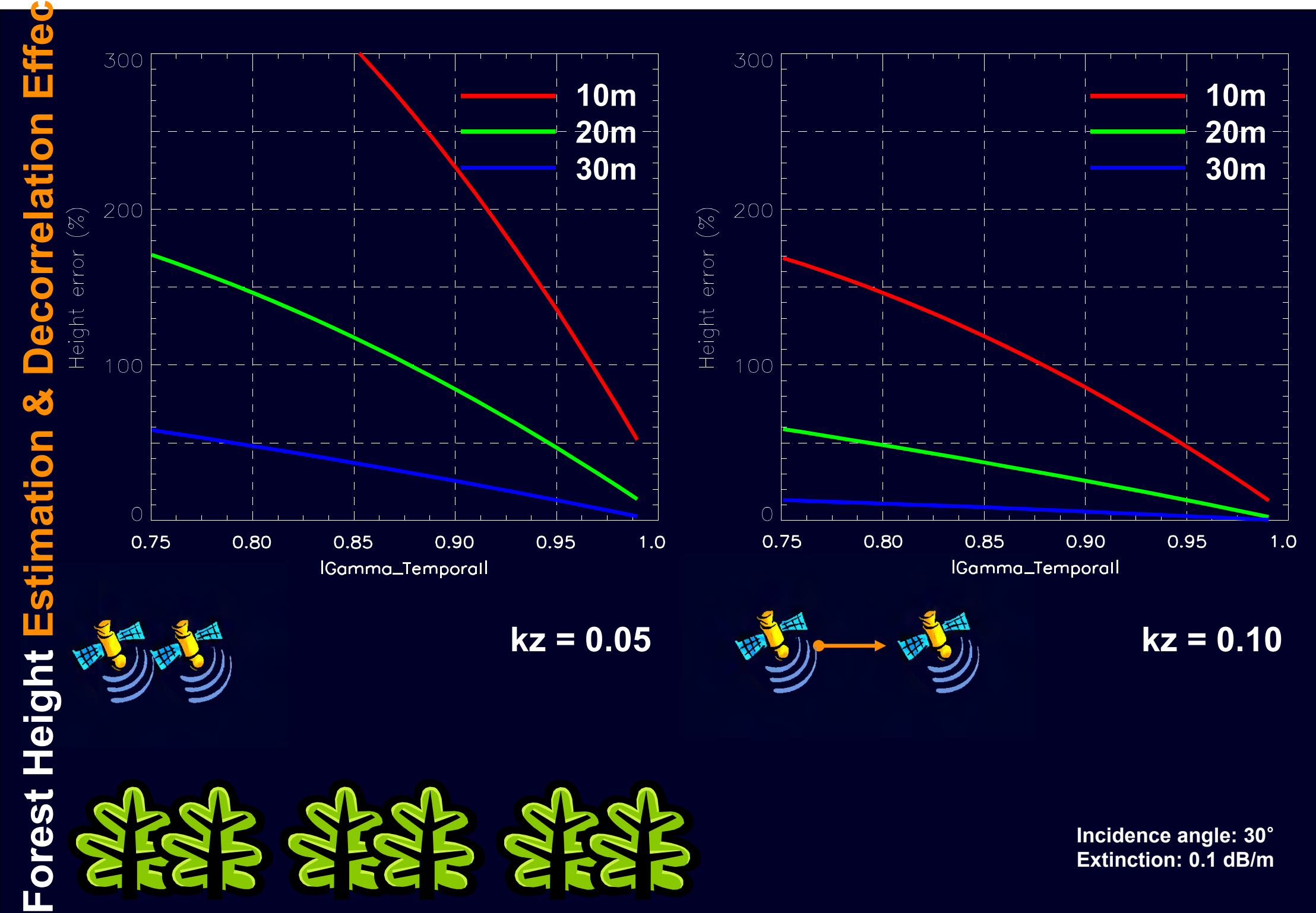
Remnningstorp Test Site: Temporal Decorrelation: P-Band



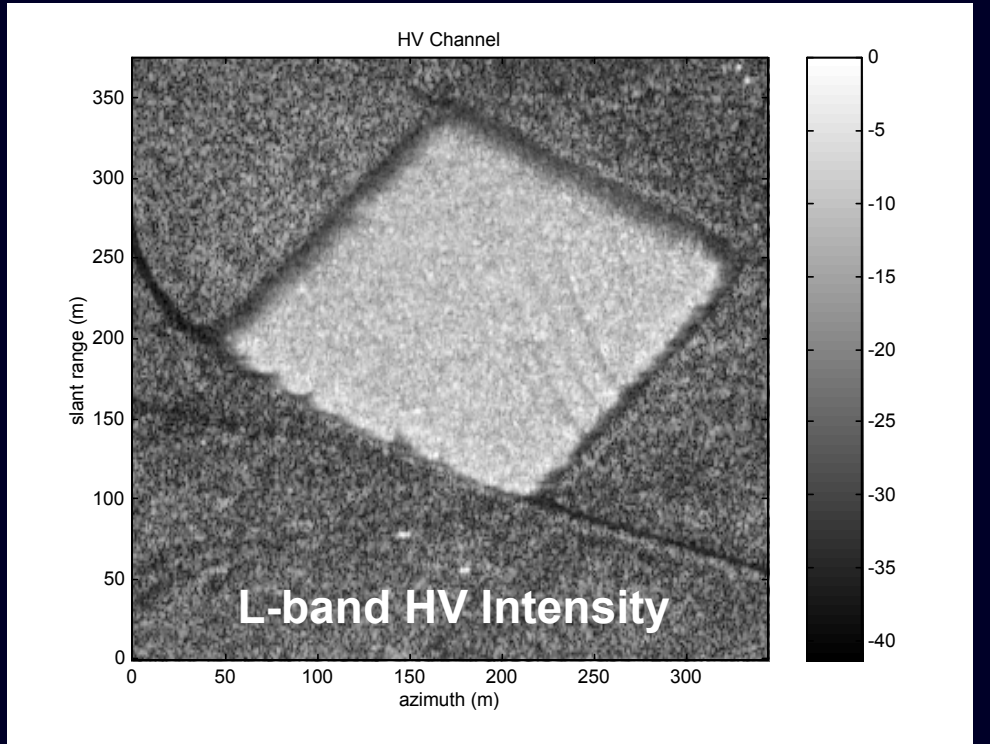
HV Amplitude Image



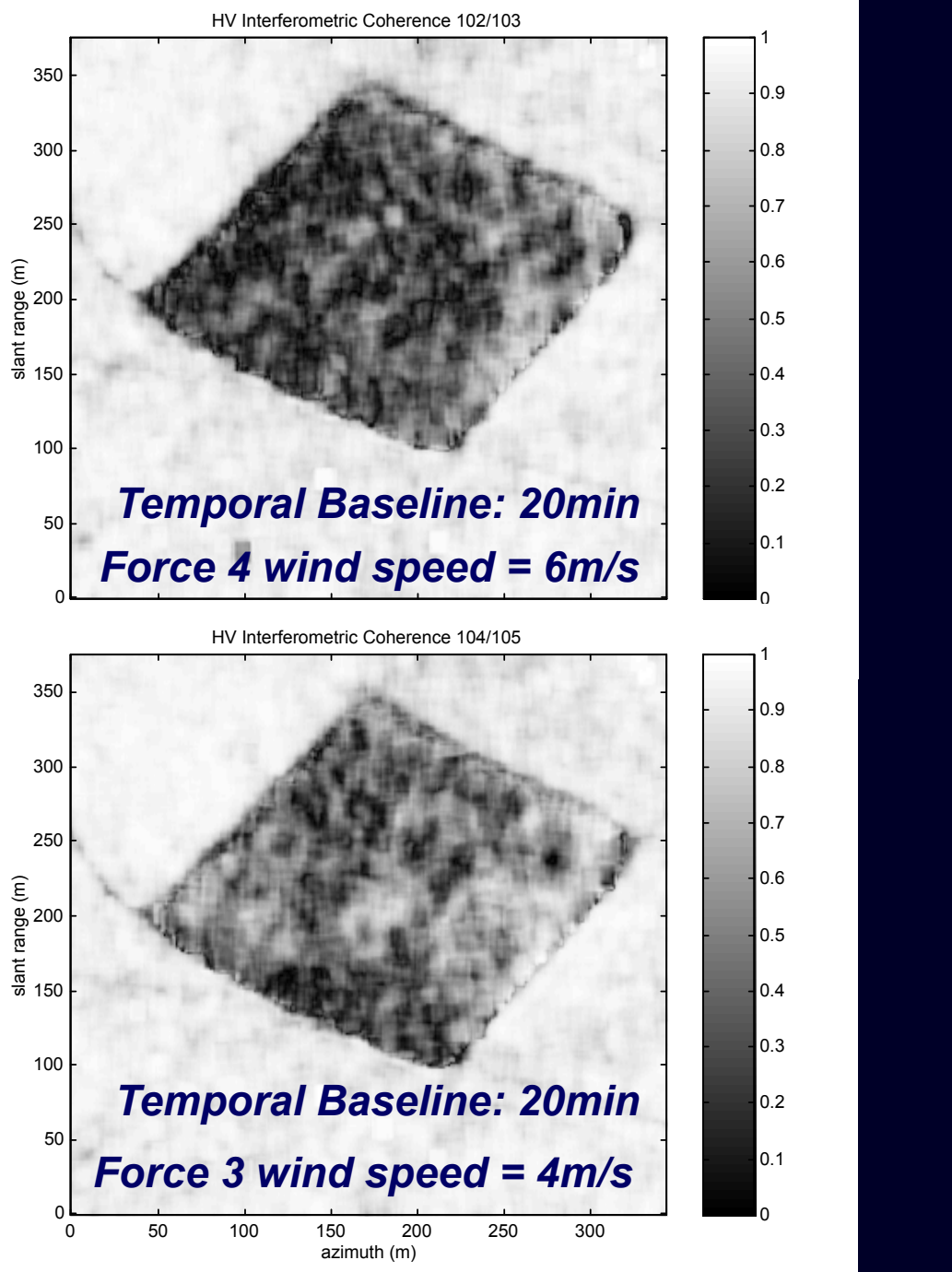
Deutsches Zentrum
für Luft- und Raumfahrt e.V.
in der Helmholtz-Gemeinschaft



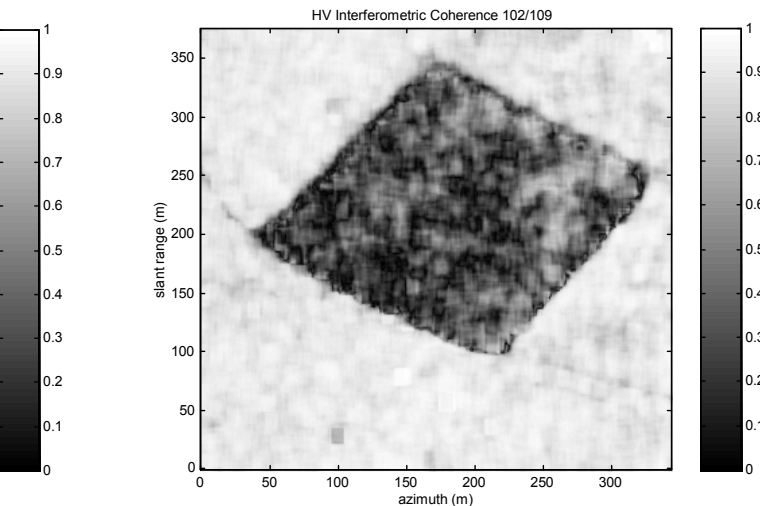
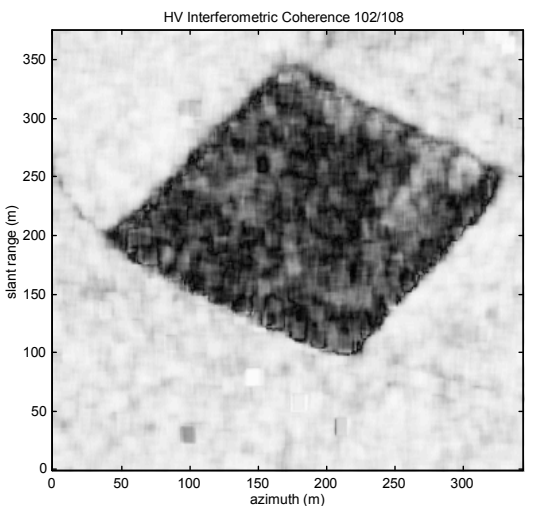
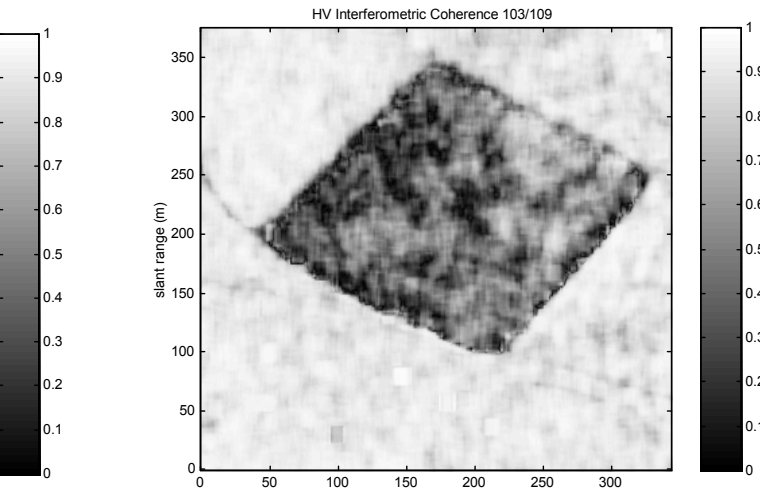
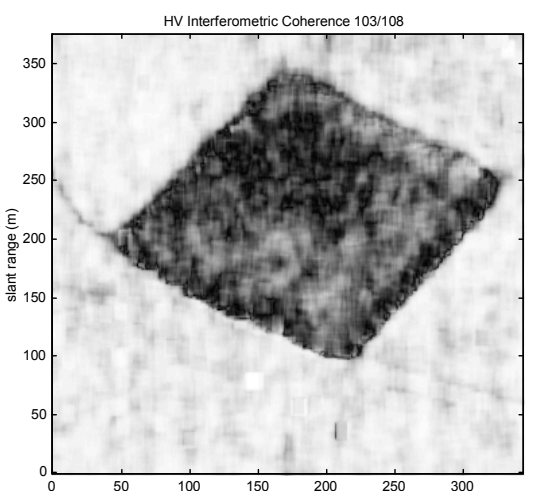
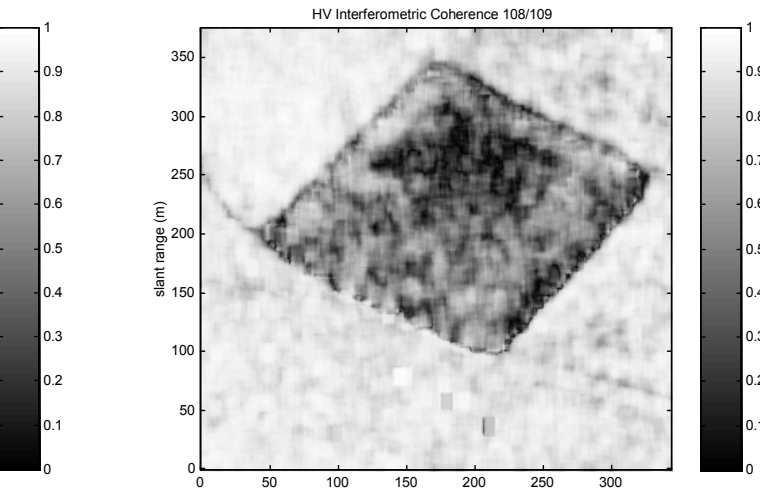
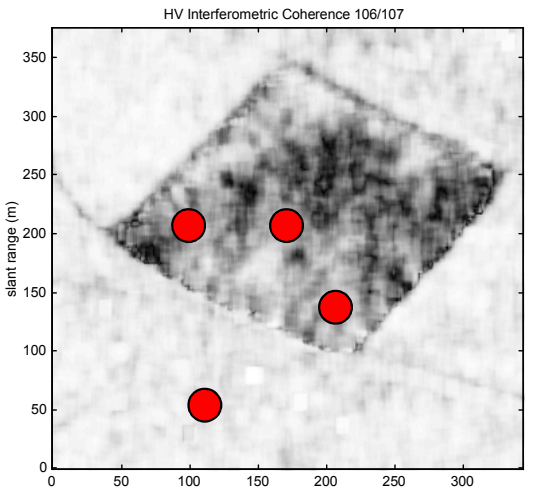
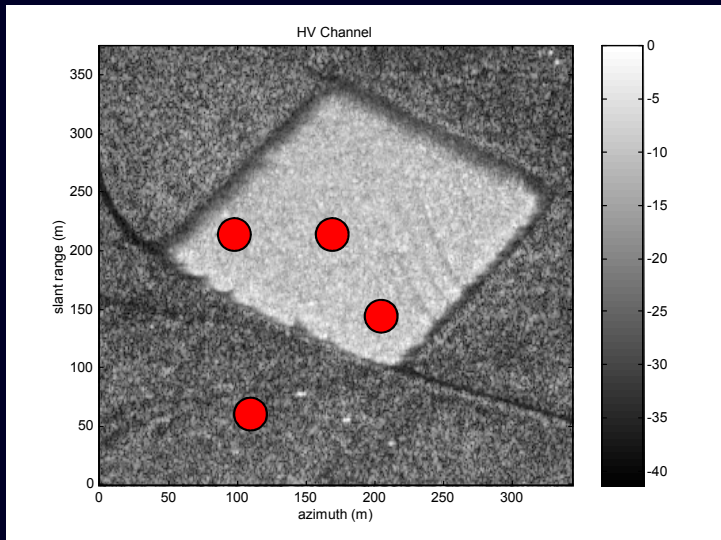
Temporal Decorrelation



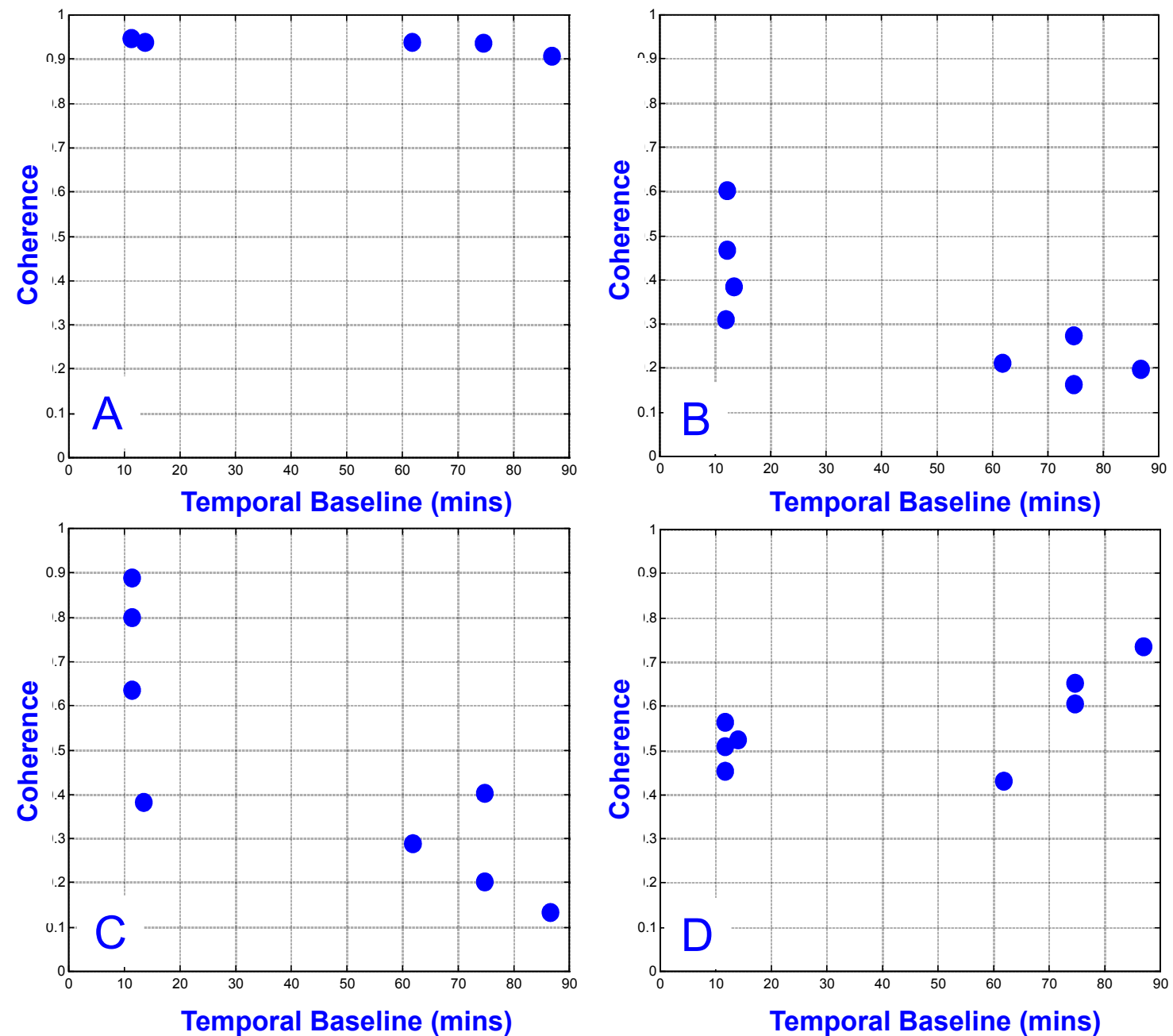
E-SAR / Test Site: Fox Covert, England



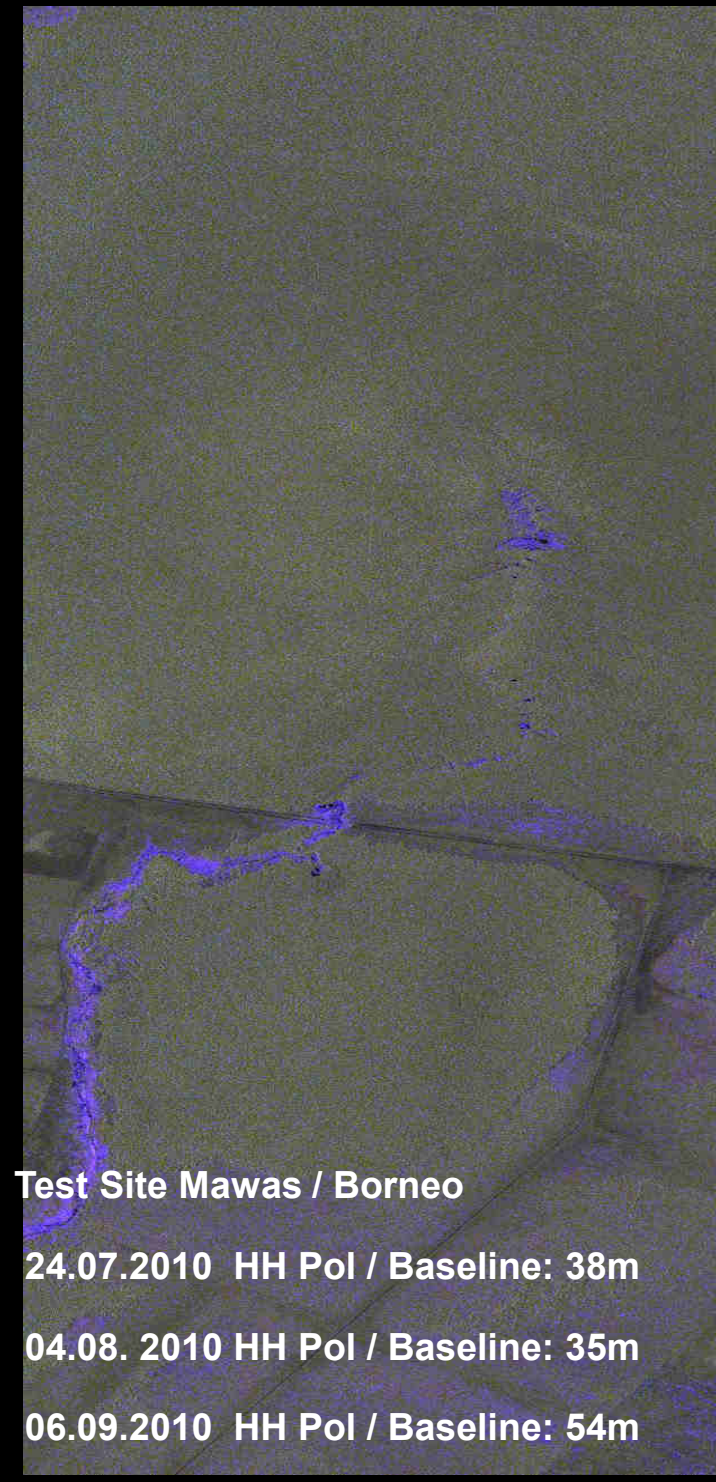
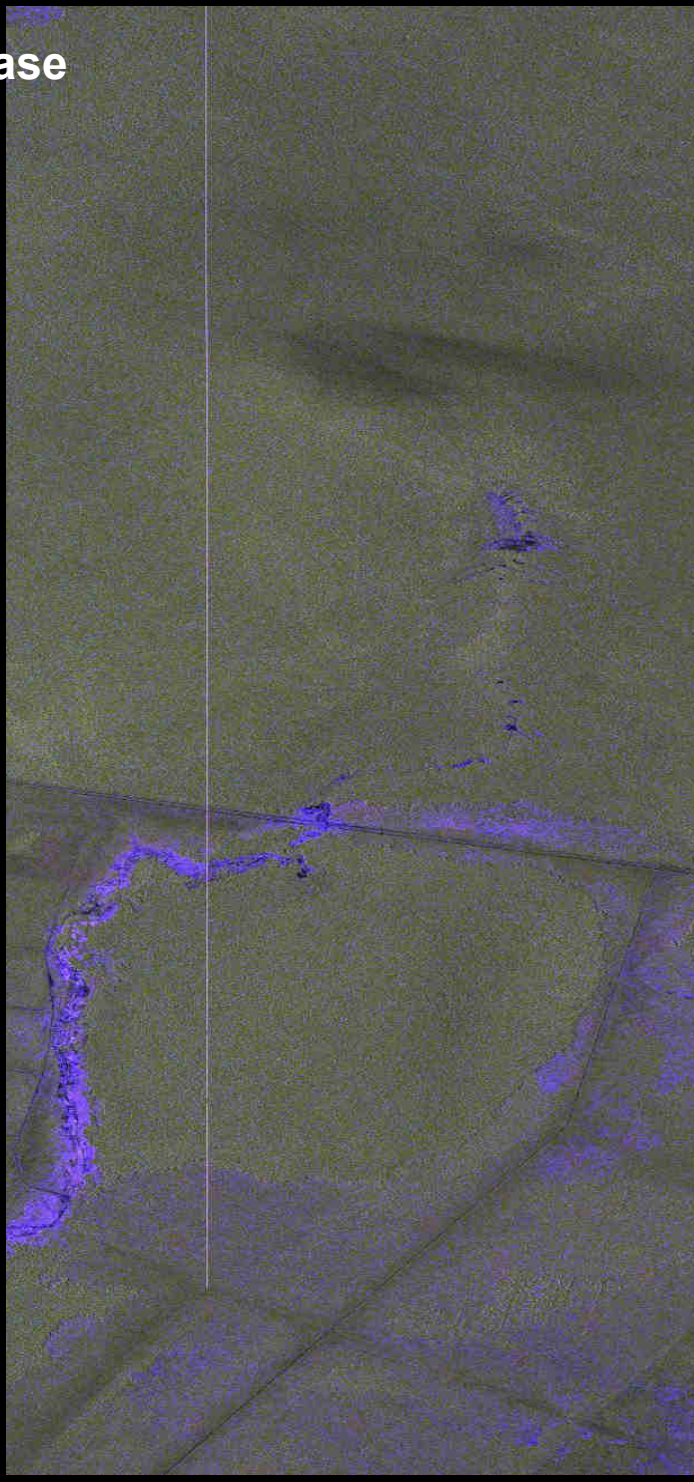
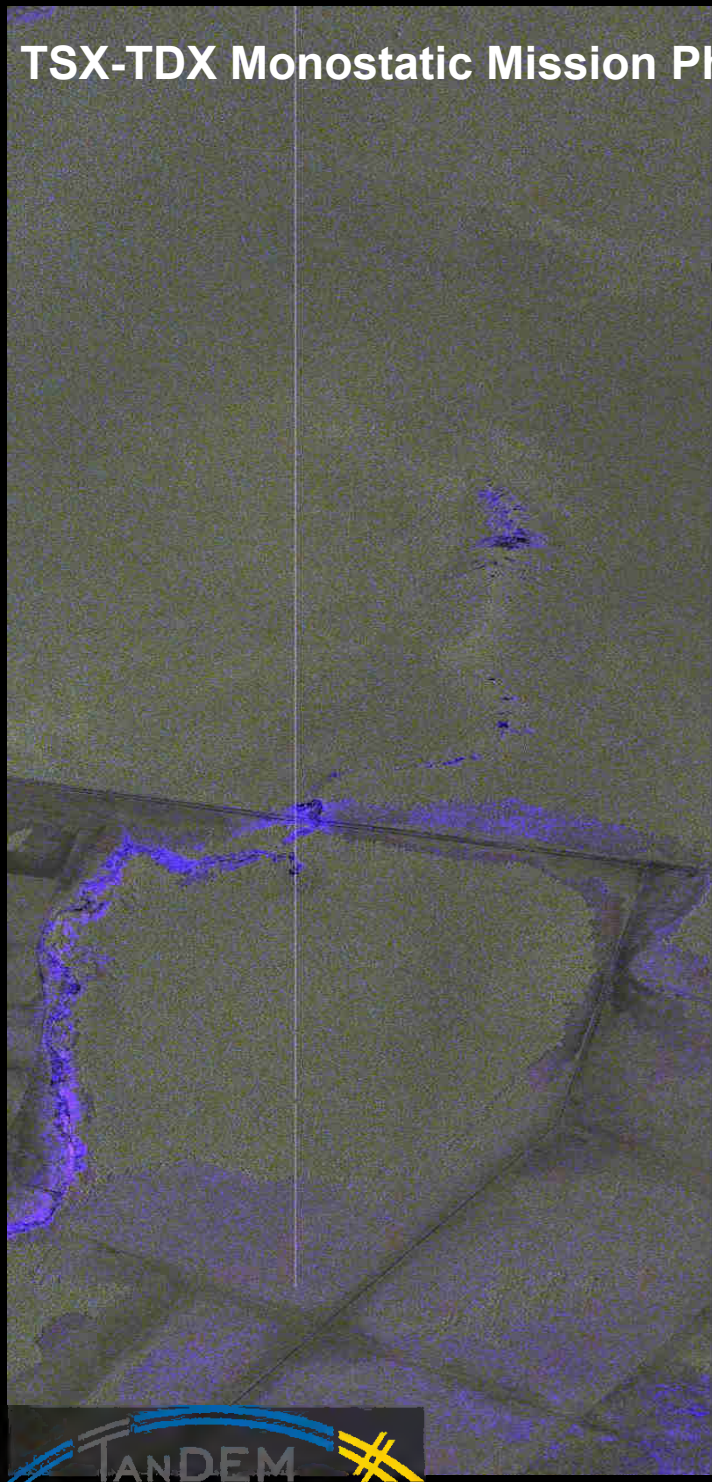
E-SAR / Test Site: Fox Covert,England



Temporal Decorrelation



TSX-TDX Monostatic Mission Phase



Test Site Mawas / Borneo

24.07.2010 HH Pol / Baseline: 38m

04.08. 2010 HH Pol / Baseline: 35m

06.09.2010 HH Pol / Baseline: 54m

TSX-TDX Monostatic Mission Phase

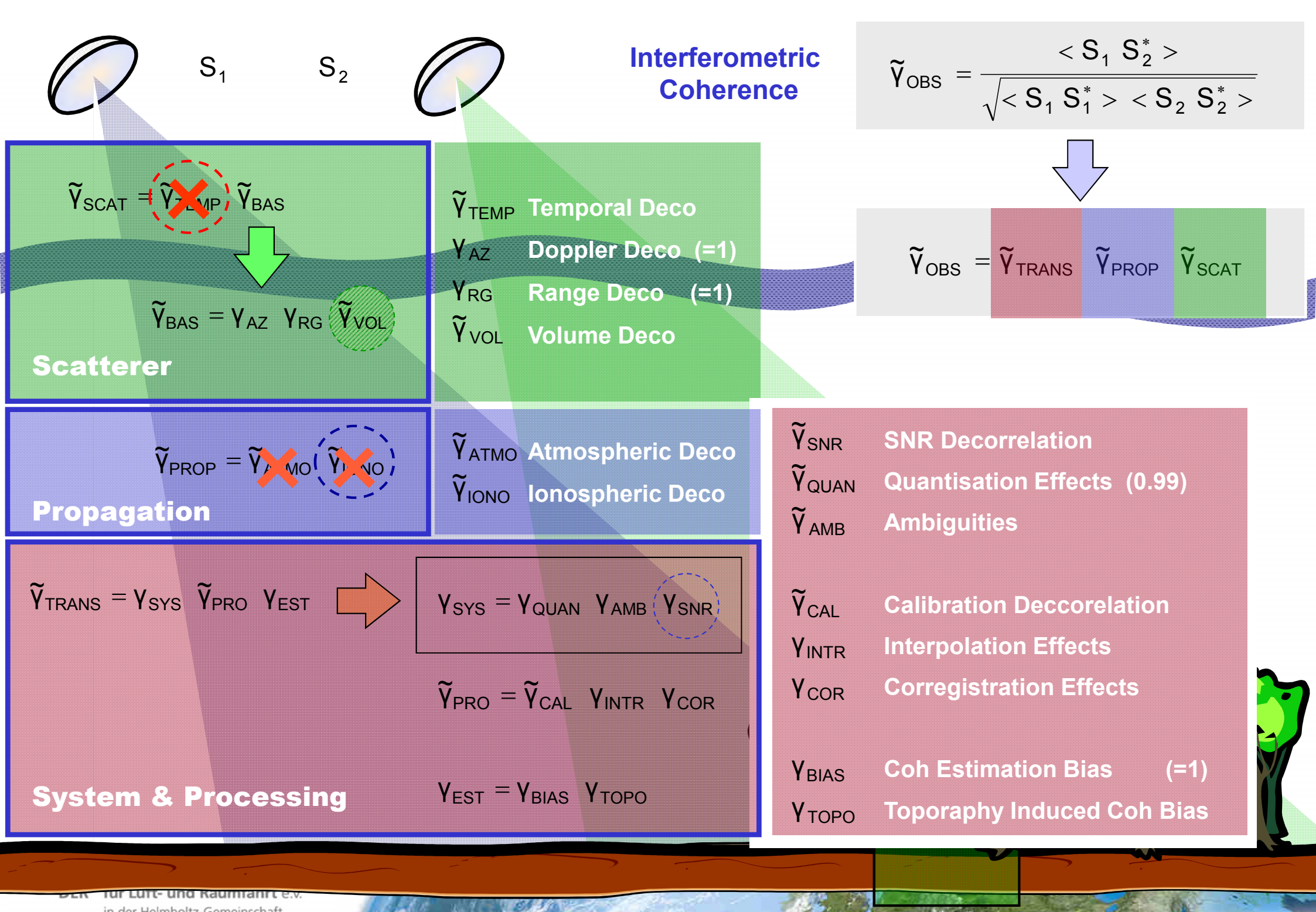
Test Site Mawas / Borneo

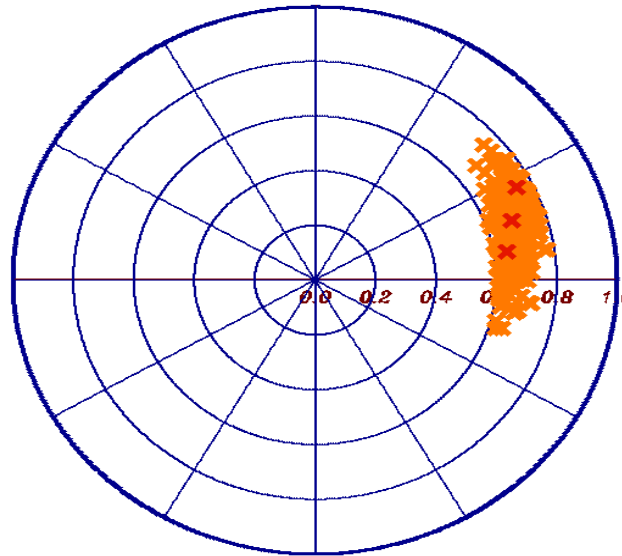
24.07.2010 HH Pol Baseline: 38m

04.08. 2010 HH Pol Baseline: 35m

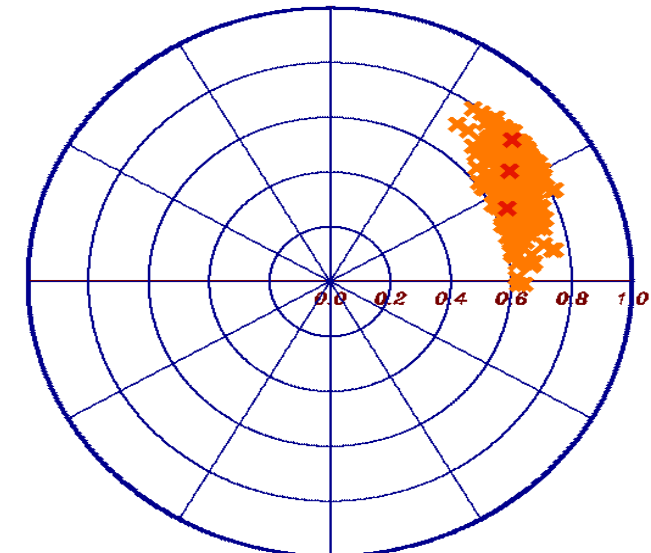
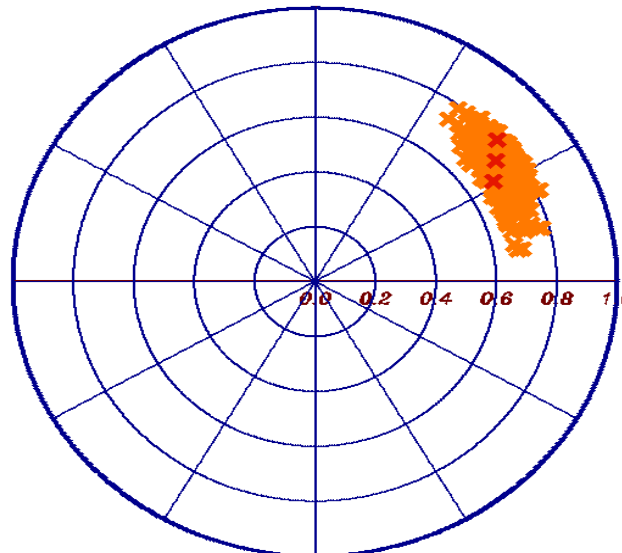
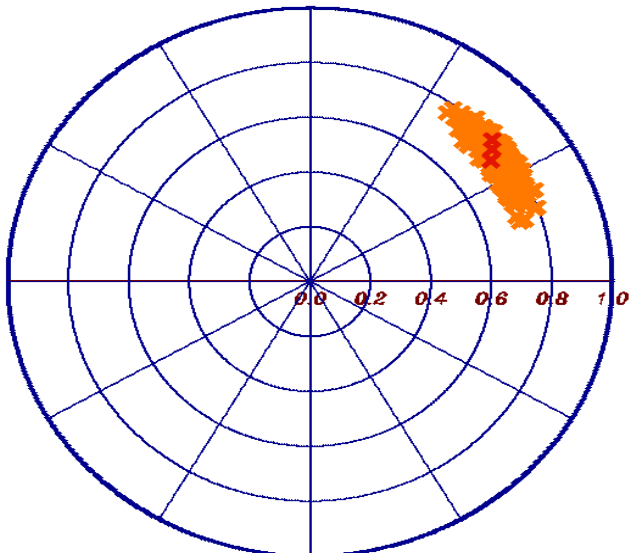
06.09.2010 HH Pol Baseline: 54m

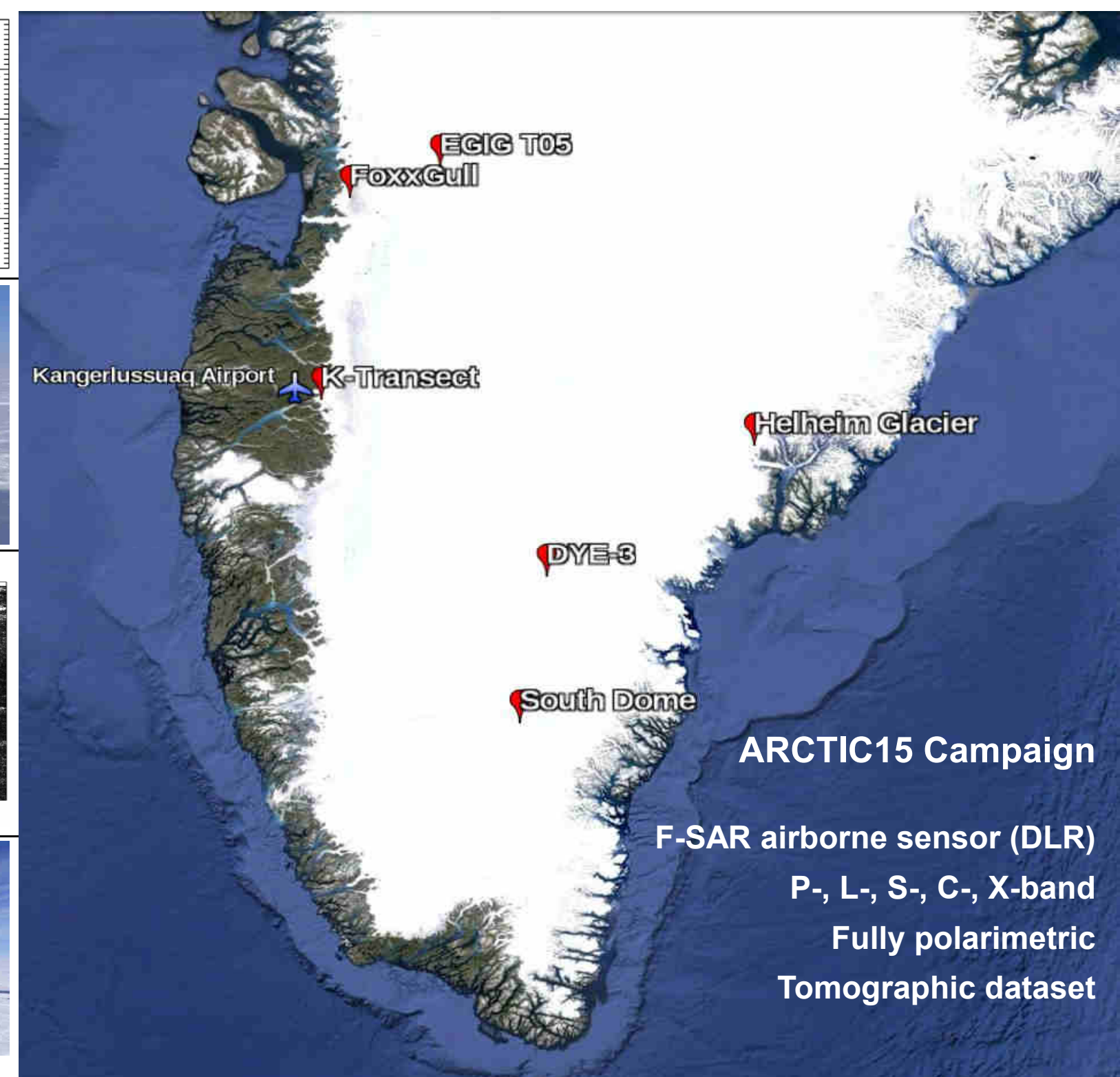
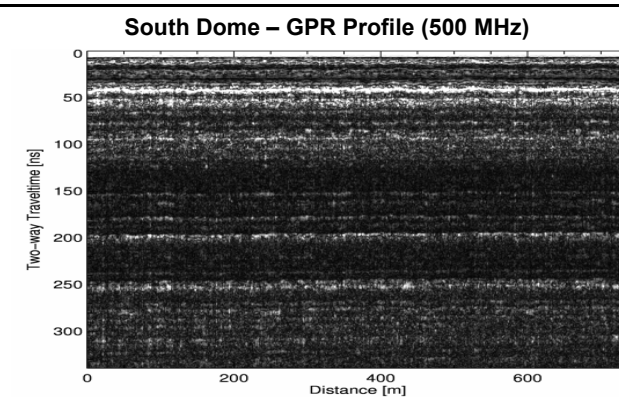
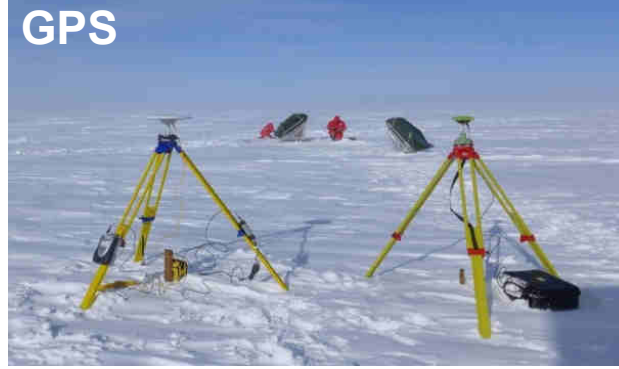
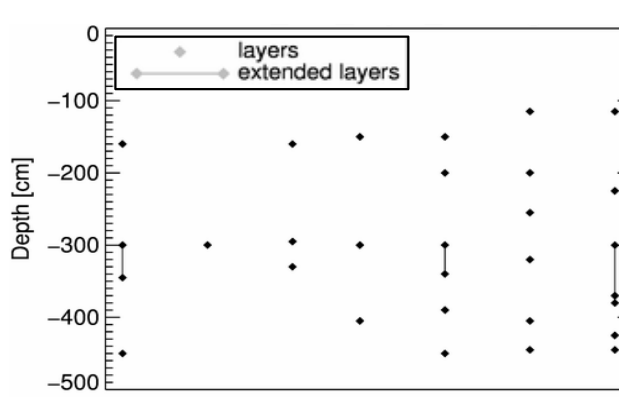






Ice & Snow Layers



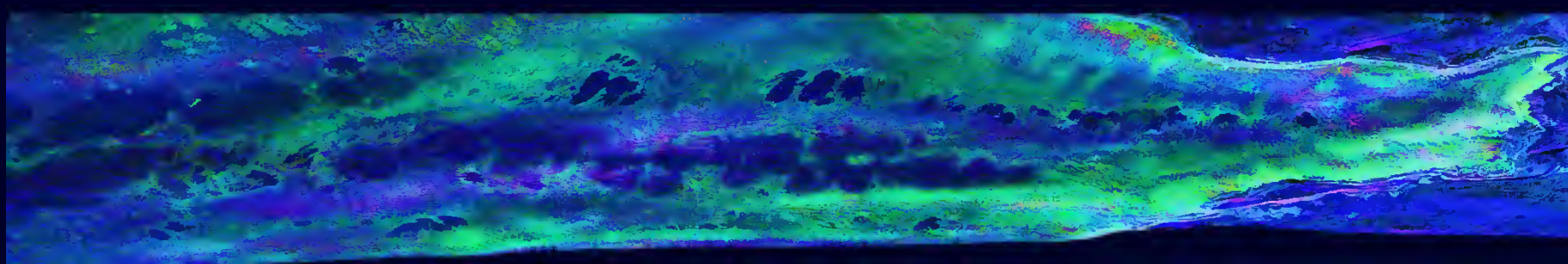


DYE-3

L-band HH+VV HH-VV HV



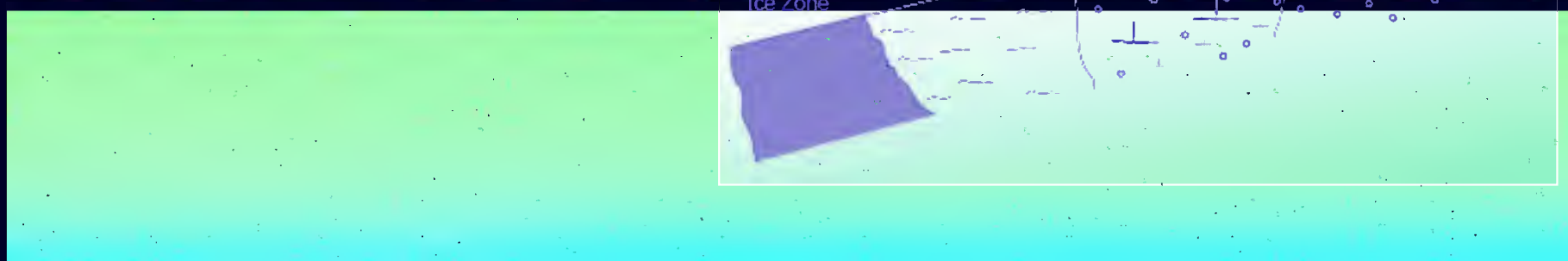
K-Transect



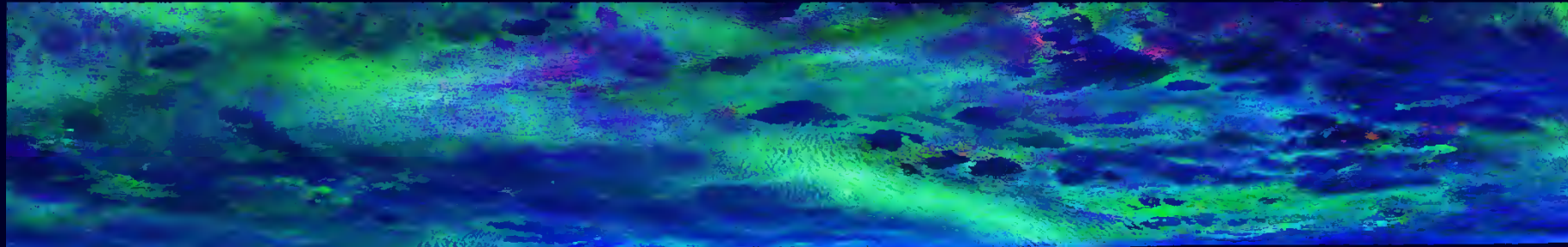
South Dome



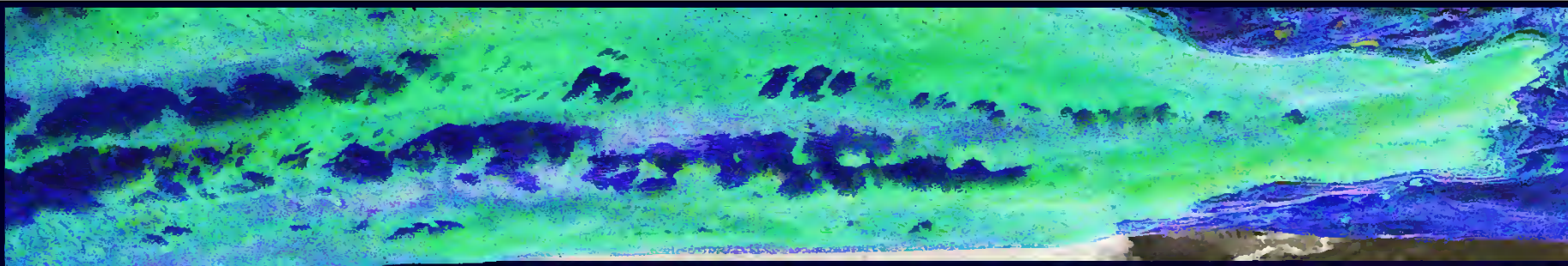
EGIG T05



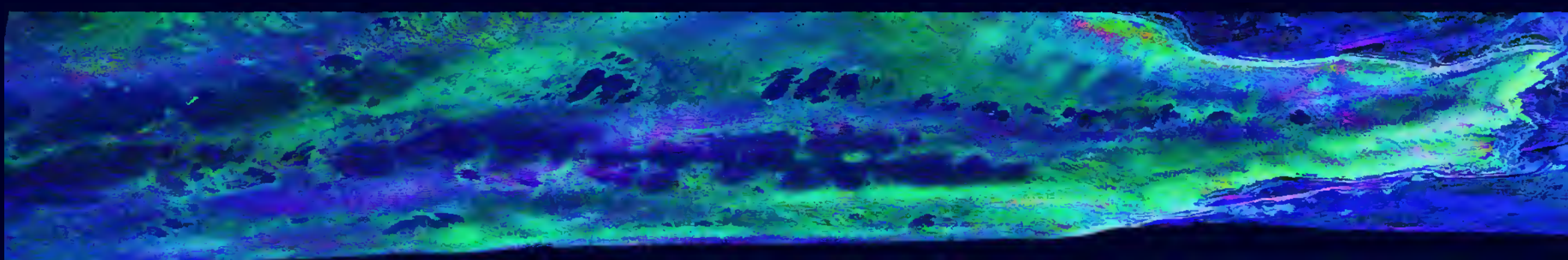
Foxx-Gull



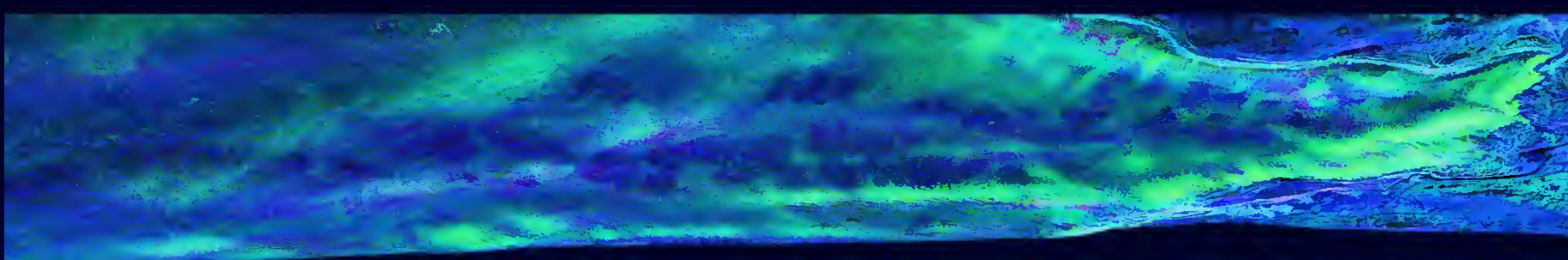
P-band



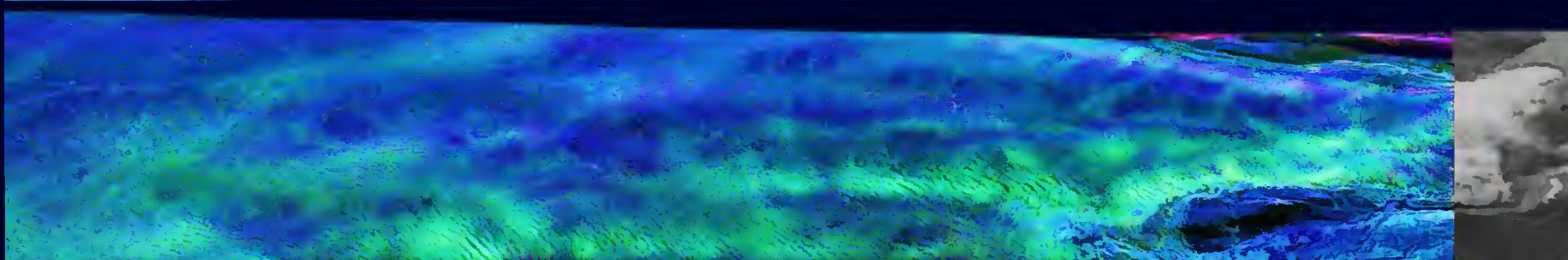
L-band



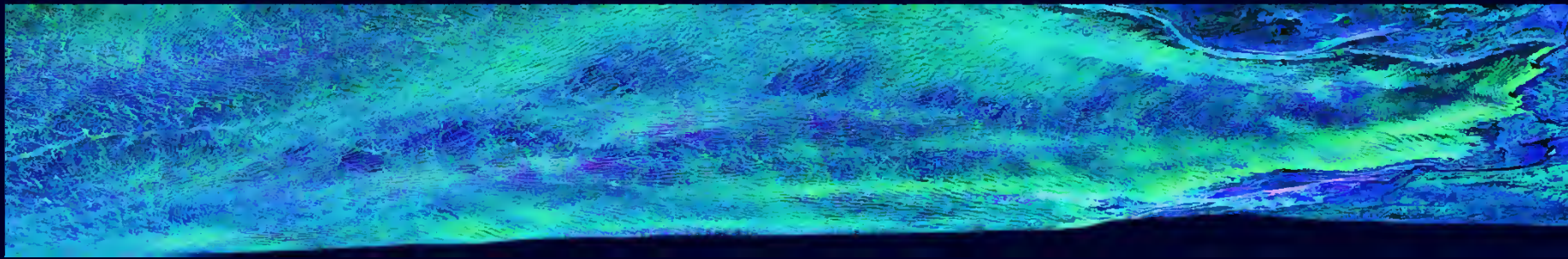
S-band



C-band



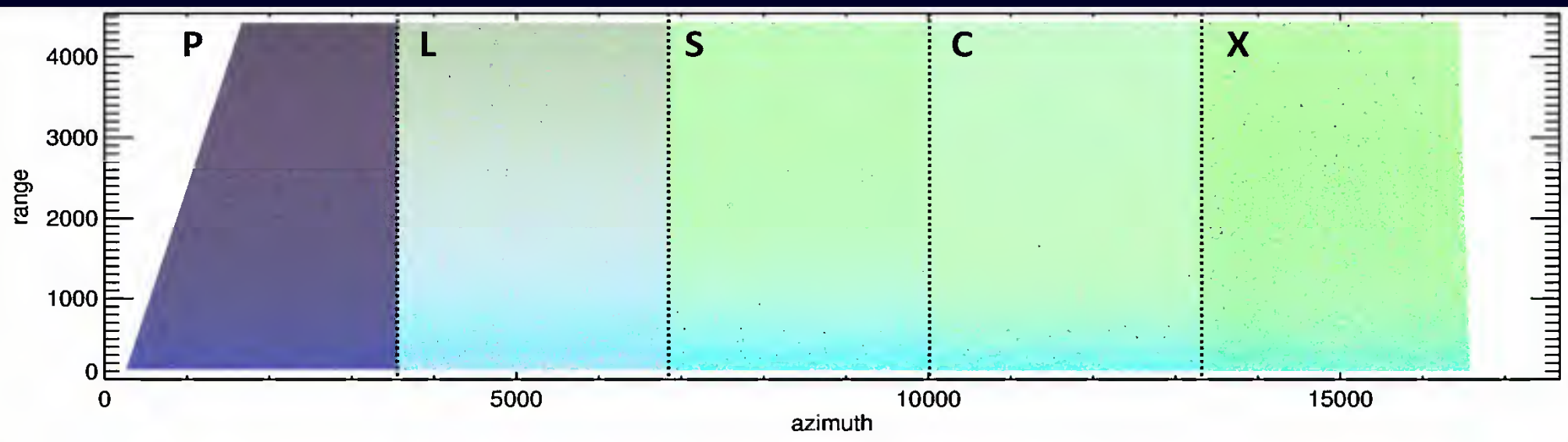
X-band



HH HV VV

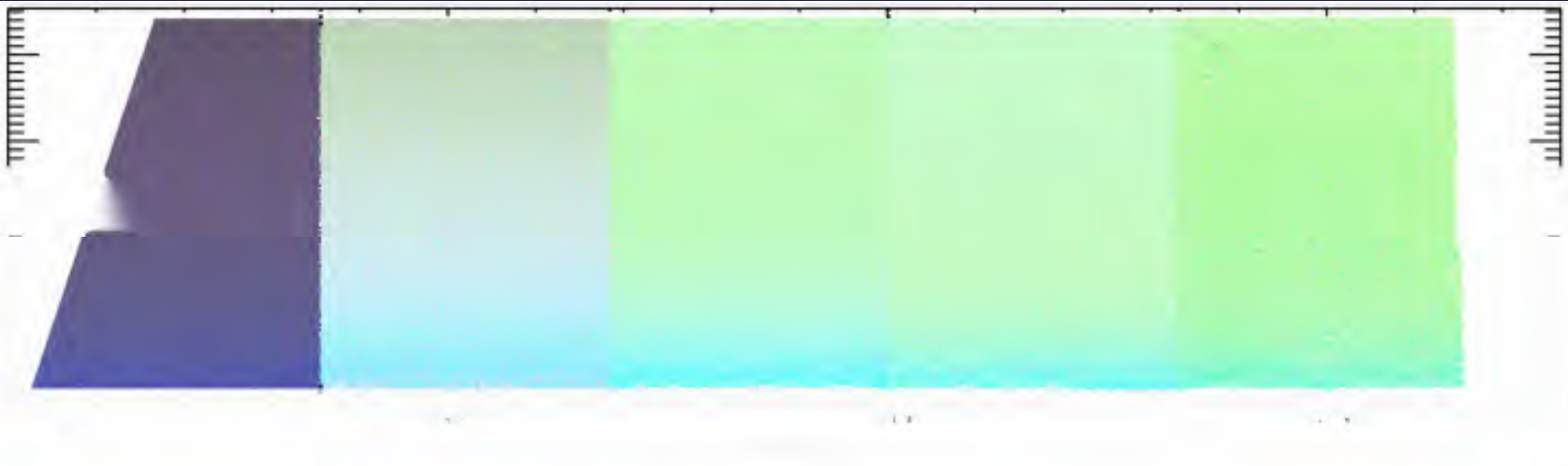
South Dome Polarimetry

HH+VV HH-VV HV

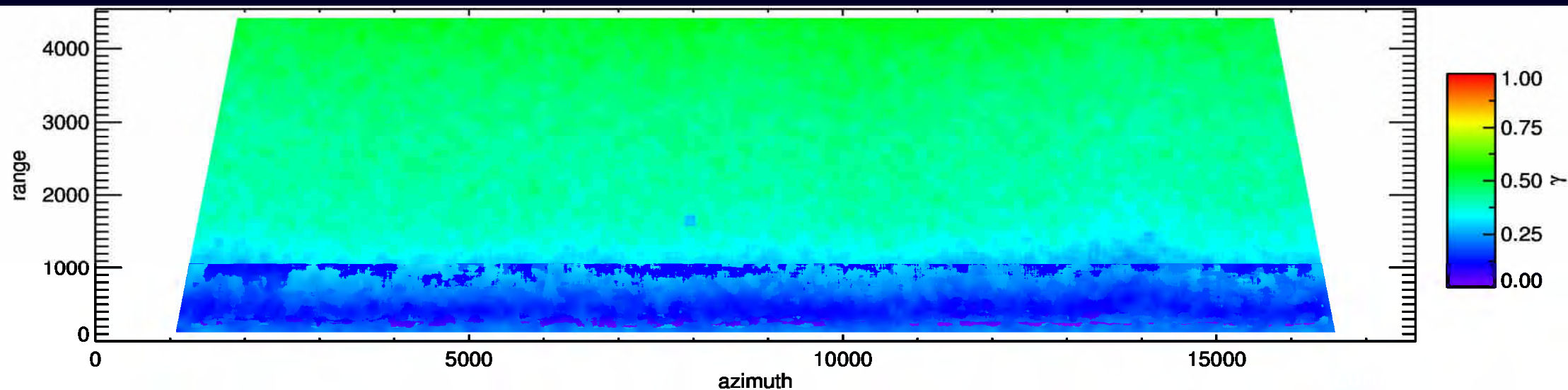


South Dome Polarimetry & Interferometry

HH+VV HH-VV HV



Horiz. Baseline: 20 m

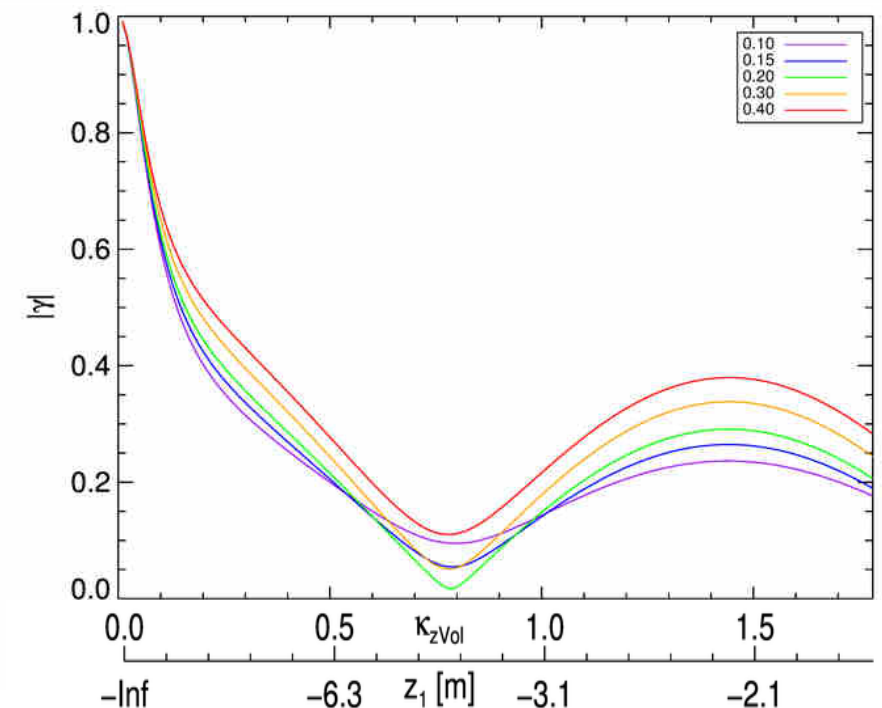
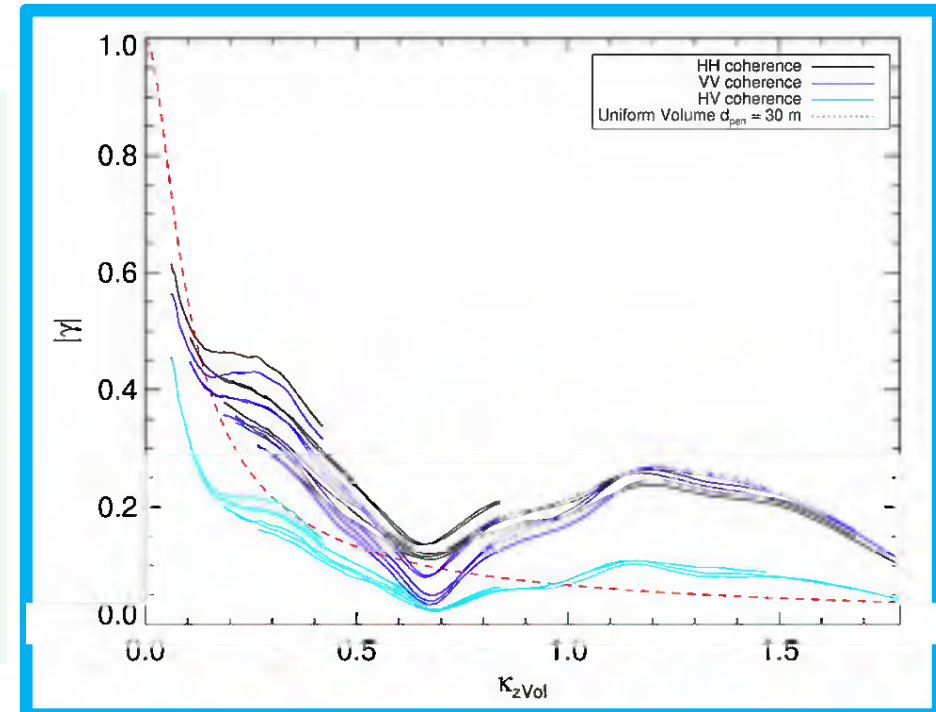
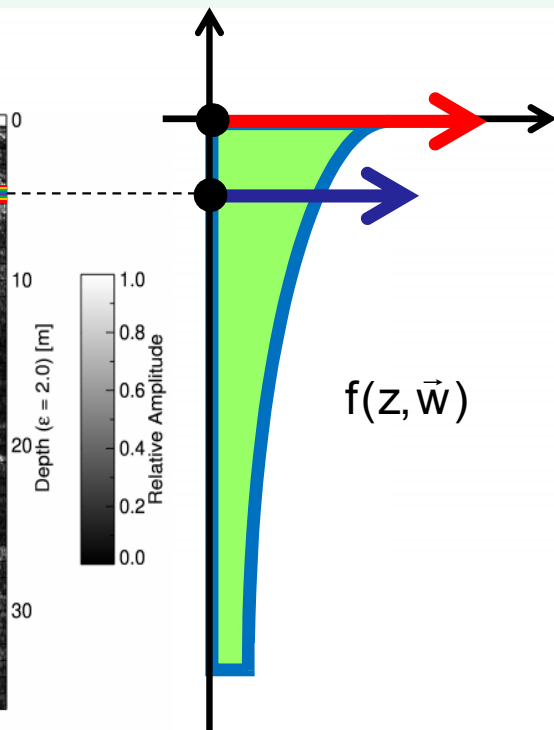
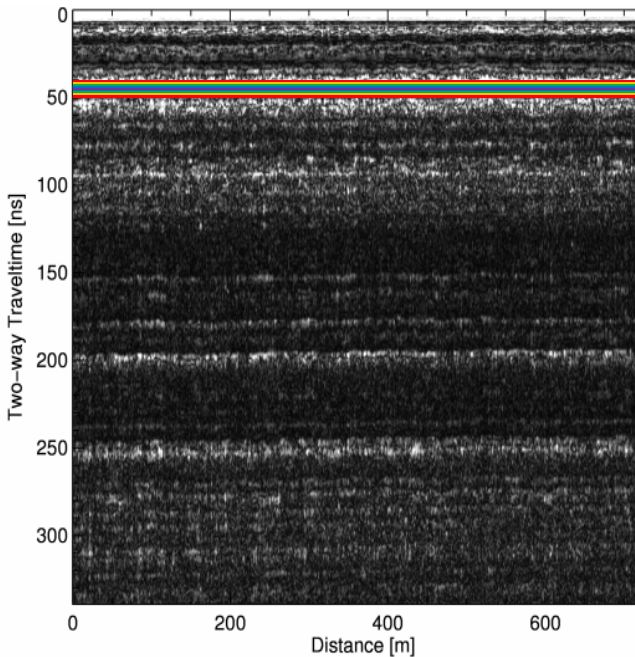


InSAR Coherence Modelling

$$\tilde{\gamma}_{\text{Vol}}(\vec{w}, \kappa_z) = e^{ik_z z_0} \frac{\int_0^{h_v} f(z, \vec{w}) e^{ik_z z} dz}{\int_0^{h_v} f(z, \vec{w}) dz} = e^{ik_z z_0} \frac{\tilde{\gamma}_v + \sum_{j=1}^N m_j \exp(i\kappa_{z_{\text{vol}}} z_j)}{1 + \sum_{j=1}^N m_j}$$

where $\tilde{\gamma}_v(\kappa_z) = \frac{1}{1 + \frac{i\kappa_{z_{\text{vol}}} d_{\text{Pen}}}{2}}$

GPR Profile @ 500 MHz

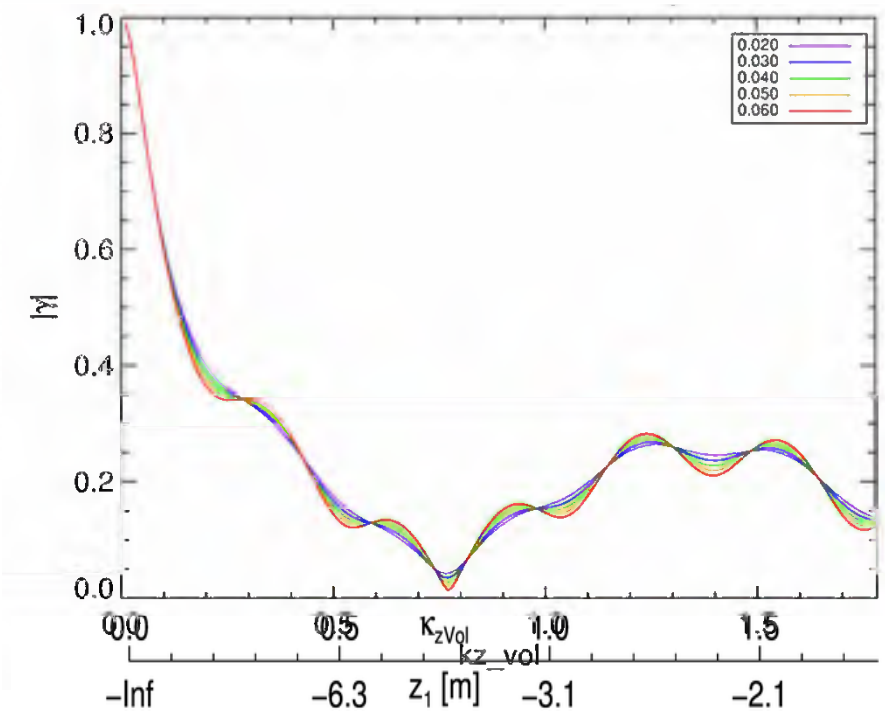
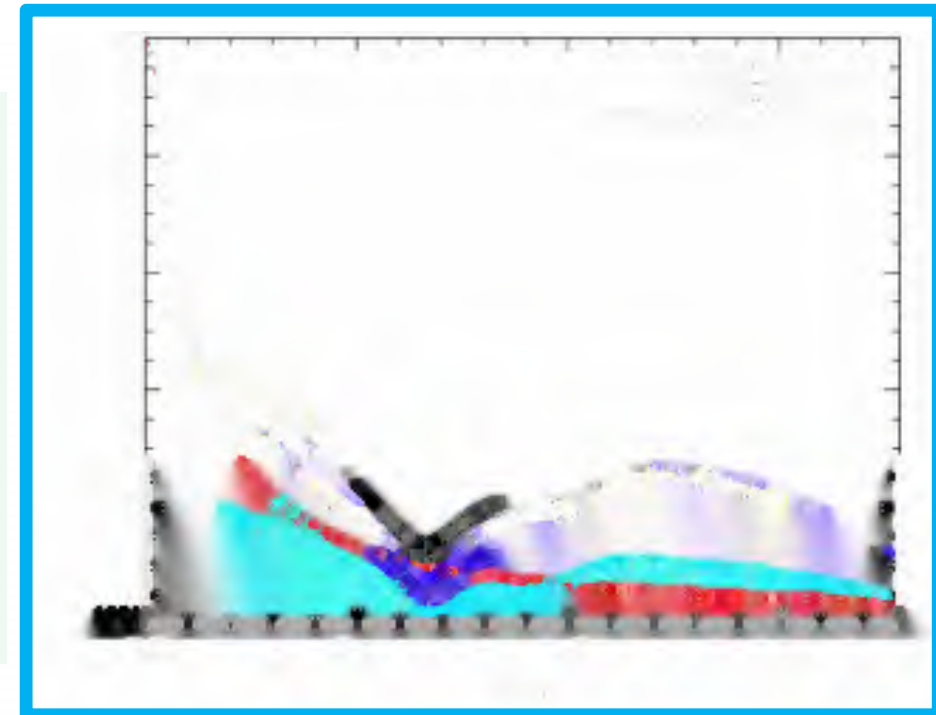
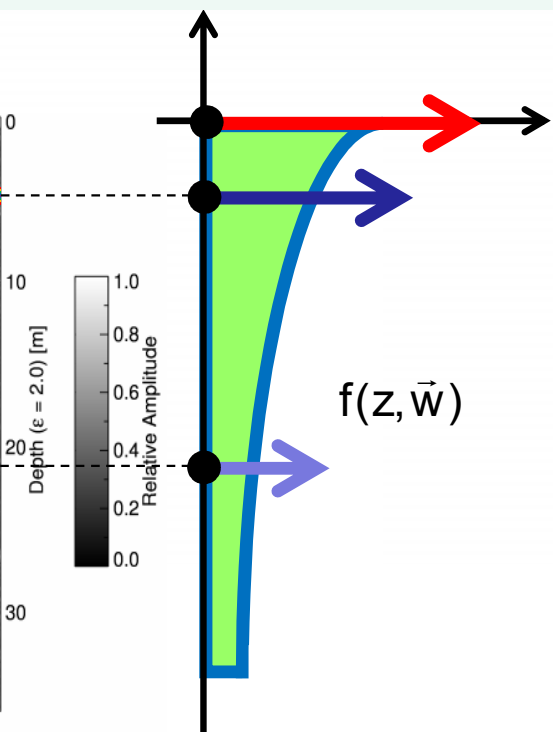
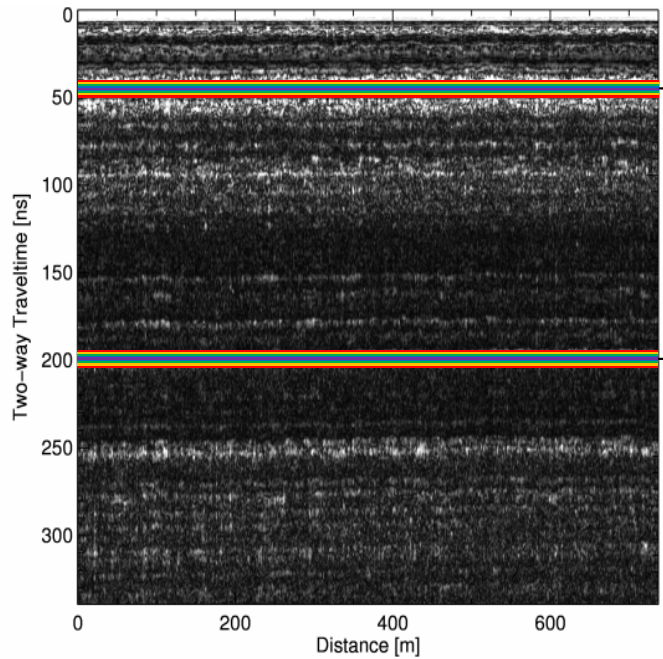


InSAR Coherence Modelling

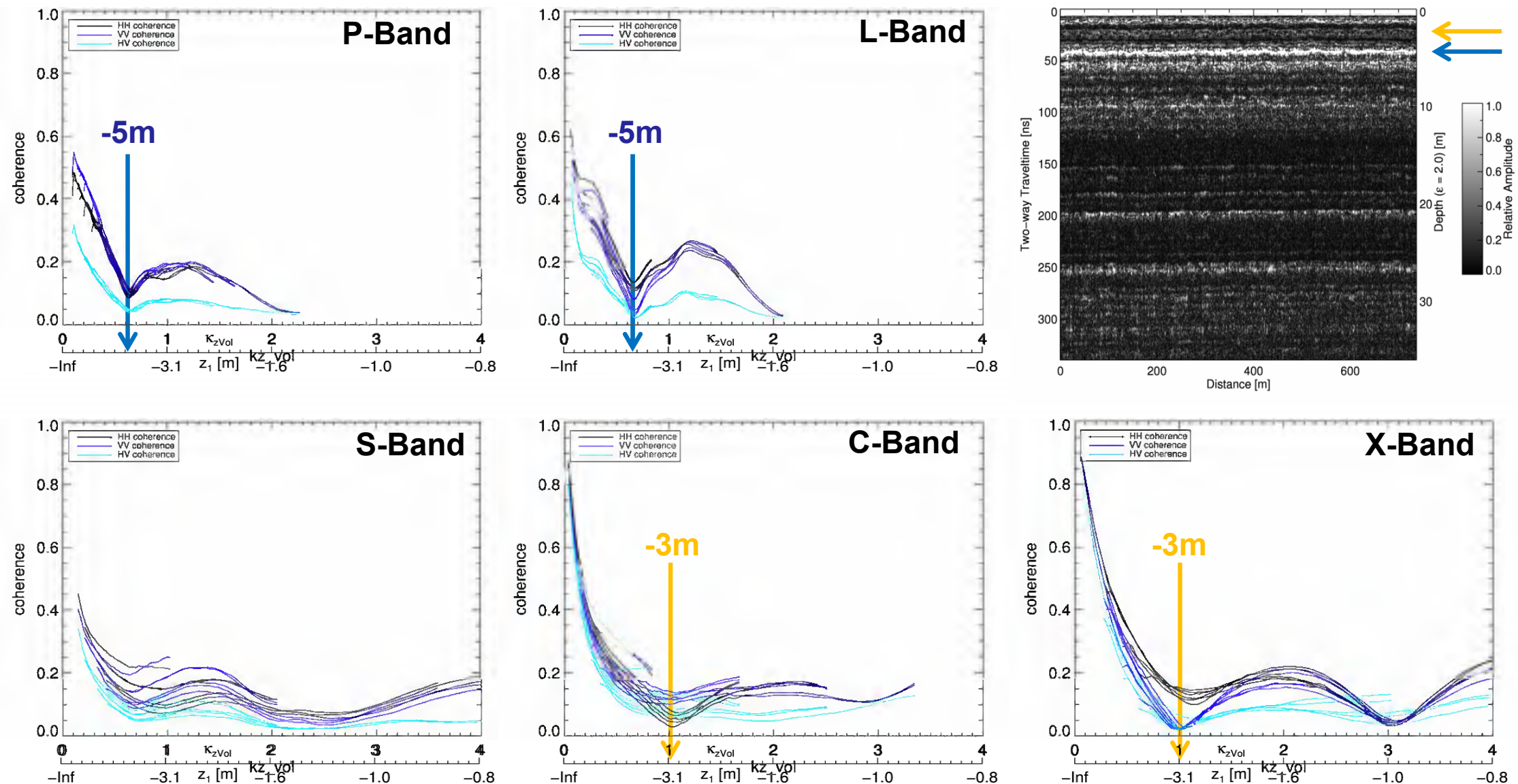
$$\tilde{\gamma}_{\text{vol}}(\vec{w}, \kappa_z) = e^{ik_z z_0} \frac{\int_0^{h_v} f(z, \vec{w}) e^{ik_z z} dz}{\int_0^{h_v} f(z, \vec{w}) dz} = e^{ik_z z_0} \frac{\tilde{\gamma}_v + \sum_{j=1}^N m_j \exp(i\kappa_{z_{\text{vol}}} z_j)}{1 + \sum_{j=1}^N m_j}$$

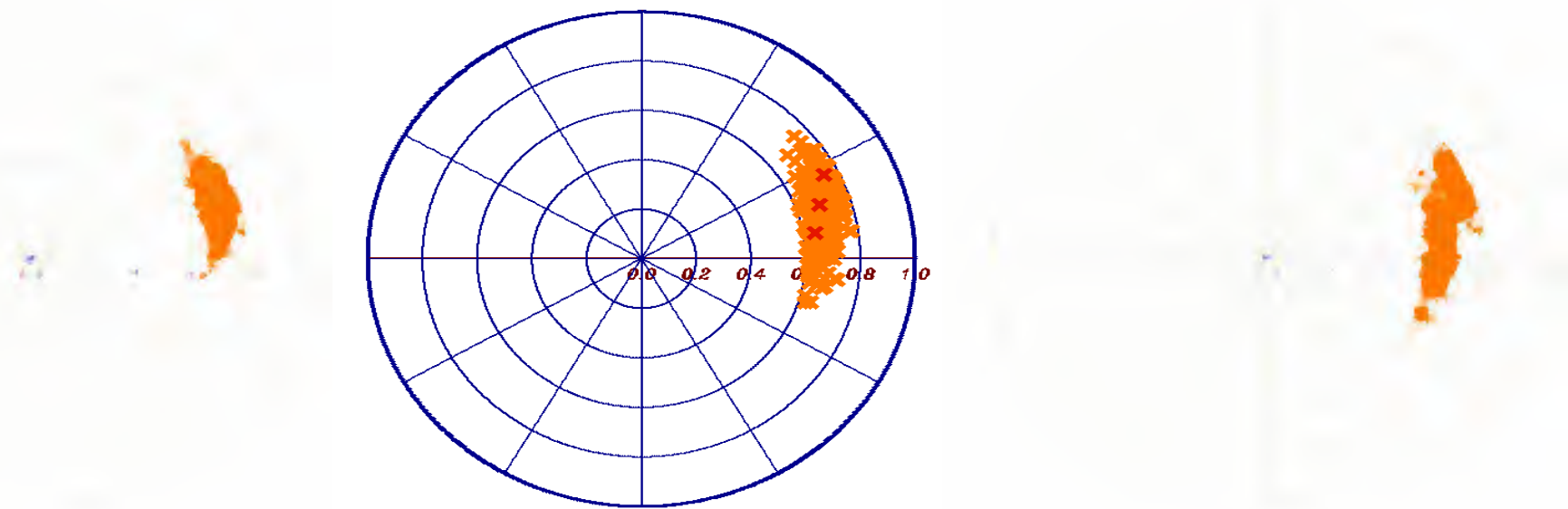
where $\tilde{\gamma}_v(\kappa_z) = \frac{1}{1 + \frac{i\kappa_{z_{\text{vol}}} d_{\text{Pen}}}{2}}$

GPR Profile @ 500 MHz

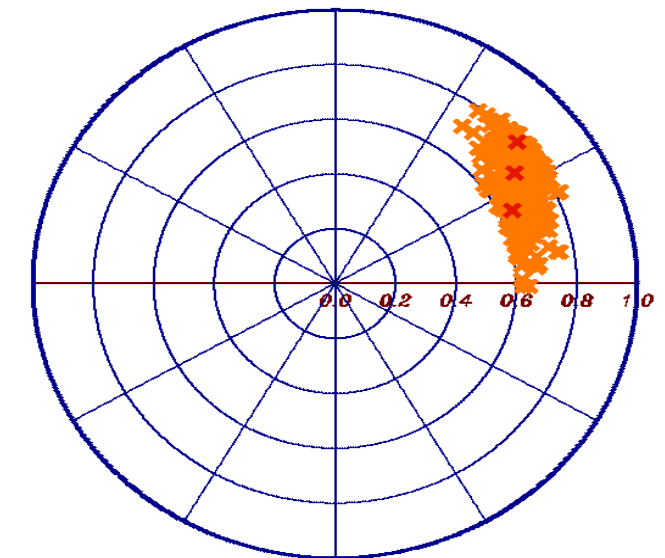
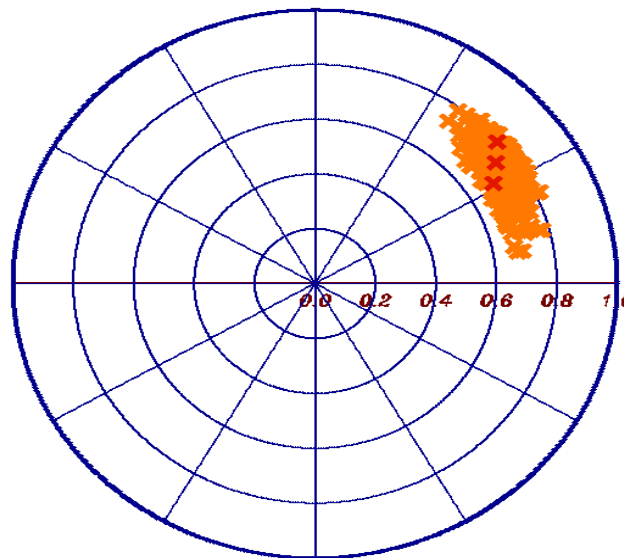
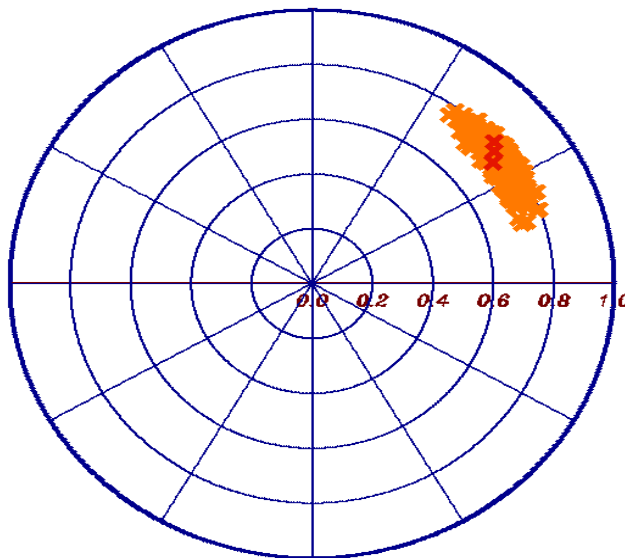


InSAR Coherence @ Different Frequencies

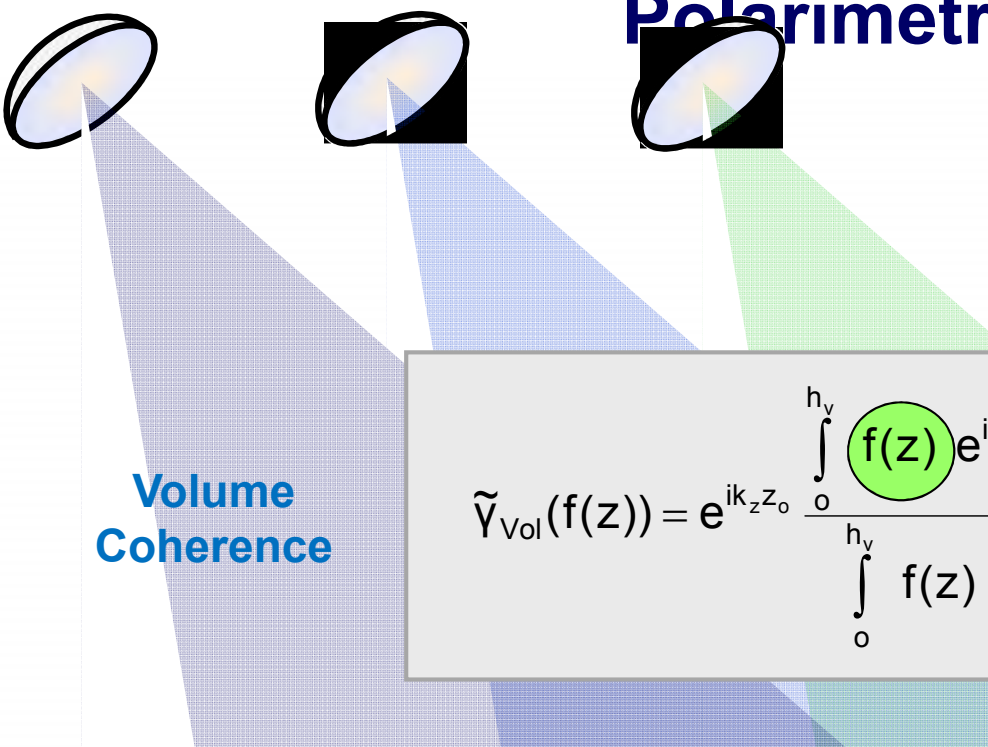




Polarimetric Coherence Tomography (PCT)

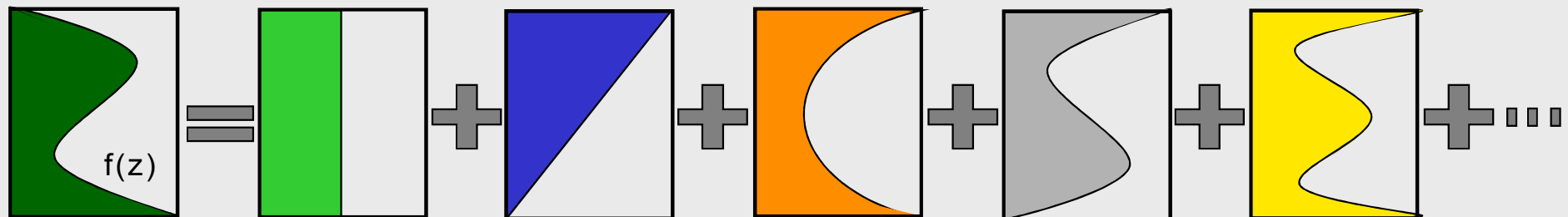
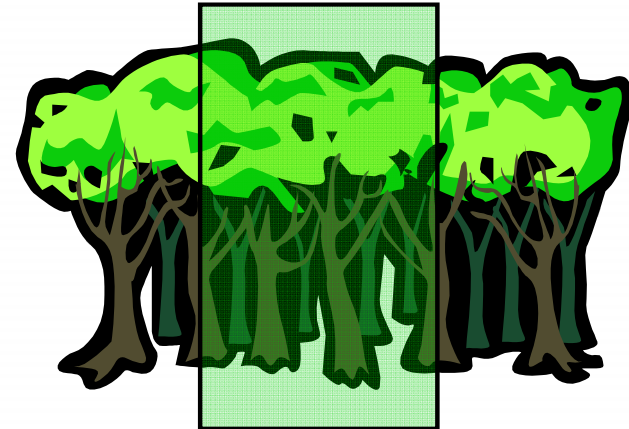
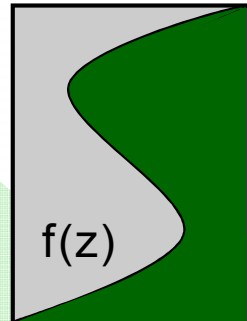


Polarimetric Coherence Tomography (PCT)



$f(z)$... vertical reflectivity function

$$\tilde{\gamma}_{\text{Vol}}(f(z)) = e^{ik_z z_0} \frac{\int_0^{h_v} f(z) e^{ik_z z} dz}{\int_0^{h_v} f(z) dz}$$



$$\tilde{\gamma}_{\text{Vol}}(f(z)) = e^{ik_z z_0} \frac{\int_0^{h_v} f(z) e^{ik_z z} dz}{\int_0^{h_v} f(z) dz}$$

$$\int_0^{h_v} f(z) e^{ik_z z} dz = \frac{h_v}{2} e^{\frac{i k_z h_v}{2}} \int_{-1}^1 (1 + f(z')) e^{\frac{i k_z h_v}{2} z'} dz'$$

$$\int_0^{h_v} f(z) dz = \frac{h_v}{2} \int_{-1}^1 (1 + f(z')) dz'$$

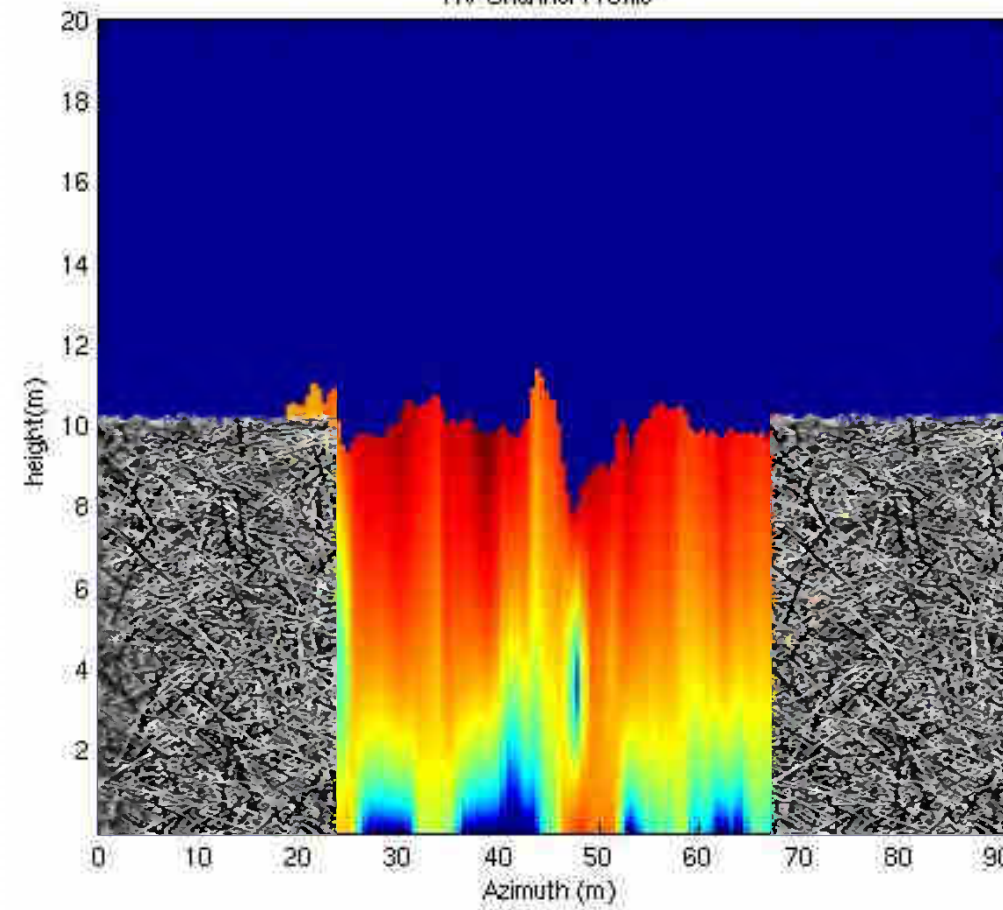
Fourier Legendre Series:

$$f(z') = \sum_n a_n P_n(z')$$

where

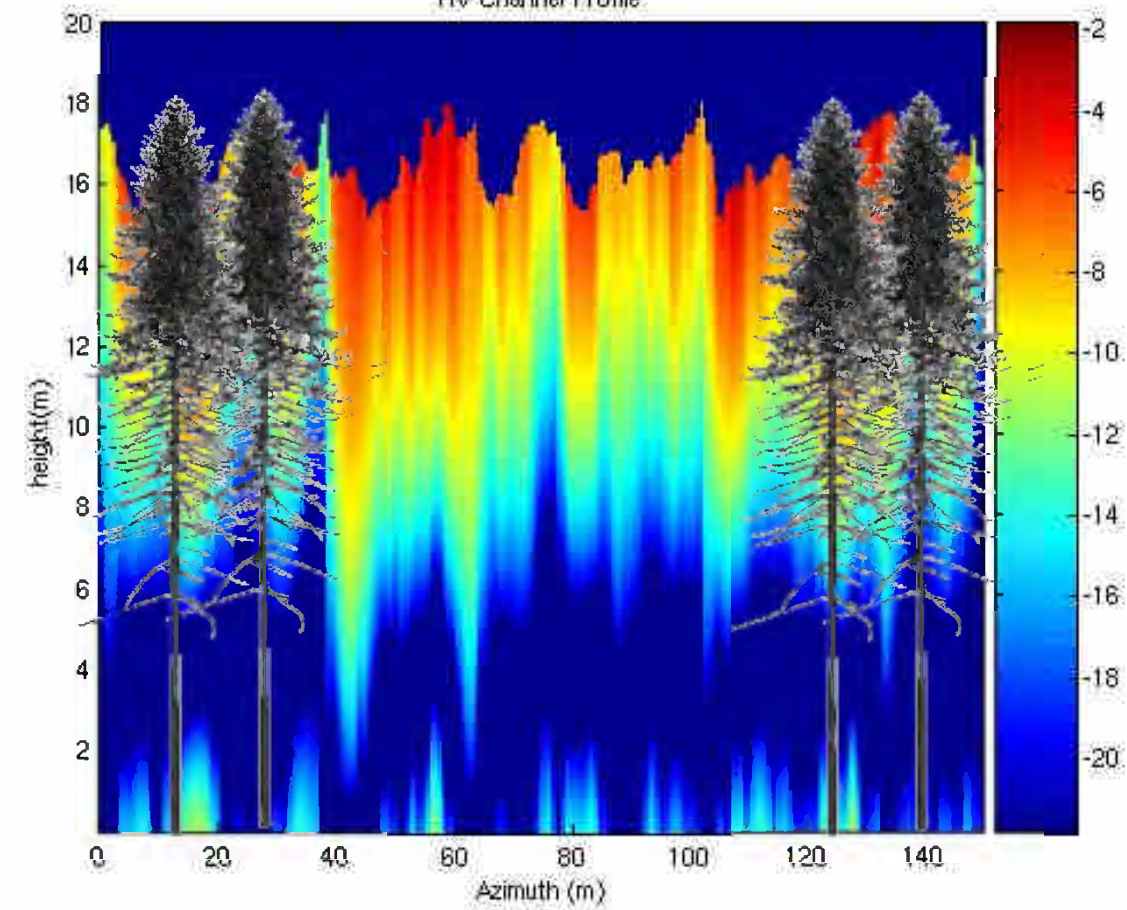
$$a_n = \frac{2n+1}{2} \int_{-1}^1 f(z') P_n(z') dz'$$

HV Channel Profile



10m Uniform Hedge

HV Channel Profile

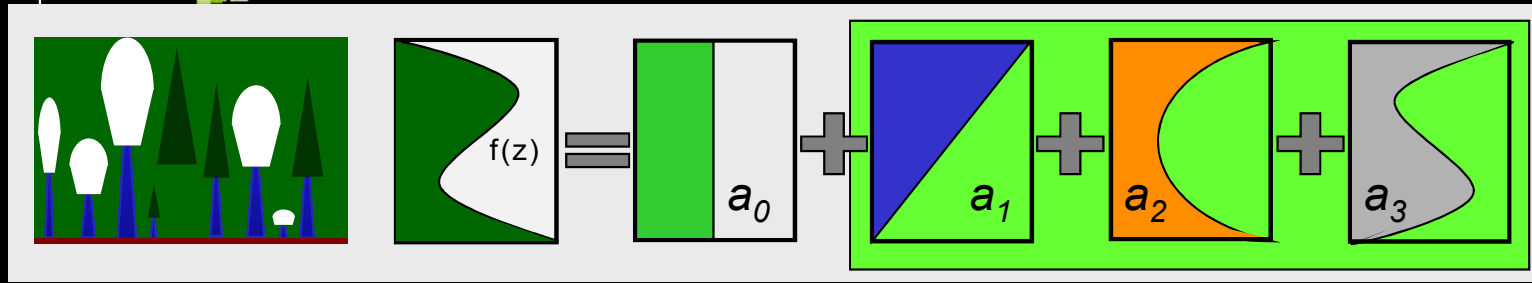
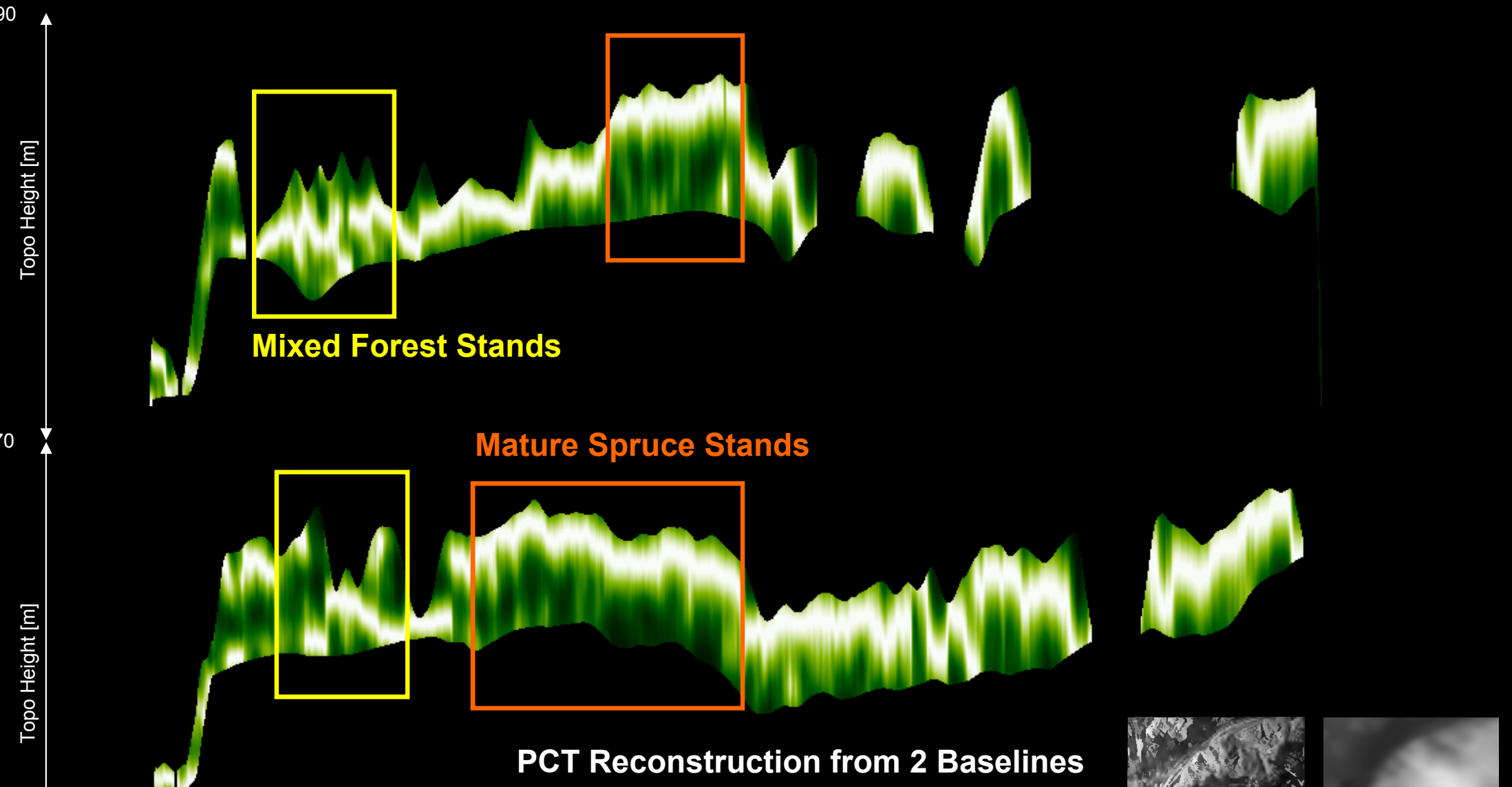


17m Scots Pine Forest

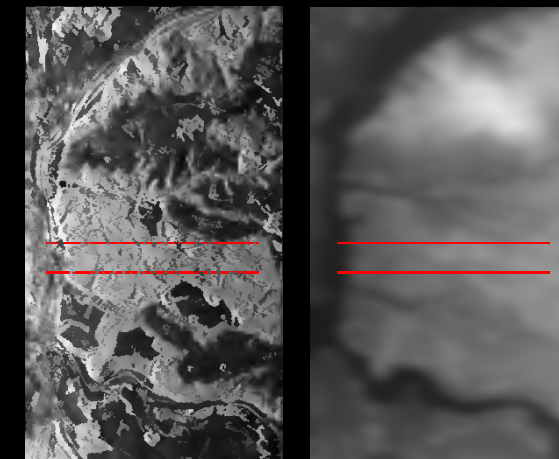
Simulations courtesy of Mark Williams:

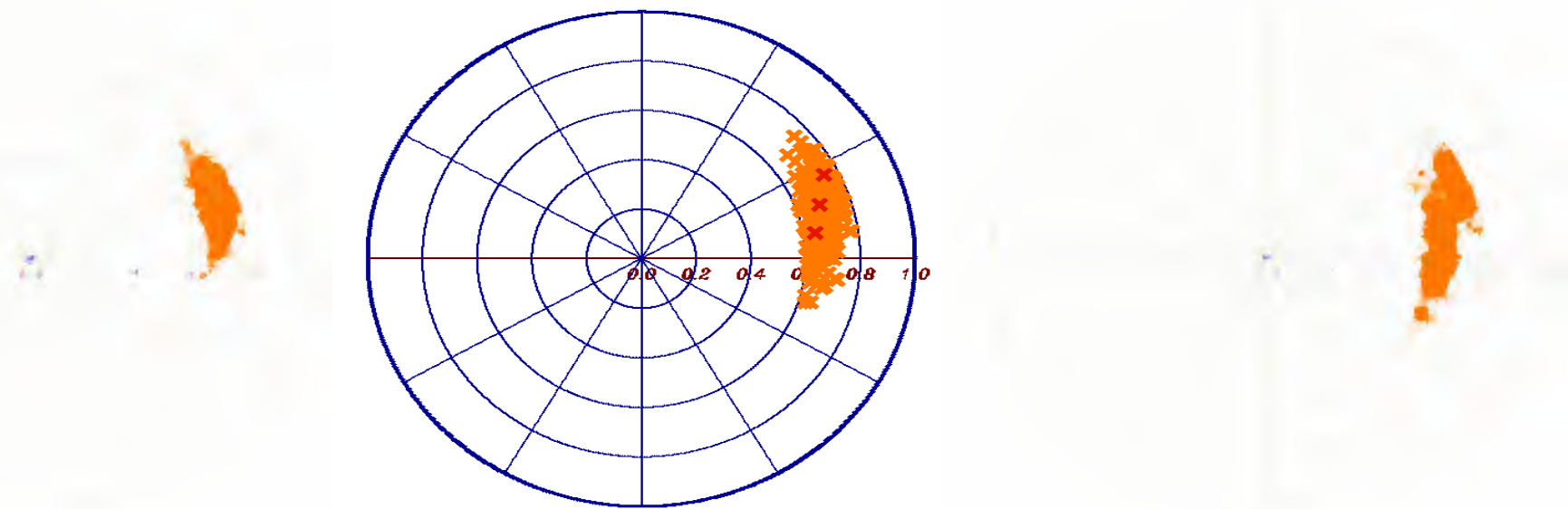
S.R. Cloude, D.G. Corr, M.L. Williams, "Target Detection Beneath Foliage Using PolInSAR", Waves in Random Media, vol. 14, pages S393 - S414., 2004



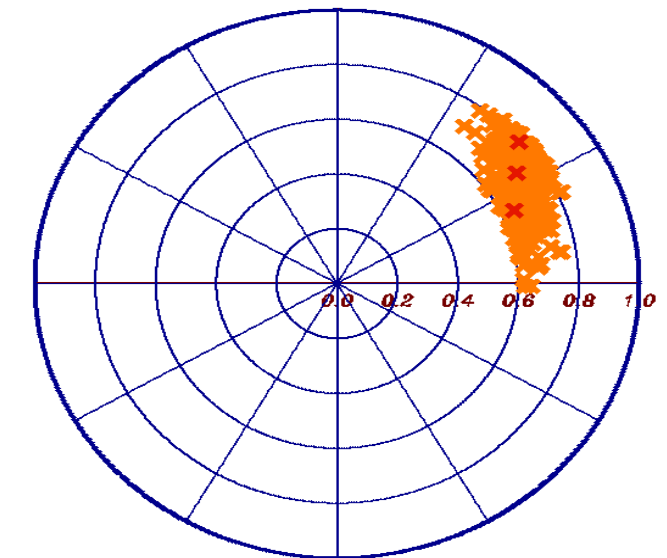
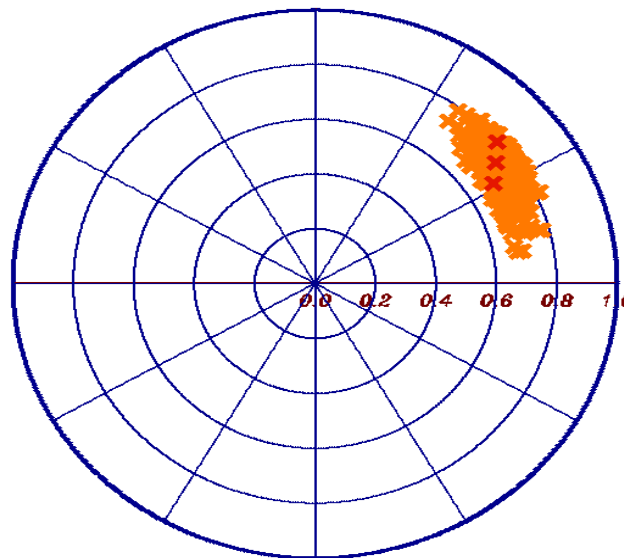
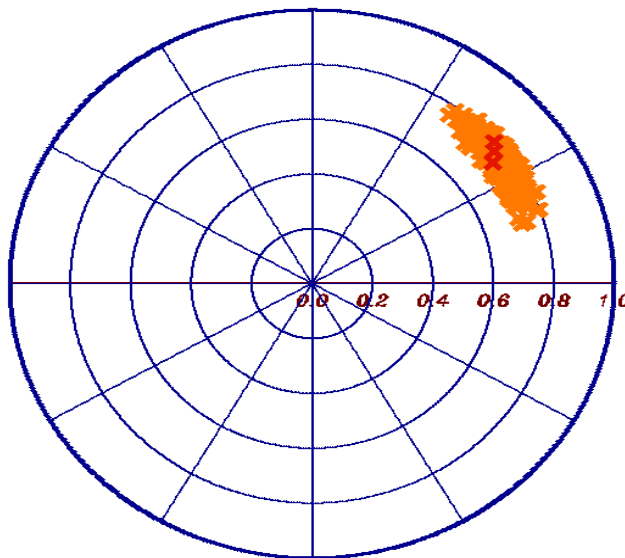


Test site: Traunstein, Germany, L-band @ HV Polarisation





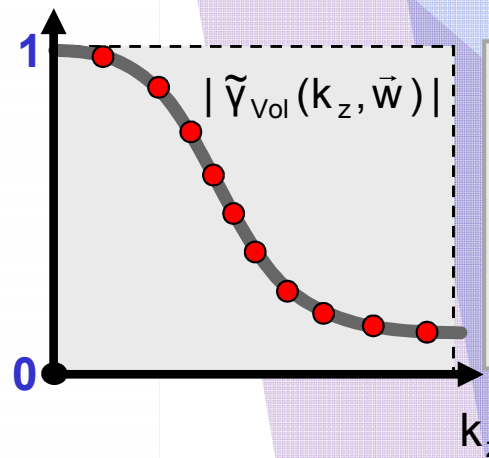
Polarimetric SAR Tomography (TomoSAR)



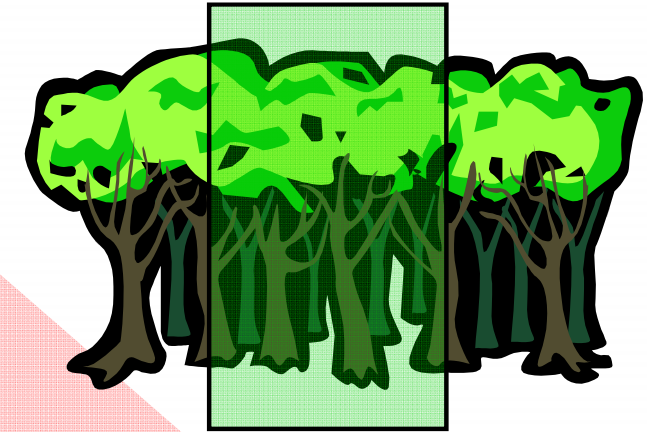
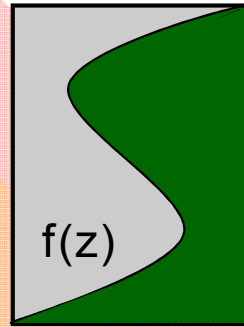
SAR Tomography



$f(z)$... vertical reflectivity function



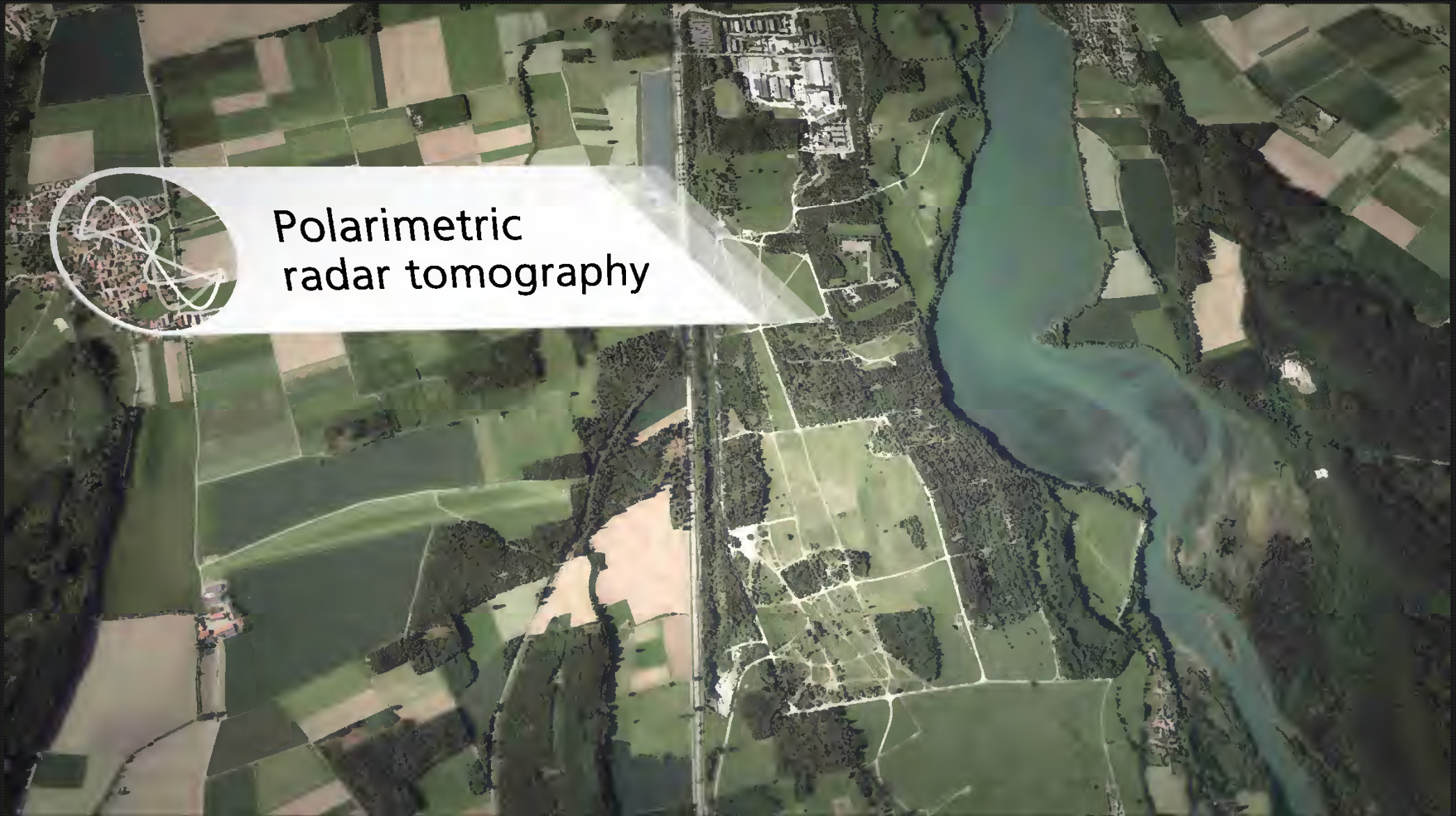
$$\tilde{\gamma}_{\text{Vol}}(f(z)) = e^{ik_z z_0} \frac{\int_{0}^{h_v} f(z) e^{ik_z z} dz}{\int_{0}^{h_v} f(z) dz}$$



$f(z)$... vertical reflectivity function

Vertical Wavenumber: $\kappa_z = \frac{\kappa \Delta \theta}{\sin(\theta_0)}$

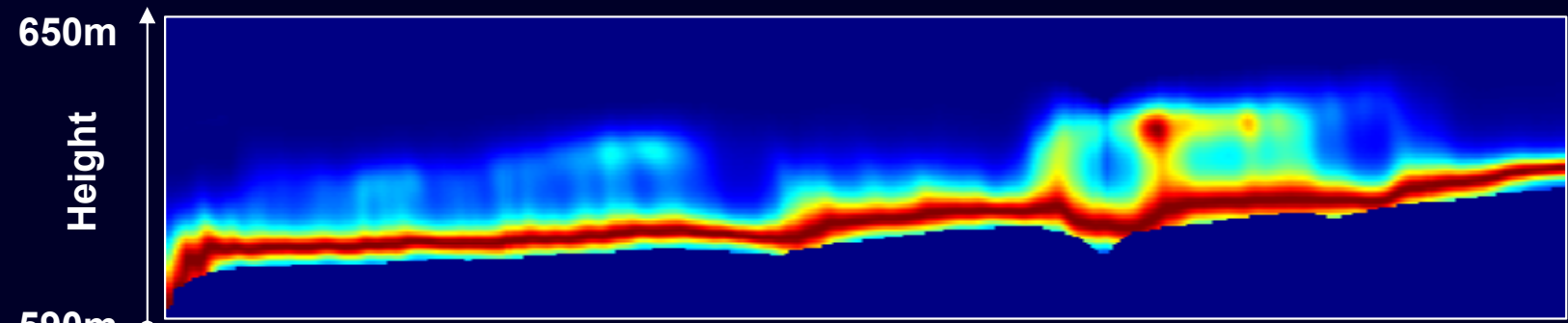




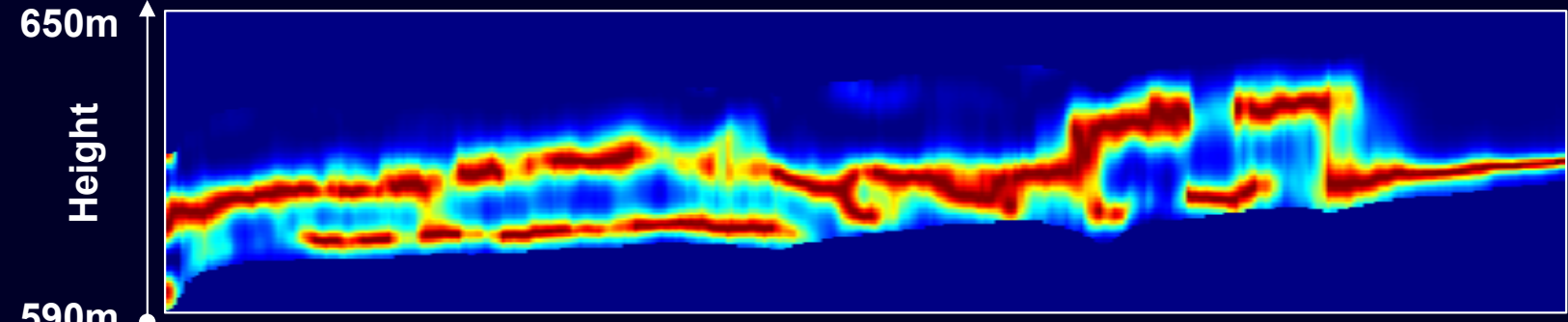
Polarimetric
radar tomography

Traunstein forest (Germany) - Capon - HH

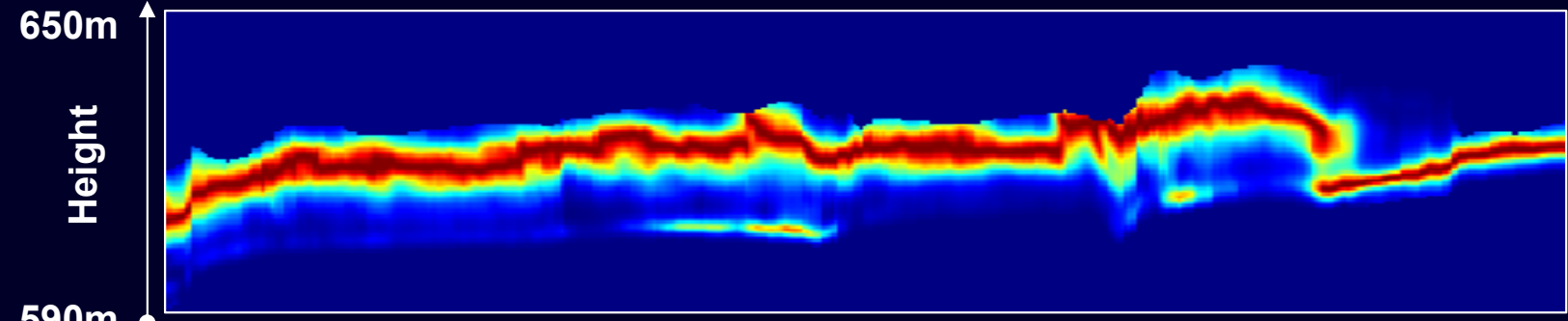
P-band



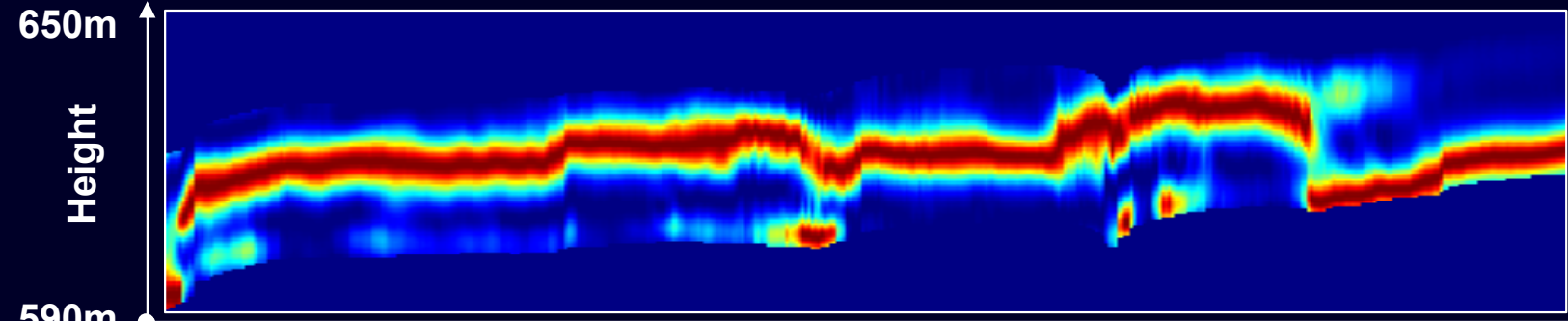
L-band



S-band

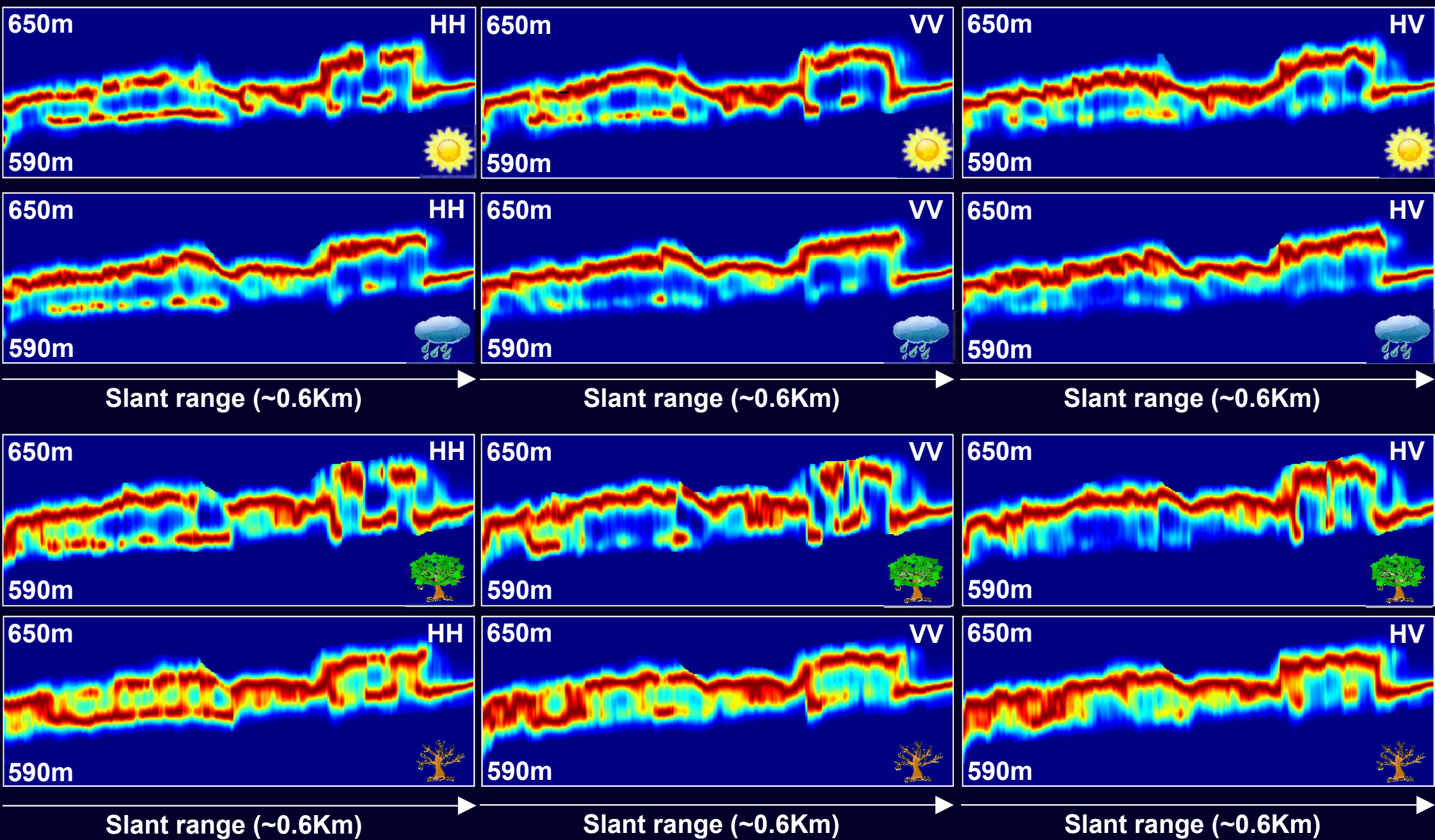


X-band



Slant range (0.6Km)

Temporal variations at L-band (Capon)

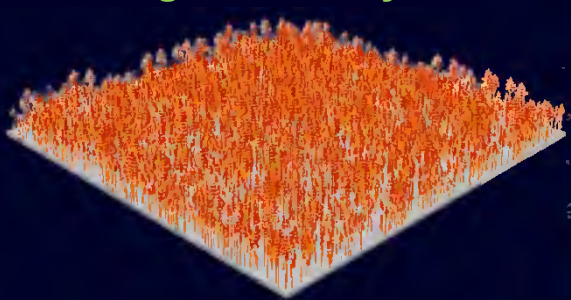


Forest Structure Characterisation

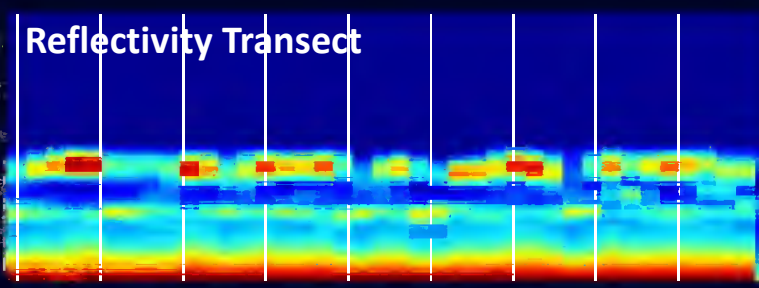


Helmholtz Alliance:
Remote Sensing and Earth System Dynamics

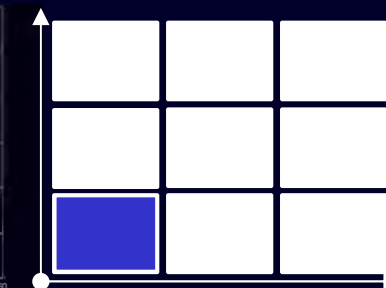
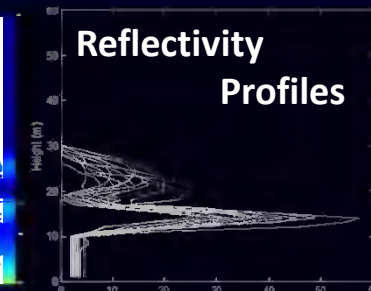
► Young forest, 50 years old



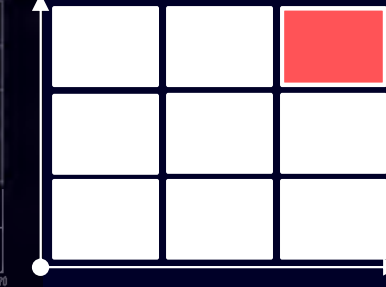
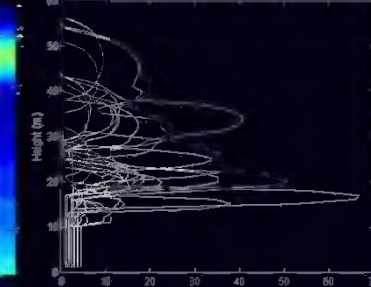
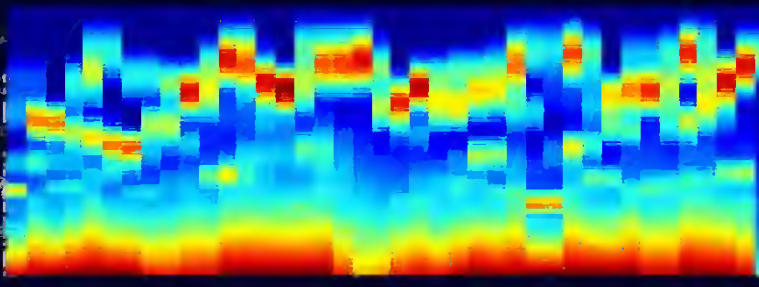
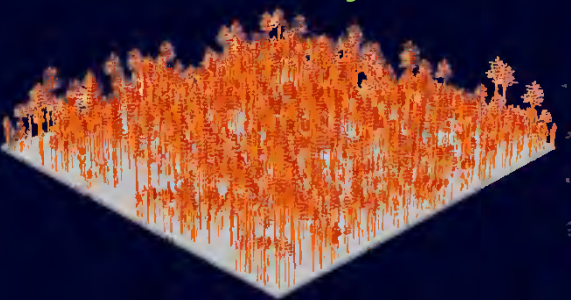
Reflectivity Transect



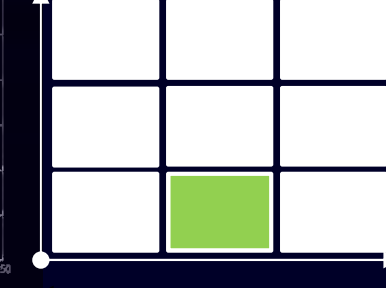
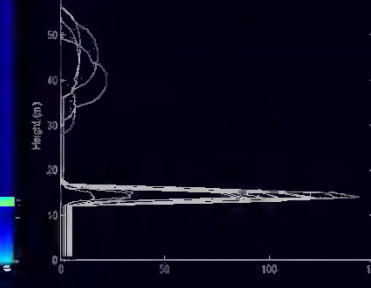
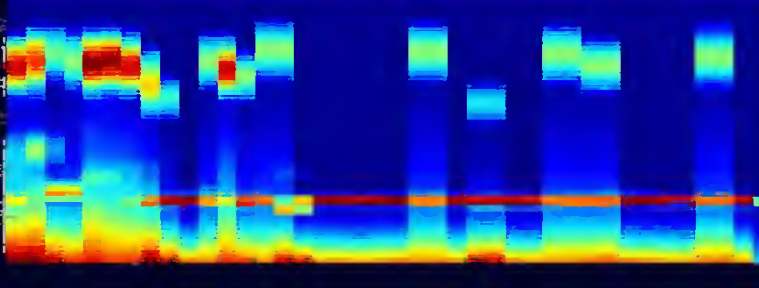
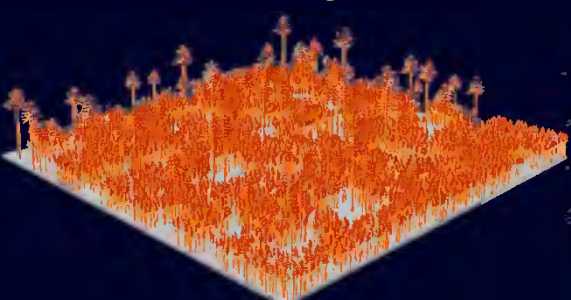
Reflectivity Profiles



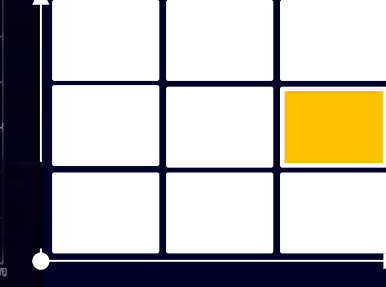
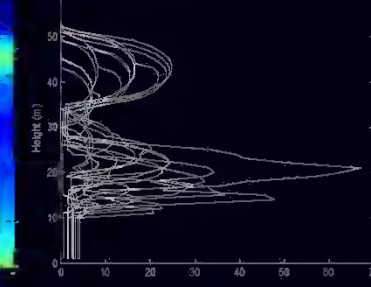
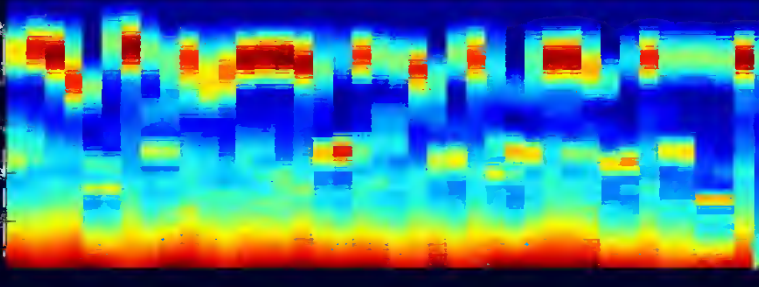
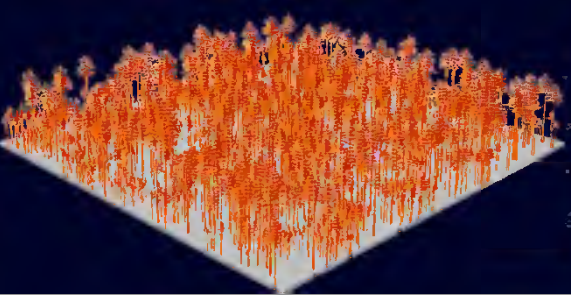
► Old forest, 500 years old



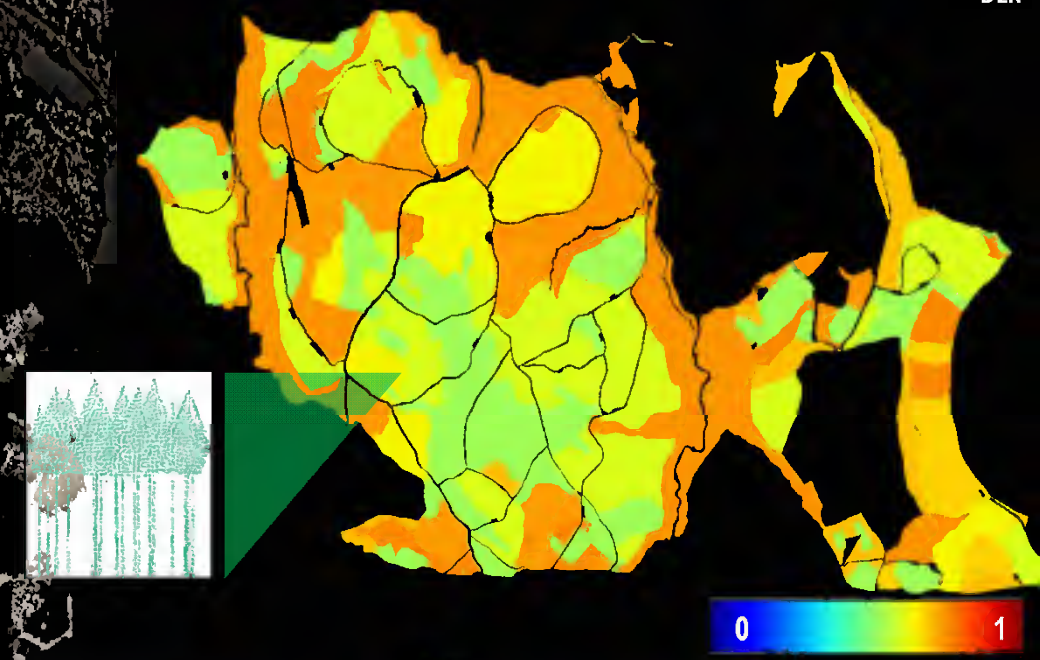
► Old forest, 10 years after a fire event



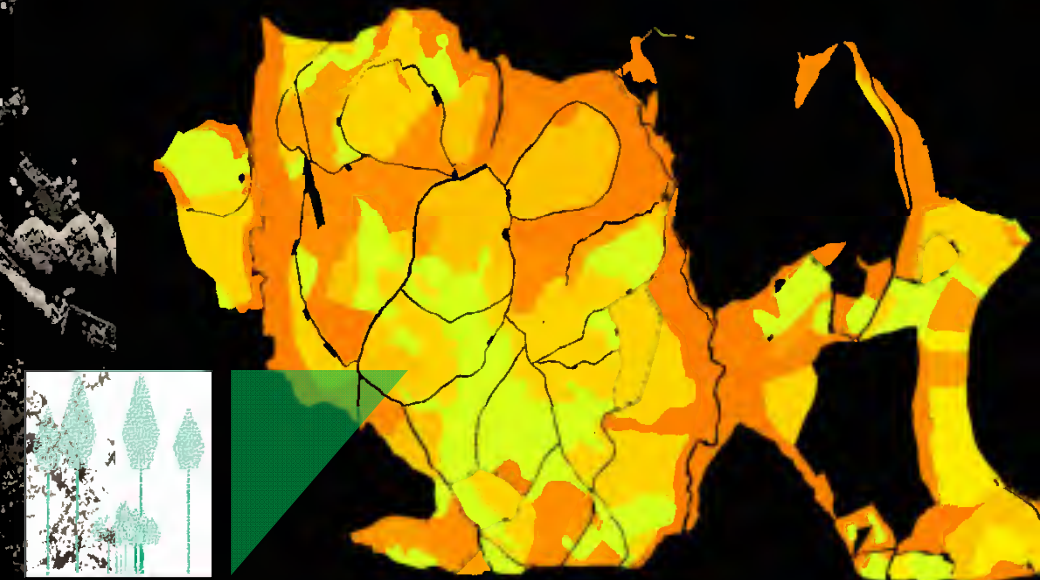
► Old forest, 200 years after a fire event



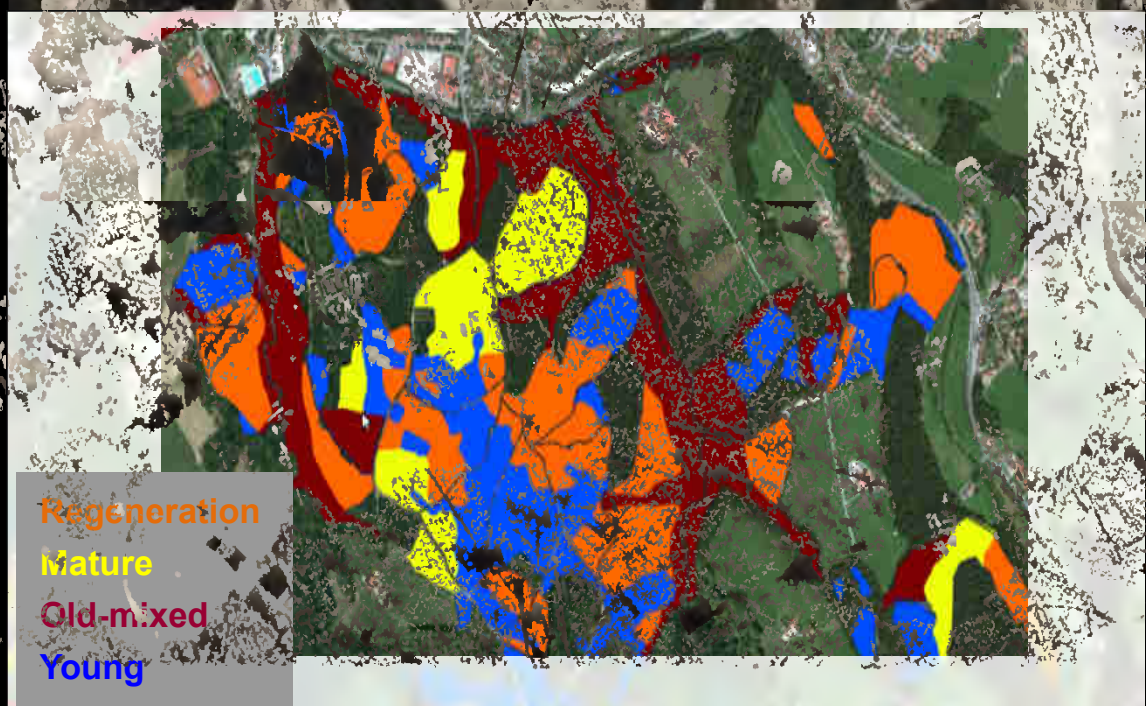
Vertical structure CM (Radar 2008)



Vertical structure CM (Radar 2012)

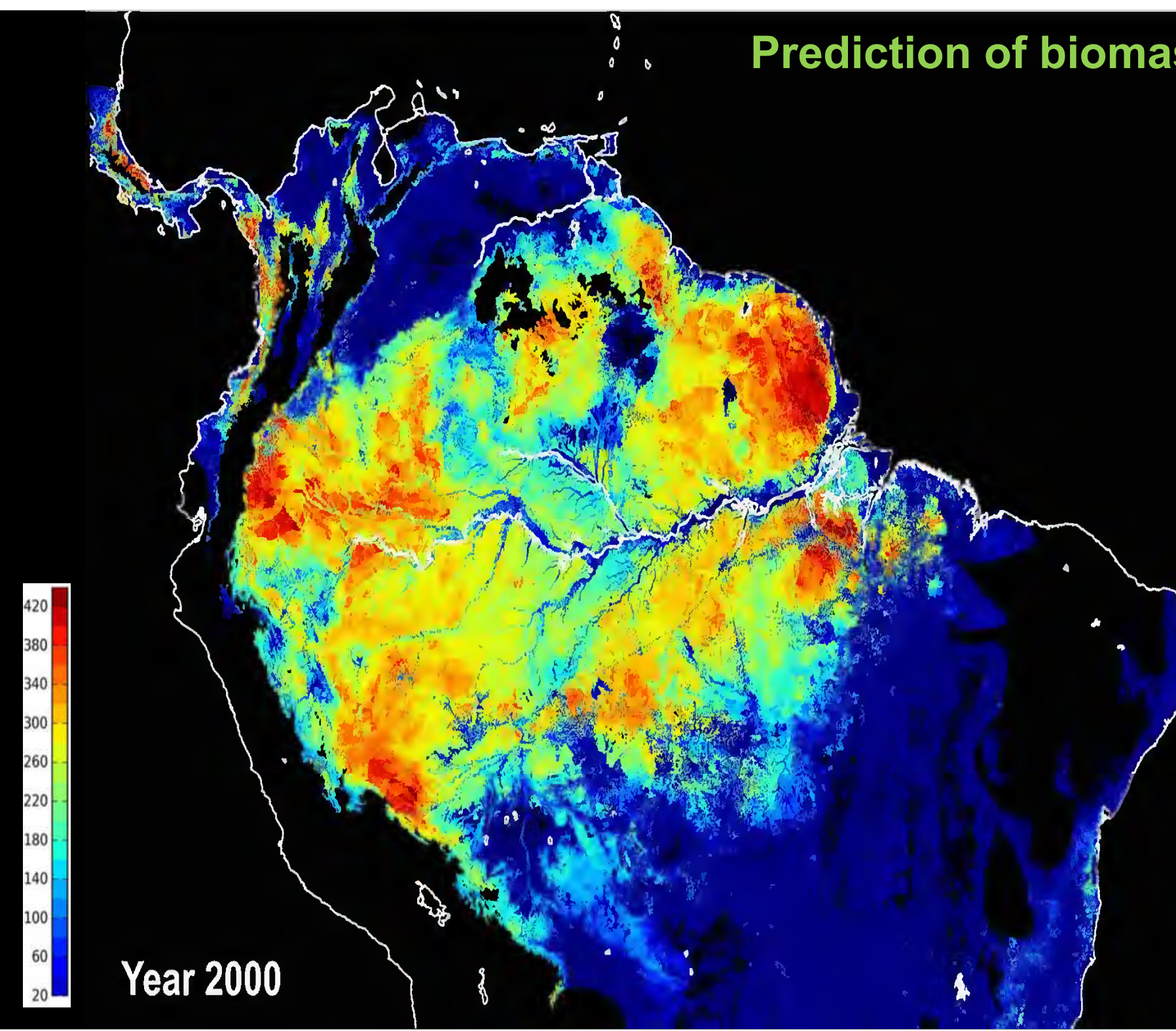


Regeneration
Mature
Old-mixed
Young



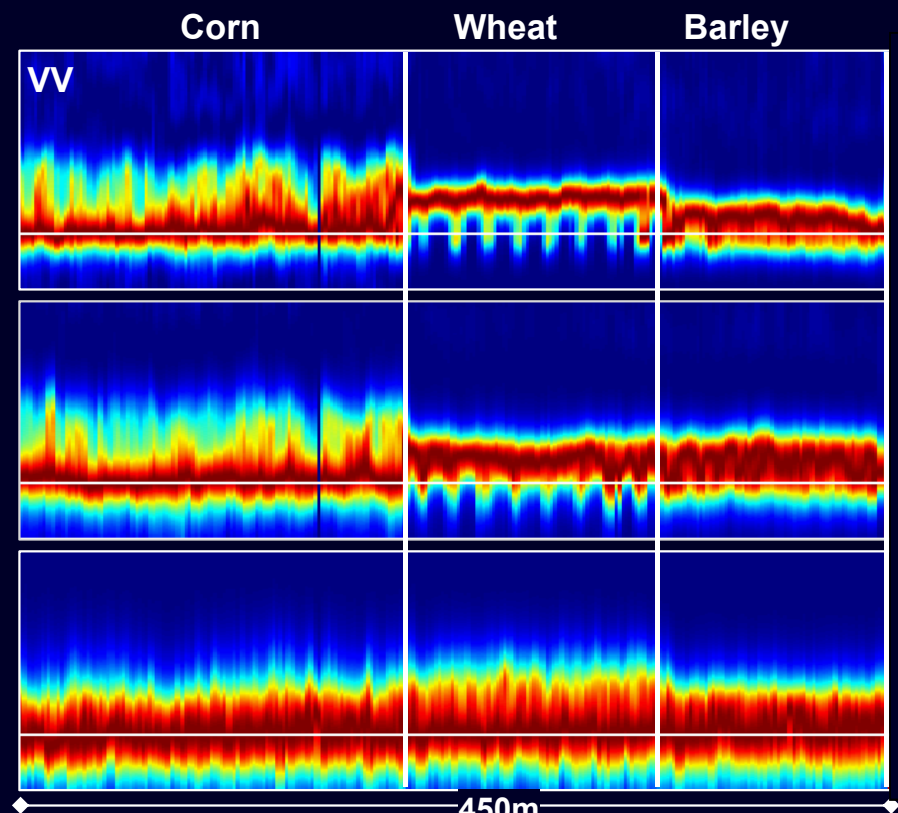
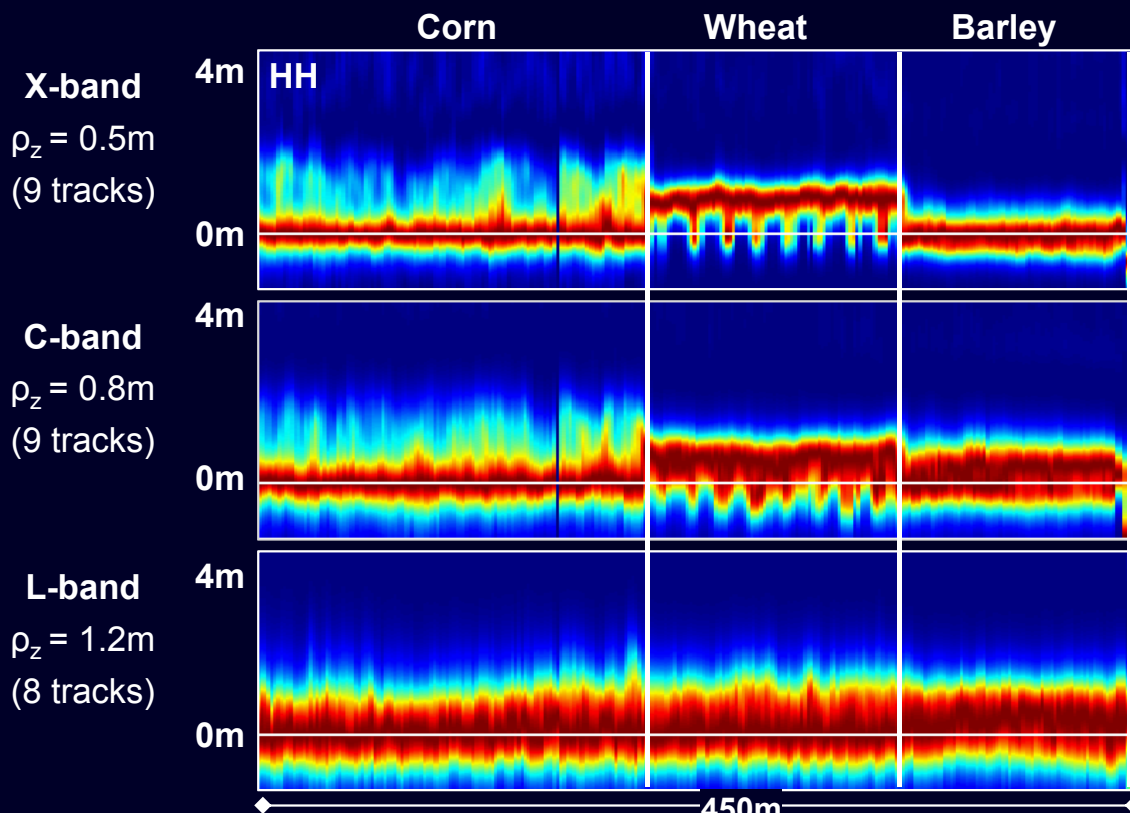
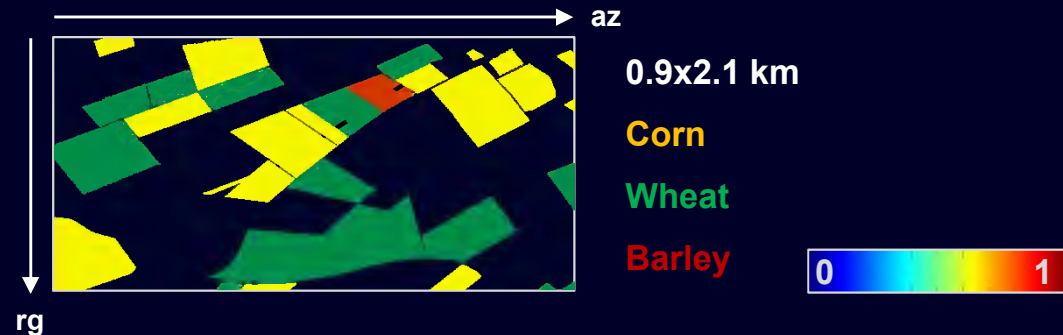
Forest Structure Classification (25x25 m): Traunstein, Germany, 2008 / 2012

Prediction of biomass dynamics



TomoSAR for Agricultural Crops

July 3



F-SAR campaign in Wallerfing (Germany), 2014:

- 8 Multi-Baseline acquisitions across the phenological cycle (May to August)
- Each acquisition: X- & C-band simultaneously, L-band
- Ground measurements (soil & vegetation)

Capon, multi-look cell $7.5 \times 7.5\text{m}$

X-band: Nlooks=200

C-band: Nlooks=200

L-band: Nlooks=100

TomoSAR for Agricultural Crops

July 3



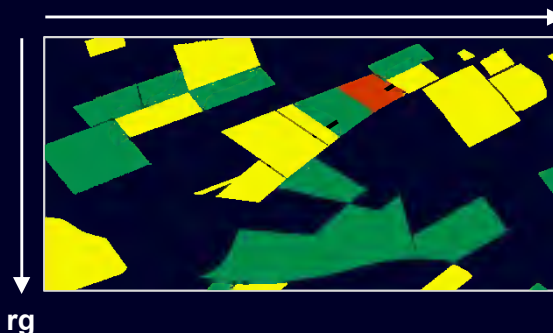
1.7m



0.8m



0.8m

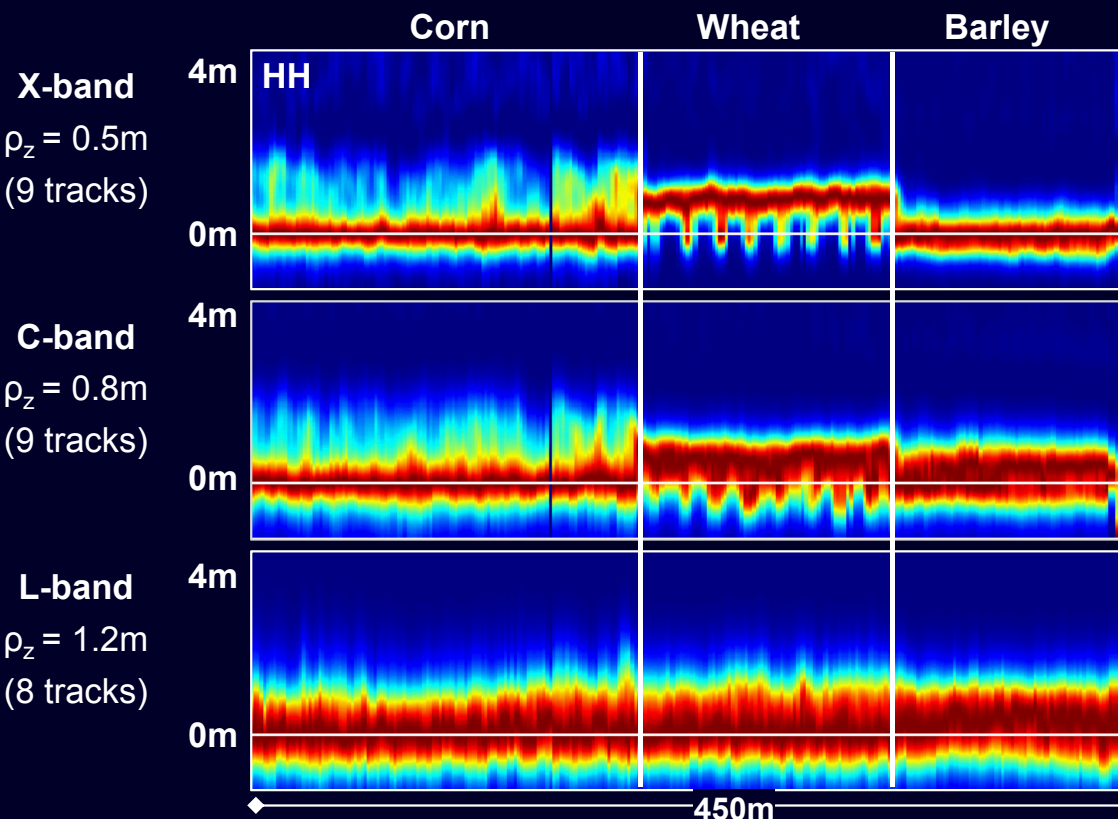


0.9x2.1 km

Corn

Wheat

Barley



F-SAR campaign in Wallerfing (Germany), 2014:

- 8 Multi-Baseline acquisitions across the phenological cycle (May to August)
- Each acquisition: X- & C-band simultaneously, L-band
- Ground measurements (soil & vegetation)

Capon, multi-look cell $7.5 \times 7.5m$

X-band: Nlooks=200

C-band: Nlooks=200

L-band: Nlooks=100

TomoSAR for Agricultural Crops

July 24



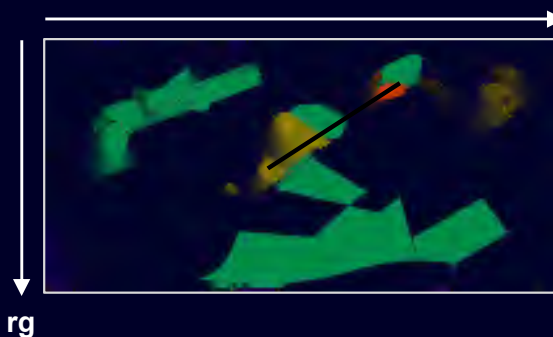
3.5m



0.8m



0.0m

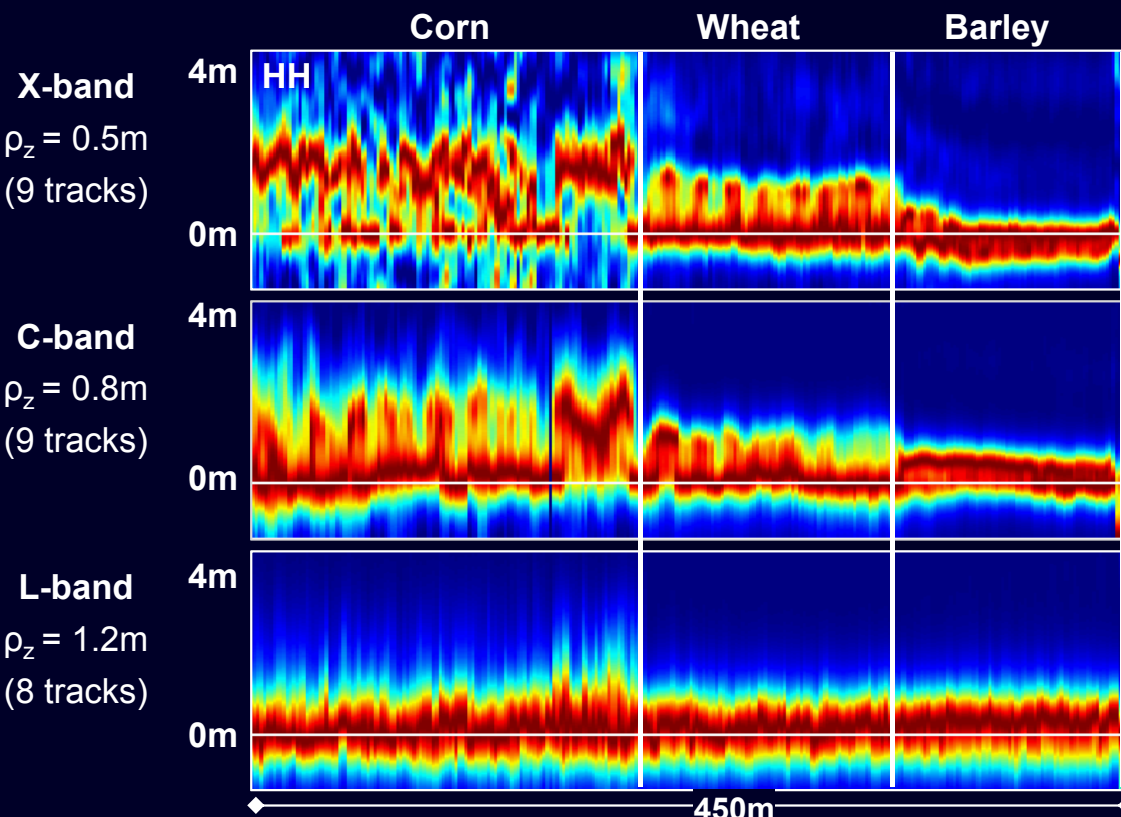
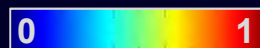


0.9x2.1 km

Corn

Wheat

Barley



F-SAR campaign in Wallerfing (Germany), 2014:

- 8 Multi-Baseline acquisitions across the phenological cycle (May to August)
- Each acquisition: X- & C-band simultaneously, L-band
- Ground measurements (soil & vegetation)

Capon, multi-look cell $7.5 \times 7.5\text{m}$

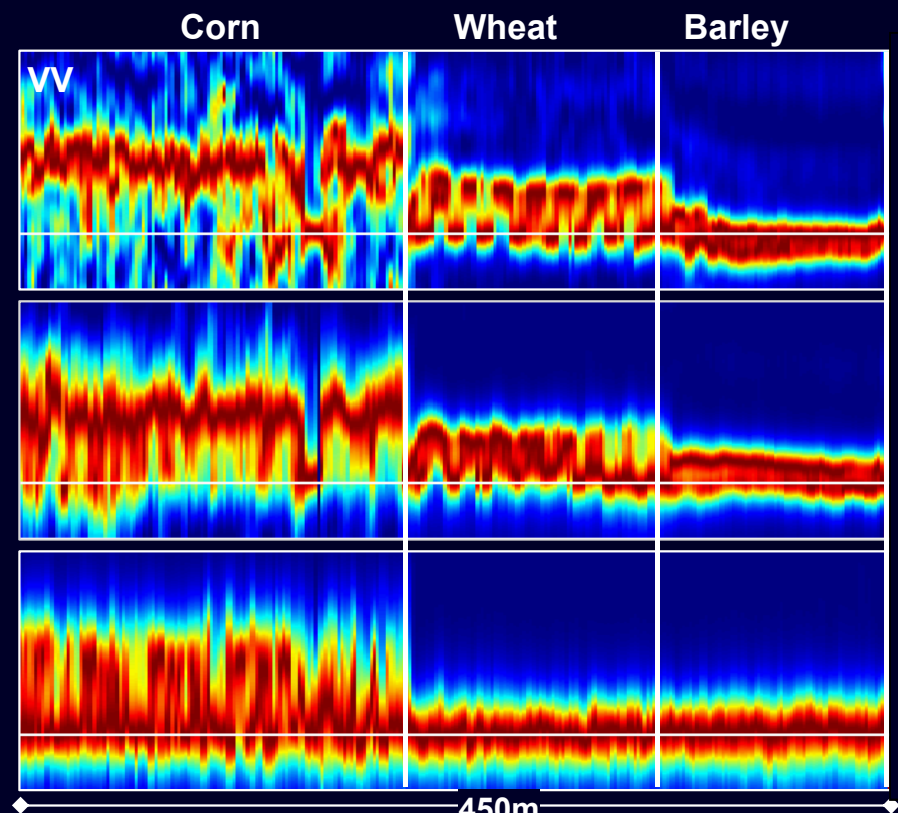
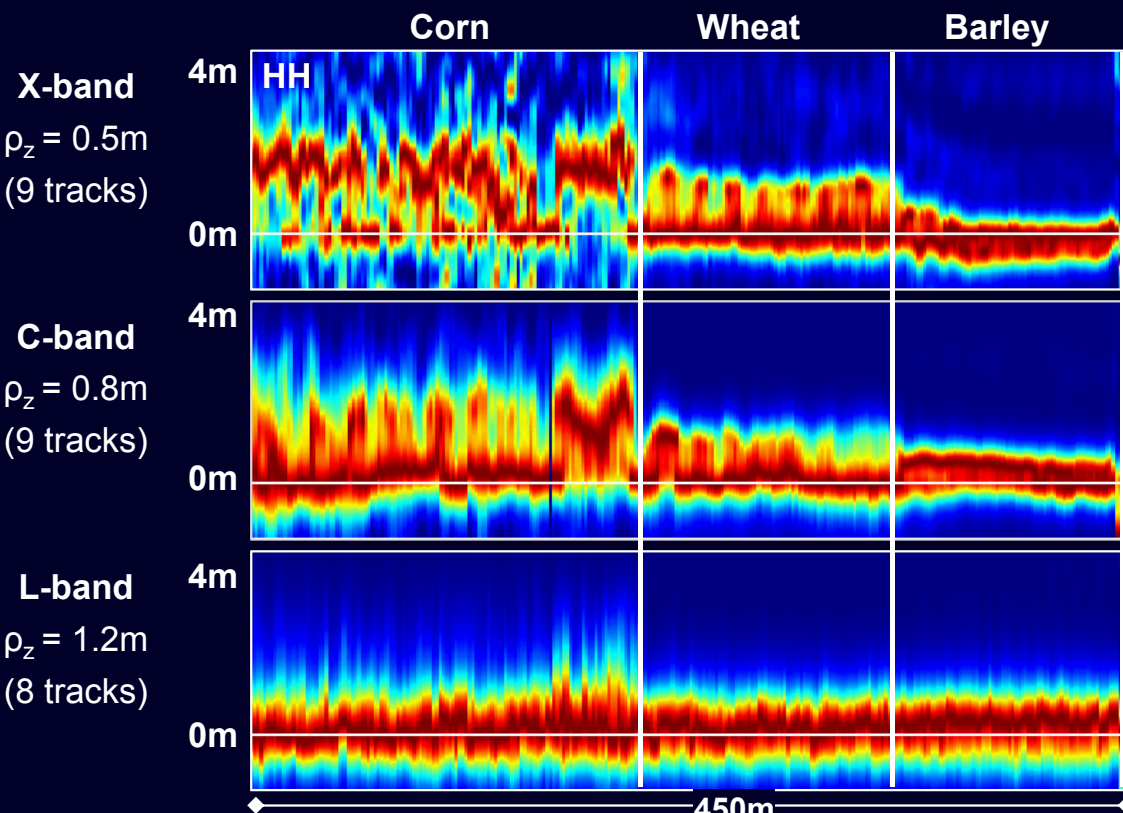
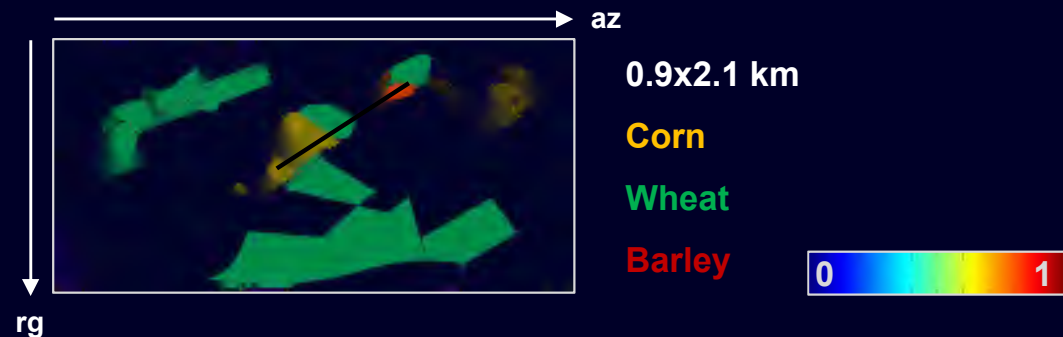
X-band: Nlooks=200

C-band: Nlooks=200

L-band: Nlooks=100

TomoSAR for Agricultural Crops

July 24



F-SAR campaign in Wallerfing (Germany), 2014:

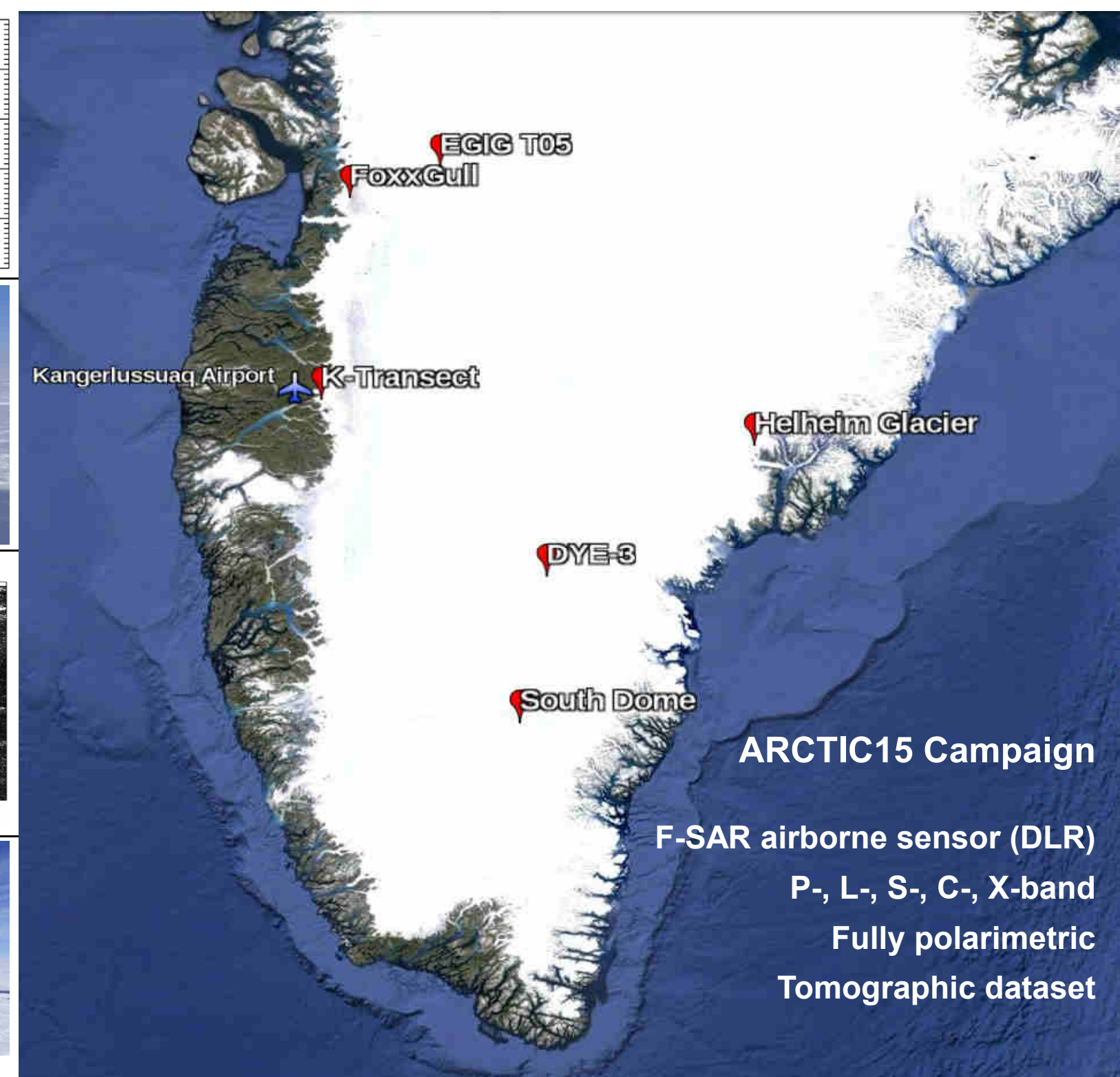
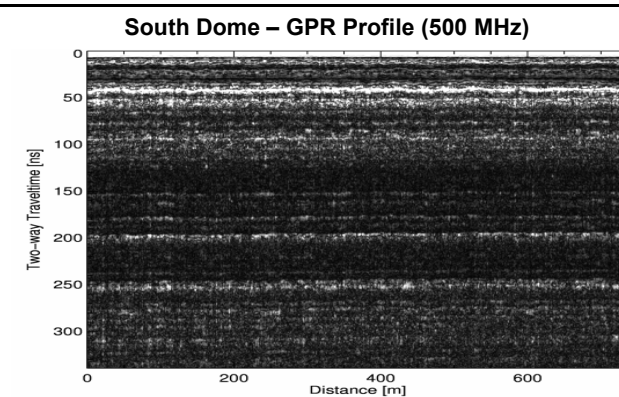
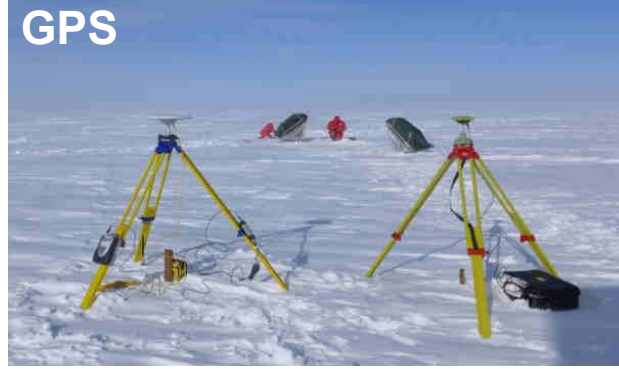
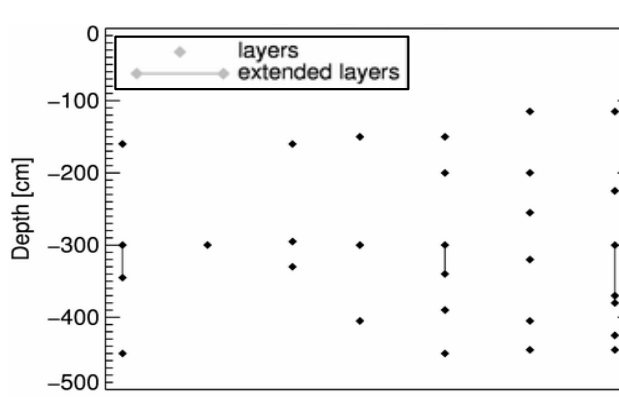
- 8 Multi-Baseline acquisitions across the phenological cycle (May to August)
- Each acquisition: X- & C-band simultaneously, L-band
- Ground measurements (soil & vegetation)

Capon, multi-look cell $7.5 \times 7.5\text{m}$

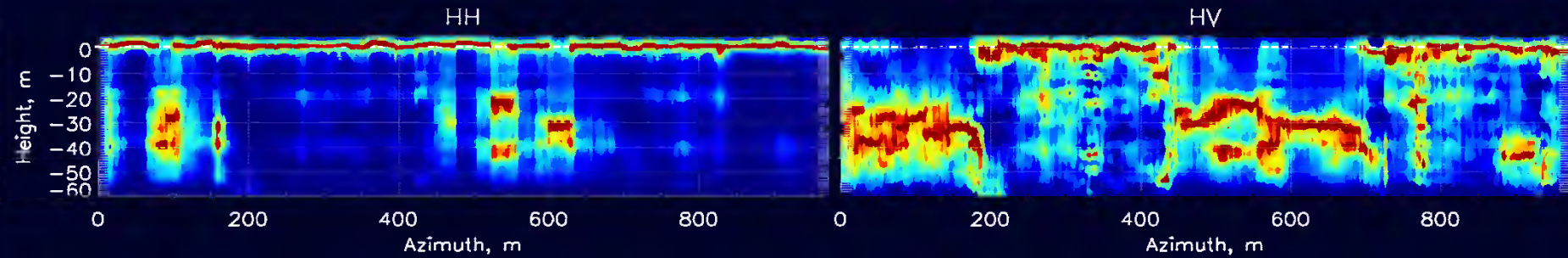
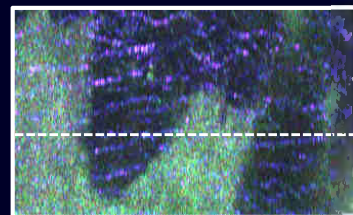
X-band: Nlooks=200

C-band: Nlooks=200

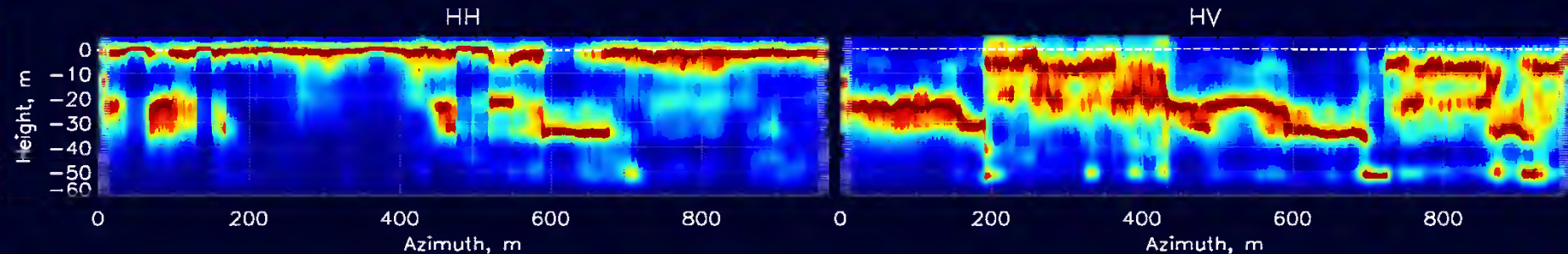
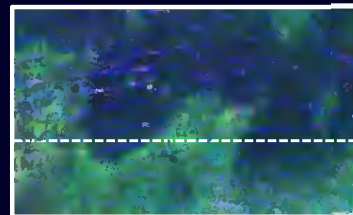
L-band: Nlooks=100



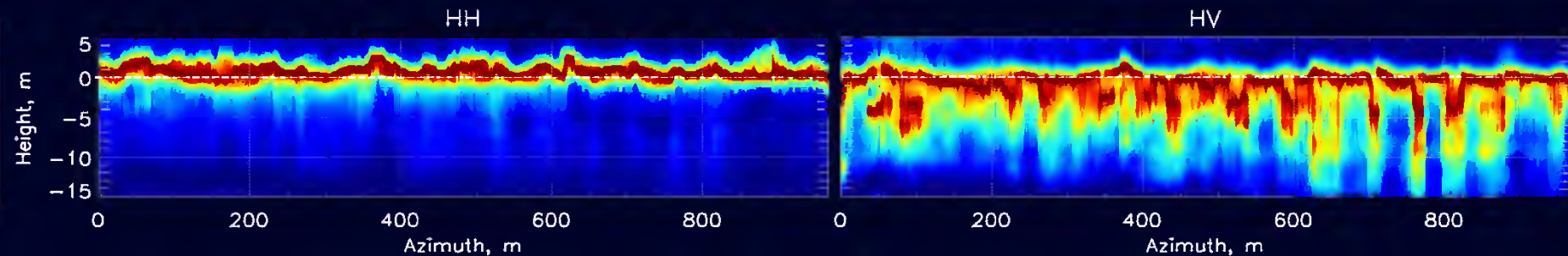
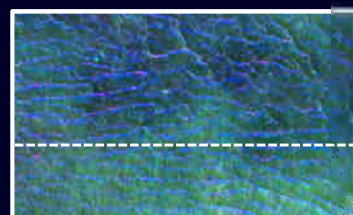
P-band



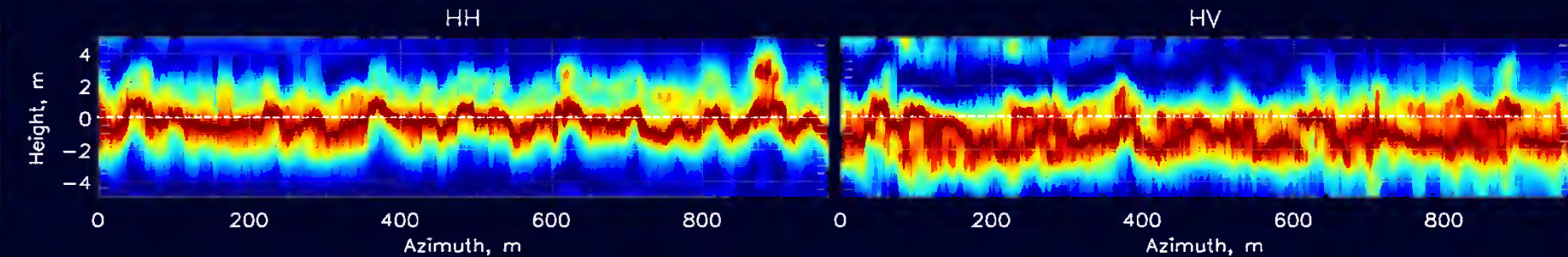
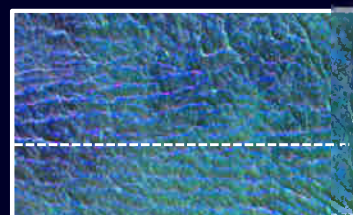
L-band



C-band



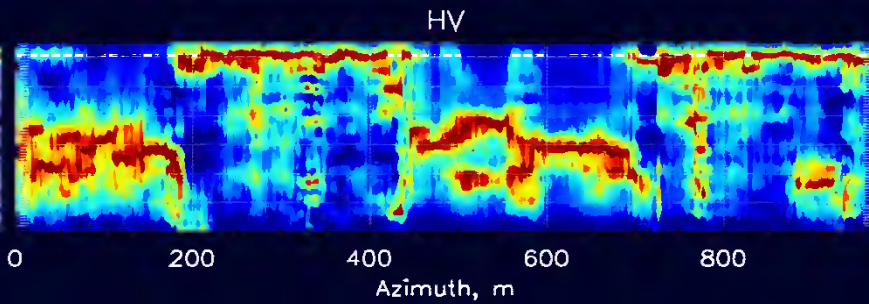
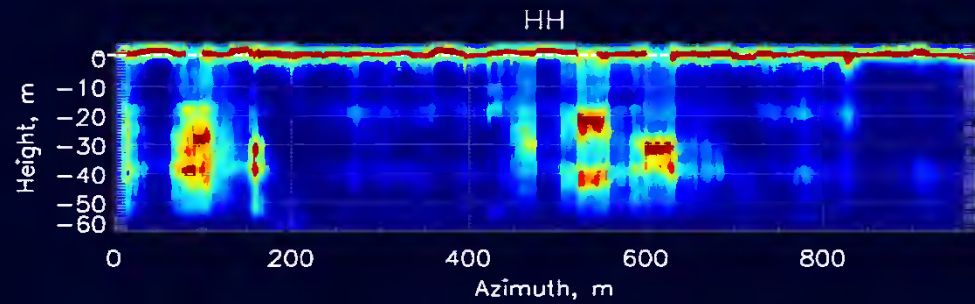
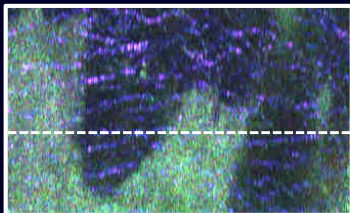
X-band



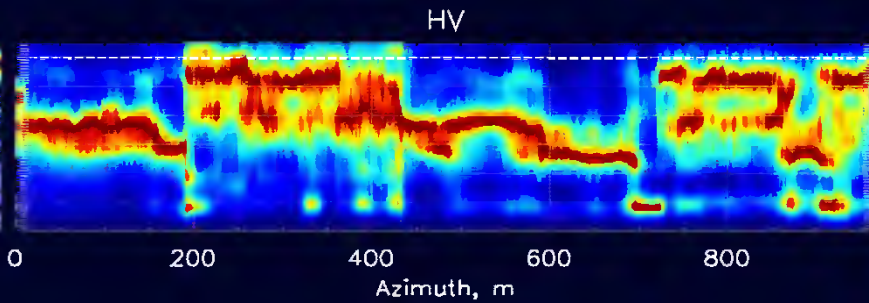
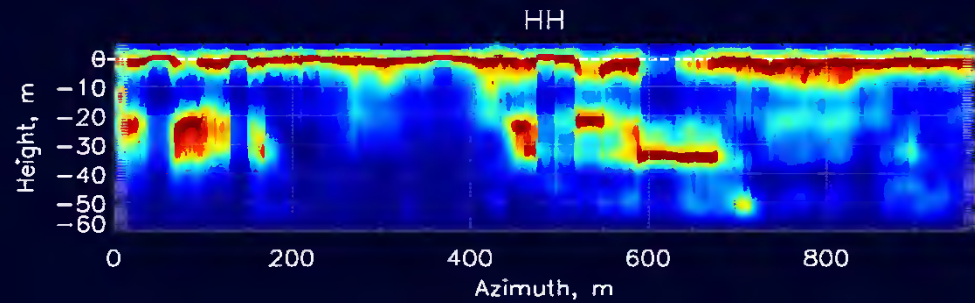
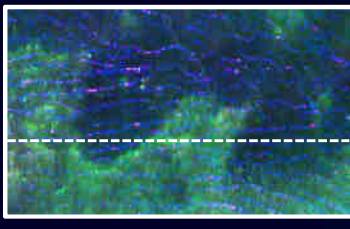
0 Norm. intensity 1

► Capon Profiles ► 20m x 20m multilook cell

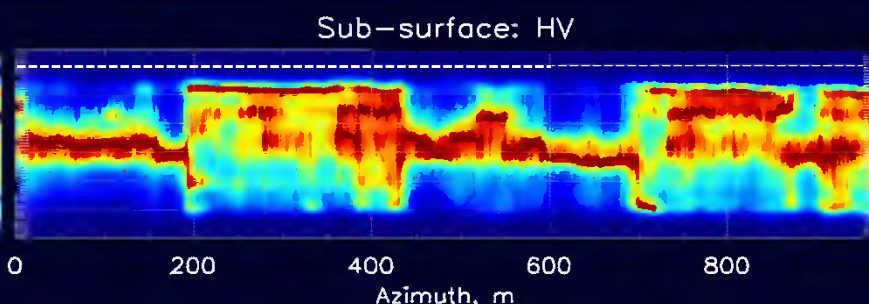
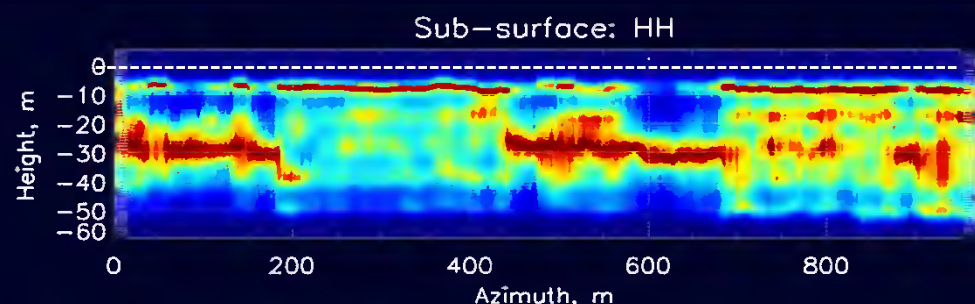
P-band



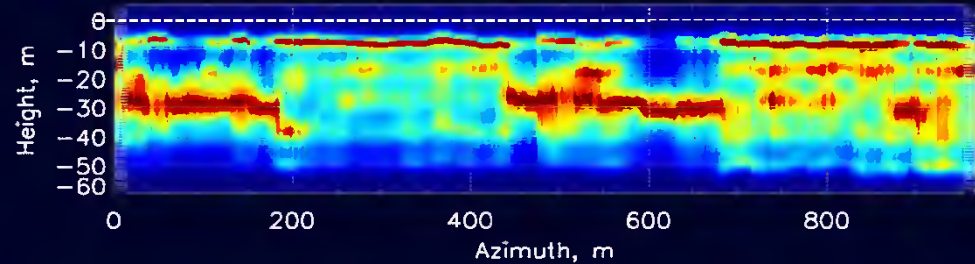
L-band



Sub-surface profiles



Sub-surface profiles + RV hyp.



0 Norm. intensity 1

► Capon Profiles ► 20m x 20m multilook cell

Polarimetric SAR



Interferometry

Konstantinos P. Papathanassiou

German Aerospace Center (DLR)
Microwaves and Radar Institute (DLR-HR)
Pol-InSAR Research Group

Oberpfaffenhofen, P.O. 1116, D-82234 Wessling
Tel./Fax.: ++49-(0)8153-28-2367/1149
Email: kostas.papathanassiou@dlr.de

